QUANTITATIVE MODELLING OF THE FLUID-ELECTROLYTE, ACID-BASE BALANCE FOR CLINICAL APPLICATION.

BY

ROBERT LOUIS FLOOD

THESIS SUBMITTED FOR THE DEGREE

OF DOCTOR OF PHILOSOPHY

THE CITY UNIVERSITY

DEPARTMENT OF SYSTEMS SCIENCE

OCTOBER 1985

To

Mandy and Ross

"Nothing puzzles me more than time and space; and yet nothing troubles me less, as I never think about them."

Charles Lamb 1775-1834

[Letter to T. Manning, 2 January 1810].

CONTENTS

FIGURES

TABLES

ACKNOWLEDGEMENT

I would like to thank Professor E. R. Carson, Dr D. G. Cramp and Dr M. S. Leaning for their support over the past two years. I would also like to acknowledge the help of my father, [redacted], and [redacted].

ABSTRACT

The thesis is introduced as a focussing project for the development of computer aided tools for clinical decision making in the maintenance of fluid volumes and distribution in critically ill patients. Initially a conceptual approach is taken with the fluid-electrolyte, acid-base balance (FAB) introduced via Systems Analysis and then via a more traditional discussion of structure, process and related abnormalities. The second distinct section considers quantitative analysis, starting with a review of extant mathematical models, and is followed by the identification and use of both statistical and mathematical techniques in an investigation into the identification and production of an appropriate quantitative tool. The third distinct section considers both practical and theoretical issues; including a microcomputer implementation of a well validated complex model, and an analysis of methodological approaches suitable for developing a model for clinical implementation.

CHAPTER 1

INTRODUCTION TO THE THESIS

1.1 BACKGROUND

In contemporary society management of scarce resources is one of man's cardinal activities. Medicine is an essential service of society, is widespread and consequently a voracious user of society's resources. As a result, there is great pressure to find ways of efficiently using the scarce resources and, hence, improve the quality of health care available for patients.

One of the most valuable resources is time (it can be considered a resource as it is available for disposal). Time is closely related to cost, for example, cost of a bed per day, cost of nursing hours and cost of internal services for patient care such as the clinical laboratory. These costs are of course closely related. Methods of improving cost efficiency are therefore greatly sought after by Central Government and Health Service administrators alike, whilst at the same time these groups and clinical, nursing and paramedical staff are concerned with maintaining and improving the quality of patient care.

It is therefore surprising to find that clinical laboratories are involved in what appears to be one of the most wasteful exercises in hospital activities. Patients in critical care for instance are subject to continual monitoring and biochemical surveillance. Samples of blood and urine are sent to Chemical Pathology laboratories for measurement and documentation. This has led to a

growing bank of data from which little useful information is extracted. Static data profiles displaying slices of information at discrete times are presented to the clinician as a decision aid. At best (although only occasionally) these profiles are accompanied by some simple statistical analysis, for example, descriptive statistics or more rarely by linear regression.

The first problem for consideration arises here. Man has limited information processing capabilities so that, no matter how sophisticated the presentation of static data profiles may be, clinicians will inevitably pass over much of the information contained in the data and many of its implications. The onus is thus on the laboratory to provide more effective support.

This gives rise to the second problem for consideration. Up to the present time patient management and quantitative decision support have been treated as separate disciplines. This has tended to lead to autonomous development and consequent mismatch between these areas of medicine. Working towards an interface between these separated areas requires that many of the gaps which have evolved be bridged. Thus, the onus is on the laboratory to provide more effective decision support but the objectives must have an emphasis on practical requirements.

1.2 OBJECTIVES OF THE RESEARCH

The solution to these problems, and therefore the aims and objectives of the research reported in this thesis, can be considered in the objectives tree of Figure 1.1. This essentially

shows the role of clinical chemistry in the data transformation activities. At the highest level (level 4) the objective is to enhance clinical decision making for diagnosis, prognosis and patient management. To achieve this objective the large number of data produced by the Chemical Pathology laboratory provide the raw material with which an appropriate decision support structure may be constructed. The extraction of maximum information by clinical data transformation (level 2) is therefore an explicit goal, see Figure 1.2.

These activities must necessarily be designed, not only for providing decision support, but also for enhancing the laboratory-clinician interface. Thus both intermediate objectives (level 3) need to be satisfied simultaneously. At this level, the provision of only decision support will certainly give rise to suboptimal results at level 4.

The transition from level 2 to level 4 will, in addition, identify the essential as opposed to the weak or redundant data available and consequently suggest areas where data production can be made more efficient (this feedback is represented in Figure 1.1. by the dotted arrow) and thus identifies the underlying objective (level 1) of optimising data production in the clinical laboratory.

The research documented in this thesis considers these objectives in the context of fluid therapy. This marks the beginning of such activities for The Centre for Measurement and Information in Medicine at The City University in collaboration with the Department of Chemical Pathology and Human Metabolism and the

Academic Department of Medical Physics at The Royal Free Hospital School of Medicine. The research programme is therefore necessarily a focussing project, looking at the many facets of the problem rather than specialising in any one area.

Fluid-electrolyte, acid-base balance (FAB) has been selected as the area of interest as it is important to many clinical problems and subsequent clinical decision making. However, as FAB is such a large domain, it would not be productive or desirable to dilute research efforts over the entire range of problems which could be encountered. It was therefore decided to investigate specifically the problem of fluid volume maintenance in acutely ill patients.

1.3 ORGANISATION OF THESIS

To ensure that the work is understood by both the Medical and the Systems reader, continual emphasis has been put on providing reading support in both areas. The basic principles of fluid dynamics are presented in Chapter 2 as both an introduction to the system of interest (SOI) and also to the Systems Approach (the underlying method of anlaysis used in this thesis). This implies a move away from the more traditional static analysis of clinical decision making, towards time-based modelling for decision support in the clinic.

A detailed analysis of FAB structure and process, and associated abnormalities follows in Chapter 3. A graph-theoretical analysis of Chapter 3 is presented in Chapter 4. This provides a diagrammatic step which is necessary to clarify areas of

controversy and weak knowledge and to identify the initial model structure.

In Chapter 5 an in-depth review of extant FAB quantitative models is documented; this identifies the approaches that have been, could be, and should be adopted in the research programme to test their suitability. Chapter 6 discusses and uses a variety of compact approaches which have not been tried in this area, whilst Chapter 7 documents the complex model (MFAB) which has been developed during the research programme. MFAB is novel in that the utilitarian objective of clinical application determines, to some extent, the structure and processes of the model. Although Chapter 6 carries its own validation (statistical confidence and so on) it was found necessary to make an extensive validation of MFAB, which is reported in Chapter 8.

The role of MFAB in fluid therapy is discussed in Chapter 9 at a practical level, where microcomputer implementation (and its attendant problems) is the main theme. In contrast, Chapter 10 is discursive in nature, considering the role of Systems Science in clinical medicine at a theoretical level.

The overall conclusions of Chapter 11 draw to a close this essentially focussing project by identifying contributions that have been made, and also by suggesting specific areas where future developments are important and, hence, would enhance the wider research programme.

In summary, Chapters 2 through to 4 provide a conceptual introduction, Chapters 5 through to 8 tackle the quantitative aspects, whilst Chapter 9 and 10 take a practical and then theoretical look at the research goals.

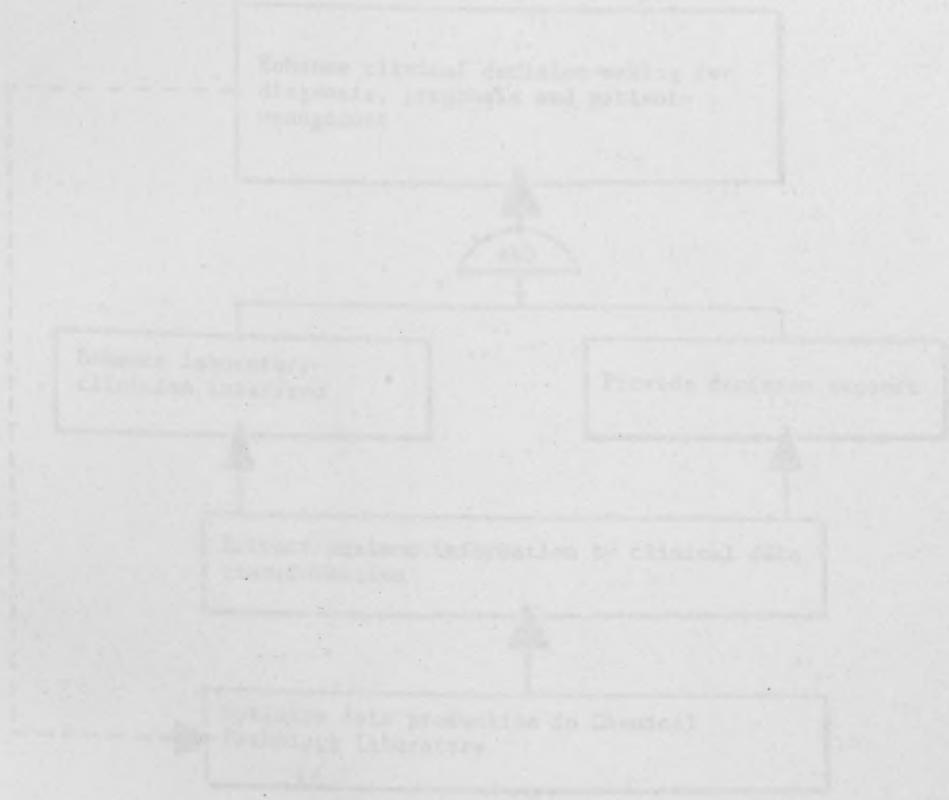

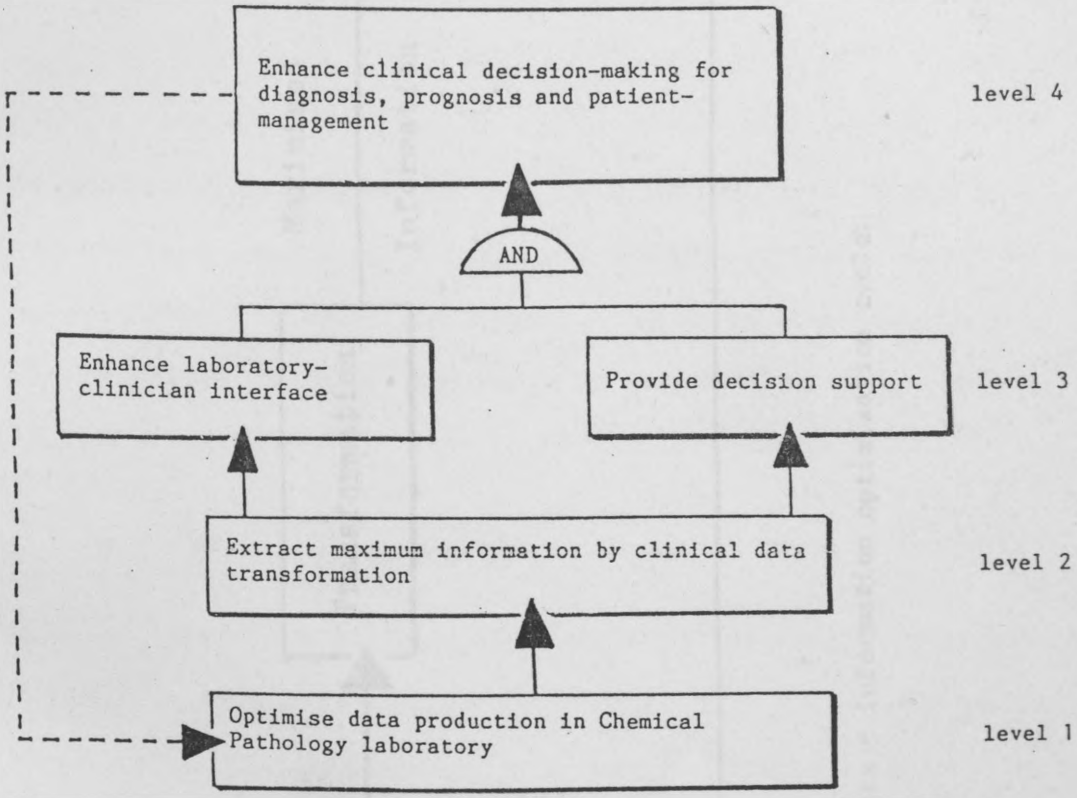

Figure 1.1 Objectives of the research goals.

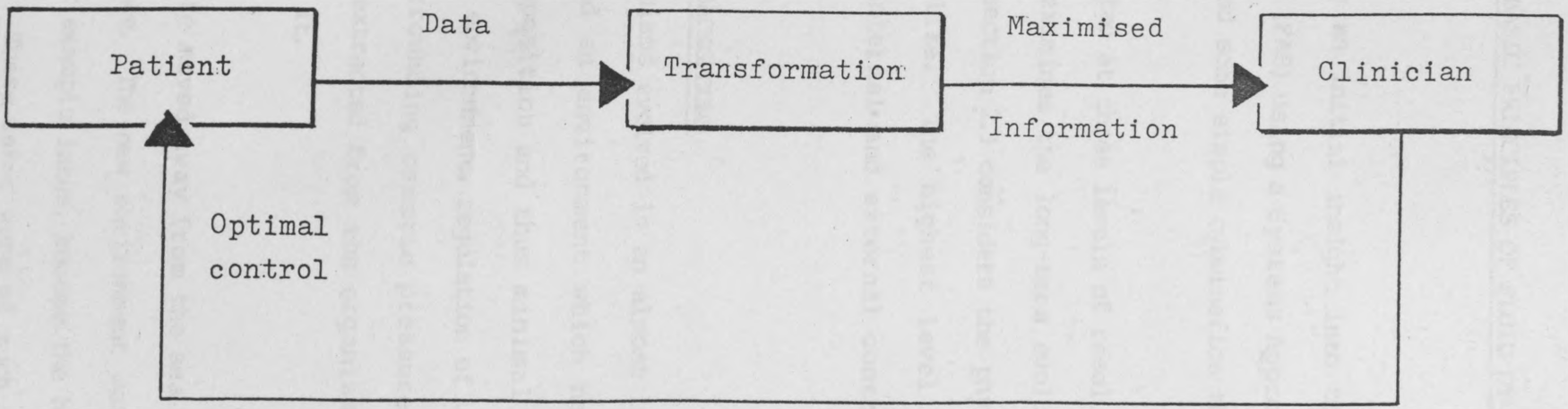

Figure 1.2 Idealised data - information optimisation cycle.

CHAPTER 2

THE BASIC PRINCIPLES OF FLUID DYNAMICS

2.1 INTRODUCTION

Chapter 2 provides an initial insight into the fluid-electrolyte, acid-base balance (FAB) using a Systems Approach. This involves organic thinking and some simple cybernetics theory.

The work is presented at three levels of resolution. At the lowest level section 2.2 examines the long-term evolution of FAB, whilst at a higher level section 2.3 considers the physiological processes that constitute life. The highest level of the day to day requirements of internal and external control is discussed in section 2.4.

2.2 EVOLUTIONARY BACKGROUND

Single celled organisms evolved in an almost infinitely large salt sea. This provided an environment which had only very small variations in composition and thus minimal disturbance to its occupants. In this environment, regulation of volume for organisms was simple as surrounding osmotic pressures remained stable. Nutrients could be extracted from the organism's environment and wastes returned to it.

Cells evolved. Life moved away from the sea taking with it this internal salt balance. The new environment was hostile. At first smaller waters, for example lakes, became the home of more complex cellular organisms. These lakes were of much smaller volume than

the seas and prone to dilution during heavy rains, or concentration during long spells of evaporation. Organisms had to evolve special mechanisms to maintain normal operating conditions, compensating for external environmental changes.

Life moved away from water. A mobile sea-like internal system was maintained around the cells, allowing vital cellular activities to occur relatively undisturbed. It is this homeostatic internal sea which is referred to as the fluid-electrolyte, acid-base system.

2.3 BASIC PHYSIOLOGY

Water is the most pervasive of all body substances, being the medium in which intracellular metabolism can continue, whilst also bathing those cells in a stable environment from which they can absorb the rich nutrient content and deposit their metabolic wastes. Furthermore, over time water is maintained as a homeostatic system through which the body supply of nutrients is matched to the rate of usage, and the production of wastes is equal to the rate of excretion. In terms of ordinary first order linear differential equations;

$$\frac{dV_B}{dt} = V_I - V_o = 0 \qquad (2.1)$$

$$\frac{dN_B}{dt} = N_I - N_o = 0 \qquad (2.2)$$

$$\frac{dW_B}{dt} = W_I - W_o = 0 \qquad (2.3)$$

where;

V = water volume.

N = nutrient content.

W = waste content.

B, I, O are subscripts relating to body, input and output respectively.

The maintenance of a homeostatic water supply ensures the satisfaction of equations (2.2) and (2.3), and consequently the continuance of life.

The complexity of the human body is vast. There are 7.5×10^7 cells in the blood alone (Guyton, 1976). It is therefore necessary to analyse the FAB system at a lower level of resolution than the cell. A convenient structural level is the functional organ and circulatory inter-connections.

Fluid exists inside the cells (intracellular fluid) and outside the cells (extracellular fluid). The latter is split between that transported around the body on continual passage through the circulatory system and pumped by the heart (plasma fluid) and the fluids which fill the spaces between the cells continually mixing with the plasma fluid via capillaries (interstitial fluid).

The plasma fluid flows past the walls of the lungs once per circulation. Oxygen diffuses from the lung alveoli into the bloodstream, attaching to haemoglobin. This oxyhaemoglobin is then transported by the circulation to the peripheral cells. The reverse holds for carbon dioxide (a waste product of metabolism),

which is removed from the peripheral cells and transported to the lungs where diffusion occurs. Carbon dioxide is then blown-off by ventilation.

Blood also acts as receiver and bulk transporter of nutrients. Vessels run through the walls of the gastrointestinal tract, the latter surrounding the passing food supply. Nutrients are actively and passively absorbed and supplied to the peripheral cells, meanwhile, the wastes are transported to the kidney, filtered and excreted.

Some substances absorbed from the gastrointestinal tract cannot be used in their raw form, therefore organs are required to perform metabolic functions, changing chemicals to more usable forms. The liver is involved in change, whilst the kidneys, endocrine glands and other functional elements, help to modify or store substances. In addition, the kidneys represent a variable resistance to ground for the analytes (the elements of analysis).

An effective circulatory volume (the component of the ECF which perfuses the tissues) must be maintained to enable the processes discussed above to continue normally.

2.4 CONTROL

2.4.1 Introduction

Control occurs at three levels, intracellular control, intraorgan control and interorgan control. Interorgan control was the main focus of the research, looking at such interrelationships as the

respiratory system and nervous system controlling whole body carbon dioxide levels; and the kidneys with the nervous system and hormonal systems controlling concentrations and contents of protons, sodium, potassium, and so on.

2.4.2 Internal Control

Internal control is almost exclusively negative feedback. Typically, a rise in a given variable triggers off some dynamic system which feeds-back a signal to the stimulant variable in an inhibiting manner. Thus, a high partial pressure of carbon dioxide (PCO_2) will cause a neural response which increases ventilation rate (VR). This in turn reduces the level of carbon dioxide by increasing the exhalation rate to the environment, see the signed-digraph immediately below,

where;

+ states that a rise/fall in the targetting variable leads to a rise/fall in the targetted variable.
- states that a rise/fall in the targetting variable leads to a fall/rise in the targetted variable.

Positive feedback does occur in good health (for example in DNA dynamics) but is usually associated with disorders, and tends to be more typical of acute rather than chronic conditions. In some disorders positive feedback leads to instability and if left unchecked will cause death. Guyton (1976) described an acute and

potentially terminal case of positive feedback following a loss of two litres of fluid from the plasma space. This would cause arterial pressure to fall, diminishing flow to the heart muscle weakening the heart, further diminishing pumping and hence blood flow. Unless external intervention occurred immediately, the cycle would repeat again and again until death.

A control system's effectiveness can be measured by its gain. Gain of the control system is the relation between how much the controlled system changes in response to the phenomena causing the change. For instance if the gain of the control system is -9 units, this says that for every one unit of change occurring 9 units are prevented from occurring, that is, there is a one-tenth dampening of the disturbance.

The concept of feedback control is well illustrated by a systems cybernetic diagram, see Figure 2.1. In this example, the controlled process is the level of carbon dioxide in the plasma. The neural system sends information via related firing rates, this registers in the respiratory centre of the medulla oblongata where desired and actual levels are compared. Any mismatch at this point will cause further changes in neural activity which will inhibit/stimulate pulmonary ventilation bringing about a decrease in the mismatch.

2.4.3. External Control

Pathological conditions and other disorders may destroy the integrity of the physiological system. Unstable positive feedback may occur, however, it is more frequent that negative feedback

control is lost, this tending to be chronic rather than acute in nature. Diabetes insipidus is an example of damage to the control unit where destruction of the supraoptic nuclei, or efferent nerves leading on to posterior pituitary gland, reduces (to varying degrees) the secretion of antidiuretic hormone (ADH), thus increasing urination.

In other cases it may be the controlled process which is affected, for example, in renal failure the kidneys may be damaged thus preventing effective control over the resistance to ground of fluid and electrolytes. Similarly, reduced abilities of the information systems or activating units may cause a loss of negative feedback control.

To compensate for diminished internal control, an external control loop (involving the clinician) is required. Clinician control takes the form of diagnosis, prognosis and patient management. This is achieved by considering patient history, current state, and the projection of these factors to a predicted future state. Clinician control is the taking of action at the current time in order to produce a predicted desired state, or to prevent a predicted undesired state.

This is the principle of feedforward control, see Figure 2.2. In response to a disturbance e on the physiological system, the clinician controller C responds in such a way as to eliminate the effect of the disturbance E on the physiological system G. Thus the effect of the error on the controlled output is given by:

$$y = (E + G.C)e \quad (2.4)$$

so that the predicted error can be removed if;

$$C = -E.G^{-1} \quad (2.5)$$

The need to predict future states is a cue for decision support tools. These tools will need to be quantitative in nature and will increasingly become computer-based.

2.5 SUMMARY

The FAB system has been considered as cybernetics applied at two levels; that of physiological and biochemical self regulation; and that consisting of the exterior control loop between clinician, patient and a computer-based decision support system.

Chapter 2 has identified some important systemic properties of FAB. Chapter 3 considers the FAB system in physiological and pathological terms whilst Chapter 4 takes a holistic view of the system, exemplifying the systemic properties identified in Chapter 2 and clarifying current physiological thinking as described in Chapter 3.

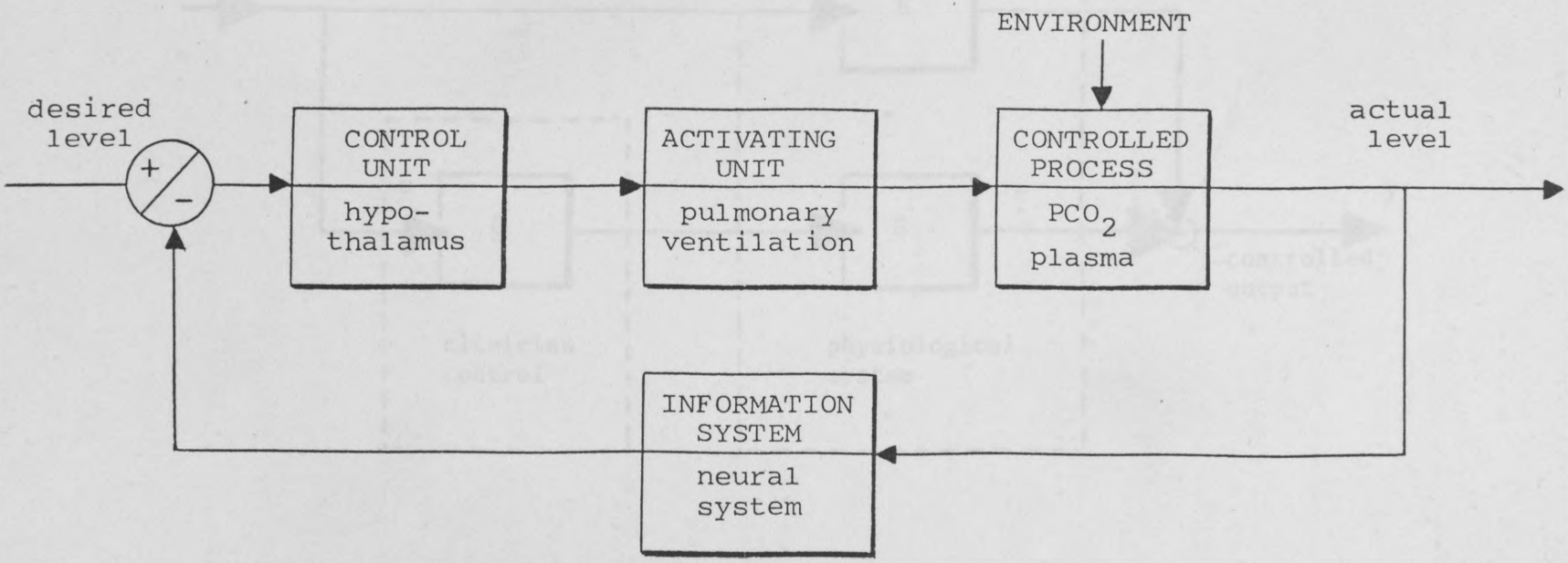

Fgiure 2.1 Systems cybernetic diagram: control of PCO2 in the plasma.

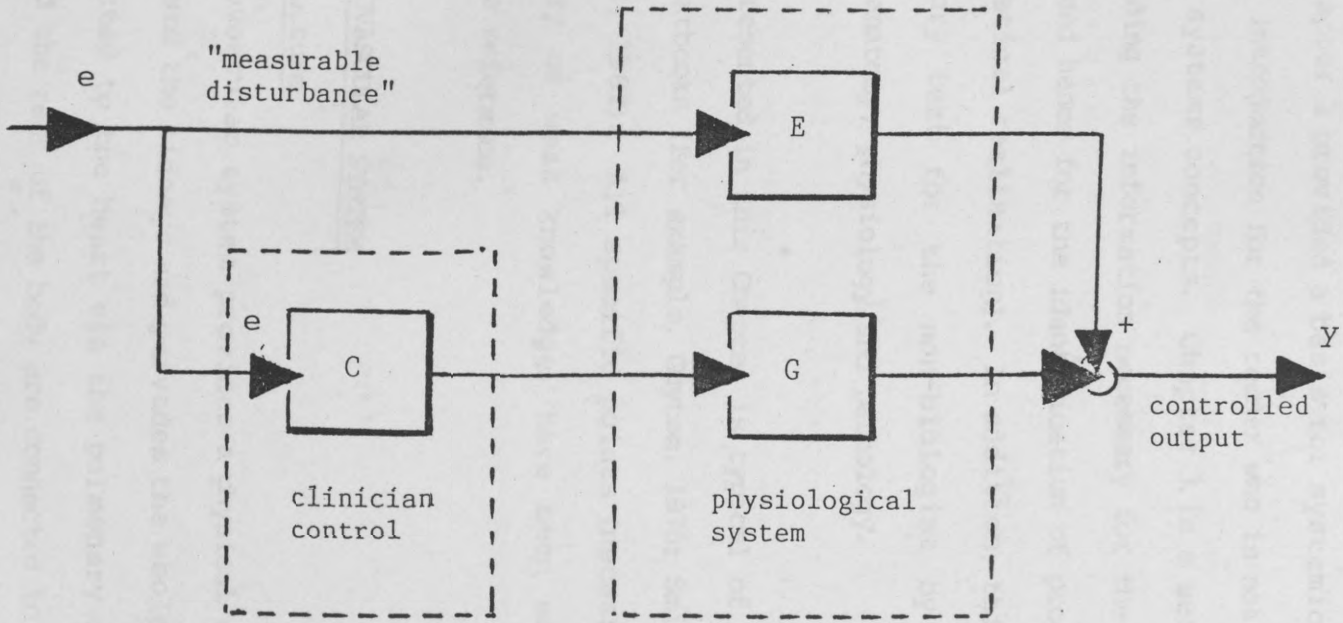

Figure 2.2 Clinical feedforward control.

CHAPTER 3

SYSTEM STRUCTURE, PROCESS AND RELATED ABNORMALITIES

3.1 INTRODUCTION

This Chapter describes the second stage in the conceptual analysis of FAB. Chapter 2 provided a basis for systemic thought and thus acts as an introduction for the reader who is not familiar with the necessary systems concepts. Chapter 3 is a sentential model of FAB, providing the information necessary for the design of a model structure and hence for the identification of processes (in advance of mathematical realisation). In addition, this Chapter acts an introductory text for the non-biologist by considering the essential anatomy, physiology and pathology.

The work presented in this Chapter is typical of many of the major medical textbooks (for example, Guyton, 1976; Smith, 1980; Gardner, 1978; Lote, 1982). All specific points (necessary for areas of controversy or weak knowledge) have been supported with an appropriate reference.

3.2 CARDIOVASCULAR SYSTEM

3.2.1 Structure

The cardiovascular system provides a physical connection between the lungs and the kidneys and pervades the whole body. The lungs are connected to the heart via the pulmonary circulation. The kidneys and the rest of the body are connected to the heart via the systemic circulation.

Each circulatory system has branches of ever decreasing size on the arterial side (away from the heart) and ever increasing sized vessels on the venous side (flowing towards the heart). The arterial and venous parts are connected via a mesh of small vessels known as the capillary bed.

The heart has four compartments, the right and left ventricles and the right and left atrium. These are separated by valves. Ventricles are positioned to receive from the atrium and supply the arteries. Atria are positioned to receive from the veins and supply the ventricles.

3.2.2 Process

The cardiovascular system transports oxygen to, and carbon dioxide from, the peripheral tissues of the body, thus maintaining short-term physiological equilibrium. In addition, nutrients are transported to, and metabolic wastes removed from, the peripheral tissues of the body, thus maintaining long-term physiological equilibrium.

Cardiac output is the most important variable in the circulatory process (Guyton, 1976). It is the volume of blood pumped by the left ventricle into the aorta and is matched over time by an equal venous return to the right atrium. Cardiac output is mainly responsible (in the shorter term) for the maintenance of an effective circulatory volume. In situations of depleted volume, arterioles can be constricted to maintain arterial filling pressure and consequently to maintain perfusion of the peripheral tissues.

Veins have thin muscular walls with relatively high compliance and volume, and can act as a sink for any temporary excess of blood, thus maintaining arterial filling pressure with relatively little effect to the venous filling pressure.

The pulsatile heart is controlled by sympathetic and parasympathetic nerves. These control cardiac pumping by either changing heart rate, or by changing the strength of contraction, or by changing both. Parasympathetic stimulation decreases heart rate and sympathetic stimulation increases heart rate. Cardiac output is regulated so that the supply of oxygen and nutrients matches the demand and ensures that the metabolic wastes do not accumulate.

The cardiovascular system has inputs into the veins from the gastrointestinal system and the microvascular system and has outputs from the capillaries into the interstitial fluid and from the arteries (via the kidneys) to the environment. The kidney exerts a variable resistance to ground.

3.2.3 Abnormalities Of Structure And Process

The majority of pathological conditions in the cardiovascular system are heart related. These cause changes in heart strength or heart effectiveness. The heart may be hypereffective if there is an inhibition of the parasympathetics to the heart which removes parasympathetic tone and increases heart rate.

Some common factors causing a hypoeffective heart are myocardial infarction (dead heart muscle caused by an occlusion), valvular heart disease (disease preventing normal valve action), inhibition of the sympathetics to the heart, congenital heart disease (existing from birth), myocarditis (inflammation of the heart muscle), cardiac anoxia (deficiency of oxygen in the heart tissues), toxicity and myocardial damage.

A non-heart related disorder is the hardening of the arteries with age or poor health, causing decreased compliance which may lead to hypertension.

3.3 GASTROINTESTINAL SYSTEM

3.3.1 Structure

The alimentary tract is open to the environment via oral inputs and anal outputs. The route between the entry and exit points consists of a strong muscular walled tube with both circular and longitudinal muscles. The route is continuous, but may be closed at certain locations where valves are present. The tube varies in diameter, expanding at the stomach reservoir and the colon. A variety of glands can be found along the passage. The walls of the tract are pervaded by a large number of blood vessels, this is especially true of the colon. Figure 3.1 shows the essential anatomy of the gastrointestinal tract.

3.3.2 Process

The primary function of the alimentary tract is to provide an entry route for water, electrolytes and nutrients. Many autoregulatory

processes ensure that substances entering the tract are mixed and are moved fast enough to supply the body's needs, whilst also moving slowly enough for digestion and absorption to take place. This is effected by the circular and longitudinal muscles.

Secretory glands play two important roles. Digestive enzymes are secreted in response to the types of substances present and mucus is secreted to maintain protection and lubrication. A variety of glands perform these functions and can be found along the entire course of the tract.

Sodium is transported actively from the gut by way of the epithelial cells, into the intercellular spaces and hence to the plasma. The resulting high local concentration of interstitial sodium leads to diffusion into the proximal blood vessels. Reduced sodium concentration in the epithelial cells augments diffusion from the gut to their interior. Potassium is transported in a similar fashion.

Chloride is transported passively. Diffusion from the upper part of the small intestine satisfies electrical gradients caused by sodium absorption. The distal ileum is capable of active chloride absorption in small quantities, this is coupled to the secretion of bicarbonate in an electroneutral exchange and, in part, causes a difference in plasma sodium and chloride concentrations.

In general, the non-specified ions obey the rule that, if monovalent they are absorbed with ease, if bivalent they are absorbed in small amounts.

Water is transported across the intestinal membrane by diffusion. The laws of osmosis are obeyed so that water passes from the plasma to the gut, instantaneously following the active and passive transport of electrolytes.

3.3.3 Abnormalities Of Structure And Process

Prevention of entry to the system may occur. This can be caused by paralysis of the swallowing mechanism brought about either by neural damage or disease, for example poliomyelitis.

Entry may be gained to the system but consequently lost during vomiting. Continual vomiting causes net body losses of electrolytes and water by the ejection of digestive fluids which would otherwise be reabsorbed.

Food transmission to the stomach may be prevented. This may be caused either by the lower last centimetres of the oesophagus failing to relax, or by the presence of a blockage.

Inflammation of the gastric mucosa reduces performance in the gastrointestinal tract. The cause may be the action of irritant foods, excoriation (removal of) stomach mucosa by peptic secretions (causing peptic ulcers) or by bacterial inflammation.

Disorders of the small intestine are relatively uncommon. They rarely have significant effects on fluid or electrolytes, usually causing problems in digestion and absorption of fats.

Constipation can reduce the output of the large intestine. This usually has little effect on the preceding processes. Diarrhoea is most commonly caused by enteritis, but may be caused by nervous tension. In the former case large quantities of fluid are made available to wash the infectious agent towards the anus. Losses from the intestine can be considered to be isotonic for all practical purposes.

3.4 MICROVASCULAR SYSTEM

3.4.1 Structure

The microvascular system is not a distinct physical entity and thus does not have a clearly defined anatomy.

The lymphatic system is a physically distinct subsystem of the microvascular system. It is a network of thin vessels that resemble veins. Lymphatic capillaries exist in almost all organs and tissues of the body, they are blind-ended and highly permeable to solutes and colloids. The lymph capillaries are ever joining, ever increasing in size, eventually draining into the venous system.

Capillaries of the systemic circulation provide the second, albeit disjointed, physical entity of the microvascular system. Capillaries proceed from the muscular arterioles, but have a much reduced diameter and a thin permeable wall. Venules lead away from the capillaries and coalesce into progressively larger veins.

The systemic circulation provides the connection from the lymphatic exit into the veins to the interstitial space. The latter provides the remaining connection from the capillaries of the systemic circulation to the capillaries of the lymphatic system.

3.4.2 Process

Water, electrolytes and to a lesser extent colloids of low molecular weight move continuously between the plasma and the interstitial fluid via the capillary bed. This movement is due to diffusion and filtration. Fluid flow from the capillaries to the interstitial space satisfies net Starling forces (a pressure gradient caused by an imbalance of hydrostatic and oncotic pressures).

Hydrostatic pressure in the systemic capillaries enters at approximately 32mmHg. This falls to about 12mmHg by the time it reaches the venules. Capillary pressure is thought to be a function of arterial pressure (which is closely regulated at the point of capillary connection) resistance of the arteriolar (which reduces pressure transmission) and the venous pressure (although some controversy over the precise contribution of venous pressure is evidenced by the variety of representations used in the models reviewed by Flood et al, 1984a).

Oncotic plasma pressure is a combination of approximately 20mmHg osmotic effects caused by protein and approximately 8mmHg caused by an imbalance of diffusive ions. This latter phenomenon is known as the Gibbs-Donnan equilibrium and is caused by a net negative electrical charge of non-diffusible colloids in the plasma.

However, small proteins (almost exclusively albumin) leak through the capillaries, but in normal health will easily enter the lymphatic system and are thus cleared from the interstitial fluid at a rate equal to the entry rate. Equally the capillary filtration rate of other analytes is matched by the lymphatic return rate in good health.

3.4.3 Abnormalities Of Structure And Process

Lymphatic obstruction can occur due to a variety of abnormalities. Filariqsis is an infection caused by nematodes of the superfamily filariqdea (which is especially common in the tropics). Blockage occurs due to inflammatory reactions and may over time totally occlude drainage from peripheral parts of the body. Surgical trauma often prevents drainage from localised areas of the body, but these effects usually disappear after several months as new lymph channels develop.

Increased capillary permeability can be caused by disease states where the integrity of the capillary endothelium is destroyed. This may be caused by burns (local) or damage to the membranes of the capillary by histamine or polypeptides in allergic reactions. Thus analyte redistribution may occur locally or throughout the whole body.

3.5 FLUID AND ELECTROLYTES

3.5.1 Structure

The distribution of these analytes can be considered as occuring within five spaces, the intracellular space, the interstitial space, the plasma space, the gastrointestinal space and the renal space.

3.5.2 Process

Expansion or contraction of the extracellular fluid may occur and is recognisable by changes in the arterial pressure (of the plasma space) and/or oedema (in the interstitial space). Intracellular fluid has narrower limits to which it can expand as individual cells are limited to relatively small increases in volume before their integrity is lost.

Distribution of body water can be explained by the presence of substances which have a significant impact on either the electrochemical or osmotic activity within the five above mentioned spaces. In the steady-state, overall electrolyte concentrations in the extracellular space and intracellular space are equal, however, individual electrolyte concentrations vary between compartments as a result of the Gibbs-Donnan effect and/or active electrolyte pumps. Changes in osmolality causing an osmotic gradient are an important means of water movement between compartments since osmotic gradients are not tolerated across semi-permeable membranes.

Expected osmotic contributions of electrolytes are affected by intermolecular attraction/repulsion, which respectively decreases or increases osmotic activity. Attraction generally overrides repulsion leaving approximately 93 per cent of the expected osmotic activity.

The major intracellular ion is potassium and the major extracellular ion is sodium. The sodium pump ensures that potassium is held almost entirely in the intracellular space and sodium in the extracellular space. It is assumed that a further potassium pump exists which maintains a higher potassium intracellular concentration than sodium extracellular concentration (Lote, 1982). A magnesium/calcium pump is also thought to exist (Lote, 1982). The electrochemical gradient set up by the active pumping of cations is offset by passive anion diffusion.

The electrolytes (and urea) that contribute significantly to water distribution are considered below. The reference concentrations in plasma are those of The Staff of the Division of Pathology Royal Free Hospital Group (1979).

Sodium (reference range for plasma 136-148 mmol l^{-1}): Sodium is an essential electrolyte. Intake occurs via food, drinks and added salt with food. Intake is thus variable depending on diet and taste but is mainly due to added salts. The optimum intake is about 75 mmol day^{-1} with a minimum requirement of 20 mmol day^{-1}.

About 50 per cent of total body sodium exists in the extracellular compartment. The skeleton holds about 40 per cent of that and has only a small exchange with other body fluids as most sodium is absorbed on to hydroxyapatite crystals producing a non-exchangeable pool.

Sodium intake has a significant variance and therefore absorption and losses require close regulation. A gut hormone may be involved in increasing intestinal absorption when sodium levels are depeleted. Renal sodium regulation is well recognised and consists of autoregulation of GFR, aldosterone control over sodium reabsorption (the exact dynamics are controversial) and the 'Third Factor' (which relates to the amount of diuresis not explained by the other factors, possibly brought about by the natriuretic hormone). Urine excretion of sodium is also affected by proton and potassium secretion (ionic swapping) and transmembrane dynamics are affected by acidity.

Potassium (reference range for plasma 3.8-5.0 mmol l^{-1}): Potassium is an essential electrolyte. Intake varies widely with dietary food and fluid habits. The optimal intake is about 75 mmol day^{-1} with a minimum requirement of 40 mmol day^{-1}.

Plasma potassium concentration requires precise regulation since it determines membrane polarisation. Renal potassium control is effected by autoregulation of GFR and aldosterone (the exact dynamics are controversial). Potassium does not hold high priority in renal regulation (although high ECF concentration will cause

significant changes in aldosterone secretion) probably because cell pumps control the bulk of body potassium.

Acidity alters the sodium-potassium swap in the kidney and affects transmembrane dynamics. Insulin release due to a rise in plasma glucose concentration results in uptake of glucose and potassium into the cells.

Chloride (reference range for plasma 95-105 mmol l^{-1}): Chloride is an essential ion. Its dynamics are closely related to those of sodium so that regulation is passive against active sodium control and therefore is indirectly related to aldosterone (although Lote, 1982, has pointed out that there is some evidence supporting the idea of active renal chloride control). In addition, chloride excretion varies in the renal tubule in relation to the regeneration of bicarbonate and is also excreted alongside ammonium ions as part of the exchange for sodium during proton elimination.

Magnesium (reference range for plasma 0.7-1.0 mmol l^{-1}): Magnesium is an essential electrolyte. Intake is gained mainly from green vegetables. The optimum rate is about 12 mmol day^{-1} with a minimum requirement of about 3 mmol day^{-1}.

Approximately half the body magnesium is in bone, the rest is mostly intracellular in bound form, although a small plasma presence also exists, partly in bound form.

Magnesium is specifically associated with the function of a number of intracellular structures and organelles. Magnesium also

activates enzyme systems and affects neuromuscular activity. In large doses it acts as a vasodilator, lowering blood pressure.

Magnesium is regulated by hormones, mainly PTH, which can reduce urinary excretion and increase gastrointestinal absorption. Magnesium is actively taken into cells by a pump which possibly regulates the magnesium and calcium ratio. It is also taken into the cells (albeit in very small amounts) under the influence of insulin promoted glucose entry.

Proximal tubular reabsorption of magnesium and calcium is closely related to sodium regulation, although during magnesium deficiency magnesium retention will rise whilst sodium retention is unaffected. Active magnesium reabsorption occurs in the distal tubule and collecting duct against an electrochemical gradient.

Calcium (reference range for plasma 2.1-2.6 mmol l^{-1}): Calcium is an essential electrolyte. It has many dietary sources, being particularly abundant in milk, egg and cheese. Intake varies widely around a mean of 20 mmol day^{-1} but apparently has little effect on renal losses.

Small amounts of calcium are found in the plasma, where about half is bound to albumin. An enormous reservoir exists in the bone which can readily compensate for plasma deficiences. Calcium has a number of roles ensuring calcification of bones and teeth, cellular metabolic regulation and blood clotting.

Absorption is usually passive in the duodenum against an electrochemical gradient. Absorption therefore depends on body requirement as well as supply rate. Factors controlling calcium dynamics are 1,25 dihydroxycholecalciferol (Vitamin D) stimulation of gut absorption, PTH enhancement of renal tubule reabsorption and calcitron control over the rate of skeletal reabsorption.

Phosphate (reference range for plasma 0.7-1.25 mmol l^{-1}): Phosphate is an essential electrolyte. Dietary sources are wide in variety. Minimum daily requirement is about 25 mmol with an optimum daily intake around a mean of 40 mmol, although high variance is common. Absorption by the gastrointestinal system is around a constant value of 75 per cent of the dietary intake.

Phosphate is mainly found in the bone, but is also present in the extracellular space and to a lesser extent intracellularly. Phosphate plays a variety of roles, occuring intracellularly as adenosine triphosphate (ATP) the final common energy providing compound for many reactions (including cell pumps) and in its acidic form or basic salt ($H_2PO_4^-$ and HPO_4^{2-} respectively) these phosphate compounds form buffer systems in the urine and the cells. Phosphate shares the same controllers as calcium.

Bicarbonate (reference value for plasma 24-32 mmol l^{-1}): Bicarbonate is an essential electrolyte. The main aspects of interest are related to HCO_3^- metabolism which is discussed in section 3.7.

Urea (reference value in plasma 3.0-6.5 mmol l^{-1}): Urea is a waste product of protein metabolism. It has been incorporated within the discussion on electrolytes for completeness. Urea diffuses evenly throughout the body and has to be continually removed to enable protein metabolism to proceed. As kidney urea excretion is dependent only on GFR it is an excellent test of renal function.

3.5.3 Abnormalities Of Structure And Process

All conditions of fluid and electrolytes under this heading arise from abnormal conditions of other subsystems, whereby abnormal concentrations and distributions occur.

3.6 KIDNEY

The kidney plays a vital role in the maintenance of FAB, controlling both fluid-electrolyte and acid-base factors in an integrated fashion. This intimate relationship explains why a disturbance in one aspect is frequently reflected by an imbalance in other aspects. As a consequence of these complexities it was found necessary to make a detailed account of the renal system. The work of Smith (1980), Lote (1982) and Gardner (1978) form the basis of the following discussion.

3.6.1. Structure

There are two kidneys and each kidney shows two distinct regions, a dark outer region (cortex) and a paler inner region (medulla). The latter is also divided into a number of conical areas (renal pyramids) the apex of which extends towards the renal pelvis

forming a papilla. The renal pelvis is the expanded upper part of the ureter, see Figure 3.2b.

The basic functional unit of the kidney is the nephron, see Figure 3.2c. The number of nephrons per kidney is quoted in millions, varying between authors with a range of 1-2.5 million (more recent works tends towards the lower value). A nephron is a blind-ended tubule, the blind end forms a capsule (Bowmans capsule) surrounded by a knot of blood capillaries. There are two populations of nephrons in the human kidney, one whose loops of Henle penetrate deep into the medulla, with glomeruli in the inner third of the cortex (juxtamedullary nephron), and one with short loops of Henle extending only a short distance into the medulla and having glomeruli in the outer two thirds of the cortex (cortical nephron).

The proximal tubule follows on from the Bowmans capsule, it is initially convoluted but becomes straight and leads into the loops of Henle. The cells of the convoluted section have a brush border of millions of microvilli which substantially increase the surface area available, the cells also have a relatively dense population of mitochondria. In contrast, the cells of the straight part of the proximal tubule have a less dense brush border and contain a less dense population of mitochondria. The cells along the descending limb of the loop of Henle extend few microvilli as do the cells of the thin ascending limb, whereas, the thick ascending limb is without a brush border.

In the region where the ascending limb enters the cortex it is closely associated with the glomerulus and afferent arterioles and

consists of maculla densa cells, termed the distal tubule. These tubules collect in groupings of about six and are served to the collecting duct, pouring successively into the duct of Bellini, draining the renal calyx and hence serving the ureter and bladder.

On the concave medial surface of each kidney is the hilius, a slit through which the renal artery and vein, the lymphatics, the renal nerve and renal pelvis pass. The structure relating to renal blood supply is shown in Figure 3.2a. The renal artery branches to form several interlobar arteries, giving rise to arcuate arteries which pass along the boundary between the cortex and the medulla. From the arcuate arteries branches travel out at right angles through the cortex towards the capsule. These are the interlobular arteries and are connected to the glomerular capillaries via the afferent arterioles.

The glomerular capillaries are intimately related to a second arteriole (rather than a venule) the efferent arterioles. These portal blood vessels carry blood away from a capillary network directly to a second capillary network. Efferent arterioles from nephrons in the outer two thirds of the cortex branch to form a dense network of peritubular capillaries which surround the cortical tubular elements. The efferent arterioles in the inner one third of the cortex give rise to some peritubular capillaries, but also give rise to capillaries which have a hairpin structure, passing into and out of the medulla, where they are adjacent to the loops of Henle and collecting tubules. The medullary and peritubular capillaries ultimately connect with the renal vein.

3.6.2 Process

Ultrafiltration occurs from the glomerulus into the Bowmans capsule, with molecular size being the main determinant whether a substance enters the filtrate or not (molecular shape and charges are less influential). The rate of filtration is governed by Starling forces (see under microvascular process) and the permeability of the capillaries. Little change in GFR occurs within the range of 90-190 mmHg of renal arterial pressure due to autoregulation. There is some controversy over the precise autoregulatory process, with Lote (1982) suggesting that the most widely accepted explanation is the myogenic theory, that is, an increase in wall tension of the afferent arterioles due to increased perfusion pressure causes automatic contraction of the smooth muscle fibres in the vessel wall, increasing resistance to flow and causing constant flow.

In the proximal tubule, a constant amount of the ultrafiltrate is reabsorbed (often quoted as being about 80 per cent). Sodium is reabsorbed by an active process (hence the presence of many mitochondria in the local cells and an extensive brush border which increases the surface area available for reabsorption) where efflux from the lumen occurs mainly through the cells passively down an electrical gradient (of about -70mv) and actively out of the cell (see Figure 3.3), however, there is a high back flux through intercellular channels. This is also thought to be the reabsorption process for potassium, magnesium and calcium (Lote, 1982). As chloride has to pass a 70 mv opposing gradient, it seems

reasonable to postulate that there is a co-transport mechanism allowing passive entry and extrusion alongside sodium (and possibly other cations).

Micropuncture studies point to the proximal tubule as the place where phosphate reabsorption occurs. This appears to happen only in the presence of sodium and thus probably has some co-transport attachment to sodium. Urinary phosphate excretion under normal conditions is less than 20 per cent of that in the ultrafiltrate, however, excretion shows a sharp equivalent incremental rise (with respect to filtration) over a given phosphate concentration. This implies nephron homogenity with respect to phosphate. (Note: renal phosphate dynamics are discussed in further detail in section 3.7 on acid-base dynamics).

Approximately 90 per cent of filtered bicarbonate is reabsorbed in the proximal tubule. This reabsorption occurs as a result of active proton secretion. Bicarbonate reabsorption behaves as if it were T_m-limited (Tubular maximum, that is, the maximum tubular reabsorptive capacity for a given solute) where the T_m can be shifted by the rate of proton excretion. (Note: renal bicarbonate dynamics are discussed in further detail in section 3.7 on acid-base dynamics).

Urea is excreted at a fairly constant 40-50 per cent of that filtered. As sodium chloride and associated analytes leave the ultrafiltrate, urea concentration rises and so urea is reabsorbed passively down its concentration gradient.

Most of the filtered glucose is reabsorbed in the proximal tubule so that in good health a negligible amount is excreted. Glucose possibly follows sodium passively, however, an apparent T_m-limited reabsorption curve appears at times to be splayed, which implies nephron heterogenity with respect to glucose. (Note: glucose dynamics are discussed in further detail in section 3.11).

Water dynamics are determined by osmotic forces in the proximal tubule, consequently the remaining filtrate is isotonic up to the loops of Henle and the isotonic reabsorbed mixture passes (after cellular extrusion) into the efferent capillaries according to Starling forces (where efferent capillaries have a high concentration of non-filterable proteins and thus exert high oncotic pressure which promotes capillary acceptance).

The loops of Henle are complex systems which enable urine osmolality in the final stages of the nephron to become high. Paradoxically, this occurs in such a way that the filtrate leaving the loops of Henle is actually in a dilute form.

The functional aspects of this system are not initially obvious, however, the following simple description should make clear the dynamics of the 'counter-current multiplier', refer to Figure 3.3. Consider only the major ions, sodium and chloride alongside water. Probably chloride (but possibly sodium) is actively extruded from the thick wall of the ascending limb of the loop of Henle, the alternative of the two ions follows passively. The walls of the thick ascending limb are impermeable to water, consequently the

osmolality of the interstitium and hence the remaining part of the loop of Henle have a raised osmolality. The higher osmolalities occur the further the loop of Henle penetrates the medulla as a result of flow, that is, new isotonic filtrate enters the descending limb and more concentrated filtrate rises into the thick ascending limb whereupon further ion extrusion continues and the remainder of the nephron again experiences a raised osmolality. The system's approximate steady-state osmolalties are displayed in Figure 3.3. The counter-current multiplier is seen to be effective in the remaining distal nephron, which again passes through the hyperosmolar interstitium and on to the collecting tubules thus ensuring a concentrated urine. Blood also follows this route via capillaries of similar architecture so that ultimately a net (but controllable, see below) water flow occurs from the nephron to the plasma.

This latter process is significantly affected by the circulating concentration of ADH, so that water conservation can occur via increased permeability of the targeted epithelium in response to ADH levels. Further reabsorption of ions also occurs in the distal nephron. A raised aldosterone concentration increases sodium and chloride reabsorption and thus alters the sodium-proton exchange and the proton-potassium competition for secretion into the urine (Note: hormone dynamics are discussed in further detail in section 3.8).

3.6.3 Abnormalities Of Structure And Process

Renal diseases may affect primarily the functions of either the glomerulus or the renal tubules. In the latter stages of chronic

renal damage (for instance in glomerulonephritis, an advancing cortical disease) the functional mass of the kidney is reduced and there is a progression in renal insufficiency called uraemia. An increase in blood urea concentration is evidence of renal failure.

Structural damage to the medulla of the kidney involving the long loops of Henle (which generate concentration gradients) may lead to water depletion. For instance, during atrophic pyelonephritis and obstructuve uropathy selective loss of these nephrons causes selective loss of concentrating ability without major disturbances of overall glomerular function.

Nephrotic syndrome is where the glomerular filtration barrier becomes permeable to plasma proteins, this reduced protein resistance to ground causes proteinuria. Albumin is the smallest plasma protein and is therefore filtered most readily in nephrotic syndrome.

Metabolic acidosis of all types of renal disease is of tubular rather than glomerular origin, being the reduction in the ability of the tubules to absorb bicarbonate ions and excrete hydrogen ions. Metabolic alkalosis is also of tubular origin and relates to renal impairment where excess bicarbonate can not be excreted.

Renal non-response to ADH due to a functional abnormality of the tubule (typically a spontaneous problem of an immature males kidney or side effects of some drugs) leads to a massive diuresis and is known as nephrogenic diabetes insipidus.

An adrenal tumour may cause primary or secondary aldosteronism. As aldosterone stimulates the active ion pump that exchanges protons (and potassium ions) for sodium and chloride ions, then the hypersecretion of aldosterone is liable to cause metabolic alkalosis and hypokalaemia.

3.7 ACID-BASE DYNAMICS

3.7.1 Structure

The distribution of protons and buffers can be considered as occuring within four spaces; the intracellular space, the interstitial space, the plasma space and the renal space.

3.7.2 Process

The theory related to acids and bases which is necessary for the understanding of the acid-base processes is contained in Appendix 1. The principal buffer systems of the body fluids are shown in Table 3.1, which is a consolidation of two tables from Gardner (1978). Each system is discussed below.

The bicarbonate/carbon dioxide system is of major importance. The acid component (that is carbon dioxide) is physically regulated by the respiratory system (see under section 3.10). The conjugate base (that is bicarbonate) is regulated by the kidney (see under section 3.6) although this is not as rapid as respiratory control. The renal regulatory dynamics of bicarbonate are shown in Figure

Buffer System	Body Fluids Regulated	Percent Contribution
CO_2/HCO_3^-	Blood, ECF	64
HHb/Hb^- and $HHbO_2/HbO_2^-$	Blood	29
H. Protein/ Protein$^-$	Blood, ECF, ICF	6
$H_2PO_4^-/HPO_4^{2-}$	Blood, ECF, ICF, Urine	1
P$^-$ organic/ P organic	ICF	-
NH_4^+/NH_3	Urine	-

Table 3.1 Principal buffer systems in body fluids (source, Gardner, 1978)

3.4. This system is a better buffer against the normal acidic end-products of metabolism than against alkalinization, as the addition of acids pushes this system towards its pK value.

Haemoglobin is the second principal buffer of the blood. As buffers are only physiologically useful in the range pH = pK $\pm$ 1 many of the acid-base dissociations/associations of the protein side chains are unimportant, however, the imidazole side chain of histidine with a pK of around 6-7 is well suited to buffering. Haemoglobin has a very high histidine content of 36 residues per molecule and is thus an important buffer.

Plasma proteins, especially the abundant albumin, make some contribution to blood buffering in accordance with their dissociating/associating side-chains. Intracellular proteins are likely to be important buffers.

Phosphate is present as phosphoric acid which is tribasic (that is it has three pK values). At physiological pH values most phosphate is in the form $H_2PO_4^-$ or HPO_4^{2-}, thus:

$$H_2PO_4^- \rightleftharpoons H^+ + HPO_4^{2-}$$

which has a pK of 6.8. As phosphate concentration in plasma is low it is a relatively unimportant plasma buffer, however, as phosphate concentration rises substantially in urine during the renal concentration processes its nephrotic buffering role is important. See Figure 3.5 for further details of the buffering role of phosphate in urine.

The second urinary buffer of major importance is the ammonium ion. Some measure of control over ammonia excretion is given by physio-chemical considerations. The more acidic the tubular luminal fluid is the steeper the NH_3 concentration gradient between the cell and the tubular lumen and hence the faster NH_3 diffuses out of the cell into the urine to form NH_4^+. As intracellular NH_3 concentration falls, deamination of glutamine is promoted, synthesising out further NH_3 and thus replenishing the ammonia supply (Curthoys et al, 1973). See Figure 3.6.

3.7.3. Abnormalities Of Structure And Process

All conditions of acid and base under this heading arise from abnormal conditions of other subsystems whereby abnormal concentrations and distributions occur.

3.8 HORMONAL SYSTEMS

Two main hormone systems are present in the fluid-electrolyte balance; the antidiuretic hormone (ADH) and the renin-angiotensin-aldosterone (RAA) system.

3.8.1 Structure

The distribution of these two hormones can be considered as occuring within the plasma space only. ADH storage occurs at the posterior pituitary gland (which is directly open to the blood circulation) and is connected to the hypothalamus (the point of synthesis) by the nerve fibres of the hypothalamus-hypophyseal nerve tract. There appears to be no significant aldosterone storage and the point of synthesis is therefore directly open to the blood circulation. Renin is also synthesised in the juxtaglomerular apparatus and appears to be stored there.

3.8.2 Process

The stimuli which give rise to the release of these hormones and the way the stimuli integrate within the control units is a matter of some controversy. This is evidenced by the variety of stimuli used in the models reviewed in the proceeding Chapter (see also Flood et al, 1984a).

There is strong evidence to support the idea that osmoreceptors in the vicinity of the supraoptic area of the hypothalamus regulate the release of ADH according to alterations of the plasma osmolality (Verney, 1948; Dunn , 1973). A rise in ECF osmolality promotes ADH release. Some evidence also suggests that arterial pressure may play a role in ADH release. A fall in arterial pressure promotes ADH release.

Once in the circulation, ADH freely enters the kidney filtration process and thus has unrestricted access to the target receptors on the peritubular side of the collecting tubule cell. A complex biochemical process is then activated which gives rise to increased water permeability of the tubule and consequently fluid loss in urine can be reduced.

Renin release is thought to be as a result of decreased body sodium content. This is probably detected by changes in the pressure of the renal afferent-arterioles caused by a diminished effective circulating volume when sodium content is low. Renin, which is released from the juxtaglomerular apparatus, enters the systemic circulation where it acts on a plasma protein producing angiotensin I which rapidly converts to angiotensin II. Angiotensin II is a potent vasoconstrictor and also acts on the zona glomerular of the adrenal gland to promote synthesis and release of aldosterone (Beketov and Korneliuk, 1981). There are also thought to be other stimuli which lead to the syntehsis and release of aldosterone, for instance, high plasma potassium concentration, maculla densa detection of reduced distal tubular sodium (very controversial) and possibly a fall in arterial pressure or ECF.

It has been shown that aldosterone is necessary for normal sodium reabsorption to occur although it is not always sufficient. Normally, however, circulating aldosterone freely enters the renal filtration process whereupon sodium reabsorption from the distal convoluted tubule is stimulated. This is loosely coupled to proton and potassium secretion. An escape mechanism also appears to be available so that in cases of abnormal aldosterone level, sodium excretion returns to normal (Marver and Kokko, 1983).

3.8.3 Abnormalities Of Structure And Process

All conditions of ADH and aldosterone under this heading arise from abnormal conditions of other subsystems whereby abnormal concentrations arise.

3.9 PROTEIN DYNAMICS

3.9.1 Structure

The distribution of proteins can normally be considered as occuring within three spaces, namely the intracellular, the interstitial and the plasma spaces. In renal disorder proteins may also enter the renal space. The liver is the site of protein synthesis and degradation.

3.9.2 Process

There are three major types of protein present in the plasma; albumin, globulins and fibrinogen. The principal function of albumin is to provide colloid osmotic pressure which prevents plasma loss via the capillaries. Globulins and fibrinogens play vital roles in the immune response and blood coagulation respectively.

The rate of synthesis of plasma proteins by the liver is dependent on the concentration of amino acids in the blood. If excess proteins are available in the plasma, but insufficient are present in the cells, then plasma proteins are used to form tissue proteins. (This is a simplistic view but is sufficient for the purposes of the current research programme).

In addition, about 400 g of body protein are synthesised and degraded every day as part of the continual flux of the amino-acids, which illustrates the general principle of reversible exchange of amino acids among the different proteins of the body. Thus, the plasma proteins, the amino acids of the blood and the tissue proteins are in a continual shared dynamic equilibrium.

The liver has four important functions in protein metabolism:

1. deamination of amino acids;
2. formation of urea for removal of ammonia from the body fluids;
3. formation of plasma proteins;
4. interconversions among the different amino acids and other compounds important to the metabolic processes of the body.

Protein metabolism is regulated by hormones. The growth hormone is significant in paediatric cases although the precise mechanism is unknown. Of greater importance to the current work is the presence of insulin, as a lack of insulin reduces protein synthesis to almost zero.

3.9.3 Abnormalities Of Structure And Process

Any abnormality of the liver can give rise to impaired protein metabolism, for example, in the disease states of hepatitis, cirrhosis and acute yellow atrophy. All other conditions of proteins under this heading arise from abnormal conditions of other subsystems whereby abnormal concentrations and distributions occur.

3.10 RESPIRATORY SYSTEM

3.10.1 Structure

Carbon dioxide diffuses throughout the whole body. The respiratory activating unit is the lungs from where carbon dioxide can be 'blown off' to the environment. The lungs are directly open to the environment via the nose and mouth and bronchial air passages. The respiratory units comprise of a respiratory bronchiole, alveolar ducts, atria and alveolar sacs (of which there are an estimated 300 million). Alveolar walls are extremely thin and within them is a dense network of interconnecting capillaries. The respiratory membrane is on average 0.5 of a micron thick and has an overall surface area of about 70 m^2.

3.10.2 Process

The reflex regulation of respiration originates in the stretch receptors of the lung and transmits neural messages via vagus nerves. Separate reflexes for inspiration and expiration are recognised. It is thought that chemoreceptors control the absolute degree of ventilation.

Carbon dioxide is transported in the blood as dissolved carbon dioxide and carbonic acid, which dissociates to protons and bicarbonate in plasma and erythrocytes.

Under normal conditions the metabolic production of carbon dioxide will be equal to its ventilation rate. This homeostasis is aided by a large body pool of carbon dioxide which acts as a non physio-chemical 'buffer' against changes in the acidic free gaseous carbon dioxide (for any given change a large pool will determine a lower change in concentration than a small pool).

The excretion of carbon dioxide is carried out by the perfusion of blood supply delivering carbon dioxide to the alveolar epithelium, this diffuses over the semi-permeable membrane of the alveolar and is removed by ventilation. This is regulated to a large extent by the respiratory centre located in the medulla oblongata.

Ventilation affects oxygen as well as carbon dioxide, thus, identifying the relative importance of the two gases as stimulants to ventilation is crucial. Haldane and Priestley (reported by Gardner, 1978) showed that carbon dioxide regulation is more important than oxygen regulation. Measured PCO_2 and PO_2 of their own alveolar varied enormously and negligibly respectively to the three cases:

1. on top of Ben Nevis;
2. at the bottom of a mine in Cornwall;
3. in a hyperbaric pressure chamber at Oxford.

Gray (1945), in the now famous 'Grays multiple factor theory', mathematically predicted the response of ventilation to PCO_2, PO_2 and blood pH in an additive fashion. However, since then Cunningham et al (1963) have shown that a decrease in PO_2 multiplies the response of alveolar ventilation to changes in carbon dioxide concentration. The precise response of the respiratory centre to these three stimuli is still somewhat controversial today.

3.10.3 Abnormalities Of Structure And Process

Abnormalities of the lungs will often be reflected by abnormal carbon dioxide excretion and consequently a low or a high PCO_2. Respiratory acidosis can be caused by defective ventilation (caused by depression of the respiratory centre in head injury or viral infections) defective diffusion (controversial as carbon dioxide diffuses twenty times faster than oxygen, thus oxygen related problems should appear as paramount) and defective perfusion (caused by pulmonary infarction, tumours or general destruction of lung tissue producing inadequate or non-uniform perfusion of pulmonary capillaries). Respiratory alkalosis can be caused by hyper-ventilation in disease states or by passive over-ventilation by incorrectly adjusted artificial ventilation.

3.11 GLUCOSE DYNAMICS

(Reference range for plasma 2.9 - 4.8 mmol l^{-1}).

3.11.1 Structure

The distribution of glucose can be considered as occuring within four spaces; the intracellular space, the interstitial space, the plasma space and the renal space.

3.11.2 Process

Blood glucose concentration is controlled strictly within very narrow bounds because glucose is the only nutrient that can be used by the brain, retina and germinal epithelium in sufficient quantities to supply them with their required energy. Important features of blood glucose regulation include the effect of increased insulin secretion on returning an elevated blood glucose level back toward normal (by promoting movement into the cells, accompanied by potassium ions and to a much lesser extent magnesium ions) and the effect of increased glucagon secretion which helps return a depressed glucose concentration back to normal. A further important regulatory feature relates to the liver, where the hepatic cells readily take up or release glucose in the form of glycogen (easily converted back to glucose) in response to increased/decreased plasma glucose concentration respectively.

3.11.3 Abnormalities Of Structure And Process

All conditions of glucose under this heading arise from abnormal conditions of other subsystems whereby abnormal concentrations and distributions occur.

3.12 CONCLUSION

Chapter 3 has drawn together the essential knowledge relating to FAB and identifies areas of weak knowledge and also points to areas of controversy. However, translating this information into a model design involving both structure and process requires a method which is capable of converting the less strictly structured information in the sentential model of Chapter 3 into a further conceptual model of more clearly defined structure. This is the task set for Chapter 4.

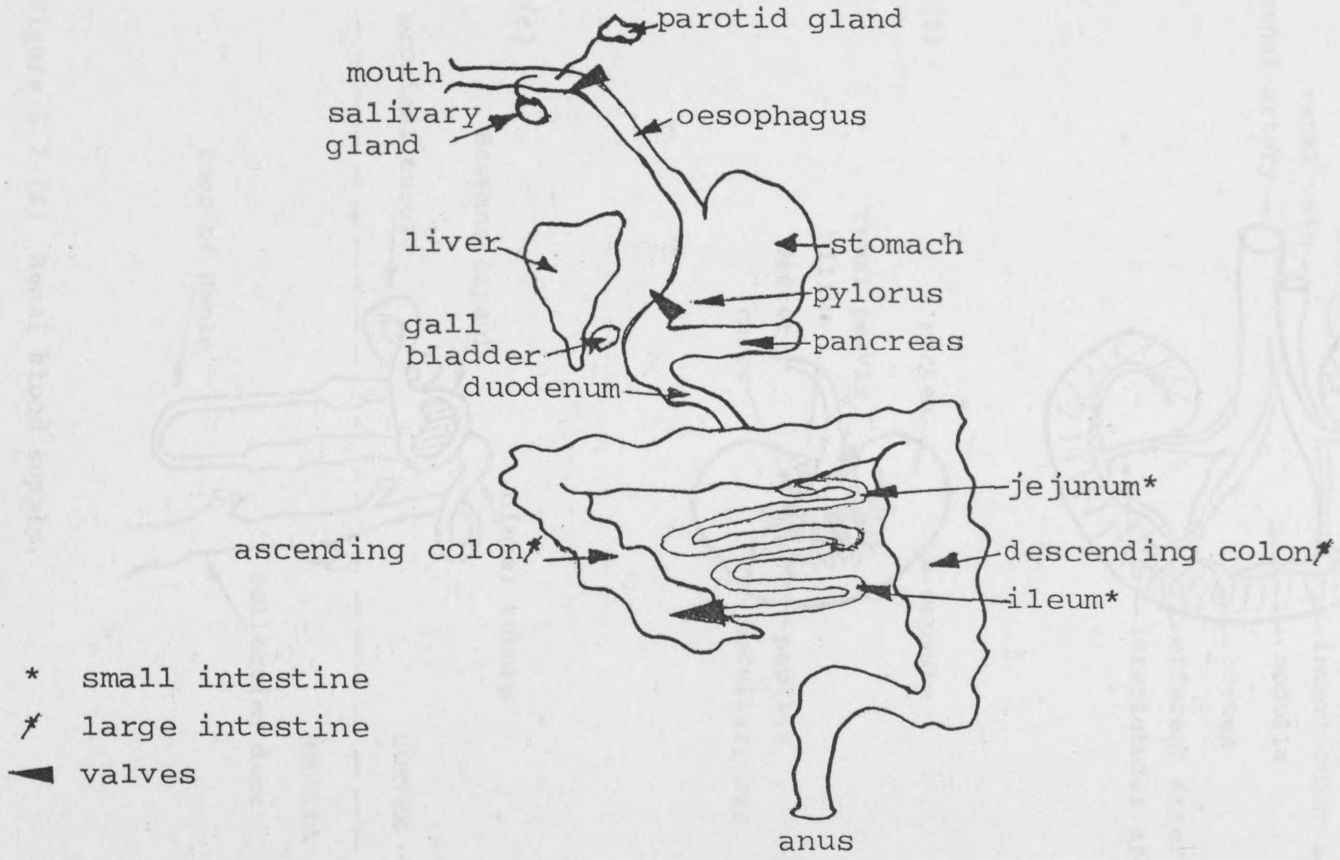

Figure 3.1 Anatomy of the gastrointestinal tract.

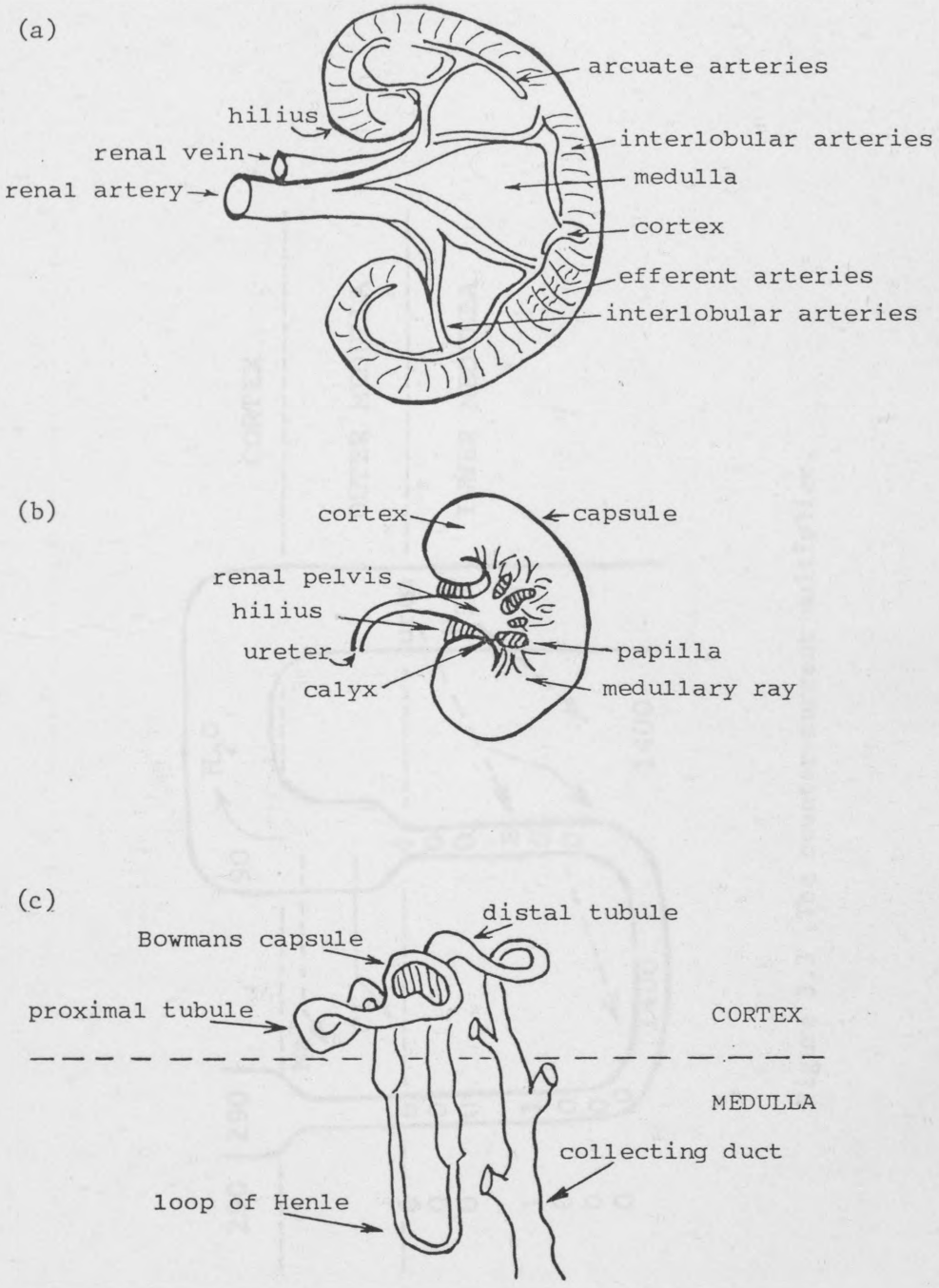

Figure 3.2 (a) Renal blood supply.

(b) Renal structure.

(c) Nephron structure.

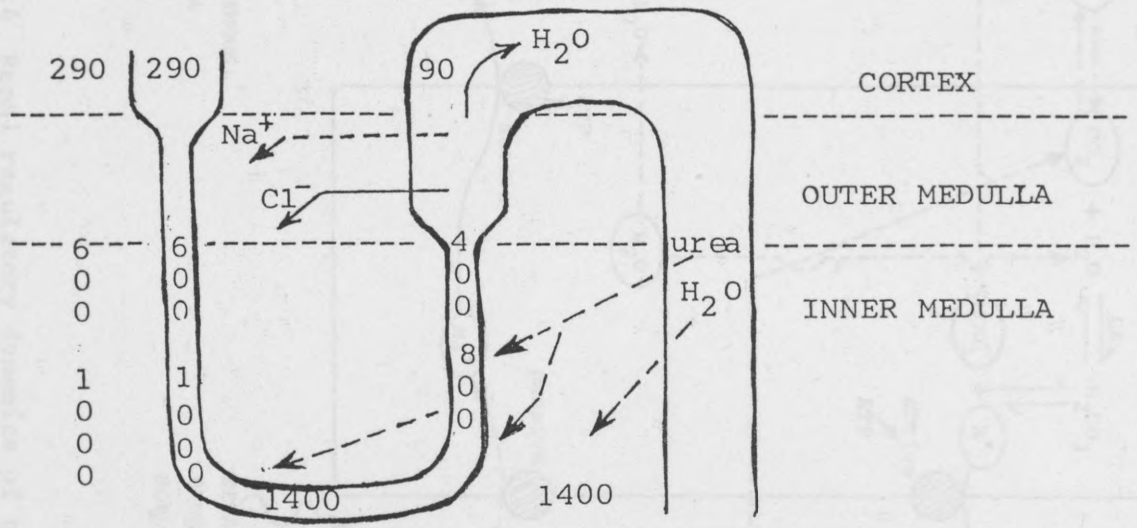

Figure 3.3 The counter-current multiplier.

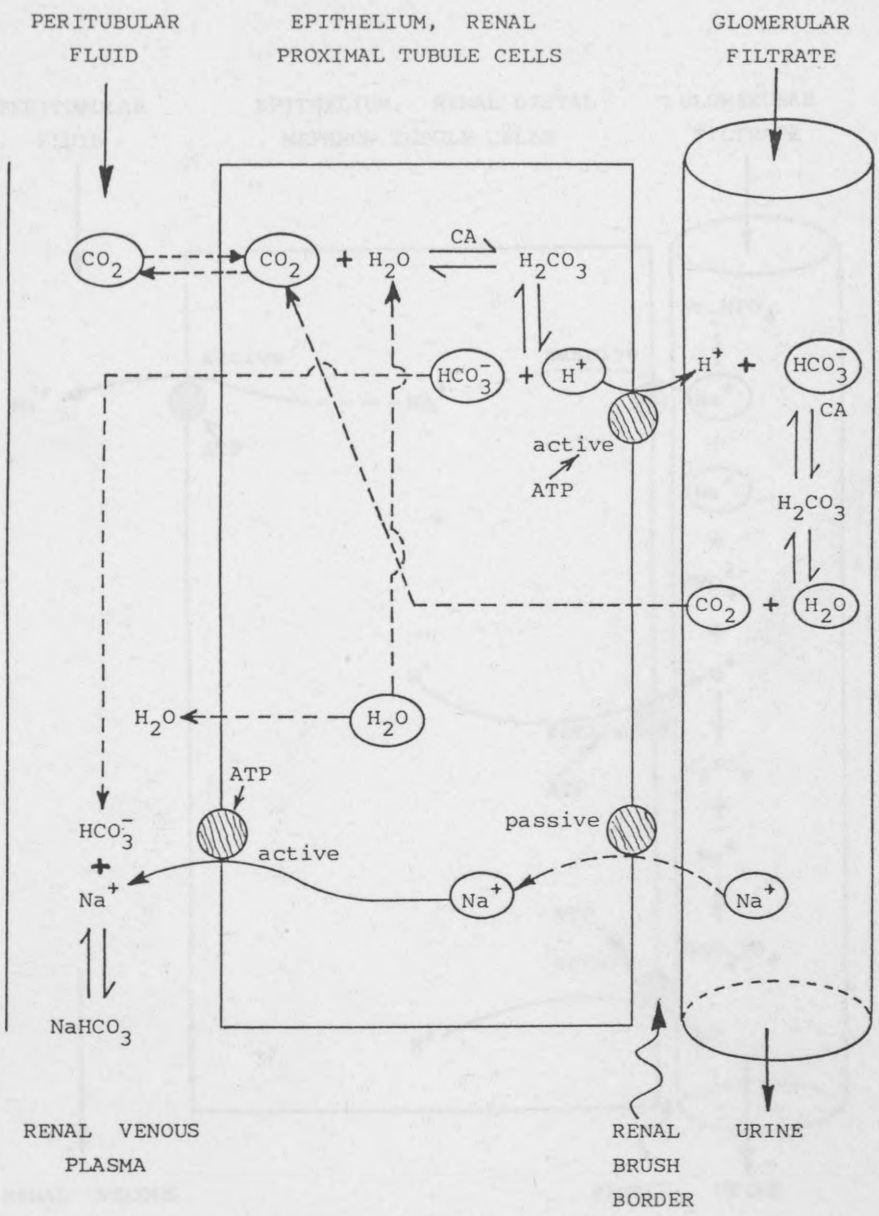

Figure 3.4 Renal regulatory dynamics of bicarbonate.

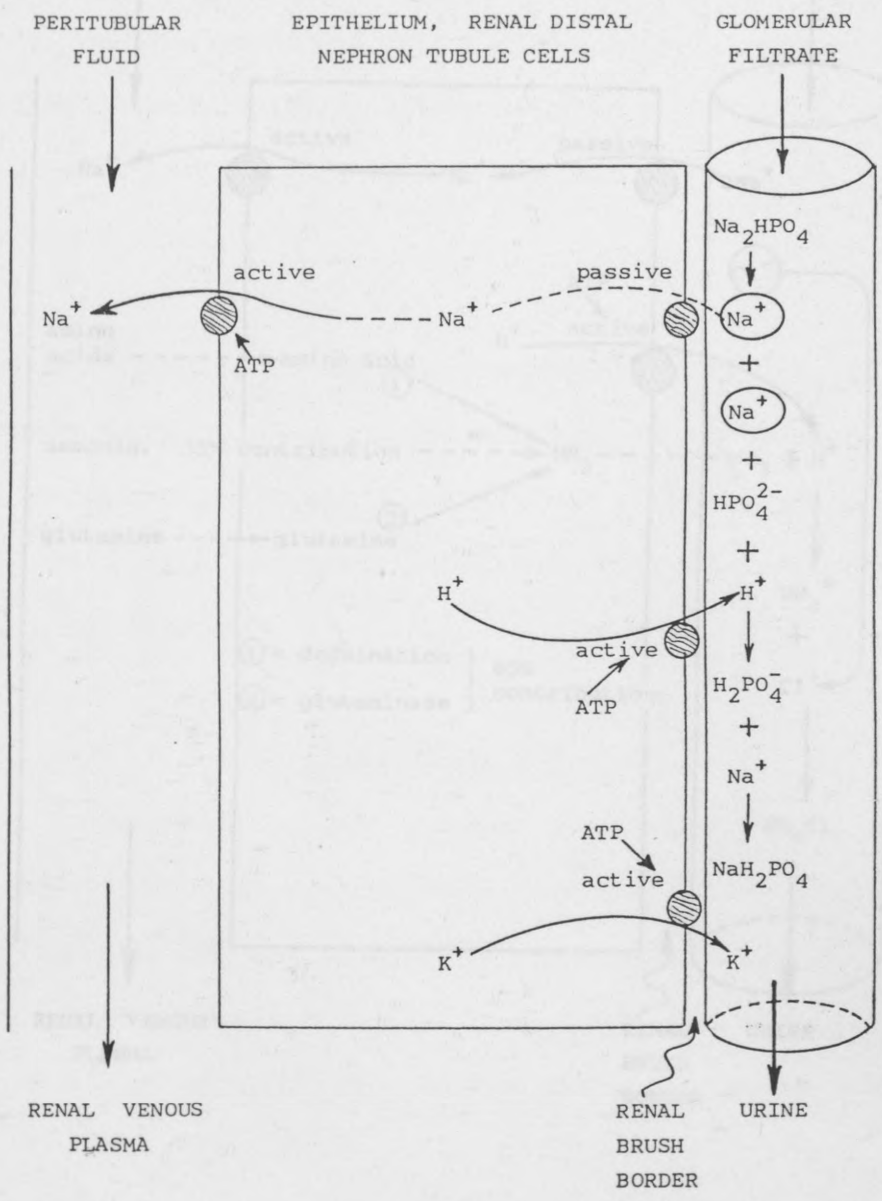

Figure 3.5 Buffering role of phosphate in urine.

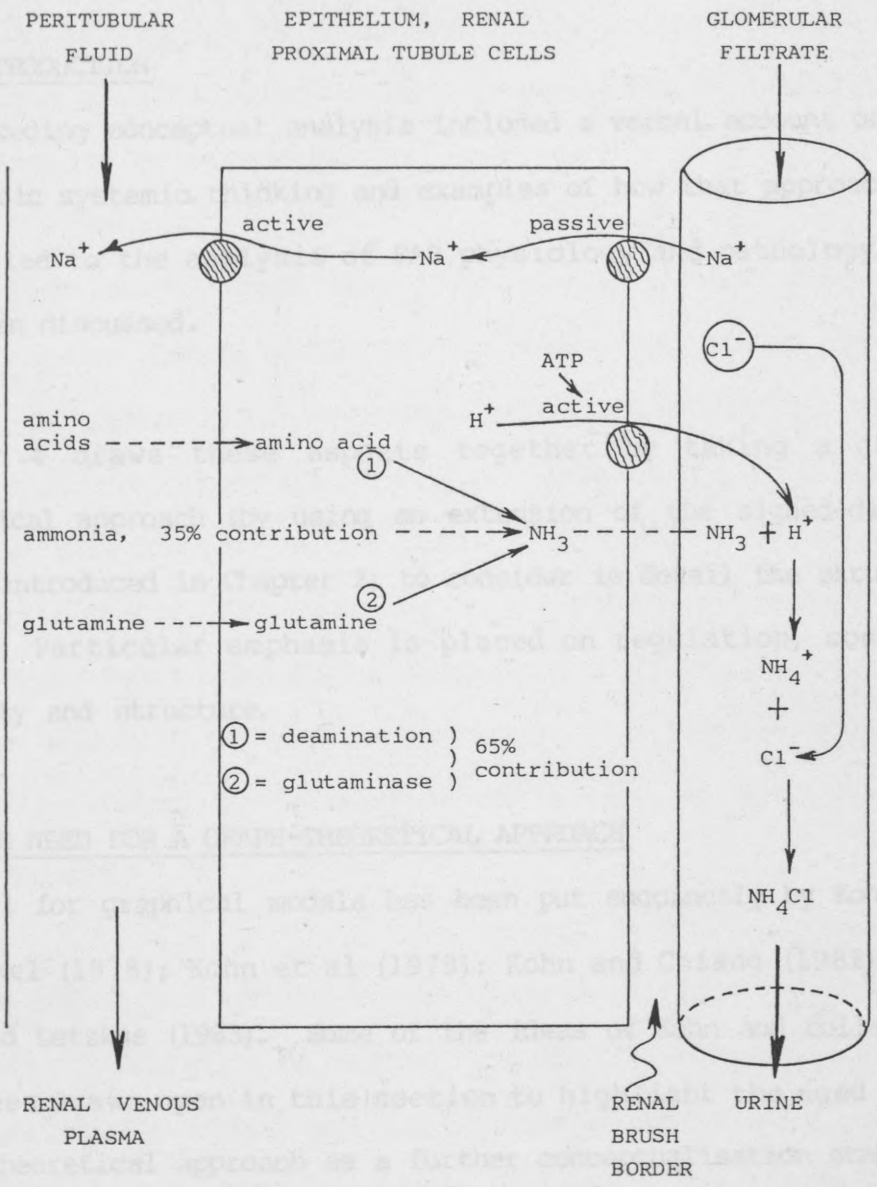

Figure 3.6 Buffering role of ammonium in urine.

CHAPTER 4

GRAPH-THEORETICAL ANALYSIS

4.1 INTRODUCTION

The preceding conceptual analysis included a verbal account of FAB. Some basic systemic thinking and examples of how that approach can be applied to the analysis of FAB physiology and pathology have also been discussed.

Chapter 4 draws these aspects together by taking a graph-theoretical approach (by using an extension of the signed-digraph method introduced in Chapter 2) to consider in detail the structure of FAB. Particular emphasis is placed on regulation, control, stability and structure.

4.2 THE NEED FOR A GRAPH-THEORETICAL APPROACH

The call for graphical models has been put succinctly by Kohn and Garfinkel (1978); Kohn et al (1979); Kohn and Chiang (1982); and Kohn and Letzkus (1983). Some of the ideas of Kohn and colleagues have been drawn upon in this section to highlight the need for a graph-theoretical approach as a further conceptualisation stage.

FAB displays the five main attributes of complexity (complexity arises when one or more of the following five attributes are found: significant interactions, high number of parts, non-linearities, broken symmetry, and non-holonomic constraints; Yates, 1978) hence there is pressure to utilise a simple and convenient method of analysing these phenomena. Graph-theory is a simple and convenient method that can satisfy the middle part of the iterative modelling

process (the process being the development of sentential or cognitive models followed by diagrammatic models followed by mathematical models) by providing a diagrammatic approach which allows some quantitative analysis to be made from which qualitative assessment can be undertaken.

Kohn and co-workers noted some advantages associated with graph-theory. System control properties may not be self evident from the solution of parametrised equations, although sensitivity analysis will quantitate the control features. Expanding this idea, Kohn and co-workers observed that a complete catalogue of the degrees of sensitivity of a model's behaviour to the values of its parameters may give far more information than is needed. Furthermore, the effects relating to local regulation are jumbled with the synergistic effects that arise from the presence of each element in a larger system.

In some situations (as for the objectives of this Chapter) only qualitative information is required to identify the important sites of regulation and control and the sequence of events underlying the observed behaviour to the structural features of the system.

4.3 ANALYSIS OF FAB

4.3.1 Introduction

Four signed-digraphs have been developed using the information contained in Chapter 3 and by seeking expert criticism. The signed-digraphs have been designed to show all of the essential features related to control and regulation of FAB, see Figures

4.1-4.4. The theory used to analyse these models is contained in Appendix 2.

4.3.2 Connectivity

The signed-digraphs can be considered in terms of connectivity. Ignoring analyte intakes (which are not intrinsically part of the physiological-biochemical system, rather they are a part of the behavioural system) it can be seen that Figures 4.1, 4.2 and 4.3 are strongly connected, that is they are connected of degree 3, hence each digraph constitutes a distinct system in its own right. Figure 4.4, however, is weakly connected, that is it is connected of degree 1. This implies that the graph does not represent a system, or, at least one distinct system is embedded in the representation.

Removing the partial graph of the phosphate aspects (that is, $[HPO_4^{2-}]_{PL}$ and $[HPO_4^{2-}]_U$) from Figure 4.4 leaves a subgraph which is unilateral, that is connected of degree 2. This suggests that the buffering capacity of phosphate is incidental among its many other activities. Control of the acid-base system is thus held in the remaining subgraph, so that theoretically the acid-base system would remain intact without the presence of phosphate. The remaining subgraph, however, is not strongly connected. Drawing out the strongly connected parts identifies four distinct systems, namely:

1. respiratory-blood-gas system;
2. bicarbonate-plasma-pH system;
3. ammonium-urine-pH system;
4. protein system.

Of these, only the bicarbonate system and the ammonium system contain elements of acidity and hence are the controllers of acid balance. Protein involvement in acid-buffering is important but can be seen as incidental among its other activities. The output of the respiratory system is clearly a controlled process.

4.3.3 Structure And Stability

The vertices of the signed-digraphs of Figures 4.1-4.4 have been assigned a number (see Tables 4.1-4.4 respectively) hence four adjacency matrices have been drawn up (see directly underneath Tables 4.1-4.4 for the related matrices). The eigenvalues of the matrices have been calculated to help assess the stability of the models, see Table 4.5.

The presence of eigenvalues with a positive real part is evidence that there is instability in the model and the presence of imaginery parts is evidence that there are inherent oscillatory features in the model. These observations hold for matrices A, B and C. Matrix D is a special case where all the roots are either zero or very small, so that the frequence domain representation:

$$\frac{1}{(s-\lambda_1)(s-\lambda_2)....(s-\lambda_3)} \qquad (4.1)$$

can be simplified to:

$$\frac{1}{s^n} \qquad (4.2)$$

if all λ_i's are assumed to be zero. This is a pure multiple integral and will lead to growth followed by decay. These observations were supported by pulse process simulations of the

networks using the related sets of equations detailed in Appendix 3.

The eigenvalues of the models and the related pulse response simulations contradict the view that all four systems are inherently stable (although they may exhibit oscillatory behaviour) and thus raises the following questions:

1. Is the linear representation inappropriate for what is known to be a highly non-linear set of systems?
2. Is the theory related to the control and the sequence of events an incorrect model?

VERTEX NUMBER	LABEL	VERTEX NUMBER	LABEL
1	Plasma volume.	14	Active transport K^+(IS-IC).
2	Capillary filtration rate.	15	$[Na^+]_{IC}$
3	Interstitial volume.	16	$[Na^+]_{IS}$
4	Capillary hydrostatic pressure.	17	Diffusion Na^+(IS-IC).
5	Interstitial hydrostatic pressure.	18	Active transport Na^+(IS-IC).
6	$[Pr^-]_{PL}$	19	Ratio $[K^+]_{IS}/[K^+]_{PL}$
7	$[Pr^-]_{IS}$	20	$[K^+]_{PL}$
8	Lymphatic pressure.	21	Diffusion K^+(PL-IS).
9	Lymphatic flow.	22	Diffusion K^+(IS-PL).
10	Intracellular volume.	23	Ratio $[Na^+]_{IS}/[Na^+]_{PL}$
11	$[K^+]_{IC}$	24	$[Na^+]_{PL}$
12	$[K^+]_{IS}$	25	Diffusion Na^+(PL-IS).
13	Diffusion K^+(IC-IS).	26	Diffusion Na^+(IS-PL).

Table 4.1 Assignment of a number to each vertex of Figure 4.1.

	1	2	3	4	5	6	7	8	9	10	11	12	13	14	15	16	17	18	19	20	21	22	23	24	25	26
1	0	0	0	1	0	-1	0	0	0	0	0	0	0	0	0	0	0	0	0	-1	0	0	0	-1	0	0
2	-1	0	1	0	0	0	0	0	0	0	0	0	0	0	0	0	0	0	0	0	0	0	0	0	0	0
3	0	0	0	0	1	0	-1	0	0	0	0	-1	0	0	0	-1	0	0	0	0	0	0	0	0	0	0
4	0	1	0	0	0	0	0	0	0	0	0	0	0	0	0	0	0	0	0	0	0	0	0	0	0	0
5	0	-1	0	0	0	0	0	1	0	0	0	0	0	0	0	0	0	0	0	0	0	0	0	0	0	0
6	0	-1	0	0	0	0	0	0	0	0	0	0	0	0	0	0	0	0	0	0	0	0	0	0	0	0
7	0	1	0	0	0	0	0	0	0	0	0	0	0	0	0	0	0	0	0	0	0	0	0	0	0	0
8	0	0	0	0	0	0	0	0	1	0	0	0	0	0	0	0	0	0	0	0	0	0	0	0	0	0
9	1	0	-1	0	0	0	0	0	0	0	0	0	0	0	0	0	0	0	0	0	0	0	0	0	0	0
10	0	0	0	0	0	0	0	0	0	0	-1	0	0	0	-1	0	0	0	0	0	0	0	0	0	0	0
11	0	0	-1	0	0	0	0	0	0	1	0	0	1	0	0	0	0	0	0	0	0	0	0	0	0	0
12	0	0	1	0	0	0	0	0	0	0	0	0	-1	0	0	0	0	0	1	0	0	0	0	0	0	0
13	0	0	0	0	0	0	0	0	0	0	-1	1	0	1	0	0	0	0	0	0	0	0	0	0	0	0
14	0	0	0	0	0	0	0	0	0	0	1	-1	0	0	0	0	0	0	0	0	0	0	0	0	0	0
15	0	0	-1	0	0	0	0	0	0	1	0	0	0	0	0	0	-1	0	0	0	0	0	0	0	0	0
16	0	0	1	0	0	0	0	0	0	0	0	0	0	0	0	0	1	0	0	0	0	0	1	0	0	0
17	0	0	0	0	0	0	0	0	0	0	0	0	0	0	1	-1	0	1	0	0	0	0	0	0	0	0
18	0	0	0	0	0	0	0	0	0	0	0	0	0	0	-1	1	0	0	0	0	0	0	0	0	0	0
19	0	0	0	0	0	0	0	0	0	0	0	0	0	0	0	0	0	0	0	0	-1	1	0	0	0	0
20	1	0	0	0	0	0	0	0	0	0	0	0	0	0	0	0	0	0	-1	0	0	0	0	0	0	0
21	0	0	0	0	0	0	0	0	0	0	0	1	0	0	0	0	0	0	0	-1	0	0	0	0	0	0
22	0	0	0	0	0	0	0	0	0	0	0	-1	0	0	0	0	0	0	0	1	0	0	0	0	0	0
23	0	0	0	0	0	0	0	0	0	0	0	0	0	0	0	0	0	0	0	0	0	0	0	0	-1	1
24	1	0	0	0	0	0	0	0	0	0	0	0	0	0	0	0	0	0	0	0	0	0	-1	0	0	0
25	0	0	0	0	0	0	0	0	0	0	0	0	0	0	0	1	0	0	0	0	0	0	0	-1	0	0
26	0	0	0	0	0	0	0	0	0	0	0	0	0	0	0	-1	0	0	0	0	0	0	0	1	0	0

Matrix A

VERTEX NUMBER	LABEL	VERTEX NUMBER	LABEL
1	Capillary hydrostatic pressure.	11	Plasma volume.
2	Effective circulating volume.	12	Drinking rate.
3	Juxtaglomerular excitement.	13	$[ADH]_{PL}$
4	$[Renin]_{PL}$	14	Distal nephron permeability.
5	$[Ang]_{PL}$	15	Hypothalamus pituitary....
6	$[AngII]_{PL}$	16	Carotid sinus ....
7	Venous pressure.	17	Arterial pressure.
8	Great vein and atria...	18	Supraoptic nucleus ....
9	Urine flow rate.	19	Extracellular osmolality.
10	Glomerular filtration rate.		

Table 4.2 Assignment of a number to each vertex of Figure 4.2.

Matrix B:

	1	2	3	4	5	6	7	8	9	10	11	12	13	14	15	16	17	18	19
1	0	0	0	0	0	0	0	0	0	1	0	0	0	0	0	0	0	0	0
2	0	0	1	0	0	0	1	0	0	0	0	0	0	0	0	0	1	0	0
3	0	0	0	1	0	0	0	0	0	0	0	0	0	0	0	0	0	0	0
4	0	0	0	0	1	0	0	0	0	0	0	0	0	0	0	0	0	0	0
5	0	0	0	0	0	1	0	0	0	0	0	0	0	0	0	0	0	0	0
6	0	0	0	0	0	0	1	0	0	0	0	0	0	0	0	0	1	0	0
7	0	0	0	0	0	0	0	1	0	0	0	0	0	0	0	0	0	0	0
8	0	0	0	0	0	0	0	0	0	0	0	0	0	0	-1	0	0	0	0
9	0	0	0	0	0	0	0	0	0	0	-1	0	0	0	0	0	0	0	0
10	0	0	0	0	0	0	0	0	1	0	0	0	0	0	0	0	0	0	0
11	1	1	0	0	0	0	0	0	0	0	0	0	-1	0	0	0	0	0	-1
12	0	0	0	0	0	0	0	0	0	0	1	0	0	0	0	0	0	0	0
13	0	0	0	0	0	0	0	0	0	0	0	1	0	0	0	0	0	0	0
14	0	0	0	0	0	0	0	0	-1	0	0	0	0	0	0	0	0	0	0
15	0	0	0	0	0	0	0	0	0	0	0	0	1	0	0	0	0	0	0
16	0	0	0	0	0	0	0	0	0	0	0	0	0	0	-1	0	0	0	0
17	0	0	0	0	0	0	0	0	0	0	0	0	0	0	0	1	0	0	0
18	0	0	0	0	0	0	0	0	0	0	0	0	0	0	1	0	0	0	0
19	0	0	0	0	0	0	0	0	0	0	0	0	0	0	0	0	0	1	0

VERTEX NUMBER	LABEL	VERTEX NUMBER	LABEL
1	Activity of granular cells.	9	$[Na^+]_{PL}$
2	Antinomycin D production.	10	$[ALD]_{PL}$
3	Renal Na^+ excretion.	11	Extracellular osmolality.
4	Glomerular filtration rate.	12	$[Na^+]_{PL}$
5	Capillary hydrostatic pressure.	13	$[Na^+]_{UF}$
6	Cardiac ouput.	14	Zona Glomerulosa.
7	Effective circulating volume.	15	Excitement of sodium sensitive....
8	Renal K^+ excretion.		

Table 4.3 Assignment of a number to each vertex of Figure 4.3.

Matrix C:

	1	2	3	4	5	6	7	8	9	10	11	12	13	14	15
1	0	0	0	0	0	0	0	0	0	1	0	0	0	0	0
2	0	0	1	0	0	0	0	0	0	0	0	0	0	0	0
3	0	0	0	0	0	0	0	0	0	0	0	-1	0	0	0
4	0	0	1	0	0	0	0	1	0	0	0	0	0	0	0
5	0	0	0	1	0	0	0	0	0	0	0	0	0	0	0
6	0	0	0	0	1	0	0	0	0	0	0	0	0	0	0
7	0	0	0	0	0	1	0	0	0	0	0	0	0	0	0
8	0	0	0	0	0	0	0	0	-1	0	0	0	0	0	0
9	0	0	0	0	0	0	0	0	0	0	1	0	0	-1	0
10	0	1	-1	0	0	0	0	1	0	0	0	0	0	0	0
11	0	0	0	0	0	0	1	0	0	0	0	0	0	0	0
12	0	0	0	0	0	0	0	0	0	0	1	0	1	1	0
13	0	0	0	0	0	0	0	0	0	0	0	0	0	0	-1
14	0	0	0	0	0	0	0	0	0	-1	0	0	0	0	0
15	1	0	0	0	0	0	0	0	0	0	0	0	0	0	0

VERTEX NUMBER	LABEL	VERTEX NUMBER	LABEL
1	Respiratory rate.	7	$[HCO_3^-]$ PL
2	Partial pressure carbon-dioxide.	8	Urine pH.
3	Extracellular pH.	9	$[NH_4^-]$ U
4	$[Pr^-]$ PL	10	Renal ammonium production.
5	Protein synthesis rate.	11	$[HPO_4^-]$ U
6	$[HPO_4^-]$ PL	12	Renal bicarbonate regeneration.

Table 4.4 Assignment of a number for each vertex of Figure 4.4.

Matrix D:

	1	2	3	4	5	6	7	8	9	10	11	12
1	0	-1	0	0	0	0	0	0	0	0	0	0
2	1	0	1	0	0	0	0	0	0	0	0	0
3	0	0	0	0	0	0	1	1	0	0	0	0
4	0	0	-1	0	-1	0	0	0	0	0	0	0
5	0	0	0	1	0	0	0	0	0	0	0	0
6	0	0	-1	0	0	0	0	0	0	0	1	0
7	0	0	-1	0	0	0	0	0	0	0	0	-1
8	0	0	0	0	0	0	0	0	1	0	0	0
9	0	0	0	0	0	0	0	-1	0	-1	0	0
10	0	0	0	0	0	0	0	0	1	0	0	0
11	0	0	0	0	0	0	0	1	0	0	0	0
12	0	0	0	0	0	0	1	0	0	0	0	0

MATRIX	A		B		C		D	
EIGENVALUE	Real	Imaginery	Real	Imaginery	Real	Imaginery	Real	Imaginery
1	0.95	0.85	0.00	0.00	0.00	0.00	0.00	0.00
2	0.95	-0.85	0.00	1.00	0.00	0.00	0.00	0.00
3	1.15	0.00	0.00	-1.00	0.00	0.00	0.00	0.00
4	0.98	0.47	-0.50	0.87	0.00	0.00	0.00	-0.00
5	0.98	-0.47	-0.50	-0.87	0.00	0.00	0.00	0.00
6	0.11	1.23	1.00	0.00	0.00	0.00	0.00	0.00
7	0.11	-1.23	-0.00	0.00	0.00	0.00	0.00	0.00
8	0.62	0.69	0.00	0.00	0.00	0.00	0.00	0.00
9	0.62	-0.69	0.00	0.00	0.00	0.00	0.00	0.00
10	-0.87	1.17	0.00	-0.00	0.00	0.00	0.00	0.00
11	-0.87	-1.17	1.00	0.00	0.00	0.00	0.00	0.00
12	-0.11	0.88	0.00	0.00	1.00	0.00	0.00	0.00
13	-0.11	-0.88	0.00	0.00	0.00	0.00		
14	-0.77	0.82	0.00	0.00	0.00	0.00		
15	-0.77	-0.82	0.00	0.00	0.00	0.00		
16	-1.24	0.00	0.00	0.00				
17	-0.86	0.24	0.00	0.00				
18	-0.86	-0.24	0.00	0.00				
19	0.00	0.00	1.00	0.00				
20	-0.00	0.00						
21	-0.00	0.00						
22	0.00	0.00						
23	0.00	1.00						
24	0.00	-1.00						
25	0.00	0.00						
26	0.00	0.00						

Table 4.5 Eigenvalues of the matrices A, B, C and D relating to the signed-digraphs of Figures 4.1, 4.2, 4.3 and 4.4 respectively.

It is clear that signed-digraphs are no more than sets of causal relationships between elements, linear in nature and independent of time. A pulse process simulation of a multicycle signed-digraph makes the assumptions of time dependence, parameter values of 1 for all the independent variables and that each discrete time step of the simulation exactly determines the length of time it takes to move between any two related vertices. Thus, gross errors are introduced into the simulation as soon as any pulse transmission moves from one cycle into another.

Tracing a pulse through any one cycle is meaningful however, as the response of controllers can be assessed.

Control loops of the signed-digraphs were analysed individually by tracing single cycle pulse responses and were all found to have an odd number of negative signs, which implies negative feedback control. Thus, there appears to be no evidence to suggest that the theory related to the control features is incorrect. On the contrary there is evidence to support the idea that the theory may be correct (albeit partially).

4.4 CONCLUSION

Graph-theory has been found useful in the identification of distinct systems and the sequences of events and areas of control within those systems. The idea of simulating pulse processes was found to have some value. The tracing of a pulse around a single cycle shows whether the cycle is stable or otherwise, however, when pulses move between cycles large errors are introduced.

Consequently further tracing of pulse transmissions is not meaningful. Other more sophisticated graphical methods which solve some of the problems associated with multicycles are available, for instance Petri nets (Peterson, 1977) and Bond graphs (Thoma, 1975). However, increased sophistication leads to a higher degree of quantification which moves away from the objectives of this Chapter. The sophisticated methods were therefore not used.

The benefits of developing the signed-digraphs are clear. They provide an important bridge between poorly structured sentential or cognitive models and the highly ordered language of mathematics. Furthermore, the consolidation of currently accepted physiology has led to the identification of areas of control which are often associated with weak knowledge and/or controversy (for instance, the integration of hormonal stimuli). Particular attention has been paid to these aspects in the following stages of the modelling process. The signed-digraphs therefore provide a comprehensive qualitative knowledge base.

Chapters 2, 3 and 4 have dealt with the conceptual aspects of the FAB system and provide the necessary basis for the more rigorous quantitative modelling approaches of Chapter 5, 6 and 7.

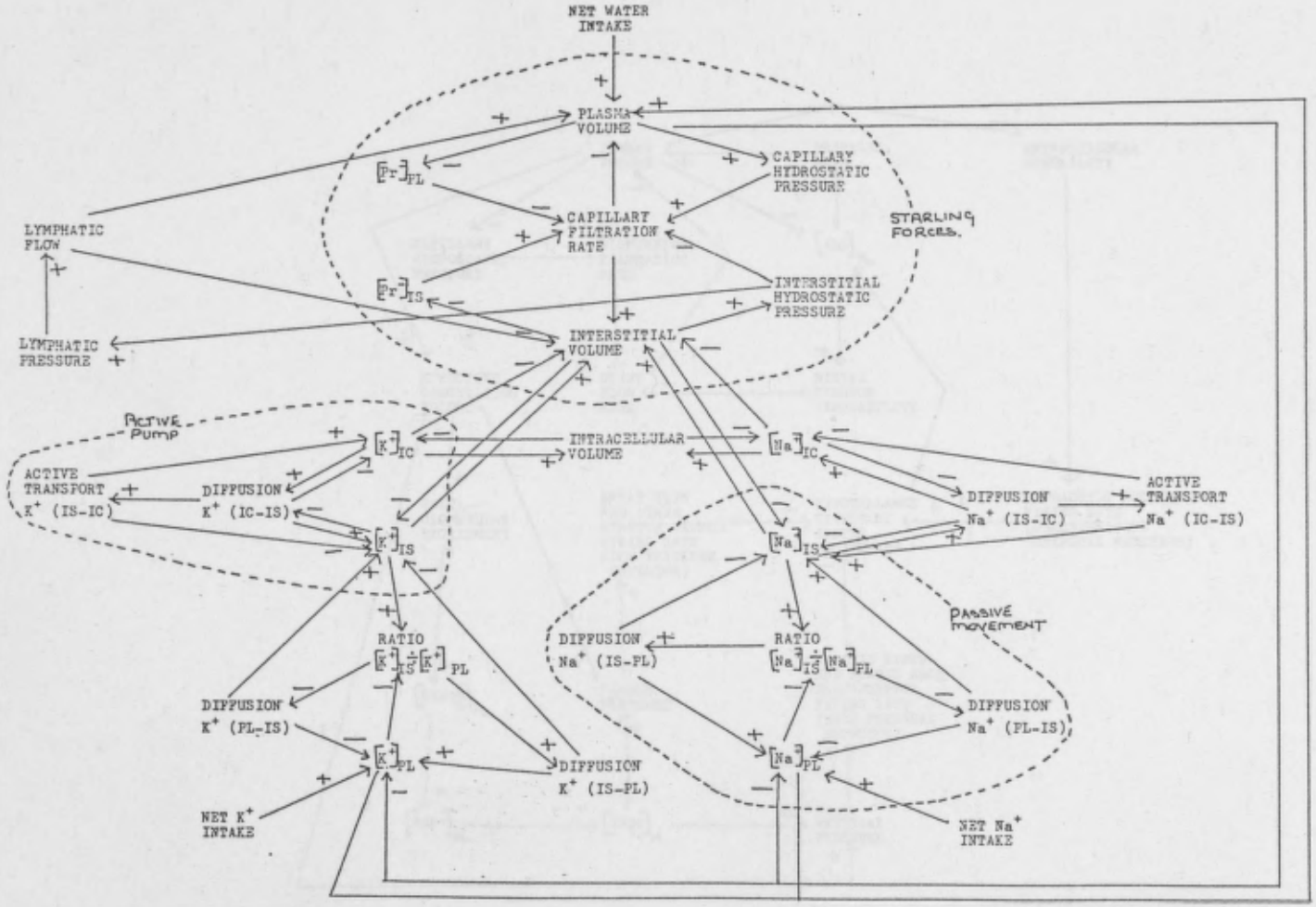

Figure 4.1 Signed-digraph of fluid and electrolyte distribution.

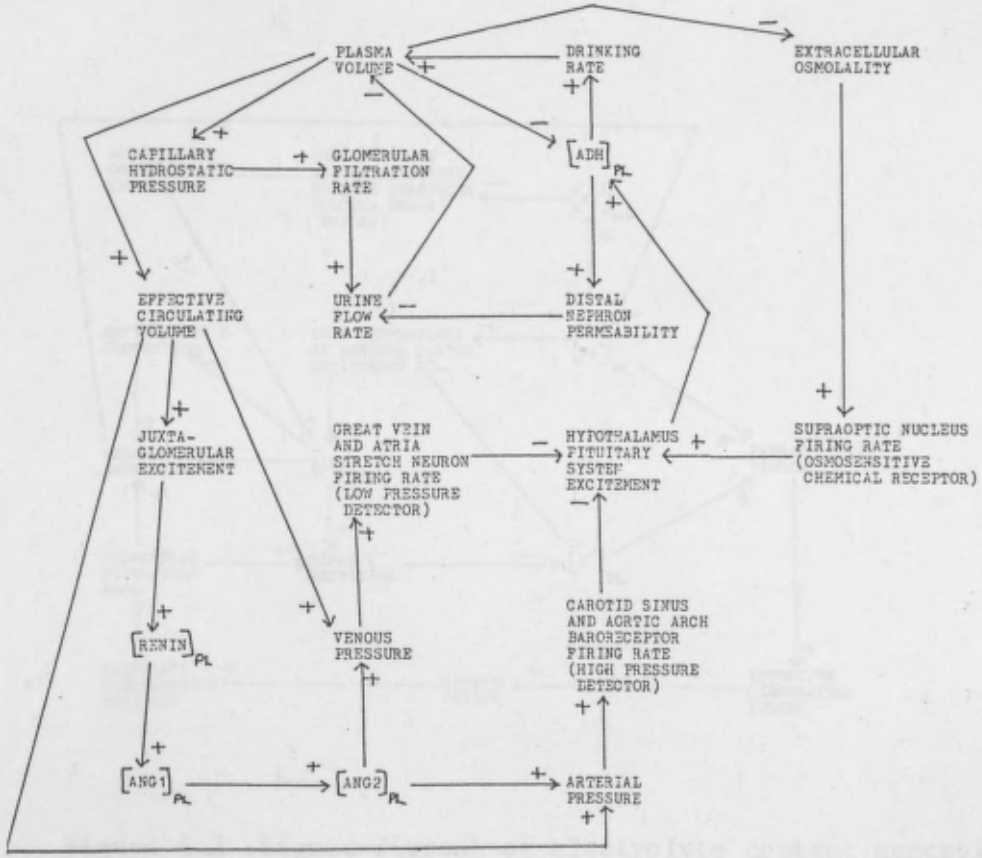

Figure 4.2 Signed-digraph of fluid volume control.

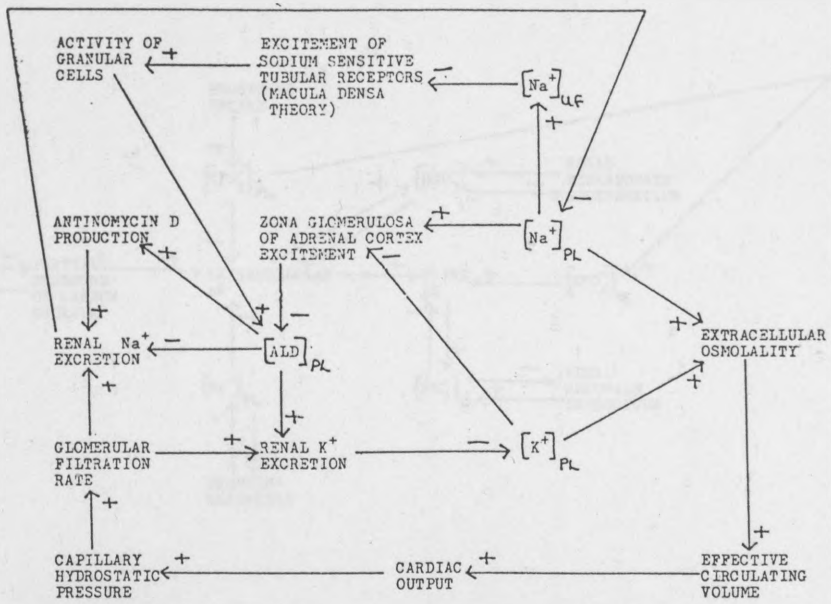

Figure 4.3 Signed-digraph of electrolyte content control.

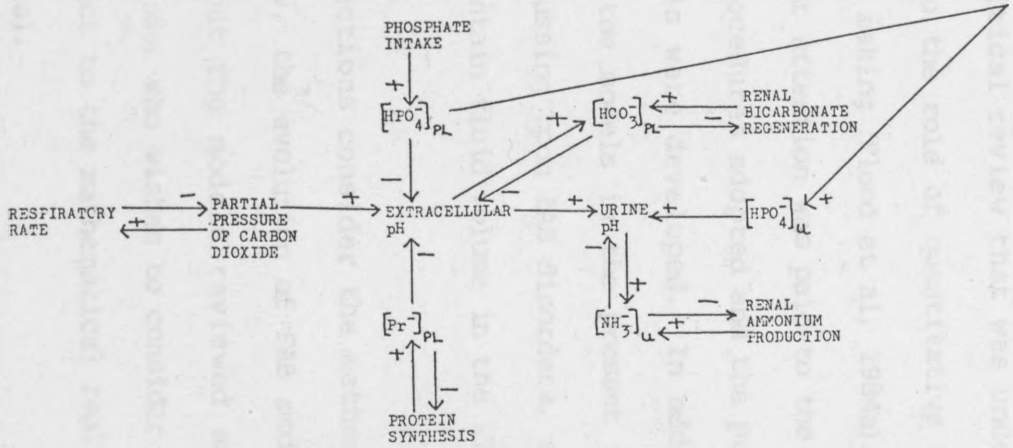

Figure 4.4 Signed-digraph of acid-buffer dynamics.

CHAPTER 5

REVIEW OF EXTANT QUANTITATIVE MODELS

5.1 INTRODUCTION

The previous three Chapters provide the conceptual basis for the remainder of the thesis whilst this Chapter marks the beginning of the quantitative approach. Documented below are the essential features of a critical review that was undertaken as part of an investigation into the role of quantitative FAB models as aids to clinical decision making (Flood et al, 1984a). In carrying out the review, particular attention was paid to the relationships between the modelling procedures adopted and the purposes for which the particular models were developed. In addition, the potential applicability of the models in the present research programme is considered by focussing upon FAB disorders, such as in the context of seeking to maintain fluid volume in the ITU patient.

The following sections consider the method of selection of the models for review, the evolution of FAB models, some qualitative observations about the models reviewed and finally a general overview. The reader who wishes to consider the review in greater detail with respect to the mathematical realisation is referred to Flood et al (1984a).

5.2 MODEL SELECTION

An extensive literature search revealed approximately one hundred papers as candidates for review. These related to sub-systems, equivalent systems and super-systems of the SOI. The majority were

of the first category, the largest proportion of which were renal models. A more detailed breakdown of model types is given in Figure 5.1 Reduction of the number of models to a manageable size for review was achieved using the decision tree depicted in Figure 5.2. Aspects of the FAB system modelled in the chosen papers are analysed in the matrix shown in Figure 5.3. This highlights aspects of the system for which substantial previous work exists, and suggests areas which may pose some difficulties in the present programme of model development, that is, from the sum of the columns Σ c. In addition, the physiological span of the model representations can be assessed from Σr, the sum of the rows.

5.3 EVOLUTION OF FAB MODELS

Amongst the very early models of body water regulation were those of Yoshitoshi et al (1955), Meredith (1957), Talbot et al (1959), Elkington (1960), Pace (1961) and Yoshitoshi and Nagasaka (1962). Fincham (1963) examined the hormonal mechanisms of water and sodium reabsorption and their mode of interaction with GFR.

From these earlier models evolved a second generation of models, including Deland and Bradham (1966) and Koshikawa et al (1964). The latter was criticised by Nagasaka et al (1969) on the grounds of a poor representation of renal function. A modified model was presented with the addition of ADH dynamics. The widely cited model of Reeve and Kulhanek was published in 1967 with its two compartmental representation of body water regulation, together with sub-models for ADH and drinking.

Among the more significant models which followed, describing the homeostatic regulation of body water and renal response to oesophageal water infusion, were those of Millerschoen and Riggs (1969) and the similar treatment by Toates and Oatley (1970). Subsequently Merletti and Weed (1972) presented a more detailed mathematical model of the body fluid control system where all aspects of ADH dynamics were assumed to be relevant. The validity of this model was limited since many of the functions incorporated were not well-based on experimental data and a number of assumptions were not made explicit.

In contrast, Koushanpour et al (1971) and Badke (1972) described less complex models for body water and salt regulation. The latter was based on segmental processing of urea, salt and water along the nephron and included the effects of hormonal and haemodynamic regulation.

Respiratory models have evolved from the multiple factor theory proposed by Gray (1945). This was followed by models representing cyclic ventilation including those of Defares et al (1960), Grodins and James (1963), Horgan and Lange (1963), Milhorn et al (1965) and Grodins et al (1967). It was upon this last model that Ikeda et al (1979) based the respiratory component of their FAB model. Subsequent developments included the dynamic gas exchange models of Emery et al (1971) and Murray-Smith and Pack (1974).

The earliest mathematical models of the circulation can be traced back to the end of the 18th century with attempts to describe

pressure/flow relationships in the major arteries. In more recent times significant developments have occurred in the Netherlands, with the analogue computer models produced by Noordergraaf et al (1963) and Beneken (1965) providing accurate representations of the circulatory anatomy. A widely used benchmark from that time is PHYSBE developed by McLeod (1965). The problem of long-term circulatory dynamics was addressed by Guyton and Coleman in 1967.

Early models of the overall control of circulation included those of Boyers et al (1972), Dick (1968) and Dickinson and Shephard (1971). Others, such as that of Coleman et al (1970) considered in addition the blood flow dynamics of the artificial kidney.

A trend of increasing complexity of representation continued culminating in the now classic model of Guyton et al (1972). It was upon this work that the subsequent models of Cameron (1977) and Ikeda et al (1979) were substantially based (respectively without and with acid-base components).

A large number of research groups have made substantial contributions to the development of renal models. Most of those of relevance to the current investigation are contained within the papers referred to above.

5.4 MODEL REVIEWS

5.4.1 Introduction

In carrying out the review of the chosen models, emphasis was placed on their worth in relation to factors such as fulfilling the objectives for which they were formulated, their basis in

physiology, the level and classification of model adopted and the extent of their validity.

5.4.2 The Models

5.4.2.1 A model of body water and salt regulation (Badke, 1972)

There are six main aspects to this model, the water and salt compartments, the drinking system, the cardiovascular system, the hormonal system and the kidney. Of these, only the drinking system (a behavioural subsystem) was not considered since fluid input in the ITU, the application domain of interest, is strictly controlled. The elements and relationships of the model are depicted in Figure 5.4. This model was developed, as an extension of that reported by Reeve and Kulhanek (1967), to include additional features of sodium regulation and its associated mechanisms.

The physiological basis of the model reflected currently accepted knowledge. Reabsorption in the proximal tubules is represented as a two step process whereby a fixed quantity of water is reabsorbed as a result of fixed active transport of solute and then a variable quantity is reabsored by osmotic forces. Thus tubular fluid at this point remains isotonic.

The more controversial hormonal control systems are considered as follows. Renin is released following either a decrease in renal artery pressure or rise in distal tubular sodium concentration (maculla densa theory). As a separate effect, aldosterone is released in response to low sodium concentration, high potassium concentration and decrease in left atrial pressure.

The cardiovascular representation, based on Guyton and Coleman (1967) has been criticised by those authors as being unable to predict accurately cardiac output and arterial pressure in response to kidney stress and water loading. The incorporation of this cardiovascular representation does imply a real limitation.

One interesting feature of the model is the simplified compartmental description of salt and water. Physiologically, the flow of substances following ingestion is as follows:

gastro-intestinal tract → plasma → interstitial fluid → intracellular fluid

with output from the kidney. In many models a detailed representation has been provided for this process regardless of its appropriateness to the level of modelling being adopted. As the process sets up osmotic pressures which have to be satisfied rapidly, Badke has dispensed with a multicompartmental realisation and adopted a simple representation for water redistribution.

Sections of the Badke model other than the kidney are typical of mainstream FAB compartmental modelling. The detail of the kidney model is too great for the current programme, particularly since the complexity would increase substantially with the inclusion of an acid-base component.

A difference equation approach is adopted for solution of the partial differential equations. The lumped portions of the model are solved using a fourth order Runge Kutta routine. In this way

new values of the variables can be calculated at intervals of five minutes of simulation time. More rapid transients of less than five minutes duration are assumed unnecessary for the prediction of the states of body salts and water. The program, written in FORTRAN, requires thirty seconds for the simulation of 72 hours on a PRIME 550 computer.

The author tested the validity of the completed model by examining responses to: salt-restricted starvation, saline infusion, diabetes insipidus and the absence of aldosterone. Badke claimed reasonable correspondence with experimental data although this was difficult to judge from the paper.

5.4.2.2 A steady-state control analysis of the Renin-angiotensin-Aldosterone system (Blaine et al, 1972)

The motivation for considering an in-depth analysis of the RAA system stems from its perceived important role as a controller in the maintenance of FAB. The precise role played by the RAA system is a matter of some controversy. The authors produced this paper in an attempt to clarify some of the thinking associated with this system. As such the paper yields considerably more than a signed-digraph representation but less than would be provided by a fully quantitative simulation model.

On the basis of the conceptual form of the model, two principal mechanisms are suggested for control of the RAA system, the baroreceptor (stretch) hypothesis related to afferent glomerular arteriolar pressure and secondly the maculla densa theory where a

response to alterations in sodium concentration at the maculla densa cells is postulated. These hormone release factors are the only negative feedback effects contained in the system.

The major uncertainty highlighted by Blaine et al relates to the hormonal release mechanism. The precise nature and combination of these stimuli are the major elements requiring solution. Even as recently as 1982, Lote stated that sodium reabsorption 'probably constitutes the major unsolved problem of renal physiology at the present time'.

The representation adopted for the systemic circulation is a highly simplified one, which allows a string of functions to relate extracellular fluid volume to GFR. Also of note is the processing of ultrafiltrate through a series of lumped renal compartments.

The validity of such a model is difficult to ascertain. Functional relationships are drawn from a range of empirical evidence and are therefore soundly based. On the other hand, the inability of the model to produce quantitative outputs makes a rigorous validation procedure inappropriate (see under modelling philosophy, subsection 10.3.2). The model does, however, have considerable potential as a test-bed for assessing the validity of a number of candidate hypotheses relating to hormonal release mechanisms.

5.4.2.3 A model framework for computer simulation of overall renal function (Cameron, 1977)

The model is effectively a simplified version of the circulatory representation of Guyton et al (1972). Specific simplifications

relate to: extracellular protein distribution and lymphatic return, systemic and pulmonary circulation, cardiac output, arterial pressure and autonomic nervous integration. Refinements were made to the representations of plasma colloid osmotic pressure, ADH and blood viscosity. In essence the dominant dynamic models are retained.

Quantities which vary either very slowly or imperceptibly when renal parameters are disturbed have been assumed to be constant. Quantities with very rapid dynamics have been set to the equilibrium solutions of their corresponding differential equations. Twelve state variables have been retained.

In terms of control action, ADH secretion is increased by raised plasma osmolality, increased autonomic nervous activity or reduced blood volume. Renin is modelled implicity, since its only function is to catalyse angiotensin formation. Angiotensin release is sensitive to renal blood flow and salt delivery to the distal nephron (maculla densa theory). Aldosterone secretion is increased by a raised ratio of extracellular potassium to sodium concentration and by reduced arterial pressure. The influences of the catecholamines and prostaglandins are neglected since the kidneys are not among their primary targets.

The kidney is represented by a single compartment, with overall relationships modified by GFR, ADH, aldosterone and sodium plasma

concentration. The model, with its relatively simple renal dynamics, appears well able to simulate a range of pathological conditions in which the kidney plays a vital role. The author did, however, intend to increase the complexity of the renal dynamics by increasing the number of functions involved, rather than adopting a multicompartmental representation of the nephron such as can be found in Cage et al (1977). In contrast to many other modelling efforts, Cameron combines the simple renal sub-model with a complex cardiovascular representation.

Model validation was carried out by comparison of simulation results with experimental data. Particular effects studied were those following renal nervous excitation, unilateral nephrectomy, aldosterone loading and acute water loading. The model responses were generally within the range of published results for the corresponding experimental or clinical situations.

Although Cameron did not make clear his modelling objectives, the model was primarily used for its heuristic potential, particularly regarding regulatory mechanisms. With relatively minor changes, it could be used predictively.

5.4.2.4 Systems analysis of the renal function (Bigelow et al, 1973)

This paper is one of a series which also includes DeHaven and Shapiro (1967; 1970). The mathematical model was developed in three stages. Originally DeHaven and Shapiro (1967) produced a realisation with four major components; plasma, red cells,

interstitial and intracellular spaces. These were considered as homogenous compartments with compositional gradients existing only between them.

A black box kidney sub-model was subsequently incorporated to provide for urine of a different salt and electrolyte content than that of plasma. At this stage the model emphasised the intrinsic control of renal function over the composition and volume of the blood. Overall, 129 chemical species were defined by 29 components.

A further step in model development (DeHaven and Shapiro, 1970) saw the effects of ADH integrated into the existing model. The final step (Bigelow et al, 1973) was concerned with the integration of a gastointestinal sub-model and arterial pressure effects, together with a number of modifications to the model enabling transient as well as the steady-state behaviour to be examined.

In terms of control action ADH was not modelled explicity using a hypothalamus-pituitary gland representation. Rather ADH was modelled implicity according to a relationship between urine and plasma osmolalities in conjunction with urine flow.

Bigelow et al (1973) made the explicit decision to exclude the RAA system from the model. In effect, it was assumed that water diuresis or conservation is the major cause of changes in urine osmolality and that conservation of salt (generally recognised as important for volume maintenance) is not available in the model.

Despite the exclusion of the RAA system, the model responded reasonably well to water loading, hypertonic saline infusion, hypertonic urea solution infusion and controlled rehydration after dehydration.

The clinical applicability of the model is limited by its complexity. The size of the model is such that its mathematical solution requires a large number of partial derivative calculations in a Jacobian matrix technique. A second problem envisaged relates to the simulation of pathological conditions. In a model such as this, a substantial number of changes in the partial derivatives (functional parameters) would be required before solving the model.

5.4.2.5 Simulation and research models as teaching tools (Deland et al, 1978)

This paper continues a series which includes DeLand (1971; 1975), Deland and Bradham (1966) and DeLand et al (1972). The kernel chemical model was described in Deland and Bradham (1966) and is divided into five general (location) compartments: gaseous venous plasma, intra-red cellular, plasma, interstitial, and intracellular (less red cells). Each location in turn includes a number of substances including: H_2O, Na^+, K^+, Ca^{++}, Mg^{++}, Cl^-, SO_4^{2-}, HPO_4^{2-}, HCO_3^-, all other anions, protein and H^+. Later developments of the kernel biochemical model included time-dependent aspects of kidney and metabolic functions. Other additions to the model included the ability to simulate clearance of each species from the body by the kidney (as a function of the composition of plasma) extracellular volume and GFR. Cross-coupling was included with the necessary

conservation of charge, and output volume was made variable according to body composition and kidney funtion. Therapeutic fluids were included as a further input to the system.

The aim of this model was the development of a teaching aid for medical students. Thus attention was paid to the provision of a user-friendly interface. The accuracy of the simulation was optimised to periods of 8 - 12 hours (the time which usually occurs between clinician visits) however, a course of treatment can be followed over days. Furthermore, the model may be restarted to compare alternative therapeutic hypotheses, which is an important feature in models designed for the purpose of aiding clinical decision making.

An algorithm has been incorporated which uses clinical information (such as body weight, surface area and sex) in the calculation of values such as the initial volumes and distribution of water and the content and distribution of electrolytes. This tunes the model to the patient which is also an essential prerequisite for a clinical decision making tool.

The essence of the work by DeLand et al is similar to that of DeHaven and his co-workers. Both of these groups include in their models phenomena such as electrochemical balance and the exchange of ions in the kidney, including the transport of ions across the epithelium. As such they contrast with most of the other large scale models of FAB, where the representation of relationships remains at a physiological level and rarely includes biochemical details. However, very detailed biochemical realisations are

unlikely to be successful as models designed for the enhancement of clinical decision making with the constraints necessarily imposed in such cases (although simplified versions might be successful).

Model verification was carried out in two phases. First the reference standard state was assessed and then performance following forcings was examined. Typical forcings were infusion of isotonic and hypertonic NaCl solutions and $NaHCO_3$ stress. These perturbations were analysed both qualitatively and quantitatively. The validity of each of the sub-models was examined individually in addition to overall model assessment.

As a teaching tool pragmatic validity was attained as the objectives of the modellers were satisfied (implementation costs were less than one dollar per hour per console). The possibilities of making use of this model in current investigations are limited on the one hand by the lack of quantitative detail on the model, and yet enhanced on the other by the theoretical validity attained by using well known and universally accepted laws.

5.4.2.6 Control of blood volume and extracellular fluid osmolality in humans (Fadali et al, 1979)

The model developed by Fadali et al makes use of linearisation techniques particularly in describing changes in osmolality. Whilst this is acceptable for describing small perturbation dynamics, errors will occur in describing the response to larger changes since the system is not intrinsically linear. The model also includes a number of highly simplified physiological relationships, for instance, it is assumed that the body content of

solutes is static, since the authors wished to exclude all hormones other than ADH in order to maintain mathematical simplicity. The title of the paper is therefore misleading as it is the content of ions which determines the volumes held whereas ADH controls osmolality, Lote (1982). Current physiological knowledge suggests that to control volume, it is essential to have a dynamic representation for solutes, therefore, aldosterone would have to be included (this does not necessarily require an explicit representation of the RAA system).

Another important aspect of blood volume control that was omitted (although autocontrol rather than active control) is the variable rate of glomerular filtration. Approximately twenty per cent of extra glomerular filtrate (over the nominal rate) can be made available for processing and possibly excretion. Thus the decision of Fadali et al to include a static GFR has to be questioned.

The method of validation was not specifically discussed, however comparisons with experimental data were made. The authors claimed comparable osmolality and urine flow changes. It was noted, however, that for small amounts of water injection the model produced unrealistically large quantities of urine flow. The authors suggested this was because the model failed to begin ADH secretion before the osmolality had returned to normal. However, because solute dynamics were excluded, a further likely reason would seem to be the inability of the model to conserve ions and hence maintain osmolality and short-term volume expansion.

Linearisation of non-linear functions seems unlikely to be responsible since the observed errors relate to small perturbations.

Although the nature of the assumptions incorporated limits the usefulness of the model, a first order exponential delay function adopted for gastrointestinal absorption may be relevant to the current research programme.

5.4.2.7 Mathematical models of respiratory regulation (Grodins and James, 1963)

The model is concerned with the distribution and concentration of carbon dioxide. The compartments of the model are shown in Figure 5.5.

Several assumptions had to be made before the model could be formulated. These were: that the lungs be regarded as a box of constant volume and homogenous content ventilated by a continuous stream of gas; expired air, alveolar air and arterial blood are in continuous equilibrium; the respiratory centre could be lumped with all other tissues into a single homogenous reservoir with constant blood flow; and arterial blood, venous blood and tissue have the same linearised carbon dioxide absorption curve.

The model was soundly based on a series of measured data. However, its performance against experimental data was not discussed, and thus its validity is somewhat uncertain.

This model has potential for the current research in that the transients of the real system can be omitted, and consequently integration for the solution of the equations is possible over minutes rather than seconds.

5.4.2.8 Long term regulation of the circulation: Inter-relationships with body fluid volume (Guyton and Coleman, 1967)

This Chapter by Guyton and Coleman describes both a simplified model of long term circulatory regulation as well as an expanded form. The models were developed in order to analyse the long term regulation of circulation which at the date of publication had not been included in circulatory models. In developing the models, Guyton and Coleman tackled a number of features which were difficult to quantify, for example, vascular growth rate in response to reduced tissue supply. As a crude solution, an empirical functional relationship was set up between cardiac output and loss/gain in vascularity of the body. In addition (and due to a lack of physiological data plus a desire to keep the complexity of the model at a manageable level) a number of other simplifying assumptions were made, for example, vascular growth and dilation of collateral arteries were lumped together.

The success of the extended model over the simpler form is highlighted when making comparisons with experimental data, for instance, a long term rise in arterial pressure and cardiac output was shown by the simplified model in response to a two-thirds reduction in renal mass and a two and a half times increase in

urinary load. Empirical data suggested that only a transient rise in cardiac output occurs whilst arterial pressure rises and remains high. The expanded model reproduced this latter behaviour well.

The dilemma for the modeller, however, is that the resolution of the problem has involved a very considerable increase in model complexity, an increase which might prove taxing in relation to the stated objectives of the model. Uttamsingh (1981) in his model formulated to examine problems relating to acute and chronic renal failure and also renal dialysis, chose to use the simple circulatory model outlined above. Whereas this would be entirely appropriate if only normal kidney dynamics were being investigated, the problems described above make questionable its wider adoption as intended by Uttamsingh. However, utilising a complex representation may well have prevented Uttamsingh from satisfying his pragmatic objectives.

In relation to diagnosis and patient management, the models of Guyton and Coleman are potentially useful since they provide longer-term trends of variables such as arterial pressure which are of clinical relevance.

5.4.2.9 Circulation: overall regulation (Guyton et al, 1972)

The model is an extensive lumped parameter, non-pulsatile representation of the circulation, incorporating both short term and long term interactions. The time constants of the system cover the range 0.005 - 57,000 minutes thus producing a stiff set of equations. To compensate for this stiffness the authors carried out initial integration with a small step length until the rapid

time constant factors reached steady-state. The integration interval step was then increased, so that the whole system attained a steady-state without consuming excessive computer time.

The complexity of the model is apparent with three hundred and fifty-four blocks, each comprising of one or more equation. The system included the following subsystems: circulatory dynamics, vascular stress relaxation, capillary membrane dynamics, tissue fluids and pressure and gel, electrolytes and cell water, pulmonary dynamics and fluids, angiotensin control, aldosterone control, ADH control, thirst and drinking, kidney dynamics and excretion, muscle blood flow control and PO_2, non-muscle oxygen delivery, autoregulation, autonomic control, heart rate and stroke volume, red cells and viscosity, and finally heart hypertrophy or deterioration.

The model was produced as an attempt to weld together a Systems Analysis of circulatory regulation with a review of current literature. Its use is thus primarily as a quantitative review of physiological knowledge (descriptive in nature and satisfying the initial objectives) rather than being a tool for aiding decision making in the clinical environment. This work has, however, stimulated other research activity (notably Cameron, 1977) where a parsimonious approach has been adopted. The Guyton model does then have relevance to clinical decision making if appropriately applied in a systemic manner.

5.4.2.10 A model of overall regulation of body fluids (Ikeda et al, 1979)

This large scale model contains sub-models for each of the physiological processes of the system of interest in the current research programme. The model was developed in three sectors, the circulation and body fluids, respiration and the renal functions. These were considered using seven interacting blocks.

This large scale model of body fluid regulation was developed with the objective of studying problems concerning body fluid disturbance and fluid therapy. In effect it is, as the authors claimed, a Systems Approach to the diagnosis and therapy of body fluid and acid-base disorders. This work is extremely important in relation to the current research programme, as it attempts to achieve similar utilitarian objectives using the same (systems) approach.

The model was developed in order to replicate in reasonable detail the physiology of the body. Parts of the model were based on Guyton et al (1972), Grodins and James (1963), Grodins et al (1967) and Sato et al (1974) and by using literature to identify relationships and to set parameter values. Some supplementary experiments were carried out by the authors. The model described was designed to represent normal bodily functions, but in a form suitable for modification enabling pathological phenomena to be represented.

A number of physiological aspects of the model are noteworthy. For example, the cardiovascular sub-system has been represented in a highly simplified form justified on the grounds that the model was to be used to simulate the long-term behaviour of body fluids. Thus only steady-state values were calculated with rapid transients neglected.

The authors have also represented a number of controversial areas of physiology. For instance, in the model ADH secretion arises from a weighted additive sum of plasma osmolality and pulmonary venous pressure. Another example is in the factors leading to aldosterone release, which are ACTH and potassium extracellular fluid concentrations, pulmonary venous pressure, sodium supply to the distal tubule (maculla densa theory) and systemic arterial pressure. The main area of controversy in this case (the maculla densa theory) adds a relatively small component to the signal stimulating aldosterone release.

The authors have represented many of the phenomena as approximated functions rather than incorporating full details of the underlying physiological processes. For example, the RAA system is represented as an input-output type function, where the dynamics of the system from renin secretion onwards have been implicitly incorporated in the aldosterone functions (the effect of angiotensin II as a vasoconstrictor has been omitted).

The authors found that the minimum integration step length required when simulating the model was determined by the respiratory block, whose frequency characteristics were approximately ten times as

rapid as those of the other blocks. This step length is, however, too short to achieve an effective long term simulation (it is only fifteen times as fast as real time on a HP-21MX mini-computer with 64 kbytes of memory). For the purpose of the current research programme, this block requires simplification.

Model validity was assessed by comparison of the model behaviour to experimental data. Many experimental data on water loading were available and the model responses compared well to these. In addition, respiratory responses to increased partial pressure of carbon dioxide and decreased partial pressure of oxygen produced generally similar behaviour to available data, however, of all model responses these proved to be least reliable, thus strengthening the case for examining closely the representation of the respiratory system. Other tests included examining glucose metabolism and potassium dynamics in response to various perturbations, all of which were in good agreement with experimental data. Metabolic acid disturbances and intracellular buffering also produced good predictions, although metabolic acidosis was predicted less well than metabolic alkalosis. Finally, respiratory acid-base disturbances and compensation by the kidney were also considered, the time-courses of model and experimental pH-$[HCO_3^-]$ plots being in good agreement.

The clinical applicability of this model is potentially high in that all important areas of FAB are considered. The complexity of the model, however, puts in doubt its suitability for effective micro-computer implementation, that is, to produce accurate results

at an acceptable speed for the user. A simplified version of the Ikeda model could well satisfy many of the complexity constraints whilst maintaining its importance as a model containing the important features of volume regulation.

5.4.2.11 Mathematical simulation of the body fluid regulatory system in dog (Koushanpour and Stipp, 1982)

The model is a further development of earlier work by Koushanpour et al (1971). Four major sub-systems are included: gastrointestinal, cardiovascular, hypothalamus-pituitary and renal as shown in Figure 5.6.

In the work described in this paper, the authors set out to provide a general and sufficiently detailed mathematical model of the major organs involved in the regulation of body fluid volume and osmolality. The compartmental components of the model provided aggregated representations, for example, cardiovascular phenomena were derived from blood volume. In other areas a less aggregated approach was adopted, for instance the determination of transcellular water flux, which required a knowledge of water permeability of cells and the surface area of all membranes.

The model is generally consistent with currently accepted physiology. ADH for example is determined by left atrial pressure and plasma osmolality, where the effects of these on ADH is described by a linearised Taylor expansion of a postulated non-linear representation. In the cardiovascular system it is assumed that changes in the quantity of osmotically active solutes occur during perturbations in water balance. This will preclude the

effect of osmotic diuresis on solute imbalance as noted by the authors.

A further point on physiology is that the effects of aldosterone and the RAA system were not incorporated, as they are mainly features of chronic disturbances in renal function. In addition, since the major purpose of the simulation was to test the effect of short term forcings on renal function, and as the minimum response time is three to four hours before the effects of change in aldosterone concentration can be detected in urine output, it was possible to consider the RAA dynamics as being outside the system of interest.

The model has certain aspects which are not entirely compatible with the patient-relatedness requirement of the current research programme. Speciation for instance may pose problems. Many of the relationships are derived regression equations from changes in dog's response, and their direct applicability to the current clinically-related programme is limited to highlighting a methodology of interest.

Indeed, the technique used to relate two phenomena (fitting various ordered polynomials to pairs of data) allows relationships and their multiple regresison coefficients to be ascertained. A measure of the error is easily accessible by taking the square of the coefficient, for example, the multiple regression coefficient of solute-free water clearance was a high 0.976 with a square of 0.953 thus having an unexplained error of only 4.7%.

Model validity was tested by comparing the simulation results to experimental data not used in the development of the model. Simulation of intraoesophageal water infusion compared favourably with experimental data, as did the simulation of water ingestion. The model's response to intravenous ADH injection yielded good agreement with the data, whereas the response to intravenous water infusion was less satisfactory. On the other hand the model's response to repeated intermittent water loading yielded no more than an adequate agreement with the data.

One last but important observation made by the authors concerned non-homogeneous mixing effects of plasma water on plasma osmolality. These were not negligible but, due to an absence of data, a detailed analysis of the effects of time delay on the response of the model due to mixing was not attempted.

5.4.2.12 Mathematical model of the body fluid control system (in Japanese) (Kuroda et al, 1980)

The model is presented as six subsystems: plasma volume control, cardiovascular control, ADH control, the kidney and fluid and electrolytes. This model constitutes a compartmental representation of the body fluid control system which incorporates the main substances and phenomena involved. Much of the detailed discussion in the paper can only be considered in general terms, due to translation difficulties.

The sub-systems other than the hormones are very simplified representations of functional relationships. All the outputs of

the cardiovascular system, for example, are derived from only three variables, plasma volume, blood cell volume and angiotensin II. In these instances, the non-linear functions are represented by two or three segmented continuous linear functions.

ADH secretion is derived from the osmotic pressure of the extracellular fluid only. Of the three signals to the hypothalamus-pituitary system, the plasma osmolality induced signal is the most controversial. Indeed, this phenomenon may well not activate ADH secretion. If this is the case, then one of the major controlling sub-systems is incorrectly represented in this model.

The secretion of aldosterone, on the other hand, is brought about by a number of stimuli: cardiac output, extracellular potassium and sodium concentrations, and a function of the juxtaglomerular apparatus. They are weighted one-third each, except cardiac output which is weighted one-tenth. Thus the juxtaglomerular aspect is not over-emphasised, and the controversial maculla densa theory is not given undue prominence.

Model validation was carried out by comparing simulation results to experimental data for water loading experiments. Many of the results were in fair agreement, however, the urinary output of sodium was shown to relate poorly and consequently body osmolality appeared unsatisfactory. Model performance was brought closer to prototype performance by the adjustment of parameter values.

5.4.2.13 Control of water excretion by antidiuretic hormone: Some aspects of modelling the system (Toates and Oatley, 1977)

This paper follows that of Toates and Oatley (1970). A five compartmental representation was adopted as shown in Figure 5.7. These compartments represent the sub-systems of drinking, stomach, intestines, body fluid and renal control. The behavioural aspects of the system have not been considered in this review as the patient in the ITU (the area of interest of the current research programme) is under strict clinical control.

This model was developed as an aid to the understanding and calculation of body fluid changes relevant to the control of thirst. The authors attempted to take into account important factors which previous models had not included, and thus produce a reasonably comprehensive model in contrast to the generally patchy and piecemeal models which had existed prior to the 1970's.

The model was originally developed on an analogue computer, hence the first order low pass filter and other electrical analogues. Taking this approach allowed the authors to make substantial use of the work of Fincham (1963) who had earlier produced an analogue simulation. After further development, the whole system was transferred on to a digital (Elliot 4130) computer, as an ALGOL program.

An interesting technique was used to measure movements of the system away from the normal steady-state. Initial conditions of the system were set at the beginning of the simulation, and errors

were measured around those set points. It was these errors which were used to determine control responses. An implication of this technique is that patient-relatedness could be achieved by including an algorithm which calculates the normal set point values from a given set of information, that is, sex, height, weight and so on.

Of the physiology, the following points are worthy of note. The kidney is considered as a single compartment, with no explicit representation of the specific sections of the kidney where particular reabsorption and other events occur.

A second point is the lack of potassium dynamics in the intracellular compartment. This may not be compatible with the need to model the interaction of the body's electrolytes with the acid-base system. That is, the intracellular-extracellular pumps are strongly affected by pH which causes some electrolyte redistribution and would strongly affect intracellular potassium levels.

In the ADH system, the composition of signals leading to the release of the hormone omitted the factor of osmotic pressure. This assumption was made due to the difficulties associated with postulating a receptor which directly measures sodium concentration. Consequently, the errors from intra- and extracellular volumes were used as stimuli in an additive fashion.

Information for model formulation was gathered both from rat experiments and relevant literature sources. Agreement between simulated outputs and observed behaviour was in general adequate,

indicating that the authors have included most of the major variables of body fluid regulation in their representation.

5.5 GENERAL OVERVIEW

Having in the previous section considered some details of each of the models reviewed by Flood et al (1984a), a number of general points of interest can now be discussed by making use of concepts contained in Carson et al (1983).

The set of FAB models reviewed show variation in the span of the system of interest represented, the depth of complexity modelled, and the techniques of the modellers used; reflecting the range of purpose for which the models have been developed.

Models of relevance to the current research programme include that of Ikeda et al (1979), whose purpose was to study problems concerning body fluid disturbance and fluid therapy. The span of the Ikeda model approaches that desired for the current research, whereas the complexity requires some reduction.

Many researchers used the approach of lumped parameter, deterministic control system models, the majority of these being non-linear. As most of the lumped time invariant modelling resulted in a mismatch between the complexity of the postulated structure and the paucity of experimental data, rigorous identification procedures were forsaken and more empirical

approaches had to be adopted. Thus many parameter values were postulated and their values assessed by adaptive fitting, so that some acceptable value was attained.

Linear representation was achieved by Fadali et al (1979) for part of their model. Non-linear systems may be linearised for small perturbation dynamics about a steady-state. However, the intrinsic dynamics of physio-biological systems are rarely linear. Consequently, this process may involve the inclusion of a less accurate representation which will often be least accurate at the extremities of the physiological range.

The control system models occasionally incorporated sub-systems classed as strictly compartmental. Generally speaking, however, the majority of substances are under some type of active hormonal control. This latter area encompasses the majority of the controversial areas in contemporary FAB physiology. Examples include the integration of the stimulus in the hypothalamus-pituitary system before stimulation of ADH secretion and the actual stimulus leading to ADH secretion. A third example is the importance and the nature of stimuli leading to the activation of the RAA system.

Only a few of the researchers attempted to represent aspects of the system with distributed models (these generally being at higher levels of resolution, for example, the counter-current system). These distributed models included effects of flow and peripheral

circulation, thus providing concentration gradients in what are otherwise represented as homogenous compartments. Koushanpour and Stipp (1982) used a distributed sub-model to represent renal function, whilst using the lumped parameter, deterministic control system technique for the rest of the model. This approach was also adopted by Badke (1972).

When embedded in FAB models, the compartmental representation was on the whole more successful, both in efficiency of representation and accuracy of output, than the distributed models. This implies that the assumption of homogenous compartments has been relatively successful.

The review of extant mathematical models has thus highlighted approaches and problem areas, thereby providing information which can be used effectively during mathematical realisation of the FAB system.

5.6 CONCLUSION

Chapter 5 provides a basis on which the quantitative analysis of Chapters 6 and 7 is built. An important finding of Chapter 5 is the scarcity of statistical FAB models. Chapter 6 thus sets out to discuss statistical modelling in the context of the research objectives and provides an alternative approach to the complex models reviewed above and the one developed in Chapter 7.

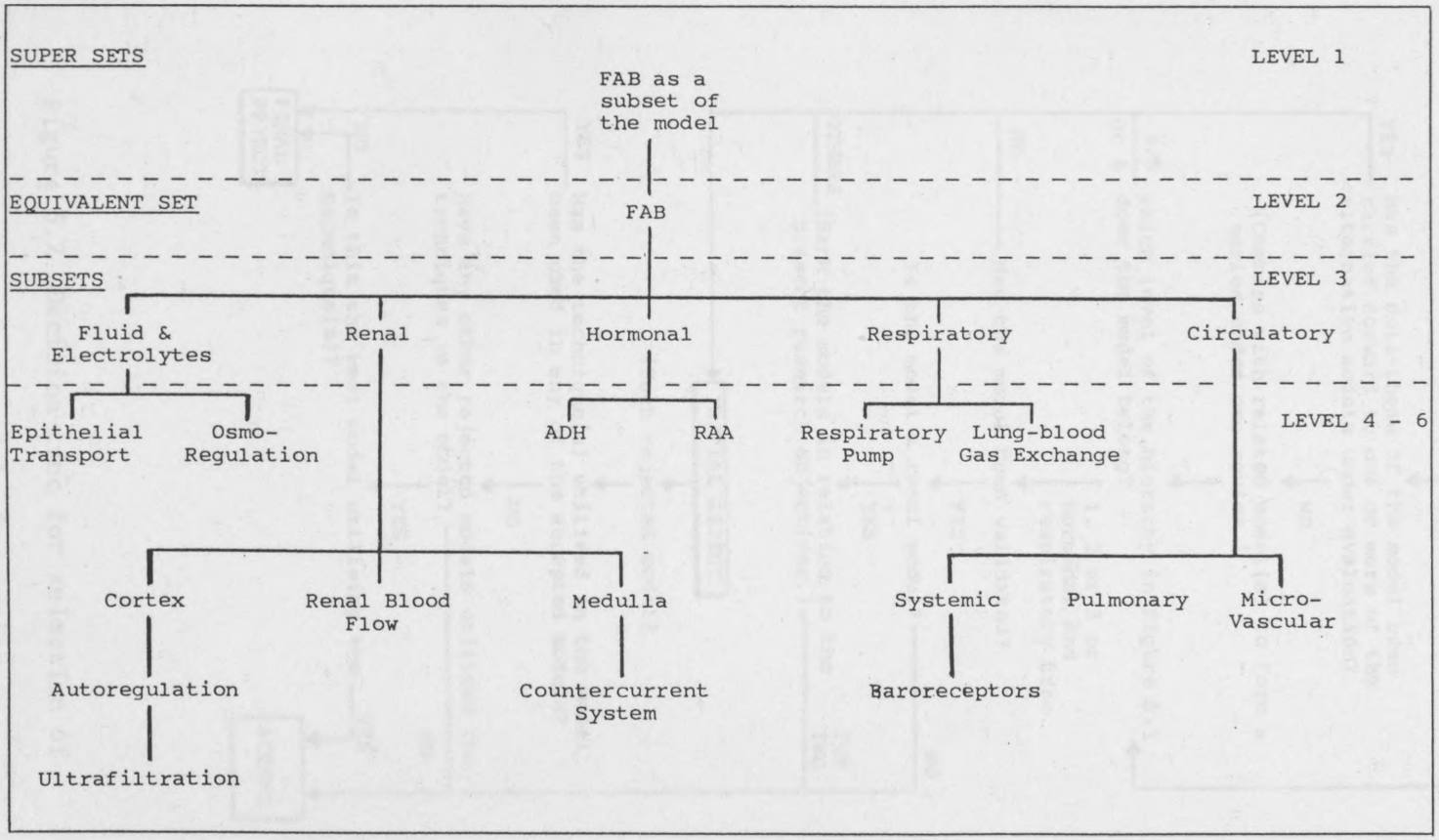

Figure 5.1 Breakdown of model types found during a critical review of extant quantitative FAB models.

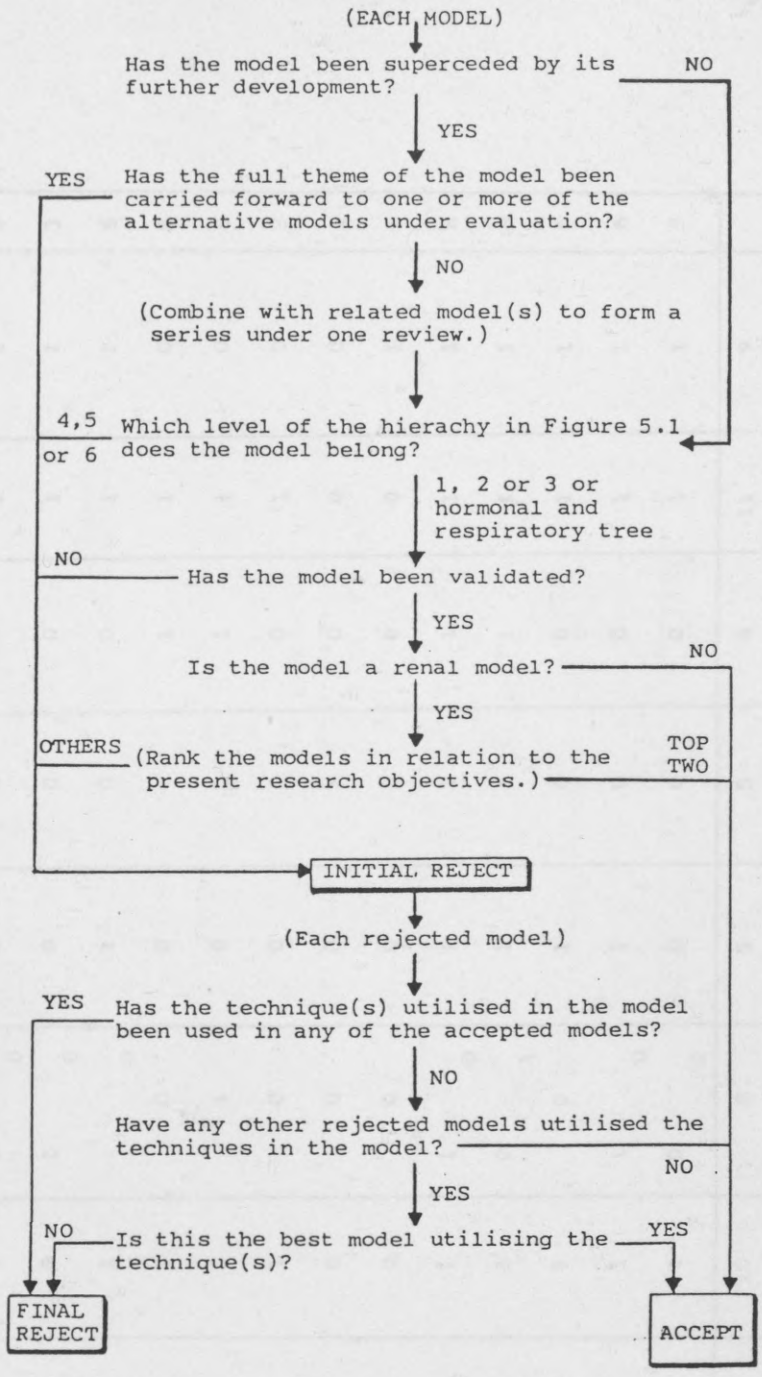

Figure 5.2 Decision-tree for selection of extant models for review

FIRST AUTHOR	ELECTRO-LYTE	ADH	RAA and ALD	VASCULAR CIRCULATION	LUNG GASES	ACID BASE	RENAL	CARDIO VASCULAR	Σ_r
Badke 1972	1	1	1 0	0	0	0	1	1	5
Blaine 1972	0	0	1 0	0	0	0	1	1	3
Cameron 1977	1	1	1 0	1	0	0	1	1	6
Dehaven 1967 - 73	1	1	0	0	1	1	1	0	5
Deland 1966 - 78	1	1	1	0	1	1	1	0	6
Fadali 1979	1	1	0	0	0	0	1	0	3
Grodins 1963	0	0	0	0	1	0	0	0	1
Guyton 1967	0	0	0	0	0	0	0	1	1
Guyton 1972	1	1	1 0	1	1	1	1	1	8
Ikeda 1979	1	1	0 1	1	1	1	1	1	8
Koushanpour 1977 - 82	1	1	0	1	0	0	1	1	5
Kuroda 1980	1	1	1 0	1	0	0	1	1	6
Toates 1970 - 77	1	1	0 1	0	0	0	1	1	5
Σ_c	10	10	8	5	5	4	11	9	

KEY: 0 = not modelled
1 = modelled
ALD = aldosterone

NOTE: '0' may imply this aspect is implicitly incorporated in the model.

Figure 5.3 Aspects of the FAB system represented in the models selected for review.

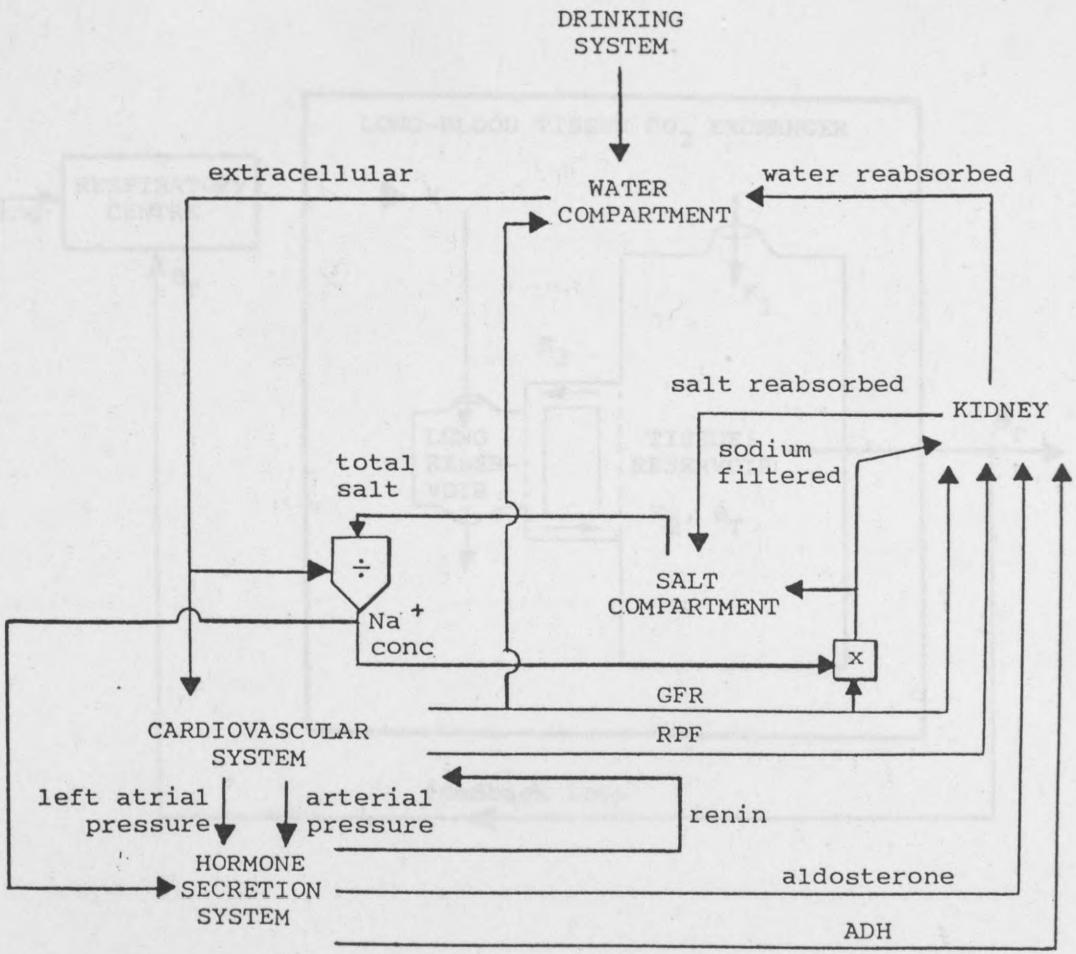

Figure 5.4 Main elements and relationships of Badke (1972).

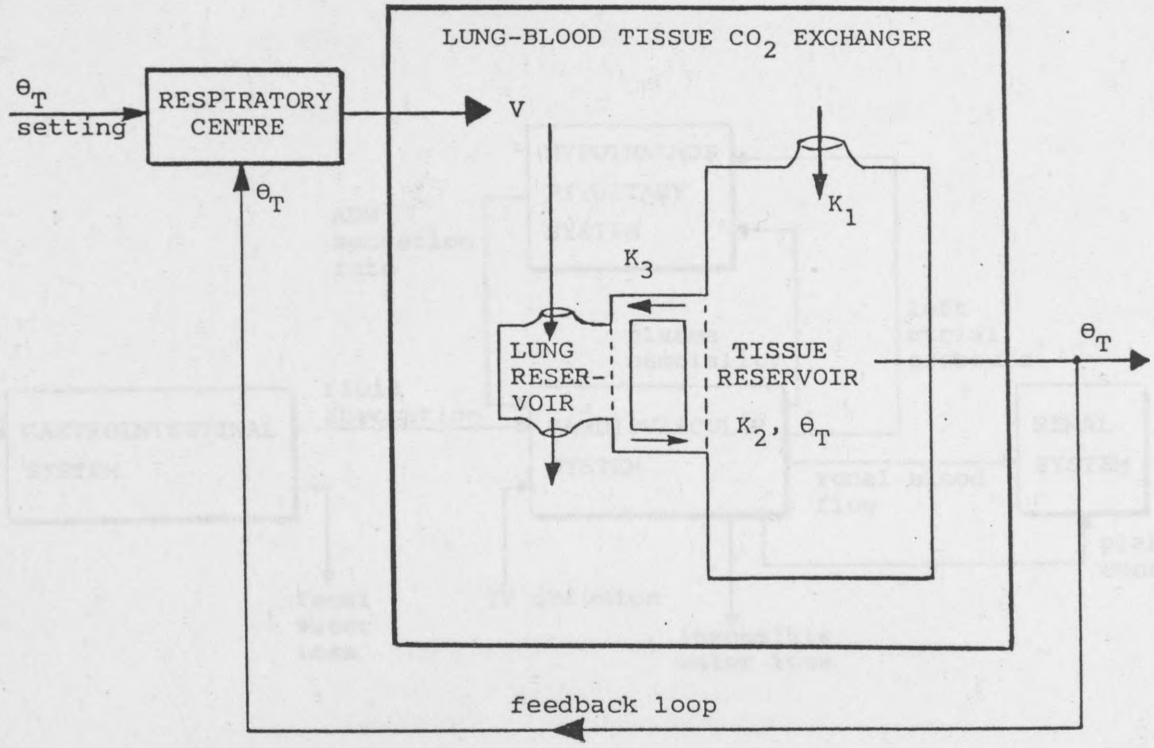

Figure 5.5 Compartmental structure of Grodins and James (1963).

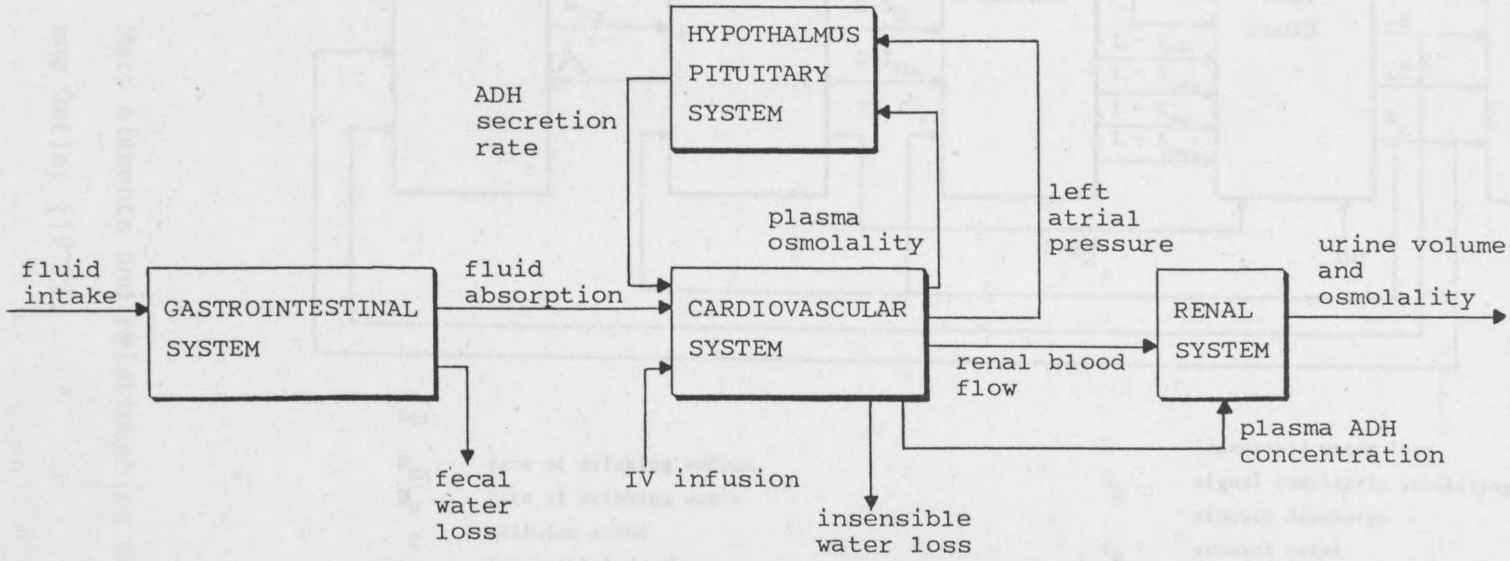

Figure 5.6 Main elements and relationships of Koushanpour and Stipp (1982).

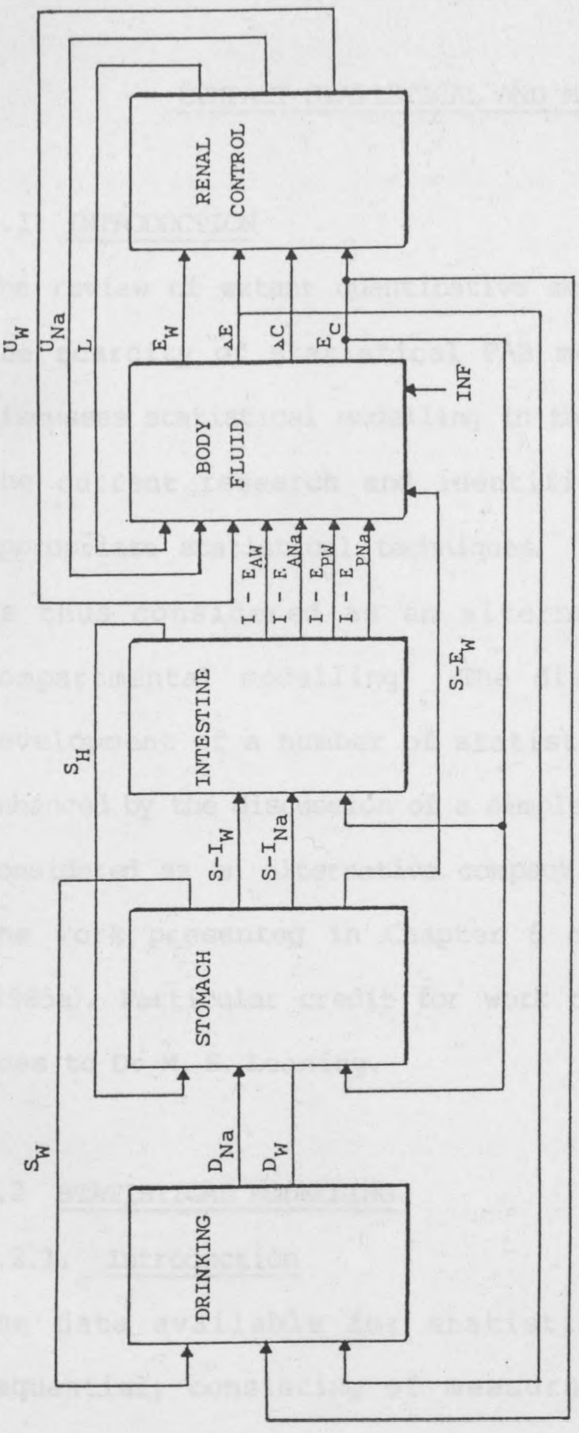

Key:

D_{Na}	rate of drinking sodium
D_W	rate of drinking water
C	cellular error
E	extracellular error
E_C	extracellular concentration of sodium
E_W	extracellular water
INF	infusion of sodium
$I - E_{ANa}$	active flow of sodium from intestine to ECF
$I - E_{AW}$	water carried by active sodium from intestine to ECF
$I - E_{PNa}$	passive flow of sodium between intestine and ECF
$I - E_{PW}$	passive flow of water between intestine and ECF
L	insensible water loss
S_H	signal completely inhibiting stomach discharge
S_W	stomach water
$S - E_W$	flow of water between stomach and ECF
$S - I_{Na}$	flow of sodium from stomach to intestine
$S - I_W$	flow of water from stomach to intestine
U_{Na}	urine sodium
U_W	urine water

Figure 5.7 Main elements and relationships of Toates and Oatley (1977).

CHAPTER 6

COMPACT STATISTICAL AND MATHEMATICAL MODELS

6.1 INTRODUCTION

The review of extant quantitative models in Chapter 5 highlighted the scarcity of statistical FAB models. Chapter 6 therefore discusses statistical modelling in the context of the objectives of the current research and identifies a number of potentially appropriate statistical techniques. Compact statistical modelling is thus considered as an alternative approach to complex compartmental modelling. The discussion is enhanced by the development of a number of statistical models, and is further enhanced by the discussion of a simple compartmental model which is considered as an alternative compact modelling approach. Much of the work presented in Chapter 6 can be found in Flood et al (1985a). Particular credit for work on the Extended Kalman Filter goes to Dr M. S. Leaning.

6.2 STATISTICAL MODELLING

6.2.1. Introduction

The data available for statistical analysis are typically sequential, consisting of measurements of blood and urine substances and other physiological variables. In general, these sequences and other physiological variables are generated in two modes. The first is laboratory based and has both a low data rate and a low sample size ($5 \leqslant n \leqslant 40$ is a typical range). The second arises in on-line monitoring, as in the ITU, and has a fast data rate and a large sample size ($n > 100$ would be expected).

The model-based techniques for estimation and prediction from data generated in both modes come under the heading of "Time-Series Analysis" (TSA). This section reviews the objectives of TSA, the approaches which are available under this heading, and identifies the particular techniques which (after analysis) appear to be most appropriate to the current research programme.

6.2.2 Time-Series Analysis (TSA)

The objectives of using TSA are for description, prediction and/or explanation (Chatfield, 1980). These are precisely the same purposes for mathematical modelling as stated by Finkelstein and Carson (1985). The essence of the latter workers' interpretation of those objectives (see 10.3.2) holds for statistical models. Statistical interpretation of the objectives (from Chatfield, 1980) are presented below.

(a) Description: obtaining simple descriptive measures of the main properties of the series.

(b) Prediction: given an observed time-series one may want to predict the future of the series. This may be closely associated to control, in that, if a movement away from a desired level is predicted then corrective action can be taken.

(c) Explanation: when observations are taken on two or more variables it may be possible to use one time-series to explain the variation in another series, therefore leading to a deeper understanding of the mechanisms which generate a given time-series.

The techniques available to help achieve these objectives can be considered under four headings:

(i) Simple descriptive techniques: by plotting data one can look for trends, seasonal fluctuations, outliers and turning points.

(ii) Probability models: using the autocorrelation function (see Appendix 4) to fit a model to the time-series and make inferences in the time domain.

(iii) Spectral analysis: using the spectral density function (not defined below as use has not been made of this method in the thesis) to fit a model to the time-series, with particular emphasis on cyclic components, and make inferences in the frequency domain.

(iv) Transfer function models: considering linear systems in which one series is considered an input series and another an output series.

The prediction element of the above discussion relates to the objectives of the current research (see Chapter 2 on feedforward control) so the task was to select an appropriate forecasting procedure. Of the four types of technique available spectral analysis (concentrating on cyclical aspects) was seen as relatively unimportant for these early investigations. The multivariate nature of the available data permitted the use of both univariate techniques (for which ARIMA modelling was selected; Box and Jenkins, 1976) and multivariate techniques (for which Transfer Function modelling was selected; Box and Jenkins, 1976). An

introduction to the theory of ARIMA modelling and Transfer Function modelling is presented in Appendix 4.

6.3 ARIMA MODELLING

6.3.1. Introduction

A file of critical care cases was made available at the Royal Free Hospital in London. Sample size was the most important criterion used in the selection of a case for analysis, as a small sample inevitably leads to sampling error. The longest time-series available was of a road traffic accident case where the patient remained in the ITU for 27 days. Measurements were taken once every 24 hours (sample step of 1 day); urine specimens were collected using a plain bottle and blood samples taken using the usual syringe method.

Two univariate time-series were selected for modelling; urine potassium concentration and plasma potassium concentration. The following subsection provides a detailed account of an ARIMA modelling exercise for urine potassium (the detail provides a step by step account which may prove useful to the unfamiliar modeller). The following subsection then presents only the essential details of the ARIMA modelling exercise for plasma potassium. A discussion of the findings is then presented.

The facilities available on MINITAB (a statistical software package) useful for ARIMA modelling are outlined in Appendix 4.

6.3.2. Urine Potassium Concentration

The extracted data are shown in Table 6.1. The reference range for urine concentration is 40-120 mmol l^{-1} (Staff of the Division of Pathology Royal Free Hospital Group, 1979).

The time-series plot (see Figure 6.1) shows two outliers which probably have arisen due to error in measurement. These could be removed by changing their actual values to their expected values,

t	1	2	3	4	5	6	7	8	9	10	11	12	13
X	54	67	141	74	63	87	91	72	93	65	58	55	56
t	14	15	16	17	18	19	20	21	22	23	24	25	26
X	57	61	92	E 68	71	80	53	57	53	15	63	E 68	68
t	27												
X	E 68												

Table 6.1 Urine potassium concentration, time-series data for road traffic accident (E means; set to expected value).

however, physiologically large changes can occur and it is difficult to determine whether the errors are due to poor measurement or physiological changes. For this reason the values were left unchanged. In addition there were three missing values which were set to their expected values.

TYPE	ESTIMATE	SD	t-RATIO
AR(1)	0.0978	0.2369	0.41
AR(2)	-0.1805	0.2287	-0.79
MA(1)	0.8531	0.1430	5.97

DIFFERENCING 1 SUM OF SQUARES = 11,052.9

DEGREES OF FREEDOM = 23 ORIGINAL SERIES = 27

AFTER DIFFERENCING = 26

Table 6.2 Final estimates of parameters of ARIMA(2,1,1) for urine potassium concentration data (initial parameters set by MINITAB).

TYPE	ESTIMATE	SD	t-RATIO
AR(1)	-0.6965	0.2069	-3.37
AR(2)	-0.7056	0.1560	-4.52
MA(1)	-0.0633	0.2779	-0.23

DIFFERENCING 1 SUMS OF SQUARES = 9,986.63

DEGREES OF FREEDOM = 23 ORIGINAL SERIES = 27

AFTER DIFFERENCING = 26

Table 6.3 Final estimates of parameters of ARIMA(2,1,1) for urine potassium concentration data (estimated initial parameters).

The correlogram of the raw data is shown in Figure 6.2. The autocorrelation function clearly damps out slowly, this implies non-stationarity of the series (which is not clear from the time-series plot of Figure 6.1). Consequently, the first differences of the series were taken. The autocorrelation function of this is shown in the correlogram of Figure 6.3. Using Bartlett's formula, the standard error ($SE(r_j)$) shows that only r_1 is significant. The partial-autocorrelation function of the first differences is shown in Figure 6.4 and the standard error test ($SE(\hat{\phi}_{jj})$) shows the first two values of the function are significant.

The interpretation of these functions is not clear cut; the autocorrelation function seems to suggest MA(1) whilst the partial-autocorrelation function seems to suggest AR(2). Furthermore, the significance of the first two partial-autocorrelations are higher than that of the first autocorrelation. ARIMA(2,1,1) was tentatively chosen with ARIMA(2,1,0) as an obvious alternative identification.

Maximum Likelihood Estimation (MLE) was the next methodological step. The ARIMA procedure on MINITAB works from initial parameter estimates of 0.1, but will allow the user to enter his own initial parameter estimates if so desired. In this first instance it was decided to compare the outcomes for both cases, thus initial parameter values had to be estimated from the autocorrelation function. This is detailed below.

For the MA part only one parameter had to be estimated:

$$r_1 = \frac{-\hat{\theta}_1}{1 + \hat{\theta}_1^2} \tag{6.1}$$

therefore:

$$\hat{\theta}_1 = \frac{1}{2r_1} \pm \left(\frac{1}{(2r_1)^2} - 1 \right)^{\frac{1}{2}} \tag{6.2}$$

so that:

$$\hat{\theta}_1 = 1.405 \pm 0.986 \tag{6.3}$$

To satisfy invertibility constraints and ensure the process is stable $|\hat{\theta}_1| < 1$ is necessary, therefore, -0.419 was chosen. For the autoregressive part, two parameters had to be estimated by solving the Yule-Walker equations:

$$\left.\begin{aligned} r_1 &= \hat{\phi}_1 + \hat{\phi}_2 r_1 \\ r_2 &= \hat{\phi}_1 r_1 + \hat{\phi}_2 \end{aligned}\right\} \tag{6.4}$$

so that $\hat{\phi}_1 = -0.492$ and $\hat{\phi}_2 = -0.382$ and $\hat{\phi}_1 + \hat{\phi}_2 = -0.874$ which is within the invertible limit.

The final parameter estimates after MLE, with initial parameters all at 0.1, are shown in Table 6.2; and with initial parameters estimated from the autocorrelation function are shown in Table 6.3. The confidence intervals respectively are:

$$\left.\begin{aligned} -0.367 < \phi_1 &< 0.572 \\ -0.629 < \phi_2 &< 0.268 \\ 0.567 < \theta_1 &< 1.139 \end{aligned}\right\} \tag{6.5}$$

and:

$$\left.\begin{aligned} -1.102 < \phi_1 < -0.291 \\ -1.011 < \phi_2 < -0.400 \\ -0.608 < \theta_1 < 0.481 \end{aligned}\right\} \qquad (6.6)$$

For the first set of confidence intervals there is less than 95 percent confidence that $|\hat{\theta}_1| < 1$ and $\hat{\phi}_1 + \hat{\phi}_2 = -0.996$ at the lower extremity of the interval which is near the invertible limit. For the second set of confidence intervals, at the lower extremity $\hat{\phi}_1 + \hat{\phi}_2 = -2.113$ which is non-convergent and thus unsatisfactory. For the first case the t-ratio is only significant for $\hat{\theta}_1$, in the second case the situation is reversed as only $\hat{\phi}_1$ and $\hat{\phi}_2$ are shown to be significant. Some of these problems are undoubtedly due to the small sample size.

As an example, the forecast for l=12 moments ahead using the final parameter estimates of Table 6.2 is detailed in Table 6.4, and is appended to the initial data in the time-series plot of Figure 6.5. The forecast is sinusoidal ($\hat{\phi}_1^2 + 4\hat{\phi}_2 < 0$) and heavily damped. The profile of the forecast approaches the mean of the forecast process as a limit since the further into the future the model predicts, the less influence the past history will have:

$$\lim_{l \to \infty} \hat{x}_t(l) = \mu \qquad (6.7)$$

PERIOD	FORECAST	95 PERCENT LIMITS	
28	61.80	18.82	104.78
29	61.31	16.89	105.37
30	62.31	18.06	106.55
31	62.54	18.08	107.00
32	62.35	17.38	107.33
33	62.29	16.89	107.70
34	62.32	16.56	108.08
35	62.34	16.22	108.45
36	62.33	15.84	108.82
37	62.33	15.48	109.18
38	62.33	15.12	109.54
39	62.33	14.76	109.90

Table 6.4 12 day forecast of urine potasium concentration using ARIMA(2,1,1) and parameters pre-MLE set by MINITAB.

Note that the 95 percent confidence limits are unsatisfactory.

An alternative process has been postulated as ARIMA(2,1,0). This is considered below both with and without the inclusion of a constant in the process. The final parameter estimates are consolidated respectively in Table 6.5 and Table 6.6. The confidence intervals respectively are:

$$\left.\begin{aligned} -0.943 < \phi_1 < -0.352 \\ -0.971 < \phi_2 < -0.392 \end{aligned}\right\} \qquad (6.8)$$

and

$$\left.\begin{aligned} -0.947 < \phi_1 < -0.331 \\ -0.984 < \phi_2 < -0.380 \end{aligned}\right\} \qquad (6.9)$$

TYPE	ESTIMATE	SD	t-RATIO
AR(1)	-0.6476	0.1506	-4.30
AR(2)	-0.6817	0.1478	-4.61
DIFFERENCING 1 SUM OF SQUARES = 10,035.8			
DEGREES OF FREEDOM = 24 ORIGINAL SERIES = 27			
AFTER DIFFERENCING = 26			

Table 6.5 Final estimates of parameters of ARIMA (2,1,0) for urine potassium concentration (estimated initial parameters).

TYPE	ESTIMATE	SD	t-RATIO
AR(1)	-0.6390	0.1539	-4.15
AR(2)	-0.6822	0.1509	-4.52
Constant	-1.381	4.104	-0.34
DIFFERENCING 1 SUM OF SQUARES 10,049.9			
DEGREES OF FREEDOM = 23 ORIGINAL SERIES = 27			
AFTER DIFFERENCING = 26			

Table 6.6 Final estimates of parameters of ARIMA $(2,1,0)\delta$ for urine potassium concentration (initial parameters set by MINITAB).

In both cases there is less than 95 percent confidence at the lower extremities of the interval that $\left|\hat{\phi}_1 + \hat{\phi}_2\right| < 1$. Confidence on convergence is thus not good. In the first case the t-ratio shows that both AR parameters are significantly different from zero, which is also true of the second case, however, the constant is not significantly different from zero. The sums of the squares of both cases approximate those found in Table 6.3 and are improved on those in Table 6.2.

As an example, the forecast for l=12 moments ahead using the final parameter estimates of Table 6.6 is detailed in Table 6.7, and is appended to the initial data in the time-series plot of Figure 6.6.

PERIOD	FORECAST	95 PERCENT LIMITS	
28	67.32	26.34	108.30
29	66.82	23.25	110.39
30	66.70	22.99	110.41
31	65.74	13.50	117.98
32	65.05	9.02	121.09
33	64.77	8.09	121.45
34	64.04	3.34	124.73
35	63.32	-1.01	127.64
36	62.89	-2.64	128.43
37	62.27	-5.80	130.35
38	61.58	-9.56	132.72
39	61.07	-11.68	133.81

Table 6.7 12 day forecast of urine potassium concentration using ARIMA (2,1,0)& and parameters pre-MLE set by MINITAB.

The forecast is sinusoidal and heavily damped with a drift (caused by δ). The steepness of the trend is the significant feature of this process, however, the 95 percent confidence limits are extremely unsatisfactory.

The better model of the above quadret appears to be ARIMA (2,1,0) using estimated parameters for MLE. This gives rise to:

$$x_t = -0.6476.x_{t-1} - 0.6817.x_{t-2} + U_t \qquad (6.10)$$

The final stage of the methodology requires some diagnostic checks. The method to be used will either confirm or reject the proposed model. Initially, the proposed model was hypothesised as having one extra parameter on p and then on q, and hence the t-ratio of the final estimate for those parameters was considered for significance. The result for the hypothesis $q=q^*+1$ (where q^* is the initial identification of q) has been discussed above, where the addition is not seen as significant for the estimated initial parameters. Thus ARIMA (2,1,1) can be rejected in favour of ARIMA (2,1,0). A similar check with the autoregressive part also showed insignificance and thus ARIMA (3,1,0) can be rejected in favour of ARIMA (2,1,0). The proposed model is thus confirmed.

Furthermore, if the modelling exercise has succeeded in transforming the observed data to random noise, then the residuals would have the properties of random numbers. This was confirmed as the sample autocorrelation of the residuals did not show serial correlation.

6.3.3 Plasma Potassium Concentration

The extracted data are shown in Table 6.8. The reference range for plasma potassium concentration is 3.8-5.0 mmol l^{-1} (Staff of the Division of Pathology Royal Free Hospital Group, 1979).

t	1	2	3	4	5	6	7	8	9	10	11	12	13	14
χ	3.6	3.4	4.0	4.0	3.5	3.6	4.1	3.7	3.5	3.4	3.4	3.4	3.5	3.9
t	15	16	17	18	19	20	21	22	23	24	25	26	27	
χ	3.6	3.6	3.3	3.4	3.7	3.9	3.4	3.6	3.5	3.1	3.6	3.7	3.2	

Table 6.8 Plasma potassium concentration, time-series data for road traffic accident. χ is plasma potassium concentration (mmol l^{-1}).

The time-series plot (see Figure 6.7) has no distinct outliers, however, the series appears to have a non-stationary downward trend which takes the series out of the reference range from t=21 onwards. This was confirmed in the (estimated) autocorrelation function (not shown). The autocorrelation and partial autocorrelations, after the first differencing of the series, are as depicted in Figures 6.8 and 6.9 respectively. The autocorrelation r_j falls off quickly after j=2 suggesting an MA(2) process, and the 95 percent confidence limits on this hypothesis show that values r_3, r_4,... are not significantly different from

zero. This finding is confirmed in the partial autocorrelation function $\hat{\phi}_{jj}$ which decays more slowly. The tentative model identification is thus ARIMA(0,1,2) δ.

Initial estimates of θ_1 and θ_2 were made from r_1 and r_2, however, these estimates were found to lie outside of the invertible region. This was probably due to large errors on r_j due to the small sample size. Allowing for an approximate standard error of 0.2 (based on $n^{-1/2}$) the invertible ranges for $\hat{\theta}_1$ and $\hat{\theta}_2$ are $0 < \theta_1 < 0.7$ and $0.25 < \theta_2 < 1.0$.

MINITAB was used to estimate the parameters of the model (using MLE and the starting value $\hat{\theta}_1 = 0.4$ and $\hat{\theta}_2 = 0.6$). The results are shown in Table 6.9.

TYPE	ESTIMATE	SD	t-RATIO
MA(1)	0.589	0.264	2.26
MA(2)	0.360	0.264	1.39
Constant	-0.0103	0.0096	-1.07
DIFFERENCING 1 SUM OF SQUARES 1.393			
DEGREES OF FREEDOM = 23 ORIGINAL SERIES = 27			
AFTER DIFFERENCING = 26			

Table 6.9 Final estimates of parameters of ARIMA $(0,1,2)\delta$ for plasma potassium concentration data (estimated initial parameters).

The errors of the estimates are fairly high and the estimates are near the invertible region ($\hat{\theta}_1+\hat{\theta}_2=0.949$). These problems are again due to the small sample size. The fitted model is thus:

$$x_t = -0.0103 + U_t - 0.589U_{t-1} - 0.36U_{t-2} \qquad (6.11)$$

In diagnostic checking the residuals of the model were found not to be serially correlated. A number of mixed models ($p\neq0, q\neq0$) with $p=5$ (based on the partial autocorrelation function) were considered, but these did not significantly reduce the sum of the squares and consequently were rejected. As an example, the forecasts for $l=20$ moments ahead for ARIMA$(0,1,2)\delta$ are shown in Figure 6.10.

6.3.4 Discussion

In the examples presented above, ARIMA models were fitted to two sequences of $n=27$ clinical data points. The forecast of the models appear reasonable, although these are not necessarily unique.

As the standard error of the autocorrelation estimate is approximately equal to $n^{-1/2}$, it is generally accepted that at least 50 data points are required in ARIMA modelling (Box and Jenkins, 1976). During on-line patient monitoring with frequent sampling this size is readily achievable, however, in data derived from laboratory results much sparser time-series are typically found.

For clinical implementation, given acceptable data rates, there remains the problem of model identification. This depends upon interpretation of the autocorrelation and partial autocorrelation functions and has a subjective element. "The interpretation of correlograms is one of the hardest aspects of time-series analysis and practical experience is a must" (Chatfield, 1980). This is not likely to become the norm for all but a few clinical staff. Automatic identification may be included in parameter estimation by selecting a model which minimises the Akaike Information Criterion (-2 ln. (maximised likelihood) +2) but a unique minimum cannot be guaranteed (Chatfield, 1980).

Other limitations of ARIMA modelling are its univariate nature and adoption of linear models. In addition, long-term clinical data are likely to contain seasonal variations at different frequencies, however, seasonal ARIMA models can handle this type of data (Box and Jenkins, 1976).

6.4 TRANSFER FUNCTION (TF) MODELLING

6.4.1 Introduction

The univariate ARIMA approach cannot take into account relations between different time-series which may be of clinical importance. For instance, in subsection 6.3.3 a falling plasma potassium concentration was forecast. If this was the only change in the patient it might have been important. However, if it had been counterbalanced by other changes (such as rising plasma sodium) it would have been of little significance. One form of bivariate relation, where one time-series corresponds to an input and another

time-series to an observable effect, or output can be investigated using discrete time TF models. Such models allow the dynamic response of the patient to be determined and hence better control exercised. Examples include control of fluid and other intakes, and drug infusions. An approach to TF modelling was developed by Box and Jenkins (1976) along the lines of their ARIMA methodology (both described in Appendix 4). As with ARIMA models, Box and Jenkins define three stages in TF model building: identification; estimation; and diagnostic checking.

Box and Jenkins stated that when the effect of noise is appreciable (which will mostly be the case for clinical measurements) a delayed first or second order system of the type:

$$y_t = \delta^{-1}(B)\ \omega(B) x_{t-b} \qquad (6.12)$$

would provide as elaborate a model as could be justified for those data. Therefore, where a choice arose, compact models were selected.

The following subsection provides a detailed account of a TF modelling exercise for drinking rate (input) and urine sodium concentration (output). A detailed account of the construction of one possible model is included (the detail provides a step by step account which may prove useful to the unfamiliar modeller). A second simpler model is then presented with only the essential details. An exercise on recursive estimation of the model parameters is followed by a discussion of the findings from the TF

modelling efforts. Details on TF models and recursive estimation can be found in Appendix 4 and Appendix 5 respectively.

6.4.2 Urine Sodium Response To Water Intake

Figure 6.11 shows the time-series "data" for water input (X_t) and urine sodium output (Y_t) with n=100. The data illustrate the way that sodium is selectively excreted in the control of total body water. The two series were obtained from a comprehensive simulation model of FAB dynamics in the human (Flood et al, 1984b) a later version of which is described in Chapter 7. This is acceptable only in that:

(a) there is currently a paucity of data for n > 30;

(b) it is the principle of the technique which is being tested, thus, as long as the data are physiologically realistic (see the validation carried out by Flood et al, 1984b) then the principle can be tested;

(c) the input can be pre-whitened (by the addition of a time-series of identically and independently distributed random disturbances with mean zero) and the output whitened;

(d) all input variables of the model may be held constant whilst the input variable of interest is varied.

The input data X_t were generated using the following function:

$$\text{Water intake} = 0.0013+0.000076R(t) \qquad (6.13)$$

where, R(t) is the pre-whitened component produced by a random number generator in the range [-5,5], the constant prefix on R(t) is used to ensure satisfaction of the constraint:

$$\text{Water intake} \geq 0 \qquad (6.14)$$

Output for urine sodium was directly accessible from computer simulation. Thus, in this investigation the nature of the input disturbance is known, however, the proceeding work assumes that it were not.

MINITAB was used to assess the type and order of the input time-series as an ARIMA process. The correlogram of the raw data (not shown) decays slowly whilst the partial autocorrelation plot (not shown) spikes at lag 1 and then tails off. This seemed to suggest an ARIMA(1,0,0) process. Taking t-ratios of the final estimates for parameters of ARIMA(2,0,0) showed that $\hat{\phi}_2$ was significantly different from zero (t-ratio of 1.02) however, the addition of a ϕ_3 or θ_1 term on the two previous processes proved to be insignificant by the t-ratios. The sums of the squares for ARIMA(1,0,0) and ARIMA(2,0,0) were not significantly different. An ARIMA(2,0,0) process was tentatively selected as being representative (although there was pressure to develop a simpler ARIMA(1,0,0) model).

A detailed account of a TF modelling exercise based on an ARIMA(2,0,0) process for the input is presented below. This is followed by the essential details of a TF modelling exercise, based on an ARIMA (1,0,0) process for the input.

Considering ARIMA(2,0,0) MINITAB was used to derive the following final parameter estimates: $\hat{\phi}_1 = 0.8676$ and $\hat{\phi}_2 = 0.1305$ with $\left| \hat{\phi}_1 + \hat{\phi}_2 \right| < 1$ although it does lie close to the invertibility limit. This suggests n=100 may be too small a sample size. The 95 percent confidence intervals were found to be:

$$\left.\begin{aligned} 0.6632 < \phi_1 < 1.072 \\ 0.0995 < \phi_2 < 0.3335 \end{aligned}\right\} \qquad (6.15)$$

so that the upper range of the confidence interval lies outside of the invertibility limit.

Thus, an input process $x_t = \nabla^0 X_t$ has been identified which is suitably stationary and can be represented by ARIMA (2,0,0) which is a member of the general linear class of autoregressive - moving average models. Using this process, any input series x_t can be transformed to an uncorrelated white noise series α_t:

$$(1-0.8676B-0.1305B^2)x_t = \alpha_t \qquad (6.16)$$

This may also be applied to y_t($\nabla^0 Y_t$) to obtain the uncorrelated white noise series β_t:

$$(1-0.8676B-0.1305B^2)y_t = \beta_t \qquad (6.17)$$

By realising the two series:

$$\left.\begin{aligned} \alpha_t &= x_t-0.8676x_{t-1}-0.1305x_{t-2} \\ \beta_t &= y_t-0.8676y_{t-1}-0.1305y_{t-2} \end{aligned}\right\} \qquad (6.18)$$

the standard deviation $\sigma_\alpha = 3.78 \times 10^{-4}$ and $\sigma_\beta = 1.36 \times 10^{-4}$ were derived. Therefore $\sigma_\beta/\sigma_\alpha = 0.36$ and thus the estimate of the impulse response function is:

$$0.36\, r_{\alpha\beta}(k) = \hat{\nu}_k \qquad (6.19)$$

From here MINITAB was used to generate the cross-correlations for $\alpha(t)$ and $\beta(t+k)$, with k representing the lag. In addition and for simplicity sake, the standard error was assumed to be $n^{-1/2}$ (0.1 for 100 samples). The results are shown in Table 6.10 where the impulse response function has also been calculated.

k	0	1	2	3	4	5	6	7	8	9	10
$r_{\alpha\beta}$	.03	.13	-.14	.13	.36	.14	.28	.30	.26	.14	-.04
SE	.10	.10	.10	.10	.10	.10	.10	.10	.10	.10	.10
$\hat{\nu}_k$	.01	.05	-.05	.05	.13	.09	.10	.11	.10	.05	-.02

Table 6.10 Cross-correlations, standard error and impulse responses of urine sodium response to water intake fitted to an ARIMA(2,0,0) process.

The values of $r_{\alpha\beta}(k)$ for k=0,...,3 are small compared with their errors, implying b=4. The estimated impulse response function is plotted in Figure 6.12. Comparing this impulse response function to examples given by Box and Jenkins (1976) the appropriate model appears to be (r,s,b)=(2,1,4), that is:

$$(1-\delta_1 B-\delta_2 B^2) y_t = (\omega_0-\omega_1 B) x_{t-4} \qquad (6.20)$$

Parameters were estimated from the following set of equations:

$$\left.\begin{array}{ll} 0 & j < b \\ \omega_0 & j = b \\ \delta_1\omega_0-\omega_1 & j=b+1 \\ \delta_1 \nu_{j-1}+\delta_2 \nu_{j-2} & j > b+1 \end{array}\right\} \qquad (6.21)$$

so that $\hat{\omega}_0 = \nu_4 = 0.13$ and:

$$\left.\begin{aligned} \delta_1(0.13)-\omega_1 &= \nu_5 = 0.09 \\ \delta_1(0.09)+\delta_2(0.13) &= \nu_6 = 0.10 \\ \delta_1(0.10)+\delta_2(0.09) &= \nu_7 = 0.11 \end{aligned}\right\} \quad (6.22)$$

thus $\hat{\delta}_1=1.08$, $\hat{\delta}_2=0.02$ and $\hat{\omega}_1=0.05$

The initial model identification was therefore:

$$(1-1.08B-0.02B^2)y_t=(0.13-0.05B)x_{t-4} \quad (6.23)$$

so that

$$Y_t = \frac{(0.13-0.05B)}{(1-1.08B-0.02B^2)} x_{t-4} \quad (6.24)$$

For this second order model, stability will only occur if the following constraints are satisfied:

$$\left.\begin{aligned} \delta_2 + \delta_1 &< 1 \\ \delta_2 - \delta_1 &< 1 \\ -1 < \delta_2 &< 1 \end{aligned}\right\} \quad (6.25)$$

however, the first constraint is not satisfied. For this reason, the alternative model $(r,s,b)=(2,0,4)$ was considered. The parameters were estimated using the following set of equations:

$$\left.\begin{aligned} 0 \qquad & j < b \\ \omega_0 \qquad & j = b \\ \delta_1\nu_{j-1}+\delta_2\nu_{j-2} \qquad & j > b+1 \end{aligned}\right\} \quad (6.26)$$

so that $\hat{\omega}_0= \nu_4=0.13$ and:

$$\left.\begin{aligned} \delta_1(0.13)+\delta_2(0.05) &= \nu_5 = 0.09 \\ \delta_1(0.09)+\delta_2(0.13) &= \nu_6 = 0.10 \end{aligned}\right\} \quad (6.27)$$

thus $\hat{\delta}_2=0.395$ and $\hat{\delta}_1=0.54$, thus the set of constraints (6.26) were satisfied ensuring stability.

Thus the following model has been identified:

$$(1-0.54B-0.395B^2)y_t = 0.13x_{t-4} \tag{6.28}$$

so that:

$$y_t = \frac{0.13}{(1-0.54B-0.395B^2)} x_{t-4} \tag{6.29}$$

The steady-state gain of the model in terms of its parameters (if x_t were held at unity) is:

$$g = \frac{\hat{\omega}_o}{1-\hat{\delta}_1-\hat{\delta}_2} \tag{6.30}$$

that is, y_t at a steady rate of 2.0.

The nature of this second order system can be assessed by calculating the roots of its characteristic equation. Alternatively, as $\delta_1^2+4\delta_2 > 0$ it is known that the roots are real and the model is "overdamped". Thus the response of this model will be asymptotic to a new steady-state following stress.

Identification of the noise model was made by assuming:

$$y_t = \nu(B)x_t+n_t \tag{6.31}$$

where $n_t = \nabla^d N_t$, so that:

$$\hat{n}_t=y_t- \hat{\nu}(B)x_t \tag{6.32}$$

Noise was identified by using the correlation functions for the input and output (after pre-whitening) by using the following equation derived by Box and Jenkins (1976).

$$\rho_{\varepsilon\varepsilon}(k) = \frac{\rho_{\beta\beta}(k) - \sum_{j=o}^{\infty} \rho_{\alpha\beta}(j)\rho_{\alpha\beta}(j+k)}{1 - \sum_{j=o}^{\infty} \rho^2_{\alpha\beta}(j)} \tag{6.33}$$

In reality only rough estimates of $\rho_{\varepsilon\varepsilon}(k)$, $r_{\varepsilon\varepsilon}(k)$, can be made using the estimated functions $r_{\alpha\beta}(k)$ and $r_{\beta\beta}(k)$. The results of applying this identification procedure are shown in Table 6.11

k	0	1	2	3	4	5	6	7	8
$r_{\beta\beta}$	1.0	0.38	0.34	0	0	0	0	0	0
$r_{\alpha\beta}$	0	0	0	0	0.36	0	0.28	0.30	0.26
$r_{\varepsilon\varepsilon}$	1.0	0.44	0.34	0.02	0	0	0	0	0

Table 6.11 Estimation of noise for ARIMA(2,0,0) process using correlation functions. (Small values set to 0).

From the $r_{\varepsilon\varepsilon}$ function a second order noise model was postulated as $r_{\varepsilon\varepsilon} > 2$ is not significant. It was postulated that the process is autoregressive (no clear directions have been given by Box and Jenkins) therefore:

$$(1-0.44B-0.34B^2)\varepsilon_t = a_t \qquad (6.34)$$

and since:

$$(1-0.54B-0.395B^2)N_t = \varepsilon_t \qquad (6.35)$$

by substituting (6.35) into (6.34) the following equation was formulated:

$$(1-0.44B-0.34B^2)(1-0.54B-0.395B^2)N_t = a_t \qquad (6.36)$$

so that the complete model becomes:

$$y_t = \frac{(0.13)x_{t-4}}{(1-0.54B-0.395B^2)} + \frac{a_t}{(1-0.98B-0.497B^2+0.354B^3+0.13B^4)} \qquad (6.37)$$

where all $\hat{\phi}$'s and $\hat{\theta}$'s are approximate starting values.

It has been previously suggested that an ARIMA(1,0,0) process might be appropriate for the given data:

$$(1-\phi_1 B)X_t = \alpha_t \qquad (6.38)$$

where $\hat{\phi}_1 = 0.96$. Since $(1-0.96B) \simeq (1-B)$, the indications are that X_t was generated by a random walk process:

$$X_t = X_{t-1} + \alpha_t \qquad (6.39)$$

The pre-whitened series α_t and transformed output series β_t were thus obtained by simple differencing:

$$\alpha_t = \nabla^1 X_t; \qquad \beta_t = \nabla^1 y_t \qquad (6.40;\ 6.41)$$

The standard deviations were $\sigma_\alpha = 0.405 \times 10^{-3}$ and $\sigma_\beta = 0.14 \times 10^{-3}$. The estimated cross-correlation function $r_{\alpha\beta}(k)$ and an approximate estimate of its standard error (SE) are given in Table 6.12 along with the estimated impulse function $\hat{\nu}_k$.

The values of $r_{\alpha\beta}(k)$ for k=0,...,3 are small compared with their SE which implies b=4. The estimated impulse function is plotted in Figure 6.13. Identification of r and s on this data is not clear cut. The drop at $\hat{\nu}_5$ between $\hat{\nu}_4$ and $\hat{\nu}_6$ is not realisable in a physical system. This effect is probably due to the large estimation errors $\hat{\sigma}_r$ in comparison with $r_{\alpha\beta}$, despite what is considered to be a reasonable sample size.

A first order model (1,0,4) was postulated as an approximate description, which leads to:

$$(1-0.75B)y_t = 0.1x_{t-4} \qquad (6.42)$$

k	0	1	2	3	4	5	6	7	8	9	10
$r_{\alpha\beta}$	-.095	.035	-.108	-.003	.234	.151	.321	.125	.074	-.094	-.127
SE	0.1	0.1	0.1	0.1	0.1	0.1	0.1	0.1	0.1	0.1	0.1
$\hat{\nu}_k$	-.033	.012	-.038	-.001	.082	.053	.112	.044	.026	-.033	-.045

Table 6.12 Cross-correlations, standard error and impulse responses of urine sodium response to water intake fitted to an ARIMA(1,0,0) process.

k	0	1	2	3	4	5	6	7	8	9	10
$r_{\beta\beta}$	1.0	.326	0	0	0	0	0	0	0	0	0
$r_{\alpha\beta}$	0	0	0	0	.234	0	.321	0	0	0	0
$r_{\varepsilon\varepsilon}$	1.0	.387	0	0	0	0	0	0	0	0	0

Table 6.13 Estimation of noise for ARIMA(2,0,0) process using correlation functions, (Small values set to 0).

with a steady-state gain of 0.4 in terms of its parameters. However, the characteristic impulse function of a (2,2,4) model is an alternative possibility, see Figure 6.13.

Identification of the noise model from $r_{\alpha\beta}(k)$, $r_{\beta\beta}(k)$ and $r_{\varepsilon\varepsilon}(k)$ (see Table 6.13) suggested a first order noise model as $r_{\varepsilon\varepsilon} > 1$ is not significant. It was postulated that the process is autoregressive, therefore:

$$(1-.387B)\varepsilon_t = a_t \tag{6.43}$$

and since:

$$(1-0.75B)N_t = \varepsilon_t \tag{6.44}$$

the following equation was formulated:

$$(1-.387B)(1-0.75B)N_t = a_t \tag{6.45}$$

so that the complete model becomes:

$$y_t = \frac{(0.1)x_{t-4}}{(1-0.75B)} + \frac{a_t}{(1-1.137B+0.29B^2)} \tag{6.46}$$

By algebraic manipulation of (6.37), based on ARIMA(2,0,0) of the input data, the following representation was achieved:

$$y_k = \underline{Z}_k^T \hat{\underline{a}} + e_k \tag{6.47}$$

where:

$$\underline{Z} = \begin{bmatrix} y_{t-1} \\ y_{t-2} \\ y_{t-3} \\ y_{t-4} \\ y_{t-5} \\ x_{t-4} \\ x_{t-5} \end{bmatrix} \quad ; \quad \hat{\underline{a}} = \begin{bmatrix} 1.520 \\ 0.362 \\ -1.000 \\ -0.135 \\ 0.210 \\ 0.130 \\ -0.127 \end{bmatrix} \tag{6.48; 6.49}$$

and similarly, manipulation of (6.46) based on an ARIMA (1,0,0) process for the input data gave:

$$\underline{Z} = \begin{bmatrix} y_{t-1} \\ y_{t-2} \\ y_{t-3} \\ x_{t-4} \\ x_{t-5} \end{bmatrix} \quad ; \quad \underline{\hat{a}} = \begin{bmatrix} 1.887 \\ -1.151 \\ 0.224 \\ 0.100 \\ -0.114 \end{bmatrix} \qquad (6.50;\ 6.51)$$

For equations (6.48; 6.49) and (6.50; 6.51) the following holds:

$$e_k = y_k - \hat{y}_{k/k+1} \qquad (6.52)$$

and:

$$\hat{y}_{k/k+1} = \underline{Z}_k^T \underline{\hat{a}}_{k-1} \qquad (6.53)$$

Assuming no error, equations (6.48; 6.49) and (6.50; 6.51) predict y_6 as 0.1148 and 0.1151 respectively, which appear reasonable.

Given a situation where a continuing data supply can be expected, the inclusion of a recursive estimator on $\underline{a}$ may well be of value. Young (1974) developed a recursive estimator for TF models (see Appendix 5 for details). The updating equations are:

$$\underline{\hat{a}}_k = \underline{\hat{a}}_{k-1} - \frac{P_k^*}{\sigma^2}\left[\underline{X}_k \underline{X}_k^T \underline{\hat{a}}_{k-1} - \underline{X}_k Y_k\right] \qquad (6.54)$$

and:

$$P_k^* = P_{k-1}^* - P_{k-1}^* \underline{X}_k \left[\sigma^2 + \underline{X}_k^T P_{k-1}^* \underline{X}_k\right]^{-1} \underline{X}_k^T P_{k-1}^* \qquad (6.55)$$

The initial conditions for $\underline{\hat{a}}_0$ may be set at those estimated above, or, $\underline{\hat{a}}_0 = [0]$. The initial conditions for $P_0 = \text{diag}[10^5, \ldots, 10^5]$ which

reflects the uncertainly. σ^2, the variance of the sequence of errors, should be set at:

$$\sigma^2 = E(\varepsilon^2 y_i) \tag{6.56}$$

that is the noise on the raw data. In practice, however, σ^2 can acceptably be set at 10 percent of E(y). The tracking of four of the model parameters of the system described by equations (6.48; 6.49) is shown in Figure 6.14 and the output of the model against the patient data is shown in Figure 6.15

The parameters remain close to their true values except for $\hat{a}_7$ (and $\hat{a}_6$ not shown) whose values show a steady fall. These parameters relate to inputs rather than outputs. The depiction of model outputs against the simulated data shows an initial prediction without correction well below the simulated data, this improves substantially on the following prediction with correction. The fit remains very good for the next 22 days from whence on a continual underestimate begins to show. This in fact becomes more prominent after 50 days (not shown).

The source of these problems is difficult to identify. Young (1974) stated that the recursive algorithm in fact generates a bias which could have led to drift on $\hat{a}_6$ and $\hat{a}_7$. Alternatively, the invertibility limit was approached during parameter estimation and may have been crossed as parameters were updated.

Additionally, the input and ouput need close scrutiny. The input data, although bounded by zero, still have wide variability whereas, the output data appear to be tightly controlled within a 2

percent peak to peak amplitude. It is generally accepted that a 6-10 percent measurement error is normally expected for biological systems, so that the TF model may be based mostly on noise. This obviously questions the ease of identification and suggests that the recursive estimation is mainly working on noise.

These considerations are important for future work in this area, however, of most importance to this thesis is the observation that in principle the technique could be used with some benefits.

6.4.3 Discussion

As was also found for the univariate data (section 6.3), a simple model may be an adequate representation of the data. The data requirements are high, and it appears that 100 sample pairs are not sufficient for the urine-sodium/water-intake experiment to perform identification for the particular subject. A more appropriate number of sample pairs might be 200. "Bumps" in the impulse function may be due to sample size problem or perhaps because the underlying dynamics are non-linear. With automatic methods of TF order determination and parameter estimation, the approach offers clinical potential where patient treatment is by physical input (for example, drugs, saline and dextrose) and monitoring ensures a high data rate. Furthermore, the method can be generalised to the multi-input multi-output case (Young, 1974). The value of recursive estimation of the parameters can clearly be seen when comparing the first estimate (without recursive estimation) to the second estimate (with recursive estimation) where a significant improvement can be seen.

6.5 COMPACT COMPARTMENTAL MODELLING

6.5.1 Introduction

State-space models (or "control system models", Carson et al, 1983) of the physiological systems and pathological processes underlying the observed variables may also be used alongside clinical time-series data. If well validated, then it may be possible to use clinical observations in comparison with the model predictions in such a way as to recursively estimate the model's parameters. de la Salle et al (1985) showed that with a simple model of thyroid disease, reasonable parameter estimates and accurate predictions can be made with as few as 3 or 4 data points. Simple state-space models thus provide an alternative approach for both low and high data rate situations. However, a necessary precondition for the use of such models is that they are theoretically uniquely identifiable (Carson et al, 1983). This is analagous to the stationarity, invertibility and stability conditions for ARIMA and TF models.

Subsection 6.5.2 presents a non-linear, stochastic compartmental model of FAB dynamics that was attained by simplifying a comprehensive deterministic model of FAB (Flood et al, 1984b; a later version of which is presented in Chapter 7). After describing the model, recursive joint state-parameter estimation is considered with the use of an Extended Kalman Filter (details of the Extended Kalman Filter can be found in Appendix 5).

6.5.2 A Non-Linear Stochastic Model Of FAB Dynamics

The model has three compartments, or states; X_1, extracellular fluid volume (normally 15 l); X_2, extracellular sodium mass (normally 2100 mmol); X_3, normalised ADH concentration (normally 1AU). The state equations are:

$$\begin{bmatrix} \dot{x}_1 \\ \dot{x}_2 \\ \dot{x}_3 \end{bmatrix} = \begin{bmatrix} -k_{01}x_1 + p_1x_3 \\ -k_{02}x_2 + p_2 \\ -k_{03}x_3 + p_3\frac{x_2}{x_1} - p_4x_1 \end{bmatrix} + \begin{bmatrix} U_1 \\ U_2 \\ 0 \end{bmatrix} + \begin{bmatrix} \zeta_1 \\ \zeta_2 \\ \zeta_3 \end{bmatrix} \qquad (6.57)$$

where; U_1 and U_2 are hourly intake rates of water and sodium (corrected for insensible losses). ζ_1, ζ_2 and ζ_3 are continuous white noises representing model uncertainty and system variability, see Figure 6.16. The measured "clinical outputs" at time t_k are given by:

$$\underline{y}_k = \begin{bmatrix} y_1 \\ y_2 \\ y_3 \end{bmatrix}_{t=t_k} \doteq \begin{bmatrix} k_{01}x_1 - p_1x_3 \\ x_2/x_1 \\ k_{02}x_2 - p_2 \end{bmatrix}_{\underline{x}=\underline{x}(t_k)} + \begin{bmatrix} \eta_1 \\ \eta_2 \\ \eta_3 \end{bmatrix}_k \qquad (6.58)$$

where y_1, y_2 and y_3 are urine flow (l h^{-1}), plasma sodium concentration (mmol l^{-1}) and urine sodium flow (mmol h^{-1}). η_1, η_2 and η_3 are discrete white measurement noises. The parameters of this model have been set at; k_{01}=0.0586 h^{-1}, p_1=0.759 l h^{-1} AU^{-1}, k_{02}=0.00446 h^{-1}, p_2=0.0, k_{03}=3.1 h^{-1}, p_3=0.119 AU l $h^{-1}mmol^{-1}$, p_4=0.904 AU $h^{-1}l^{-1}$.

Given a situation where there are a number of unknown parameters, or indeed where there are a number of parameters which are required to be patient-specific (the need for patient-specific parameters is discussed in section 10.2), then the use of an Extended Kalman Filter for recursive estimation may well be of value.

In the Extended Kalman Filter, the state vector is augmented with the unknown parameters, hence $\underline{X} = [x_1\ x_2\ x_3\ k_{01}\ k_{02}\ p_2]^T$. Assuming the parameters are constant, the extended state and output equations become:

$$\dot{\underline{x}} = \begin{bmatrix} -x_4x_1 + p_1x_3 \\ -x_5x_2 + x_6 \\ -k_{03}x_3 + p_3\frac{x_2}{x_1} - p_4x_1 \\ 0 \\ 0 \\ 0 \end{bmatrix} + \begin{bmatrix} u_1 \\ u_2 \\ 0 \\ 0 \\ 0 \\ 0 \end{bmatrix} + \begin{bmatrix} \zeta_1 \\ \zeta_2 \\ \zeta_3 \\ 0 \\ 0 \\ 0 \end{bmatrix} \qquad (6.59)$$

$$\underline{y}_k = \begin{bmatrix} x_4x_1 - p_1x_3 \\ \frac{x_2}{x_1} \\ x_5x_2 - x_6 \end{bmatrix}_{\underline{x} = \underline{x}(t_k)} + \begin{bmatrix} \eta_1 \\ \eta_2 \\ \eta_3 \end{bmatrix} \qquad (6.60)$$

or

$$\left.\begin{aligned} \dot{\underline{x}} &= \underline{f}(\underline{x}) + \underline{u} + \underline{\zeta} \\ \underline{y}_k &= \underline{g}(\underline{x}(t_k)) + \underline{\eta}_k \end{aligned}\right\} \qquad (6.61)$$

The Extended Kalman Filter updates the estimate $\hat{\underline{x}}_{k-1}$ and its estimated covariance P_{k-1} in a two-step process each time a new data point $\underline{y}_k$ becomes available.

The model and filter algorithm were tested using data simulated from the model. X_6 was simulated as a random walk, that is $\underline{\zeta} = [\zeta_1, \zeta_2, \zeta_3, 0, 0, \zeta_6]^T$, to allow for over simplification of the sodium dynamics, $\dot{X}_2$. The noise matrices were Q = diag[2.5 x

10^3,6.25 x 10^2,6.25 x 10^{-4},0,0,1] and R = diag[3.6 x 10^5,1.96,0.81]. The recursive parameter estimates for the situation in which the model is fitted to the simulated data, and the actual model outputs and simulated data are shown in Figures 6.17 and 6.18 respectively.

The results are very encouraging. Both K_{01} and K_{02} settle relatively quickly and track close to their true values, this being despite the large output variability. The fit between outputs and simulated data is very good.

6.5.3 Discussion

Given that identifiable and well validated models of the underlying pathophysiological processes are in existence, or at least are relatively easily attainable (somewhat confirmed by the review of extant models presented in Chapter 5 and the models presented in this thesis, where a basis for such models can be found), it is clear that in principle the recursive state-space approach may offer attractive possibilities. This is true not only for the technique itself, but also for the technique in relation to the types of output and the data rate encountered clinically.

The main requirement is that the model outputs relate to patient variables of particular clinical interest. The main drawbacks are that the Extended Kalman Filter is theoretically a biased estimator (Ljung, 1979) and that it requires knowledge of the noise Q and R but does not explicitly identify the noise model as in the ARIMA and TF techniques.

6.6 CONCLUSION

The three approaches to clinical time-series analysis which have been investigated above, differ in their requirements for sample size and knowledge of underlying physiological system dynamics.

The Box-Jenkins type methods need data sets of $n > 50$ which are large in chronic situations or laboratory terms, but small when sampling is frequent as in on-line monitoring. The recursive implementation of discrete TF models was found to be promising and with the existence of multivariable analysis, it is possible to say that these models may have potential in on-line monitoring and control in critical care units. The omission of physiological processes is disadvantageous unless the system dynamics are not well understood or if they are rapidly changing, as during the course of disease.

Where the pathophysiological processes underlying the clinical data are codified in validated mathematical models, schemes may be devised where model estimates and predictions are made on only a few data and updated as new data arrive. The clinical implication is clear. Such an approach will be equally effective where data rates are high.

Chapter 6 has considered non-complex models in some detail. This was a necessary exercise since the review of extant models (reported in Chapter 5) revealed a distinct paucity in this area. The lessons are clear and point to the need for substantial

research programmes concentrating in this particular field. Other methodologies for time-series should also be considered.

However, the possibilities for complex models have not been exhausted. Many complex models have been developed for reasons other than clinical implementation. The following Chapter thus documents substantial research efforts that were made in developing a complex non-linear model of FAB dynamics for clinical application.

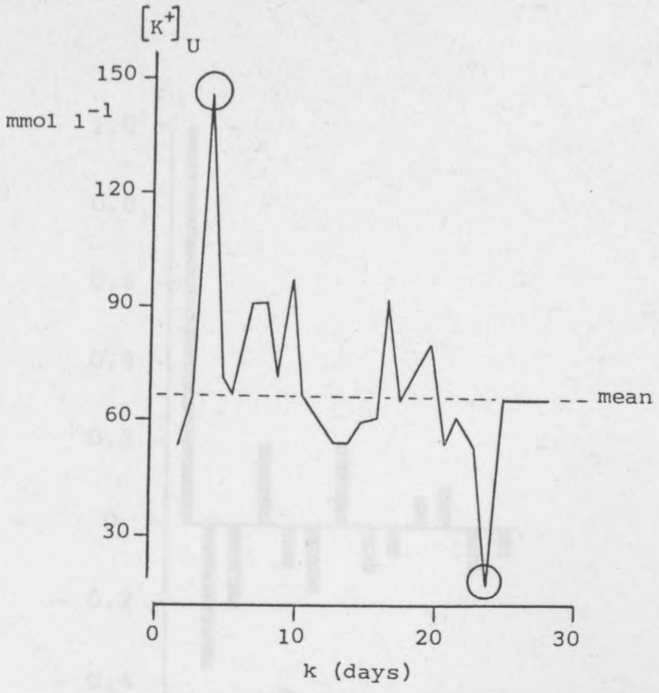

Figure 6.1 Urine potassium, $[K^+]_U$, time-series. (Dashed line shows the mean value. Circle highlights outliers).

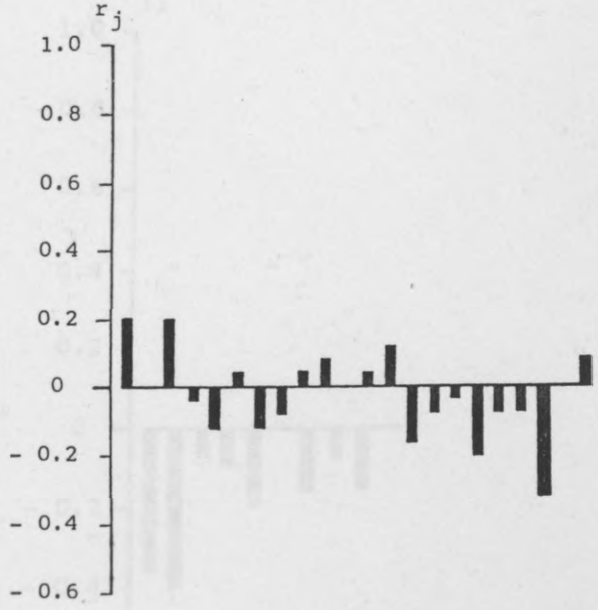

Figure 6.2 Estimated autocorrelation r_j function on data in time-series plot of Figure 6.1.

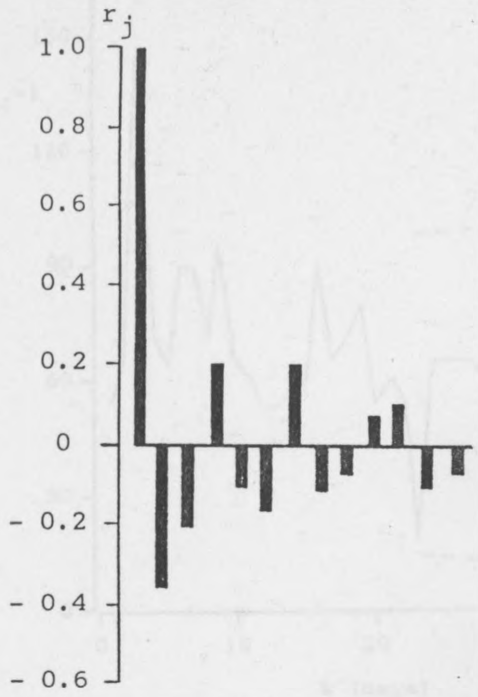

Figure 6.3 Estimated autocorrelation r_j function on first differences of time-series plot of Figure 6.1.

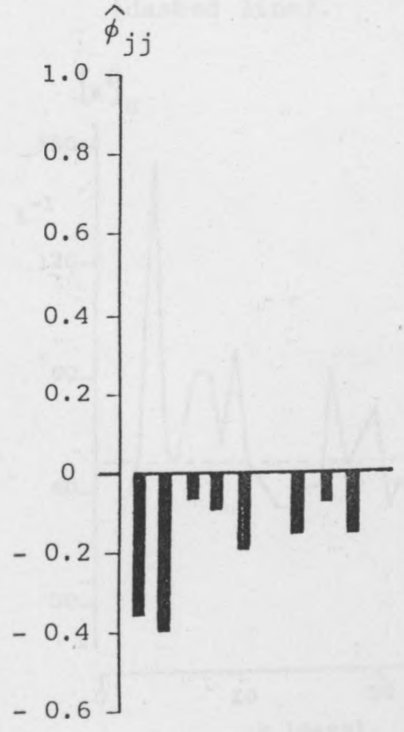

Figure 6.4 Estimated partial autocorrelation $\hat{\phi}_{jj}$ on first differences of time-series plot of Figure 6.1.

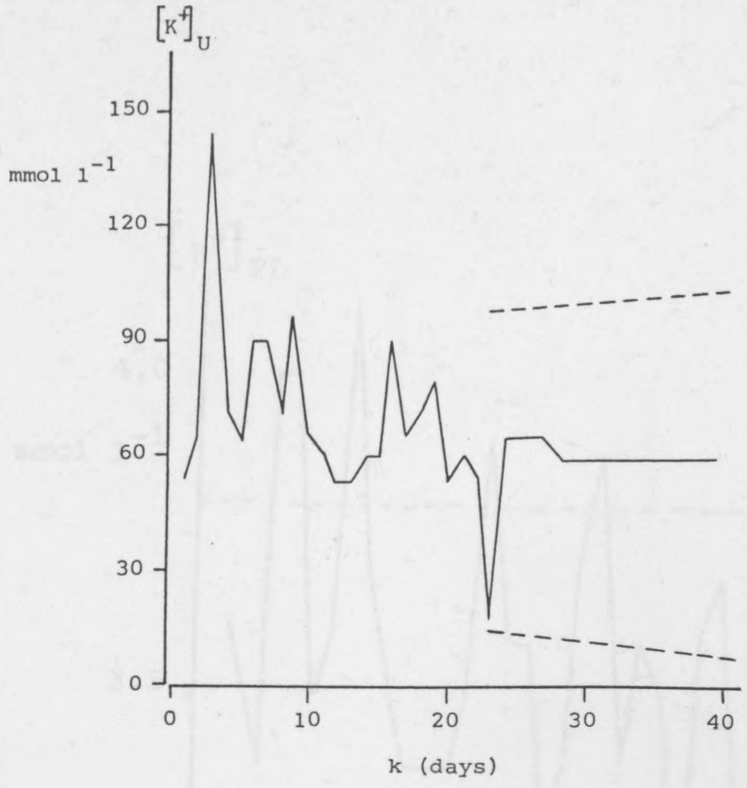

Figure 6.5 Data and 12 day ARIMA (2,1,0) model forecast (solid line) with 95% confidence intervals (dashed line).

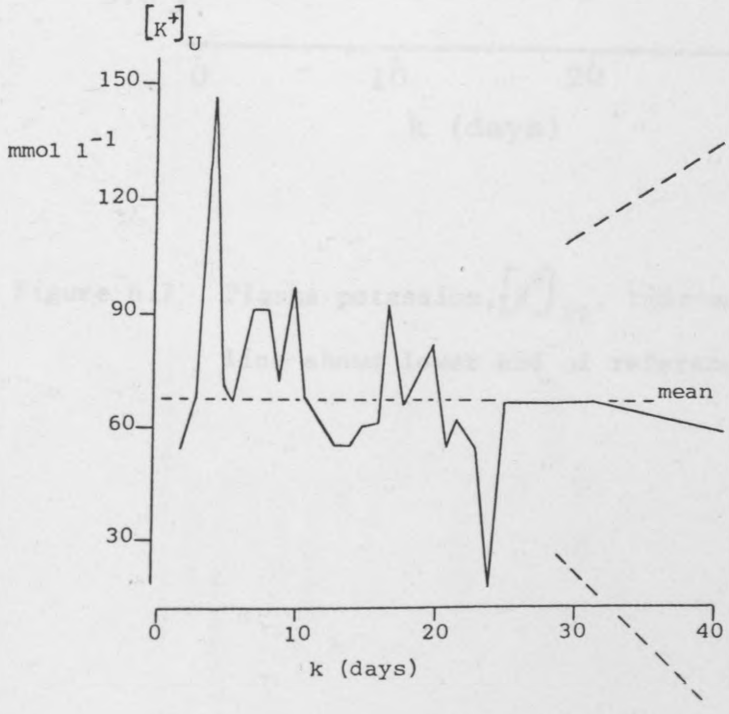

Figure 6.6 Data and 12 day ARIMA (2,1,0)δ model forecast (solid line) with 95% confidence intervals (dashed line).

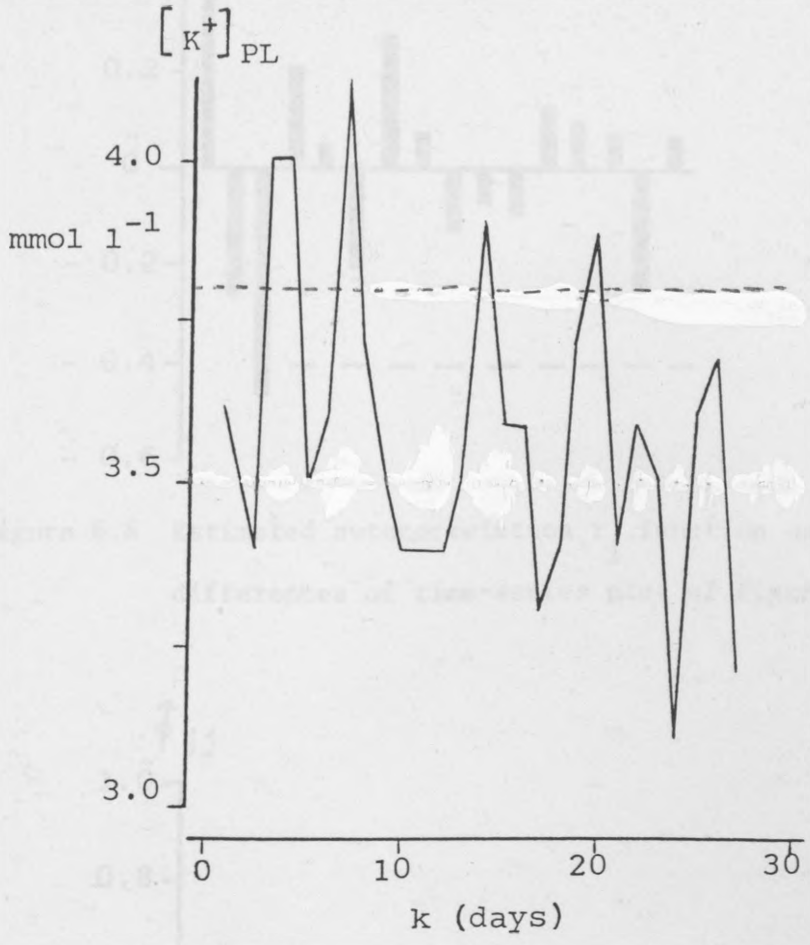

Figure 6.7 Plasma potassium, $[K^+]_{PL}$, time-series (dashed line shows lower end of reference range).

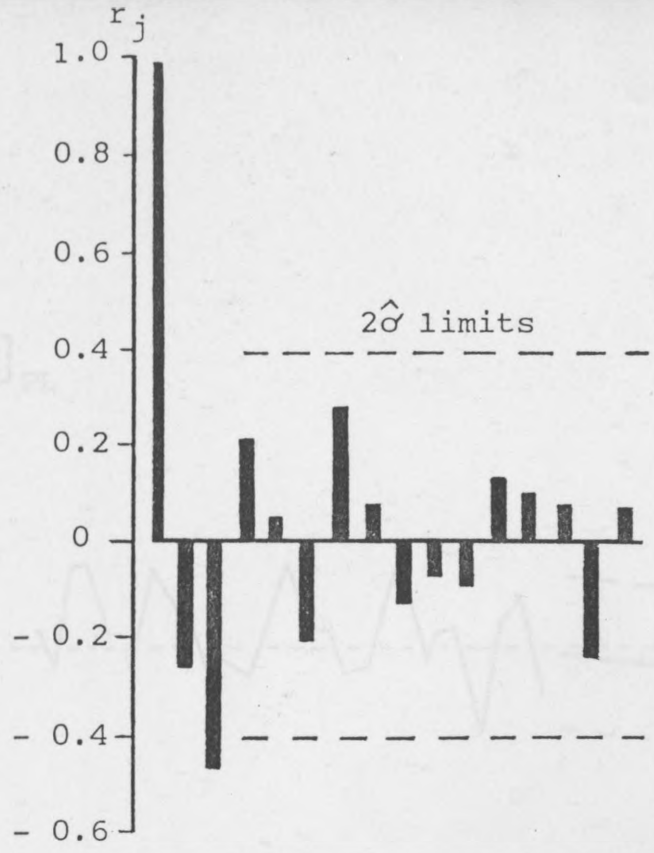

Figure 6.8 Estimated autocorrelation r_j function on first differences of time-series plot of Figure 6.7.

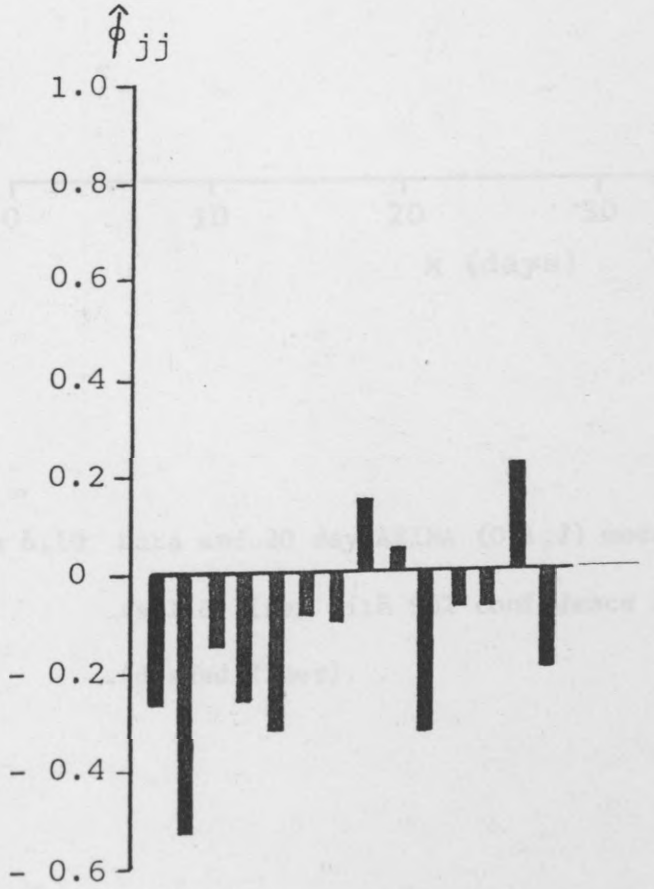

Figure 6.9 Estimated partial autocorrelation $\hat{\phi}_{jj}$ on first differences of time-series plot of Figure 6.7.

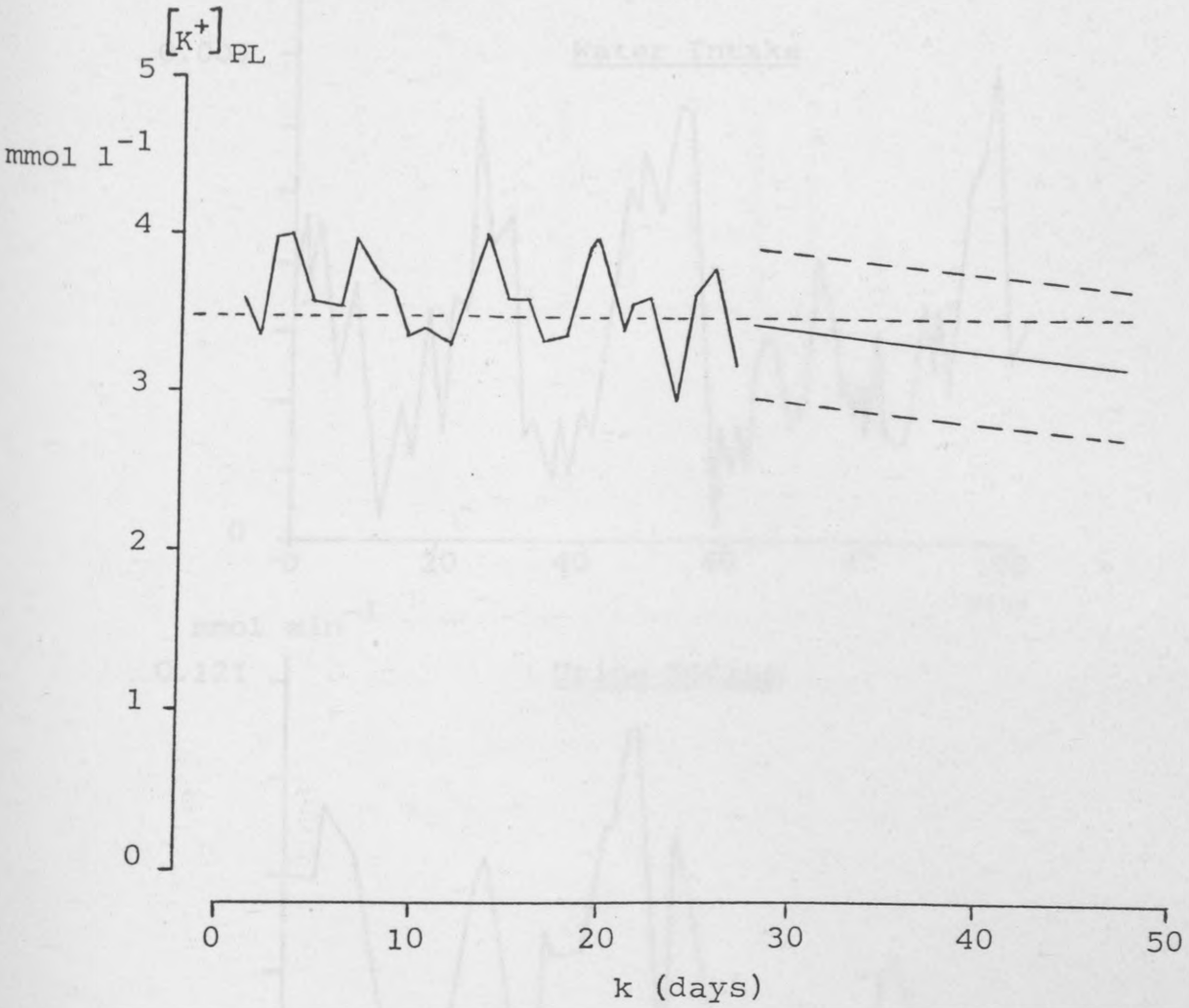

Figure 6.10 Data and 20 day ARIMA (0,1,2) model forecast (solid line) with 95% confidence intervals (dashed lines).

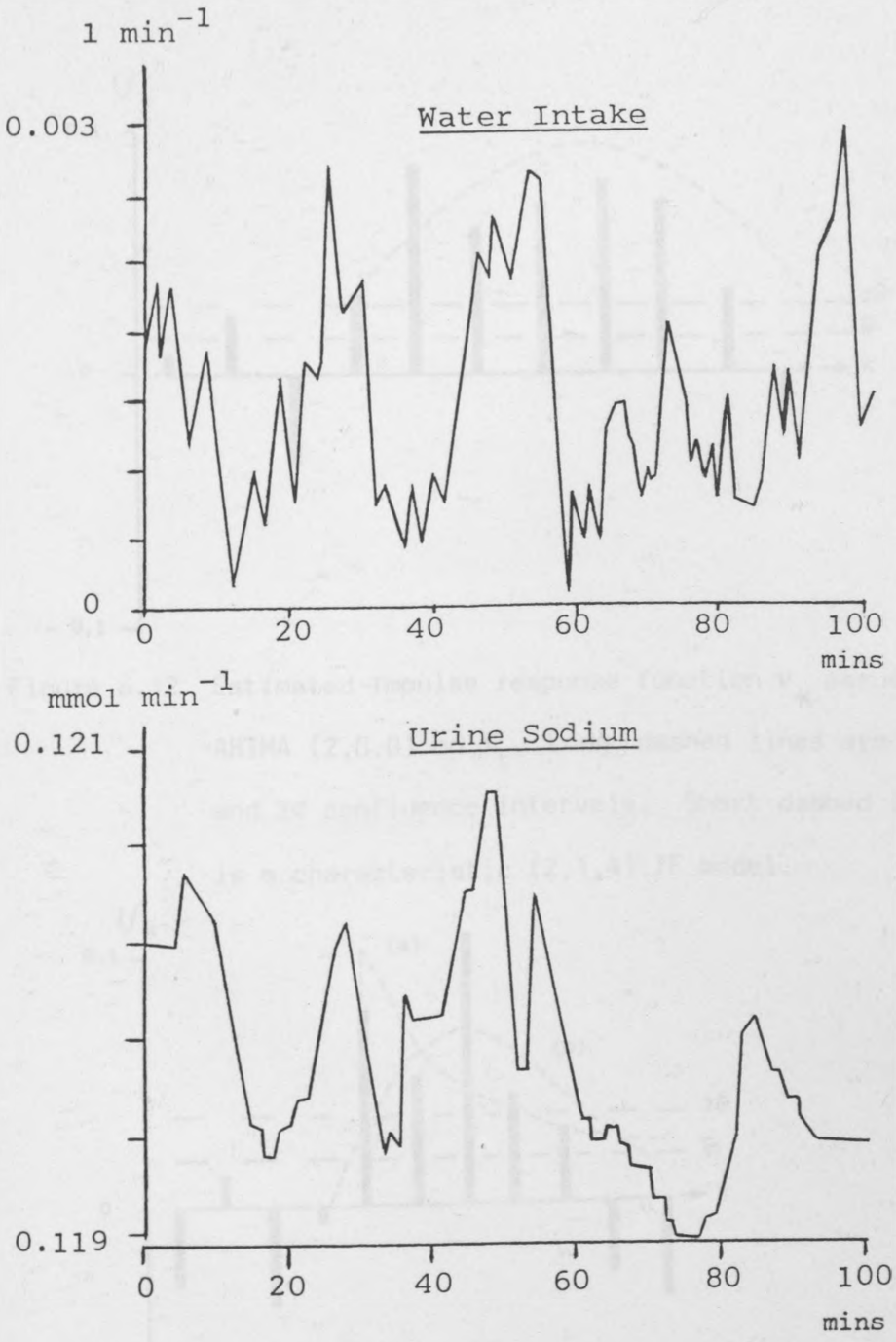

Figure 6.11 Water intake and urine sodium data generated from FAB3.

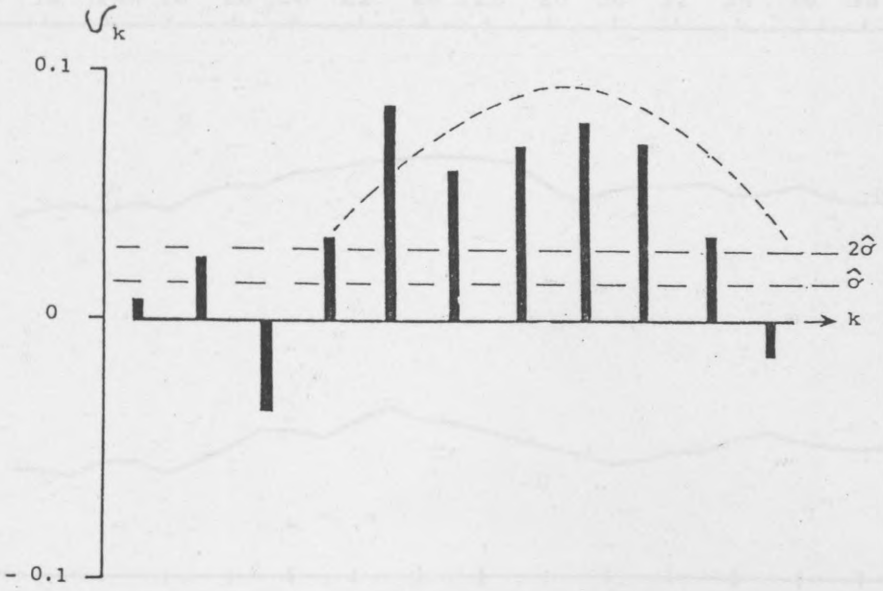

Figure 6.12 Estimated impulse response function ν_K assuming ARIMA (2,0,0) on X_t. Long dashed lines are σ and 2σ confidence intervals. Short dashed line is a characteristic (2,1,4) TF model.

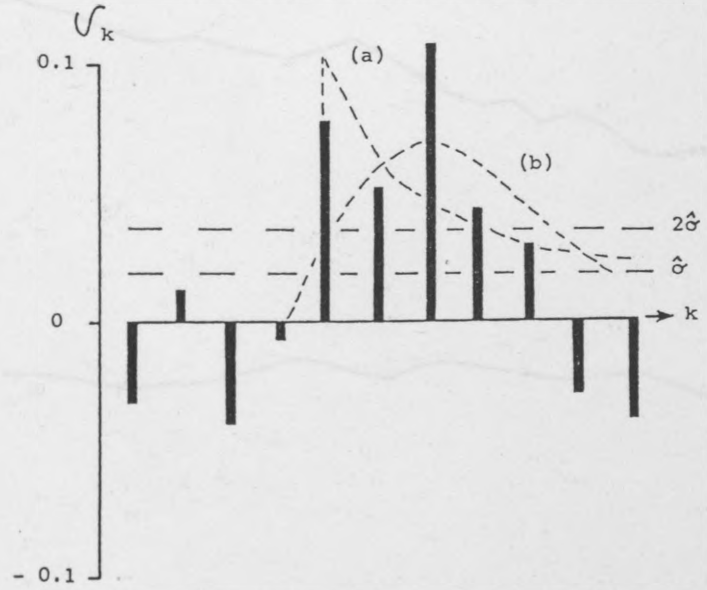

Figure 6.13 Estimated impulse response function ν_K assuming ARIMA (1.0.0) on X_t. Long dashed lines are σ and 2σ confidence intervals. Short dashed lines are characteristic (1,0,4) (a) and (2,2,4) (b) TF models.

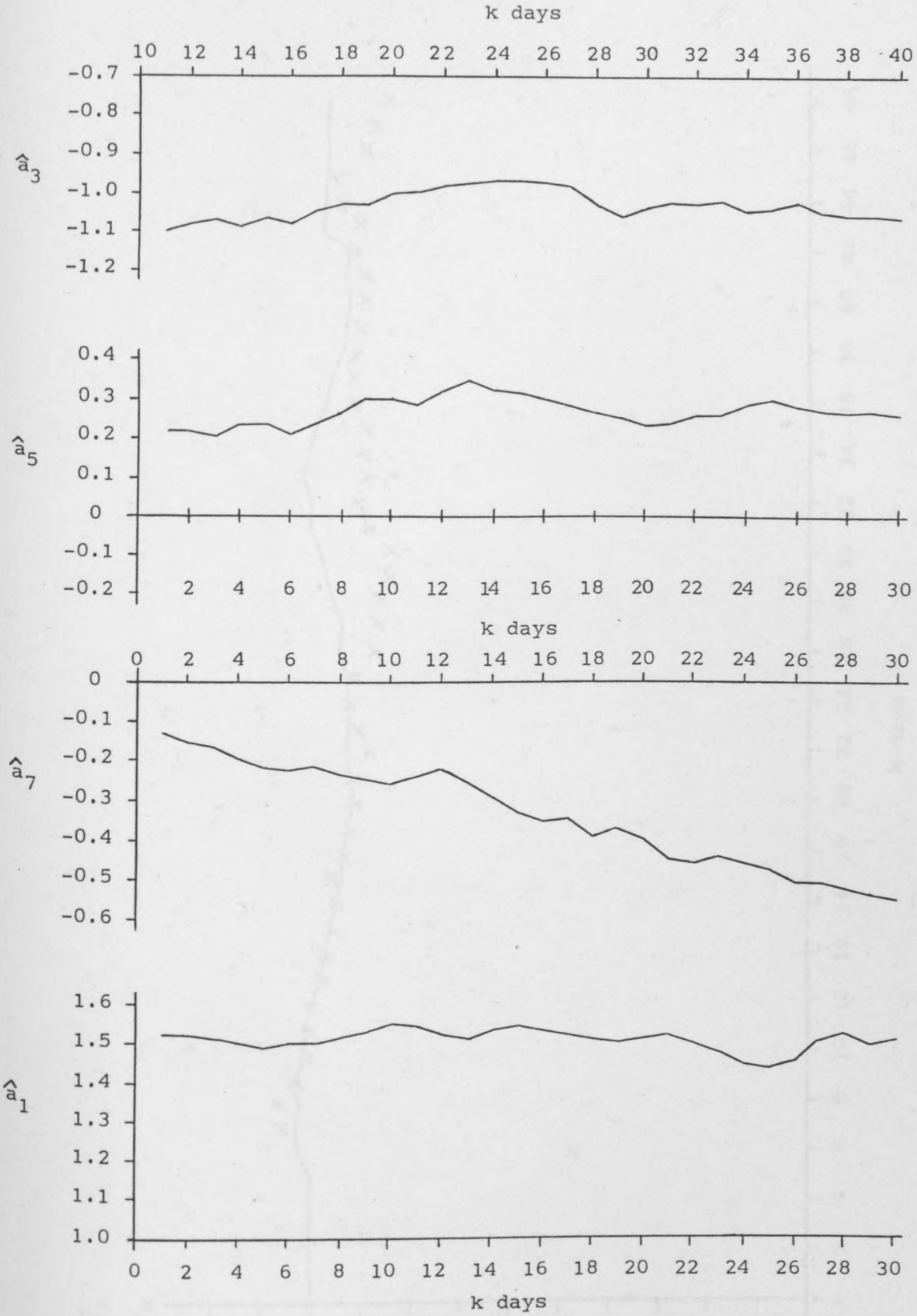

Figure 6.14 Recursive parameter estimates of TF model.

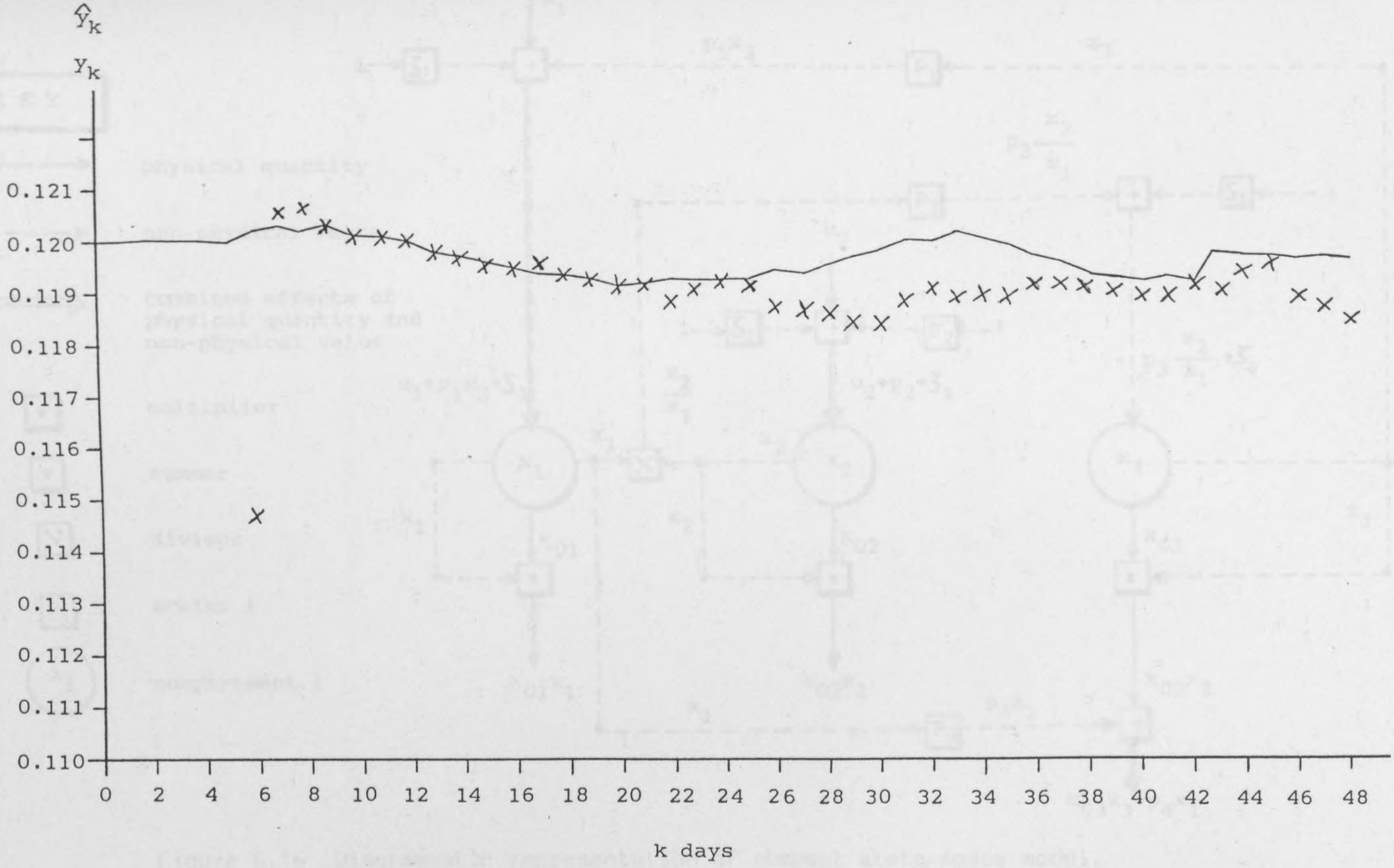

Figure 6.15 Recursive model outputs and patient data for TF model.

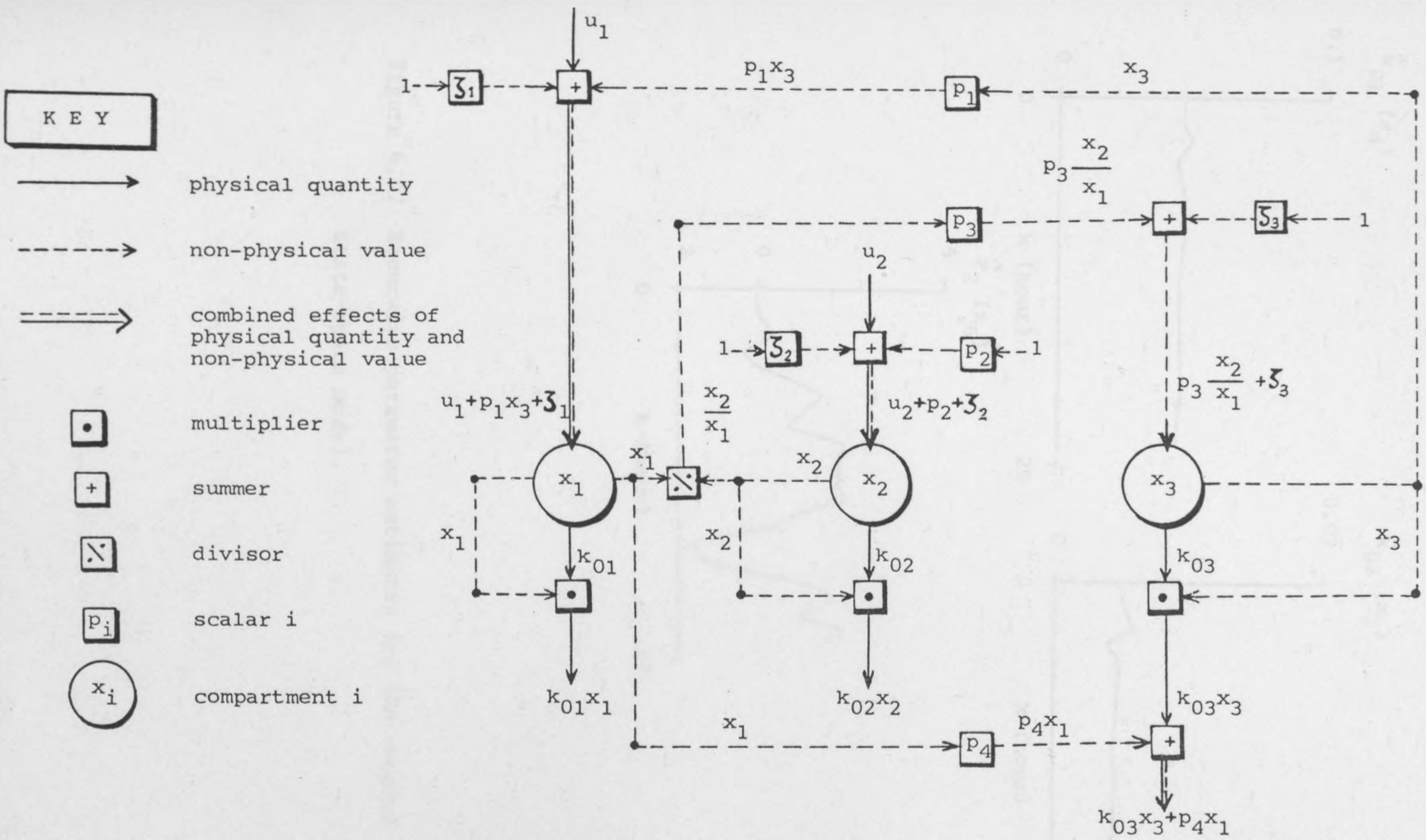

Figure 6.16 Diagrammatic representation of compact state-space model.

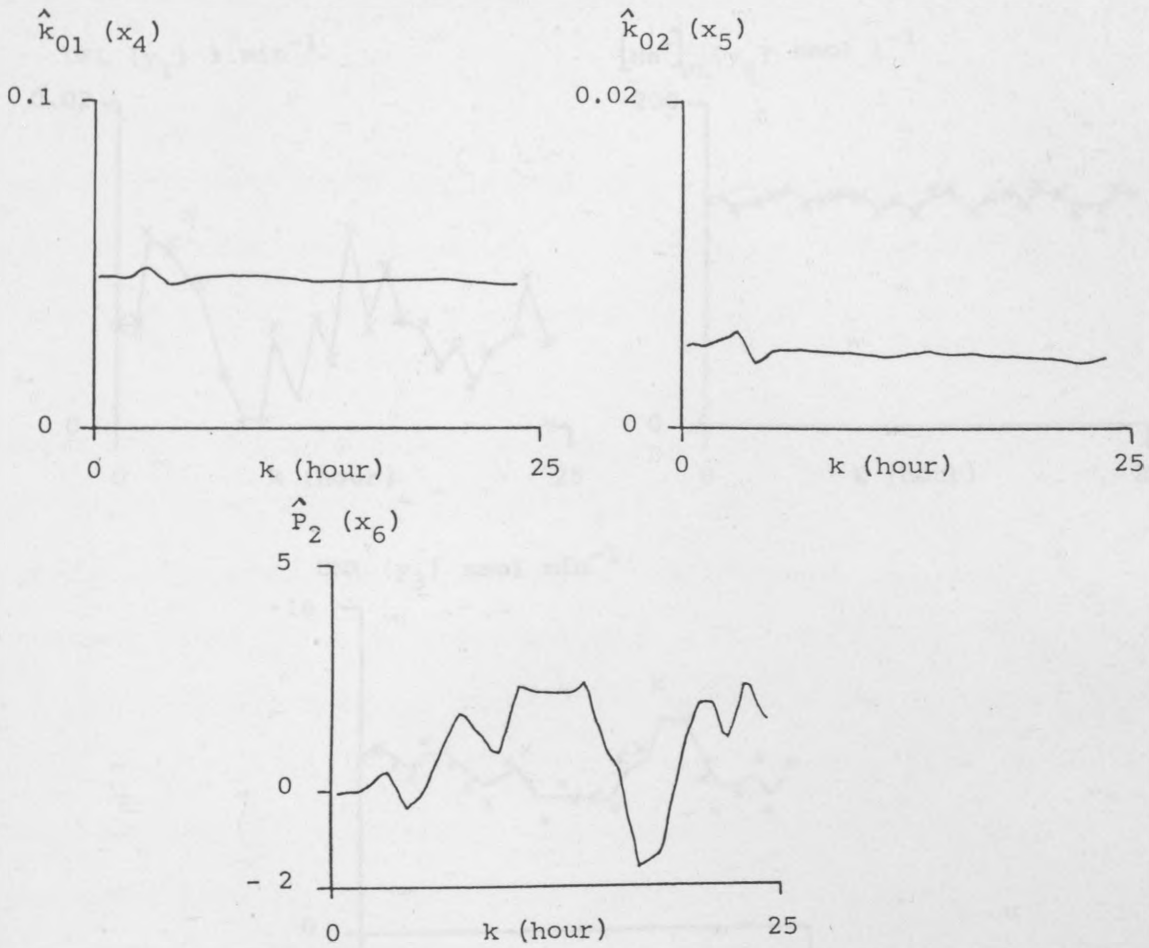

Figure 6.17 Recursive parameter estimates for the compact state-space model.

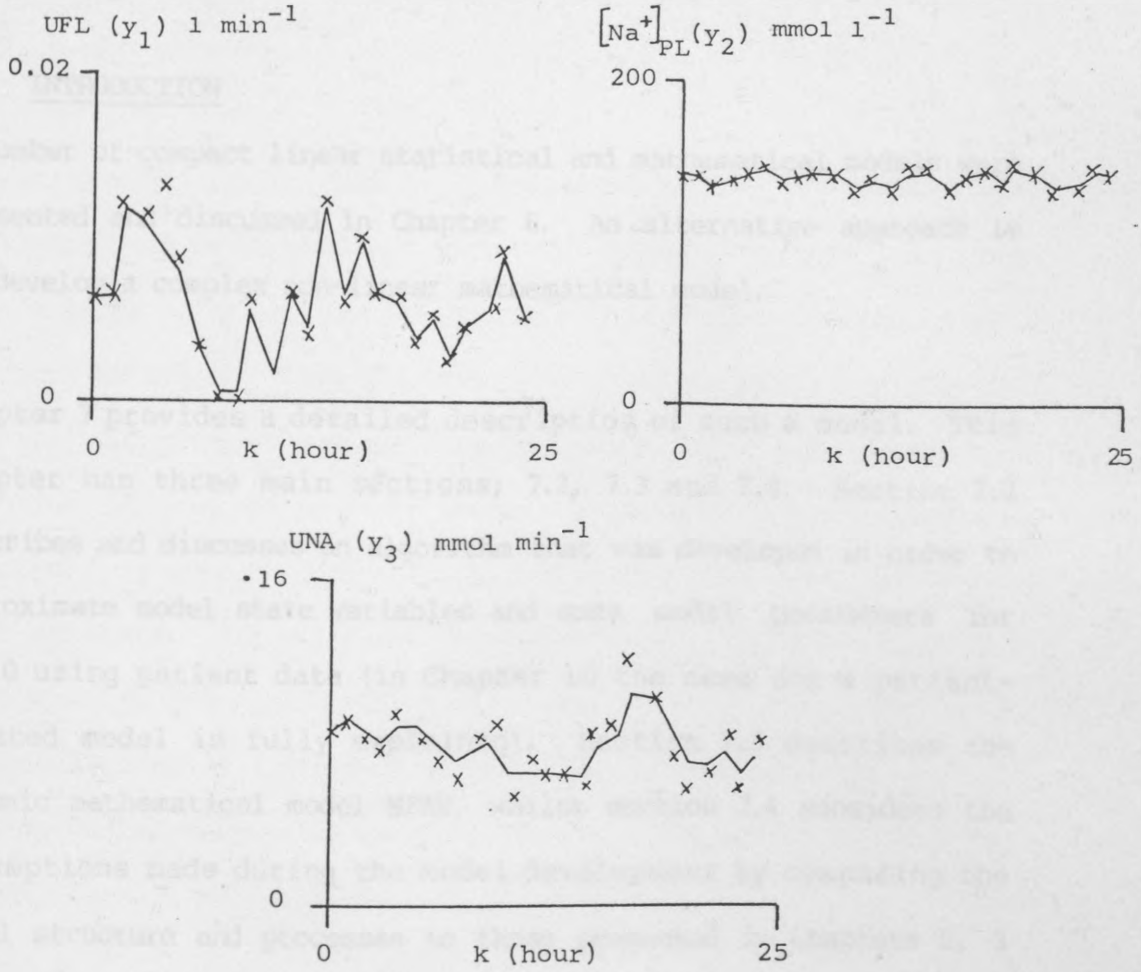

Figure 6.18 Recursive model outputs and simulated data of compact state-space model.

CHAPTER 7

MFAB: A COMPLEX MATHEMATICAL MODEL

7.1 INTRODUCTION

A number of compact linear statistical and mathematical models were presented and discussed in Chapter 6. An alternative approach is to develop a complex non-linear mathematical model.

Chapter 7 provides a detailed description of such a model. This Chapter has three main sections; 7.2, 7.3 and 7.4. Section 7.2 describes and discusses an algorithm that was developed in order to approximate model state variables and some model parameters for $t = 0$ using patient data (in Chapter 10 the need for a patient-related model is fully explained). Section 7.3 describes the dynamic mathematical model MFAB, whilst section 7.4 considers the assumptions made during the model development by comparing the model structure and processes to those presented in Chapters 2, 3 and 4.

The equations of MFAB have been developed for computer simulation and thus are presented as equations for/from a computer program. All differential equations use D operator notation $D( ) = \frac{d}{dt}$ and all unspecified nomenclature is contained in Appendix 6. The computer program is listed in Appendix 7.

7.2 PATIENT-RELATED ALGORITHM

7.2.1 Introduction

The objective of this exercise was to develop an algorithm to convert clinical data into state variables of the model, and subsequently set some parameters of the model.

State variable estimation for paediatric patients proved to be problematic as water volumes vary with growth. Firstly, children have a large interstitial volume as a percentage of body weight relative to adults. This difference normally disappears by the age of five. Of greater consequence is 'puppy fat'. Adipose tissue contains reduced amounts of water relative to lean body mass. Representing this is difficult as its diminution with age has a high variance. In addition, differences in fluid volumes and distribution for patients older than seventy have prevented effective state variable estimation. It was therefore decided to develop the algorithm for patients between the age of fifteen and seventy inclusive.

The first step of the algorithm determines total body water. The next step distributes the total body water between the intracellular, interstitial and plasma spaces. By using normal values for the concentration of analytes and knowing the fluid volumes for each space, the algorithm then derives analyte contents. Subsequently, related model parameters are adjusted.

Allometric and multiple regression techniques were considered as methods of producing the necessary equations. These are discussed in the following subsections.

7.2.2 Allometric Approach

A non-linear allometric approach was initially tried. Tables relating age and height to weight (Diem and Lenter, 1970) were used to heuristically develop equations estimating patient weight. An obesity factor was calculated by dividing actual weight less expected weight all by expected weight. The obesity factor was used to place the patient on a spectrum of thin-normal-fat and the percentage body weight of water was estimated from Table 7.1.

Variances between the surface of the data and the surfaces created by the non-linear equations were reduced using an optimisation hill

	MALE	FEMALE
THIN	65	55
NORMAL	60	50
FAT	55	45

Table 7.1 Percentage body weight of water according to obesity and sex. Source, Smith (1980).

climbing technique, however, the sums of the squares of the errors remained unacceptably high. It was therefore concluded that this heuristic technique could provide little confidence.

Multiple regression was seen to provide a quick and efficient solution to the problem. It is a well known identification technique with easily attainable measures of validity. This technique is the topic of the next subsection.

7.2.3 Multiple Regression Approach

A literature search revealed that this area has been thoroughly researched. The historical progression is presented in Table 7.2. The linear multiple regression analysis of Hume and Weyers (1971) proved to be of particular interest. Thirty males and thirty females had their total body water calculated using an intravenous tritium technique. In addition, height, weight and age were noted. These data have been reproduced in Table 7.3.

The following results were given for males:

$$TBW = .195*(MHT) + .297*(MWT) - 14.01 \quad (7.1)$$

with a correlation coefficient $r = 0.95$. For females:

$$TBW = .345*(FHT) + .184*(FWT) - 35.27 \quad (7.2)$$

with a correlation coefficient of $r = 0.96$. Further statistical analysis of the data was undertaken. The results are documented in Tables 7.4a for males, and Tables 7.5a for females. These results exhibit some small discrepancies when compared with the results reported by Hume and Weyers, which may have arisen through transcription errors onto their paper.

In Table 7.4a the t-ratios show that both MHT and MWT are significant in the regression equation. Furthermore, they explain 90 percent of the variance (adjusted for degrees of freedom) of MTBW from measured total body water. Of this 90 percent, MHT explains marginally more than MWT.

In Table 7.5a the t-ratios show that both FHT and FWT are significant in the regression equation. Furthermore, they explain

YEAR	AUTHORS	CONCLUSIONS OF WORK
1945	Pace & Rathbun	Fat is anhydrous. Fat free tissues are 73% water.
1956	Allen et al	Circulating total blood volume is closely related to a combination of body weight and cube of height.
1962	Nadler et al	Added a computer correction factor to the work of Allen et al (1956).
1965	Steinkamp et al	Fat weight can be accurately predicted from body parameters other than height and weight.
1966	Hume	Produced a formula for predicting lean body mass from height and weight.
1969	Retzlaff et al	Produced equations predicting erythrocyte and plasma volumes from various indices of body size.
1971	Hume & Weyers	Produced equations predicting total body water from height and weight.

Table 7.2 Historical analysis of research into fluid volume and related estimation for the human body.

MHT	MWT	MTBW	MAGE	FHT	FWT	FTBW	FAGE
170.2	66.4	38.9	69	160.0	42.3	28.8	55
170.2	62.7	34.4	59	157.7	60.9	30.6	65
167.6	63.6	37.8	56	162.6	48.2	30.6	57
158.8	67.3	33.2	60	146.1	36.8	21.8	84
177.8	70.0	40.8	46	152.4	35.5	23.5	58
161.3	70.9	38.0	52	147.3	32.3	21.7	58
165.1	66.4	38.3	50	144.8	57.3	26.0	50
160.0	50.0	33.5	53	149.9	62.3	26.3	68
174.0	67.3	41.8	53	157.5	56.8	27.0	62
180.3	74.5	47.8	52	149.9	40.5	22.7	54
177.8	67.0	41.9	53	154.9	39.1	26.3	59
132.1	36.4	24.3	69	151.1	45.0	26.9	41
180.3	83.6	43.7	51	154.9	40.9	23.3	47
172.7	65.9	40.7	40	158.8	62.0	31.7	43
170.2	75.0	40.7	71	149.9	55.2	27.1	46
170.2	64.1	38.4	64	161.3	62.7	29.7	66
180.3	58.2	36.6	60	154.9	45.0	25.7	59
163.5	66.8	40.1	57	154.9	57.0	27.3	48
176.5	75.0	44.9	61	157.5	53.6	30.8	41
163.5	62.1	36.9	57	153.7	81.8	30.2	57
156.2	59.1	30.9	65	154.9	100.0	38.6	63
185.4	89.1	48.8	48	158.8	90.5	36.8	35
168.9	68.9	41.0	50	157.5	105.9	46.6	61
174.0	77.3	42.7	55	170.2	93.6	36.8	33
175.3	48.6	31.3	51	161.3	96.8	36.8	53
175.3	121.8	55.5	35	170.2	102.3	56.1	56
175.3	86.4	48.7	45	167.6	108.2	41.9	42
179.1	96.3	48.8	54	152.4	84.5	33.8	54
172.7	108.6	52.2	43	156.2	67.3	31.9	49
172.7	84.3	41.8	55	160.0	76.6	37.0	49

Table 7.3 Data on height, weight and total body water for 30 males and females of varying ages. Source, Hume and Weyers (1971). Where the prefixes M and F refer to male and female, and HT is height (cm), WT is weight (kg) TBW is total body water (l) and AGE is age (years).

THE REGRESSION EQUATION IS:

MTBW = -14.2 + 0.197*(MHT) + 0.296*(MWT)

COLUMN	COEFFICIENT	ST. DEV. OF COEFF.	T-RATIO = COEFF/S.D.
	-14.249	7.8008	-2.03
MHT	0.19678	0.04628	4.25
MWT	0.29571	0.02753	10.74

R-SQUARED = 90.7 PERCENT

R-SQUARED = 90.0 PERCENT, ADJUSTED FOR D.F.

THE REGRESSION EQUATION IS:

MTBW = -8.21 + 0.187*(MHT) + 0.282*(MWT) - 0.0611*(MAGE)

COLUMN	COEFFICIENT	ST. DEV. OF COEFF.	T-RATIO = COEFF/S.D.
	-8.211	9.030	-0.91
MHT	0.18665	0.04717	3.96
MWT	0.28200	0.03038	9.28
MAGE	-0.06112	0.05783	-1.06

R-SQUARED = 91.0 PERCENT

R-SQUARED = 90.0 PERCENT, ADJUSTED FOR D.E.

Tables 7.4a and b. Statistical analysis of data on males sampled using:

a. the same variables, and

b. additionally age,

data from Hume and Weyers (1971)

THE REGRESSION EQUATION IS:

FTBW = -42.8 + 0.379*(FHT) + 0.227*(FWT)

COLUMN	COEFFICIENT	ST. DEV. OF COEFF.	T-RATIOS = COEFF/S.D.
	-42.76	17.16	-2.49
FHT	0.3787	0.1169	3.24
FWT	0.22743	0.03145	7.23

R-SQUARED = 83.7 PERCENT
R-SQUARED = 82.5 PERCENT, ADJUSTED FOR D.F.

THE REGRESSION EQUATION IS:

FTBW = -50.3 + 0.408*(FHT) + 0.229*(FWT) + 0.0540*(FAGE)

COLUMN	COEFFICIENT	ST. DEV. OF COEFF.	T-RATIOS = COEFF/S.D.
	-50.34	19.20	-2.62
FHT	0.4080	0.1218	3.35
FWT	0.22879	0.03160	7.24
FAGE	0.05402	0.06051	0.89

R-SQUARED = 84.2 PERCENT
R-SQUARED = 82.3 PERCENT, ADJUSTED FOR D.F.

Tables 7.5a and b. Statistical analysis of data on females sampled using:

a. the same variables, and

b. additionally age

data from Hume and Weyers (1971)

82.5 percent of the variance (adjusted for degrees of freedom) of FTBW from measured total body water. Of this 82.5 percent, FHT explains substantially more than FWT.

Descriptive statistics for the male and female ages are shown in Table 7.6. Hume and Weyers claimed that the formulae are applicable to those over the age of 16 years. The claim was found to have an area of doubt. In the sample there were no males under the age of 35 years and no females under the age of 33 years. Furthermore, the male mean of 54.5 years has a standard deviation of 8.4 years, and the female mean of 53.8 years has a standard deviation of 10.6 years. Thus 95 percent of the males were between the ages of 37 years and 71 years, and 95 percent of the females were between the ages of 32 years and 75 years. The upper ranges approximate the age boundary set for the algorithm, however, the lower ranges do not.

	MAGE	FAGE
N	30.0	30.0
MEAN	54.5	53.8
SD	8.4	10.6
MAX	71.0	84.0
MIN	35.0	33.0

Table 7.6 Descriptive statistics for the ages of sampled males and females, from Hume and Weyers (1971); where SD is the standard deviation; and MAX and MIN are the maximum and minimum values respectively.

These latter observations required further analysis as the main effects of age on volumes and distribution of total body water occur between the age of 15 years and 25 years (Guyton, 1976).

It was decided to test the significance of age for the sampled males and females on the estimation of total body water. The results are documented in Tables 7.4b and 7.5b. The t-ratios for both MAGE and FAGE show that neither are significantly different from zero, consequently the explanation of the sums of the squares by those independent variables is very small. It was concluded that the low significance of age in the estimation of total body water would also hold (albeit with some increase in significance) for the ages 15 years to 25 years. The equations (7.1) and (7.2) had therefore been found suitable for the patient-related algorithm.

7.2.4 The Patient-Related Algorithm

MFAB is a hybrid parameter model as defined by Leaning (1984):

$$\dot{x}_i = f(x_i, p_s, \hat{p}_i, u, t) \qquad (7.3)$$

where s_i is a member or individual of s, the class of systems being modelled; x, p and u are vectors of states, parameters and inputs.

$$y_i = g(x_i) \qquad (7.4)$$

where y are the measurements.

$$x_i(0) = h(y_{i0}, z_{i0}) \qquad (7.5)$$

where z are additional measurements; f, g and h are vector functions.

$$P_i \Longleftrightarrow \underset{P_i}{\text{Max}} \sum_{k=1}^{N} L(y_{ik}, y_i, (t_k)) \qquad (7.6)$$

where L is a likelihood function.

The vector $x_i(0)$ is derived from two patient observations, height and weight.

For the male patient:

$$MTBW = 0.195*(MHT) + 0.296*(MWT) - 14.01 \quad (7.7)$$

with an r of 0.95

For the female patient:

$$FTBW = 0.345*(FHT) + 0.184*(FWT) - 35.27 \quad (7.8)$$

with an r of 0.96. The regression equations are taken from Hume and Weyers (1971).

The initial states of the fluid compartments are derived from the total body water:

$$VICF = 0.62*(TBW) \quad (7.9)$$

$$VISF = 0.3*(TBW) \quad (7.10)$$

$$VPL = 0.08*(TBW) \quad (7.11)$$

$$VA = 0.2*(VPL) \quad (7.12)$$

$$VRA = 0.025*(VPL) \quad (7.13)$$

$$VV = 0.775*(VPL) \quad (7.14)$$

with the constant parameters typical of those found in the major medical textbooks.

Having computed the compartmental fluid volumes and knowing the steady-state concentrations of the analytes of interest (Staff of the Division of Pathology Royal Free Hospital Group, 1979), the remaining state variables can be derived using the general equation:

$$Q_{ij} = (\text{steady state conc.}_{ij}).(\text{volume}_j) \quad (7.15)$$

where Q is quantity and the subscripts i and j respectively refer to the analytes and the fluid compartments. The analyte compartments derived are displayed in Figure 7.1.

Many parameters and computer variables are derived from these state variables for t = 0. The parameter ANCO, used to set the position of the Starling curve for cardiac output, is derived separately:

SA = (0.00718*(HT))*(WT) duBois and duBois (1916) (7.16)

CI = -0.029*(JAGE) + 3.9 Guyton (1976) (7.17)

$15 \leq JAGE \leq 70$

so that

CO = (CI) * (SA) Guyton (1976) (7.18)

and the Starling curve is thus set:

ANCO = CO/5 (7.19)

with cardiac output at $t > 0$ being:

CO = ANCO*f(PRA) (7.20)

Figure 7.2 clearly shows the flexibility of this approach.

7.3 THE DYNAMIC MODEL

7.3.1 An Overview

The general compartmental structure is shown in Figure 7.3 and the routes within that structure are shown in Figure 7.4. The relationships between active control, passive regulation and the analytes are defined in Figure 7.5. The connections and controls between subsystems are shown in Figure 7.6. The specific compartmental mass flows and the main causal links are identified in Figure 7.7.

The fluid and electrolytes form the basis of the model. The kidney has been included as it controls the exit of fluid and electrolytes from the system. Acid-base dynamics have been included because of the interactions that occur during electrolyte and acid-base control in the kidney and cell pump. The two hormonal systems, aldosterone and ADH, have been included as they exert control over kidney function. Protein dynamics have been included as they can be responsible for large shifts of water during poor health. The cardiovascular system is included as the observations of this system relate directly to effective circulatory volume, the main concern of clinician control over fluid balance. The micro-vascular system has been included as it is necessary for protein dynamics to be modelled. Glucose has been included as it is a common clinical input and has a significant effect on potassium transmembrane dynamics.

The model is discussed in segments of submodels whose dynamics are closely related. The order of presentation of each segment is; model description, comparisons to other models where appropriate and segmented validation either by the original authors (if extant models have been used) or in the current research programme or both. A list of all assumptions made (identified by comparing the conceptual analysis of Chapters 2, 3 and 4 to the quantitative realisation of the current Chapter) is consolidated in the following section.

7.3.2.1 Fluid and electrolytes

MATHEMATICAL MODEL:

Extracellular and intracellular osmolality is calculated from electrolyte concentrations contained there in:

IOSM = (ZINA+ZIK+ZICL+ZIHCO3+ZIMG+ZIHPO4+ZWUR+104.5)*(MAC) (7.21)

EOSM = (ZENA+ZEK+ZECL+ZEHCO3+ZEMG+ZECA+ZEHPO4+ZWUR+24.9)*(MAC) (7.22a)

D(VICF) = (IOSM − EOSM)*TCEI + MPW (7.22b)

Further insight into these equations is given by Table 7.7

ELECTROLYTE	EXTRACELLULAR CONCENTRATION mEq l^{-1}	INTRACELLULAR CONCENTRATION mEq l^{-1}
Na^+	140.0	9.0
K^+	4.5	140.0
Cl^-	104.0	4.0
HCO_3^-	24.0	9.0
Mg^{++}	3.0	30.0
Ca^{++}	5.0	0.45
HPO_4^-	1.1	10.0
UREA	2.5	2.5
OTHERS	24.9	104.05
SUBTOTAL	309.0	309.0
MULTIPLY BY THE MOLECULAR ATTRACTION CONSTANT (.9288)		
TOTAL	287.0	287.0

Table 7.7 Electrolyte constituents of the Intracellular and Extracellular spaces in MFAB.

Thus both spaces share the same osmolality. The rates of change of the extracellular compartments include inputs from the gastrointestinal system and metabolic production, and outputs from the kidney and insensible routes. Other than environmental exchanges, fluxes also occur between the intra- and extracellular spaces of each species.

D(ENA) = ABNA-UNA-SINA-D(INA) (7.23)

D(EK) = ABK-UK-SIK-D(IK) (7.24)

D(ECL) = ABCL-UCL-SICL-D(ICL) (7.25)

D(EHCO3)= MPHCO3-UHCO3-D(IHCO3) (7.26)

D(EMG) = ABMG-UMG-D(IMG) (7.27)

D(ECA) = ABCA-UCA-D(ICA) (7.28)

D(EHPO4)= ABHPO4-UHPO4-D(IHPO4) (7.29)

D(WUR) = MPUR2-UUR (7.30)

Urea has been included here as an analyte that contributes to the fluid dynamics, although metabolic production is presented under 7.3.2.9 for protein.

The intracellular compartmental dynamics of the electrolyte were developed using the principles of Deland (1975) for ionic accounting, and the idiosyncracies of Ikeda et al (1979) for special biochemical dynamics. These two approaches are discussed below.

The structure of Deland's simple blood model assumes lumped compartments for intracellular and plasma spaces. Ions assumed to

be actively pumped are Na^+, K^+, Ca^{++} and Mg^{++}. Ions assumed to move passively are HPO_4^-, SO_4^{2-}, HCO_3^-, Cl^- and lactate. Potential across the membrane for the actively pumped ions is calculated using the Nernst-Planck equation:

$$V = \frac{R*T*\log_e}{F^o} \frac{ko}{ki} \quad \text{assuming } 38^oC \tag{7.31}$$

where; V is potential difference (mv), R is the gas constant (J $mol^{-1}K^{-1}$), F^o is Faradays constant (C mol^{-1}), T is temperature (^oC), ko is the concentration in the extracellular fluid (mEq l^{-1}), and ki is the concentration in the intracellular fluid (mEq l^{-1}). [Note: $\sqrt{ko}$ and $\sqrt{ki}$ were taken for divalent ions]. This was rearranged so that:

$$\frac{\Delta F^o}{R*T} = -\ln k_j \tag{7.32}$$

Thus k_j is a relative free energy parameter, interpreted as proportional to the work function of the active membrane pump plus the specific ion potential. Concentration ratios for the passively moving ions are then calculated

$$CR = \frac{ki}{ko} \tag{7.33}$$

Where CR is the concentration ratio [Note: $\sqrt{ko}$ and $\sqrt{ki}$ were taken for divalent ions]. The method for solution of the blood model is shown in Figure 7.8. [Note: this is a personal interpretation]. This particular model is not time dependent, tracing only the new steady-state.

The structure of the model of Ikeda and co-workers included an intracellular and extracellular space for electrolyte dynamics.

The electrolytes considered were Na^+, K^+, Ca^{++}, Mg^{++}, SO_4^{2-}, HPO_4^-, Cl^- plus organic acid. All electrolytes have an extracellular compartmental representation, only K^+ additionally has an intracellular compartmental representation.

Electrolyte interaction is included for some phenomena. For example, if the blood becomes more acidic then K^+ flux to the cells increases. If the intracellular fluid becomes more acidic then Na^+ flux from the cells increases (this representation assumes an infinite source/sink for sodium as an intracellular compartment was excluded). Intracellular acidity increases only if blood acidity increases, see Figure 7.9. These relationships do not achieve electroneutrality for two reasons. Firstly, the exchange between H^+, K^+ and Na^+ is not equal by charge. Secondly, Na^+ charges either arrive in the extracellular space from the unaccounted intracellular source, or having been accounted for in the extracellular space then disappear into the intracellular sink.

One other important transmembrane electrolyte movement has been represented by Ikeda and co-workers. Insulin promoted glucose dynamics moves K^+ into the cell and indirectly moves Na^+ out of the cell. The return to a normal state is then a function of the glucose dynamics. For similar reasons to the above case, electroneutrality is not maintained.

In principle, these idiosyncracies from Ikeda and co-workers model are acceptable. In practice they are only acceptable if strict accounting occurs and if appropriate control towards a normal state are included. The integration and development of Deland's

principles and Ikeda et al's idiosyncracies was seen to be a useful marriage. The outcome is presented below. The Nernst-Planck equation can be rewritten in the form of the Nernst Potential (NP):

$$NP = -61.0*DLOG10\ \frac{ki}{ko} \qquad \text{for monovalent ions} \qquad (7.34)$$

$$NP = -61.0*DLOG10\ \frac{\sqrt{ki}}{\sqrt{ko}} \qquad \text{for divalent ions} \qquad (7.35)$$

From this the actual potential of the active cations included in the model can be calculated:

```
APNA = -61*(DLOG10(ZINA/ZENA))                                    (7.36)
APK  = -61*(DLOG10(ZIK/ZEK))                                      (7.37)
APK  = -61*(DLOG10(SQRT(ZIMG)/SQRT(ZEMG))                         (7.38)
APCA = -61*(DLOG10(SQRT(ZICA)/SQRT(ZECA))                         (7.39)
```

The charges for intracellular and extracellular spaces are approximated from the number of mM of electrolytes present in each. A constant contribution from the assumed static intracellular and extracellular anionic globulins and the dynamic anionic albumin have been incorporated:

```
CAIC = INA+IK-ICL-IHCO3+2*(IMG)+2*(ICA)-2*(IHPO4)-PIC             (7.40)
CAEC = ENA+EK-ECL-EHCO3+2*(EMG)+2*(ECA)-2*(EHPO4)
                        -(0.9926*(PALB+ISALB+SSPGLOB))            (7.41)
```

So that a charge disequilibrium between the two compartments may exist:

```
CH = CAIC-CAEC                                                    (7.42)
```

[Note: this is not the exact charge disequilibrium normally encountered, -70 mv in the intracellular compartment but does serve to simulate effects of changes away from the steady-state condition].

Any charge disequilibrium will affect the ionic pumps. This affect will be opposite for pumps working in different directions:

PPNA = SSAPNA+(CH)*(KCH) (7.43)

PPK = SSAPK-(CH)*(KCH) (7.44)

PPMG = SSAPMG-(CH)*(KCH) (7.45)

PPCA = SSAPCA+(CH)*(KCH) (7.46)

Current ability of the pumps to maintain normal cation distribtuion can be attained by normalising the pump potentials of equations (7.43)-(7.46) with the actual normal potentials of equations (7.36)-(7.39):

PDNA = APNA/PPNA (7.47)

PDK = APK/PPK (7.48)

PDMG = APMG/PPMG (7.49)

PDCA = APCA/PPCA (7.50)

With the above information the rates of change of the actively pumped cations can be derived:

D(IMG) = (IMG-(SSIMG)*(PDMG))*(TCCA) (7.51)

D(ICA) = ((SSICA)*(PDCA)-ICA)*(TCCA) (7.52)

Potassium movement into the cellular space is also promoted by glucose metabolism, stimulated by the presence of insulin:

D(INA) = ((SSINA)*(PDNA)-INA)*(TCCA)-(ZEGL-6.0) (7.53)

D(IK) = (IK-(SSIK)*(PDK))*(TCCA)+EGLKI2 (7.54)

Transmembrane movement of cations is effected by a pump simulation. To maintain electroneutrality an equal movement by charge of anions must follow the cations. Anionic movement is passive according to the laws of diffusion. An appropriate mathematical representation for net diffusion and the selection of anions forming that diffusion were developed. This is discussed below.

Diffusion across a semi-permeable membrane is a function of five main factors:

$DR \propto (CR)*(CSA)*(T)/(MR)*(D)$ (7.55)

Where, DR is diffusion rate, CSA is cross-sectional area, T is temperature, MR is molecular radius, and D is distance. Model assumptions include constant temperature. In addition cross-sectional area and distance for lumped representations can satisfactorily be assumed constant. Furthermore, a selection of molecular radii shown in Table 7.8 show that the range of sizes

ANALYTE	H_2O	UREA	Cl^-	K^+	Na^+	PORE SIZE
RADII(A°)	3.0	3.6	3.86	3.96	5.12	8.0

Table 7.8 A sample of molecular radii of model analytes. Source Guyton (1976)

particularly of the electrolytes, are not large. It was therefore assumed that the contribution of molecular radii to equation (7.55) is also constant. Equation (7.55) therefore simplifies:

$$DR \propto CR \tag{7.56}$$

The direction of movement of anions during electrical disparity has known laws. If there is negative disparity negative ions move away from that disparity. If there is positive disparity then the gradient is satisfied from both sides, negative ions moving towards the positive disparity and positive ions moving away. If cation pumps are present then passive cation movement is prevented.

Integrating these concepts produced the following two criteria for the selection of anion to accompany cation movement. Movement is a function of:

(a) the deviation of each anion away from its normal concentration ratio, and;

(b) the fractional content of each anion over all anions in the space from which the anion will move.

Realisation follows.

Anion movement will match cation movement by charge:

$$CAM = D(INA)+D(IK)+2*(D(IMG))+2*(D(ICA)) \tag{7.57}$$

Total anion content available in each space is:

$$TOTANI = ICL+IHCO3+IHPO4 \tag{7.58}$$

$$TOTANE = ECL+EHCO3+EHPO4 \tag{7.59}$$

If net cation movement is away from the cells, that is CAM < 0, then equations (7.74)-(7.76) are used. These determine the anion selection from the cellular space for cation accompaniment. If net cation movement is cellward, that is CAM > 0, then equations (7.77)-(7.79) are used. These determine the anion selection from the extracellular space for cation accompaniment.

For the former case; normalised concentration ratios for inside divided by outside are:

NCRCLIO = (ZICL/ZECL)/SSCRIOCL (7.60)

NCRHCO3IO = (ZIHCO3/ZEHCO3)/SSCRIOHCO3 (7.61)

NCRHPO4IO = (ZIHPO4/ZEHPO4)/SSCRIOHPO4 (7.62)

Fractional anion contents for the intracellular space are:

CLANI = ICL/TOTANI (7.63)

HCO3ANI = IHCO3/TOTANI (7.64)

HPO4ANI = IHPO4/TOTANI (7.65)

For the latter case; normalised concentration ratios for outside divided by inside are:

NCRCLOI = (ZECL/ZICL)/SSCROICL (7.66)

NCRHCO3OI = (ZEHCO3/ZIHCO3)/SSCROIHCO3 (7.67)

NCRHPO4OI = (ZEHPO4/ZIHPO4)/SSCROIHPO4 (7.68)

Fractional anion contents for the extracellular space are:

CLANE = ECL/TOTANE (7.69)

HCO3ANE = EHCO3/TOTANE (7.70)

HPO4ANE = EHPO4/TOTANE (7.71)

These factors are combined for each space:

```
CAMI = ((NCRCLIO)*(CLANI)/(SSCRIOCL))+((NCRHCO3IO)*
       (HCO3ANI)/(SSCRIOHCO3))+((NCRHPO4IO))*(HPO4ANI)
       /(SSCRIOHPO4))                                    (7.72)

CAME = ((NCRCLOI)*(CLANE)/(SSCROICL))+((NCRHCO3OI)*
       (HCO3ANE)/(SSCROIHCO3))+((NCRHPO4OI)*(HPO4ANE)
       /(SSCROIHPO4))                                    (7.79)
```

The combination of these factors produces a common denominator used to determine three fractions, each related to the contribution of an anion to match cation movement. The fractions sum to unity. The differential equations for intracellular anion movement are;

For CAM < 0:

```
D(ICL)   = (CAM)*((NCRCLIO)*(CLANI)/(SSCRIOCL))/(CAMI)          (7.74)
D(IHCO3) = (CAM)*((NCRHCO3IO)*(HCO3ANI)/(SSCRIOHCO3))/(CAMI)    (7.75)
D(IHPO4) = (CAM)*((NCRHPO4IO)*(HPO4ANI)/(SSCRIOHPO4))/2*(CAMI) (7.76)
```

For CAM > 0:

```
D(ICL)   = (CAM)*((NCRCLOI)*(CLANE)/(SSCROICL))/(CAME)          (7.77)
D(IHCO3) = (CAM)*((NCRHCO3OI)*(HCO3ANE)/(SSCROIHCO3))/(CAME)    (7.78)
D(IHPO4) = (CAM)*((NCRHPO4OI)*(HPO4ANE)/(SSCROIHPO4))
           /2*(CAME)                                         (7.79)
```

COMPARISON TO OTHER MATHEMATICAL MODELS:

The discussion of the fluid and electrolyte aspects from Ikeda et al (1979) and Deland (1975), presented in the above development of the fluid and electrolyte mathematical model for MFAB, are typical

of the two main approaches that have been taken. Bigelow et al (1973) is another example of the approach adopted by Deland, whilst Kuroda et al (1980) and Cameron (1977) are examples of the approach adopted by Ikeda and co-workers.

VALIDATION:

The validity of this representation lies in its theoretical credibility (the use of known laws). This is especially the case for the model MFAB as the computed intracellular state variables are not observable in the physiological system without introducing a series of non-filterable errors.

It is important that well founded laws, such as the Nernst-Planck equation and the directly proportional relationship for diffusion rate, were used. Further credibility of the use of the Nernst-Planck equation was attained by comparing the potentials of sodium and potassium derived by the model with values given by Guyton (1976). Model potential for sodium is 72.7 millivolts and for potassium is -91.1 millivolts compared to 70 millivolts for sodium and -85 millivolts for potassium given by Guyton. Furthermore, magnesium (with a model potential of -30.5 millivolts) and calcium (with a model potential of 31.9 millivolts) potentials are close in absolute value, which compares favourably with the currently accepted magnesium-calcium pump exchange theory (Lote, 1982). Similarly, the theory of an additional potassium pump over and above the recognised sodium-potassium pump exchange is consistent with the discrepancy in absolute value between the sodium and potassium potentials. The model suggests the additional pump

contributes 18.4 millivolts to the potassium potential whereas Guyton (1976) estimated the contribution to be 15 millivolts.

7.3.2.2 Cardiovascular system

MATHEMATICAL MODEL:

The cardiovascular model is a modified version of that developed by Parkin (1984). The original closed model structure is shown in Figure 7.10. It was necessary to include inputs and ouputs to open the structure for later integration into MFAB.

The equations are solved at every second of simulation time. This prevents negative compartmental volumes occurring. The range of time constants in MFAB consequently increased substantially stiffening the system. The problems arising from this are discussed in Chapter 8.

The equations with a brief commentary follow.

VRAS = VRA-VRAU (7.80)

Where the unstressed volume is the volume that gives a pressure of OmmHg, and the stressing volume is the volume that distends the walls causing increased pressure see Figure 7.11.

PRA = VRAS/CRA (7.81)

Cardiac output is derived using Starlings law:

CO = ANCO*((((PRA+4)*6.0)↑2.6)/(5000+(((PRA+4)*0.6)
↑2.6)))*(11.45) (7.82)

FA = (CO)*(HS) (7.83)

D(VA) = ((FA-FC))-UO+CFR))/15 (7.84)

so that the arteries are open to the interstitial space and the environment.

VAS = VA-VAU (7.85)

PA = VAS/CA (7.86)

The calculation of PA had to be modified due to over-sensitivity. In the physiological system, neural control over vascular tone reduces the relative change of pressure to volume. This is implicitly incorporated in the following equations:

PA = ((VAS/CA)-100)*(0.05)+100 (7.87)

PGAV = PA-PV (7.88)

FC = PGAV/RA (7.89)

so that flow in the capillaries is equal to the cardiac output for the steady-state. This flow may be inhibited or augmented by changes in the volumes of the preceeding arteries and/or the proceeding veins.

D(VV) = ((FC-FV)+(ABW-GLW+LRR+SIWI))/15 (7.90)

so that the veins are open to the gastrointestinal system, the interstitial space and the environment.

SIWI = constant (7.91)

VVS = VV-VVU (7.92)

PV = VVS/CV (7.93)

PGVRA = PV-PRA (7.94)

FV = PGVRA/RV (7.95)

D(VRA) = (FV-FA)/15 (7.96)

COMPARISON WITH OTHER MATHEMATICAL MODELS:

The cardiovascular representations of Koushanpour and Stipp (1982) and Ikeda et al (1979) derive pressures linearly from blood volume and cardiac output respectively. Non-linearities such as variable compliance and resistance are not accounted for, preventing simulation of non-heart related abnormalities.

Guyton and Coleman (1967) developed both a simple and a more complex model of the long term regulation of circulation. Uttamsingh (1981) and Badke (1972) used the simple model. However, the simpler model reproduces the long term relationship between arterial pressure and cardiac output incorrectly. The more complex model includes a substantial number of additional assumptions and features (difficult to quantify) in order to correct the relationship. Thus the latter model was deemed inappropriate for the current research. The former model is similar to that of Parkin (1984), displaying no additional benefits.

The cardiovascular element of Cameron (1977) includes all the essential elements required by MFAB, plus substantial additional factors, and was not seen as being parsimonious with respect to the research programme.

VALIDATION:

A comprehensive study of the model has been made by Dr Parkin but has not yet been documented, his expert opinion however, is that the model responds well in a qualitative sense.

A quantitative feature analysis showed that a time constant of 15 seconds for the differential equations is too long. Equilibrium between compartments occurs over 3 or 4 heartbeats, which suggests a time constant of about 5 seconds. However, this led to instability. The change from stability to instability is illustrated by Figures 7.12a and b. The required model response over the initial second is less for the case of a 15 second as opposed to a 5 second time constant. A sharp rise in model response is expected for the latter case because of the nature of numerical integration. The size of the error caused by this sharp rise leads to overcompensation in the next second and hence a larger error. This growth continues until the model 'blows up'. In the case of the 15 second time constant, the smaller error does not cause over compensation.

The number of integration steps taken at each discrete step was increased in an attempt to reduce the initial error. This was also found to cause instability. The number of steps required to reduce the steepness of the model response is very large. Small errors are associated with each step so that before the error of the steep rise can be removed, other errors at least as large enter the calculations.

The time period for each discrete step was reduced as an alternative attempt to stabilise the model with a 5 second time constant. This idea was incorporated into the whole model validation of Chapter 8 where 'Gear's Method' for stiff equations is considered.

Quantitative validation highlighted the problem of an over-sensitive arterial pressure. Equation (7.87) was formulated, implicitly representing vascular tone. The constant, set at 0.05, was attained by iterative adjustment until PA and PV were seen to respond in line with expected results of a medical expert.

7.3.2.3 Gastrointenstinal system

MATHEMATICAL MODEL:

The gastrointestinal system is adapted from Kuroda et al (1980). The s-domain representation is:

$$\text{oral input} \longrightarrow \frac{1}{(T_1 s+1)+(T_2 s+1)} \longrightarrow \text{increase in plasma}$$

with T_1 = 17 minutes and T_2 = 25 minutes. This can be rewritten using partial fractions:

$$1/8\,\mathcal{L}^{-1}\frac{1}{25s-1} - 1/8\,\mathcal{L}^{-1}\frac{1}{17s-1} \qquad (7.97)$$

Solving this for the time-domain and adapting the solution for the general equation case:

$$ABS_i = GCOMP_i*((0.125*DEXP(0.04(t)))-(0.0125*DEXP(0.059(t)))) \qquad (7.98)$$

Where ABS_i and $GCOMP_i$ respectively refer to the amount of species i absorbed at time t, and the quantity of the gastrointestinal compartment for species i at time t.

Quantitative features of this model are; absorption starts at t=0 (although time delays could be imposed), peak absorption occurs at 18 minutes, and total absorption is completed by 38 minutes.

The analytes of MFAB that can gain access to the extracellular space via gastrointestinal absorption are water, sodium, potassium, chloride, magnesium, calcium and phosphate. Other analytes are represented as the product of metabolism.

COMPARISON WITH OTHER MATHEMATICAL MODELS:

The majority of extant mathematical models have the assumption that fluid and electrolytes are absorbed at a constant rate, equal to the model's normal steady-state outputs.

The addition of a gastrointestinal system, albeit highly simplified, substantially increases the range of application for the model, for in certain circumstances gastrointestinal losses can be significant. Sodium is a good example in that about 15 percent of body sodium is turned over between the gut and the plasma every day. This potentially can be lost to the environment.

Fadali et al (1979) included a simple first order representation of the gastrointestinal system in their fluid model. This injects water into the plasma over T_j hours. Further analysis of the model was prevented as the parameter values were not specified.

Cramp and Carson (1981) presented a model, with parameter values, representing glucose ingestion. The model is a piecewise continuous function with a linear section followed by a first order exponential decay:

$$\left.\begin{array}{ll} ABS = 4 & t < 30 \\ = 4*DEXP(-0.1*(t-30)) & t \geq 30 \end{array}\right\} \qquad (7.99)$$

for a 50 gram bolus input. The area under the curve showed that just under 80 percent absorption occurs after 25 minutes for a unit impulse. This compares to approximately 87 percent for Kuroda and co-workers' model.

The models of Badke (1972), Koushanpour and Stipp (1982), and Toates and Oatley (1977) are more complex representations. These were not considered to be parsimonious in relation to the research objectives.

VALIDATION:

The quantitative features of Kuroda et al (1980) are comparable to Cramp and Carson (1981) and values presented in major medical textbooks.

7.3.2.4 Microvascular system

MATHEMATICAL MODEL:

The microvascular model is adapted from Ikeda et al (1979). The Starling equation calculating net forces for capillary filtration has been used, thus both colloid and hydrostatic pressures of the adjacent plasma and interstitial spaces have to be derived. Lymphatic return, although equal to capillary filtration in the normal steady-state, is derived from interstitial hydrostatic pressure. The equations are:

$$
\begin{aligned}
PISF &= -15 && CPISF \leq 0.9 \\
&= 87*(CPISF)-93.3 && 0.9 < CPISF \leq 1 \\
&= -6.3*((2-CPISF)\uparrow 10) && 1 < CPISF \leq 2 \\
&= CPISF-2 && 2 < CPSIF
\end{aligned}
\qquad (7.100)
$$

$$PC = (((PV)*(KCP))+PA)/(KCP+1) \qquad (7.101)$$

$$PICO = 0.25*(ZISALB) \qquad (7.102)$$

$$PPCO = 0.4*(ZPLPR) \qquad (7.103)$$

$$NCSF = PC+PICO-PISF-PPCO \qquad (7.104)$$

$$CFR = (NCSF)*(CFC) \qquad (7.105)$$

$$LRR = (SSLRR)*(24/(1+DEXP(-0.4977*(PISF)))) \qquad (7.106)$$

$$CPISF = VISF/SSVISF \qquad (7.107a)$$

$$D(VISF) = CFR-LRR-SIWL-RWL \qquad (7.107b)$$

COMPARISON WITH OTHER MATHEMATICAL MODELS:

The model structure of Ikeda et al (1979) is typical of many microvascular models incorporated into fluid dynamics simulations. The main differences occur in the derivation of capillary pressure and the parameter values associated with the flows.

Some other differences have been noted. Cameron (1977) developed equations to derive colloid oncotic pressures using the Landis-Pappenheimer formulae (Landis and Pappenheimer, 1963). Koushanpour and Stipp (1982) differed in that 2nd, 3rd and 4th order regression equations were used to derive oncotic and hydrostatic pressures. Bert and Pinder (1982) produced an analogue version with the same structure and processes.

VALIDATION:

Theoretical validity of Ikeda and co-workers model is evidenced by the similar structure of other extant mathematical models.

Derivation of capillary pressure poses the only controversy, in that, major medical textbooks differ on the estimates of the contributions of arterial and venous pressures to this variable. Future agreement is likely to be achieved. For this reason, future theoretical validity of the capillary pressure representation in MFAB may come into question. Transparency of this area of MFAB is therefore essential, and is achieved below.

The equations (7.87) and (7.93) for the calculation of arterial and venous pressures respectively are rewritten below:

$$PA = 20*(CO) \tag{7.108}$$

$$PV = 3.3*(CO)-13.6 \tag{7.109}$$

Substituting (7.108) and (7.109) into (7.101) gives capillary pressure in terms of cardiac output:

$$PC = 2.85*(CO)-11.69+2.89*(CO) \tag{7.110}$$

where PV contributes (2.85*(CO)-11.69) and PA contributes (2.89*(CO)). The percentage contribution of arterial and venous pressures to capillary pressure over some typical cardiac outputs are shown in Table 7.9.

IN PERCENT									
PV	2.25	6.25	12.5	15	17.5	19	21	22.5	24
PA	97.75	93.75	87.5	85	82.5	81	79	77.5	76
CO	4.2	4.4	4.8	5.0	5.2	5.4	5.6	5.8	6.0

Table 7.9 Comparison of the contribution of arterial and venous pressure to capillary pressure in MFAB.

One other point arises from this discussion. Cardiac output in MFAB is derived for t = 0 from the patient-related algorithm. Different steady-state cardiac outputs have differing combinations of contribution from arterial and venous pressures. Consequently, males and females with the same body dimensions, and having different cardiac outputs derived from the algorithm, will have a different combination of effects from arterial and venous pressures on capillary pressure. This is also true for members of the same sex with different dimensions.

It was concluded that, unless evidence of irregularities were found when validating MFAB at a holistic level, the Ikeda and co-workers, representation for capillary pressure would be used until such a time that concrete evidence on capillary dynamics falsifies the hypothesis.

7.3.2.5 Kidney system

MATHEMATICAL MODEL:

The renal dynamics of Ikeda et al (1979) were used to form the basis of the kidney model. Renal bicarbonate and chloride dynamics were developed during the current research programme. The equations follow with a commentary (the current author's interpretation).

Glomerular Filtration:

The first physical factor that influences glomerular filtration rate (GFR) is the normalised value of the extracellular fluid (ECF) volume divided by its steady-state value.* If the volume of

* ECF could be replaced by plasma volume.

the ECF increases then the normalised value will rise above unity. This value is multiplied by the steady-state value for the GFR. Ikeda and co-workers included this function as an implicit controlling factor supposedly brought about by information from volume receptors:

$$GFR1 = (SSGFR)*(VECF/SSVECF) \qquad (7.111)$$

The second physical factor that influences GFR is change in arterial pressure. This represents the well recognised autoregulatory mechanism:

$$\begin{aligned} GFR2 &= 0.0 && PA < 40 \\ &= 0.02*(PA)-0.8 && 40 \leq PA < 80 \\ &= -0.005*((PA-100)\uparrow 2)+1 && 80 \leq PA < 100 \\ &= 1.0 && 100 < PA \end{aligned} \qquad (7.112)$$

So that actual GFR is:

$$GFR3 = GFR1*GFR2 \qquad (7.113)$$

A third factor that also exerts influence over urinary output at the GFR stage is the so-called 'Third Factor'. This represents the effect of body fluid volume expansion on increased urinary output, not fully explained by the antidiuretic hormone or aldosterone. The assumption is that the Third Factor is brought about via plasma colloid osmotic pressure:

$$\begin{aligned} THDF &= -5.0*((PPCO/28)-1)+1 && PPCO \leq 28 \\ &= 1.0 && PPCO > 28 \end{aligned} \qquad (7.114)$$

The Third Factor and an assumed constant representing 80 percent reabsorption of the ultrafiltrate are combined with the actual GFR to produce a fourth equation for GFR. This is used to calculate net ultrafiltraiton of electrolytes:

GFR4 = (GFR3)*0.2*(THDF) (7.115)

Urine formation:

Urine excreted in the proximal tubules remains approximately isotonic. The rate at which water passes through the proximal tubules is determined by electrolyte passage rate through the proximal tubules, a constant contribution by glucose is included:

DTU = (UUR+0.312+(1.86*(DNNA+DNK)))/EOSM (7.116)

The water load passing through the distal tubule is modified by the effects of ADH so that water can be either additionally conserved or excreted:

UO = DTU-((ADH2)*0.9*(DTU)) (7.117)

Thus 90 percent of the urine filtrate is conserved, but may be modified by ADH. Equation (7.117) implies that if ADH2 becomes greater than 1.1 then water is taken into the system from an unspecified source. Furthermore, it is necessary that an obligatory urine loss of 500 ml per day is maintained to clear out wastes. Thus the constraint UO $\geq$ .0003472 has been imposed on the model.

Renal bicarbonate dynamics:

Bicarbonate is reabsorbed in the kidney as a function of the partial pressure of carbon dioxide in the plasma. If the partial pressure of carbon dioxide rises, then from the Henderson Hasselbach equation (7.153), it is known that blood acidity will rise. Equation (7.153) shows that a rise in plasma bicarbonate would offset the rising acidity. This increased need is explicitly represented by the following equations:

$$UFHCO3 = (ZEHCO3)*(GFR3) \tag{7.118}$$

$$MDUHCO3 = (-PCO2/120.0)+(4.0/3.0)+UFHCO3 \tag{7.119}$$

$$UHCO3 = \begin{cases} 0 & MDUHCO3 \leq 2 \\ 0.1638*((MDUHCO3-2.0)\uparrow 2.61) & 2 < MDUHCO3 \leq 4 \\ (MDUHCO3-3.0) & 4 < MDUHCO3 \end{cases} \tag{7.120}$$

Renal chloride dynamics:

It is assumed that chloride will match the cation excretion up to the point where all chloride available in the ultrafiltrate has been excreted (the very small contribution from phosphate has been excluded):

$$UFCL = (GFR3)*(ZECL) \tag{7.121}$$

$$UCH = (UNA+UK+UNH4+2*(UCA)+2*(UMG)-UHCO3-0.073) \tag{7.122}$$

$$UCL = \begin{cases} 0 & UCH < 0 \\ UCH & UCH \leq UFCL \\ UFCL & UCH > UFCL \end{cases} \tag{7.123}$$

Renal phosphate dynamics:

The reabosrption of phosphate is T_m (tubular maximum) limited:

UFHPO4 = (ZEHPO4)*(GFR3) (7.124)

$$\left.\begin{array}{lll} \text{UHPO4} = 5.0*(\text{UFHPO4})/22.0 & \text{UFHPO4} \leq 0.11 \\ = \text{UFHPO4}-0.085 & \text{UFHPO4} > 0.11 \end{array}\right\} \quad (7.125)$$

Renal urea dynamics:

Urea is excreted as a constant part of the urea arriving in the glomerular filtrate. It is the lack of renal urea control that makes urea a useful measure of ultrafiltrate formation. Urea excretion is therefore a measure of renal health:

UUR=0.6*(GFR3)*(ZWUR) (7.126)

Renal albumin dynamics:

Albumin is not normally excreted and urine loss is assumed to be very low in normal health.

$$\left.\begin{array}{lll} \text{UALB} = ((\text{ZPALB})*(\text{GFR3}-0.1)/10) & \text{GFR3} \geq 0.1 \\ = 0 & \text{GFR3} < 0.1 \end{array}\right\} \quad (7.127)$$

Renal calcium dynamics:

Calcium reabsorption is T_m limited:

UFCA = (ZECA)*(GFR3) (7.127)

$$\left.\begin{array}{lll} \text{UCA} = 0 & \text{UFCA} < 0.493 \\ = \text{UFCA}-0.493 & \text{UFCA} \geq 0.493 \end{array}\right\} \quad (7.129)$$

Renal magnesium dynamics:

Magnesium reabsorption is T_m limited:

UFMG = (ZEMG)*(GFR3) (7.130)

$$\left.\begin{array}{lll} \text{UMG} = 0 & & \text{UFMG} < 0.292 \\ = \text{UFMG}-0.292 & & \text{UFMG} \geq 0.292 \end{array}\right\} \quad (7.131)$$

Renal potassium dynamics:

After the autoregulatory reabsorption in the proximal tubules implicit in GFR4, a further 50 percent of potassium is reabsorbed in the loops of Henle:

PTK = (GFR4)*(ZEK) (7.132)

LHK = (PTK)*0.5 (7.133)

In normal steady-state conditions a further 90 percent of potassium is reabsorbed in the distal tubule. Excretion into the lumen may occur outside of normal steady-state conditions depending on extracellular potassium concentration and the hormonal control of aldosterone:

DNK = (0.9*(LHK))+((0.01778*(ZEK)*(ALD2)) (7.134)

A further 61 percent of potassium is reabsorbed between the distal nephron and the collecting ducts:

UK = (DNK)*0.39 (7.135)

Renal sodium dynamics:

After the autoregulatory reabsorption in the proximal tubules implicit in GFR4, a further 50 percent of sodium is reabsorbed in the loops of Henle:

PTNA = (GFR4)*(ZENA) (7.136)

LHNA = (PTNA)*0.5 (7.137)

In normal steady-state conditions a further 90 percent of sodium is reabsorbed in the distal nephron. Further reabsorption may occur outside of the normal steady-state according to aldosterone control:

DNNA = (0.9*(LHNA)-((ALD2)*0.09)) (7.138)

Approximately a further 88 percent is reabsorbed between the distal nephron and the collecting ducts in the normal steady-state. The sparing of sodium ions is facilitated when the net rate of acid secretion rises. The net rate of acid secretion is represented by the buffering agents and has the constraint $(-UHCO3+UNH4+UTA) \geq 0$ (Gardner, 1978). So that sodium excreted via the urine is:

UNA = ((DNNA)*0.11624+(UHCO3-UNH4-UTA)) (7.139)

The following analytes are considered in MFAB only by their excretion rates.

Renal titratable acid:

Titratable acid refers to the amount of buffer required to titrate urine acidity back to its normal pH. This is represented as a function of urine and plasma acidity:

UTA1 = 0 $PHU \leq 4$

= ((SSUTA)*(-2.5*(PHAA)+19.5))*(PHU-4) $4 < PHU \leq 5$ (7.140)

= ((SSUTA)*(-2.5*(PHAA)+19.5)) $5 < PHU$

UTA = UTA1+((0.001*(ALD2))+0.009) (7.141)

Aldosterone is assumed to affect titratable acid so that the alkalosis of hyperaldosteronism may be brought about. The effects of plasma acidity on titratable acid excretion are subject to a 200 minute delay:

D(PHAA) = (PHA-PHAA)/200 (7.142)

Renal ammonium dynamics:

Ammonium is an important buffer of the urine. Its excretion is a function of urine acidity:

UNH4 = ((SSUNH4)*(-0.5*(PHUA)+4.0)) (7.143)

The effects of urine acidity on urine ammonium dynamics is subject to a 300 minute delay:

D(PHUA) = (PHU-PHUA)/300 (7.144)

Renal glucose dynamics:

Glucose reabsorption is assumed to be T_m limited:

UFGL = (ZEGL)*(GFR3) (7.145)

$$\left.\begin{array}{lll} UGL = 0 & UFGL < 0.65 \\ = UFGL-0.65 & UFGL \geq 0.65 \end{array}\right\} \quad (7.146)$$

COMPARISON WITH OTHER MATHEMATICAL MODELS:

The renal model presented above differs from Ikeda and co-workers representation through the bicarbonate and chloride equations. One feature of MFAB that differs from the whole model of Ikeda and co-workers is that both bicarbonate and chloride have two distinct compartmental representations as opposed to merely renal representations. Thus, urine excretion in MFAB is related to the state of these electrolytes, for example through extracellular concentrations. Furthermore, urine losses are recorded in the mass balance equations of the respective compartmental representations.

A large number of extant renal models were identified by Flood et al (1984a). Representative models of the two main approaches can be found in Cameron (1977) and Badke (1972).

Cameron (1977) developed a simplified version of Guyton et al (1972). In the simplified model the kidney is represented by a single compartment, with overall relationships modified by GFR, ADH, aldosterone and sodium plasma concentration. The model as such, with its relatively simple renal dynamics, appears well able to simulate a range of pathological conditions in which the kidney plays a vital role. Serious consideration was given to the possibilities involved with the use of this representation. It was concluded that the simplicity of Cameron's renal representation would impose too many restrictions on the necessary addition of acid-base dynamics. Furthermore, the model of Ikeda and co-workers was developed within the mould of an integrated fluid-electrolyte, acid-base representation and has obvious advantages for that reason. Cameron did, however, intend to increase the complexity of the renal dynamics in terms of adding to the number of functions involved rather than adopting a multicompartmental representation of the nephron such as can be found in Cage et al (1977). An up-dated version of Cameron's model could be of interest if made available.

A very different representation can be found in Badke (1972). The kidney is considered in five sub-units: glomerulus, proximal and distal tubules, the loops of Henle and the collecting ducts. The first three are modelled as homogenous compartments, whilst the

last two include spatial effects and thus require partial differential equations for their representation. A difference equation approach is adopted for the solution of the partial differential equations. This model offered little in the way of acid-base dynamics and involved substantial complexity. For these reasons it was concluded that this representation is not parsimonious with respect to the research objectives.

It is interesting to note that with the one compartmental renal representation Cameron used a multicompartmental fluid and electrolyte structure, whereas with the five compartmental renal representation Badke used a single compartmental representation for salt and water. Validity of the former model was good, however, validity of the latter model was difficult to judge.

VALIDATION:

An initial validation of the renal model was made by identifying explicitly the similarities and dissimilarities between currently accepted physiology and the model representation, as shown in Figure 7.13. The qualitative features of the renal model that match currently accepted physiology include the representations for sodium, potassium, water (the three essential analytes of the model), chloride (although there is recent evidence that suggests renal chloride pumps may exist, Lote, 1982), bicarbonate, phosphate, urea and glucose. A T_m limited representation for calcium and magnesium appears to be rather crude but as their renal dynamics may be related to chloride (or anyway display evidence of some special functions) then from a theoretical viewpoint a T_m limited representation displays some of the qualitative features

that are known to occur, whilst omitting theoretical features that may not occur.

Other than the qualitative observations outlined above, validation of the kidney can only realistically be assessed when integrated with MFAB (or any other relevant model). This is the case for at least two reasons; firstly the renal subunit is an acutely open system and secondly the control of its functions lie without the system of current concern.

It was interesting to note the results of Ikeda and co-workers for water loading and saline infusion. These are the most fundamental tests of the interaction between body fluids and the kidney. Water intake led to a marked increase in urine output (the quantitative features being determined by ADH) and saline infusion raised extracellular volume causing only a slight increase in urine output (due to the third factor) and took several hours of simulation time to return to normal. These results are impressive because of the comparable quantitative features between simulation and experimental data. This does not necessarily give a green light for the similar kidney included in MFAB due to the nature of non-linear models (one change in a non-linear model ideally requires that all previous results in a validation programme be reassessed). It does, however, provide substantial confidence in the basic structure and processes that have been brought forward for MFAB.

7.3.2.6 Acid-base dynamics

MATHEMATICAL MODEL:

Bicarbonate is an integral part of both the fluid-electrolyte dynamics and the acid-base dynamics. The need to represent this electrolyte using the principles of mass flux was discussed under the heading FLUID AND ELECTROLYTES. The entry point of bicarbonate into the model is into the extracellular fluid by representation of metabolic production. Metabolic production occurs in the kidney through biochemical reaction with protons (the balance between these electrolytes can be met by using the Henderson-Hasselbalch equation).

It was therefore necessary to develop a function to represent bicarbonate metabolism. Although the bicarbonate extracellular representation of Ikeda et al (1979) is not in compartmental terms, the empirically derived equation holds some information on bicarbonate metabolism. The equation given is:

$$ZEHCO3 = STBC-(0.527*(XHB)+3.7)*(PHA-7.4)+0.375*(UHB-UHBO)/0.02226 \quad (7.147)$$

where STBC is standard bicarbonate, UHB is blood oxygen combining power, UHBO is blood oxyhaemoglobin and XHB is blood haemoglobin concentration. As the current research assumes that oxygen dynamics can be excluded and blood haemoglobin concentration is constant, equation (7.147) can be simplified to:

$$ZEHCO3 = STBC-(11.605*(PHA-7.4)) \quad (7.148)$$

This equation is an expression of what the bicarbonate concentration should be, given the current state of all other ions and blood acidity, that is:

$$STBC = \sum_{i=1}^{n} cation_i - \sum_{j=1}^{m} anion_j \quad (mEq\ l^{-1}) \qquad (7.149)$$

where n and m refer to the number of cations and anions respectively. The relationship between PHA and bicarbonate concentration is therefore defined by PB1:

$$PB1 = -11.605*(PHA-7.4) \quad (mEq\ l^{-1}) \qquad (7.150)$$

Multiplying both sides by the volume of the extracellular fluid (VECF) gives a similar relationship with respect to bicarbonate content defined by PB2:

$$PB2 = (VECF)*(-11.605*(PHA-7.4)) \quad (mEq) \qquad (7.151)$$

Metabolic production rate of bicarbonate is therefore:

$$MPHCO3 = SSMPHCO3+((VECF)*11.605*(7.4-PHA)) \qquad (7.152)$$

with a time constant in the differential equation for extracellular bicarbonate of 1 minute.

Plasma hydrogen ion concentration is calculated from the Henderson-Hasselbalch equation:

$$PHA = 6.099+DLOG10(ZEHCO3/(0.03*(PCO2))) \qquad (7.153)$$

The equation for partial pressure of carbon dioxide was derived from data given by Gardner (1978):

$$PCO2 = 2.5*(ZWCO2-23.0)+35.0 \qquad (7.154)$$

Where the whole body carbon dioxide content is represented as one compartment:

D(WCO2) = MPCO2-((VR)*(SSECO2)) (7.155)

COMPARISON WITH OTHER MATHEMATICAL MODELS:

Despite the large number of extant fluid-electrolyte models, very few have been developed in the mould of an integrated fluid-electrolyte, acid-base representation. Ikeda et al (1979) is a typical example of the models that include an acid-base element. The state variables and computed variables modelled are the same as those developed above, using the Henderson-Hasselbalch equation for acidity but different functions for the remaining variables.

VALIDATION:

Validation of these equations is difficult as they do not constitute a distinct dynamic unit. Suffice to say that the basis of the acid-base dynamics lies with the Henderson-Hasselbalch equation which holds obvious theoretical validity. Further validation has been undertaken at the holistic level, as discussed in Chapter 8.

7.3.2.7 Respiratory dynamics

MATHEMATICAL MODEL:

Respiratory dynamics are incorporated in MFAB as a controller over ventilation rate and consequently the rate of excretion of carbon dioxide. Oxygen dynamics have not been represented. A rough basis for the calculation of ventilation rate is given by Gardner (1978). He stated that ventilation rate increases approximately two times

for every 0.1 drop in plasma acidity, and increases approximately four times for every 10 mmHg rise in the partial pressure of carbon dioxide. Two exponential functions were drawn up to represent this data:

EPAVR = DEXP(7.0*(SSPHA-PHA)) (7.156)

EPCO2VR = DEXP(0.138*(PCO2-SSPCO2)) (7.157)

Normalised ventilation rate is achieved by linearly combining equations (7.156) and (7.157):

VR = (EPAVR+EPCO2VR)/2 (7.158)

COMPARISON WITH OTHER MATEHMATICAL MODELS:

Respiratory dynamics are not a common feature of fluid-electrolyte models. However, a number of respiratory models have been developed in their own right. The cyclical models of one research group include Grodins and James (1963) and Grodins et al (1967). It was upon the latter model that Ikeda et al (1979) based the respiratory component of their fluid-electrolyte, acid-base model. The authors found that the minimum integration step length required when simulating the model was determined by the respiratory unit, whose frequency characteristics were approximately ten times as rapid as those of the other blocks but too short to achieve an effective long term simulation, taking 96 minutes to simulate 1 day of real time using a HP-21MX mini-computer with 64 kbytes of memory. For the purposes of the current research programme, this representation is not parsimonious.

VALIDATION:

The exclusion of oxygen dynamics requires some explanation. This simplification is based on three points.

1. The patient is strictly controlled in the ITU.
2. The evidence of Haldane and Priestley (reported by Gardner, 1978) that under widely varying environmental conditions oxygen levels in the blood remained relatively constant whilst carbon dioxide levels varied widely.
3. Gray's multiple factor theory (Gray, 1945) states that partial pressure of carbon dioxide, partial pressure of oxygen and blood acidity act independently on ventilation rate. This is not the whole truth, however, as a part truth it does add credibility to such a representation.

The success of the respiratory model is assessed in parallel to the closely linked acid-base equations in the holistic validation of Chapter 8.

7.3.2.8 Hormonal dynamics

MATHEMATICAL MODEL:

The rate of change of ADH secretion is brought about by deviations of stimuli from set points. These are integrated as a weighted additive sum with time constant, to produce a control response targeted at the kidney. The causal factors for ADH secretion are extracellular osmolality and arterial pressure; and for aldosterone are extracellular potassium concentration, arterial pressure and the maculla densa theory. The functions used to simulate these phenomena are simplified from Ikeda et al (1979).

The responses of ADH are allowed to take effect immediately (as if being released directly from a store), however, aldosterone responds to the value of the stimuli at t=100 (as if being

synthesised from proteins). These statements need some qualification in that the time constant represents the time between stimulation by the causal factors and the time that the hormone hits its target:

```
D(ADH1) = ((WTOSADH*(EOSM-287.0))-(WTPAADH*(PA-100))
          -ADH1)/TCADH                                    (7.159)

ADH2    = 1.1/(1+DEXP(-0.5*(ADH1+4.605))*(AADH)           (7.160)

D(ALD1) = (((ZEK-4.5)*WTKALD)-((PA-100.0)*WTPAALD)
          -((LHNA-1.4)*WTNALD)-ALD1)/TCALD                (7.161)

ALD2    = 10/(1+DEXP(-0.44*(ALD1-5.0)))*(AALD)            (7.162)
```

COMPARISON WITH OTHER MATHEMATICAL MODELS:

The hormonal dynamics of Cameron (1977) are similar to the above equations according to the secretive stimuli, and different in that set point theory is not used. ADH is stimulated by hypothalamic osmoreceptors, and aldosterone by a relationship between extracellular sodium and potassium and arterial pressure. Non-linear functions were used. In addition, Cameron represented angiotensin dynamics, with extracellular sodium concentration as stimulus.

Koushanpour and Stipp (1982) were consistent with the above representations for ADH. The secretion of this hormone is stimulated by left atrial pressure and plasma osmolality, represented by a linearised Taylor series expansion of a postulated non-linear function. The effects of aldosterone and the renin-angiotensin-aldosterone (RAA) system were not incorporated, due to the effects being documented mainly during chronic disturbances in renal function. In addition, since the major purpose of the

simulation was to test the effect of short term forcings on renal function, and as the minimum response time is three to four hours before the effects of a change in aldosterone concentration can be detected in urine output, it was possible to consider the aldosterone aspect of the RAA system as being outside the system of interest. Furthermore, the transient nature of the renin-angiotensin aspect was too short to be of concern in relation to the objectives.

The objectives associated with MFAB, however, relate closely to chronic disturbances in renal function. Furthermore, as the clinical decision making period is directly related to the amount of time necessary for treatment to take effect (in most fluid-electrolyte situations a minimum of 8 hours) then 4 hours delay for aldosterone to take effect comes within the range of the system of interest, but the rapid effects of angiotensin do not. These considerations led to the representation of only the aldosterone aspect of the RAA system in MFAB.

VALIDATION:

The validity of the representation for these hormonal controllers can best be assessed in conjunction with other fluid-electrolyte aspects. The holistic validation of Chapter 8 deals with this for MFAB. Suffice to say that the equations given above for hormonal dynamics have been carried forward in a variety of prototypes and through a number of first pass qualitative and quantitative feature analyses of those prototypes. They have consistently provided a high level of agreement to the published data.

7.3.2.9 Protein dynamics

Intercompartmental exchanges of protein for the given structure of MFAB consists almost exclusively of albumin (the higher molecular weight of other globulins preventing such movements). The structure consists of an interstitial and a plasma compartment connected via the microvascular dynamics. The works of Rossing (1978) and Reeve and Chen (1973) were found to be generally useful for parameter estimates:

D(PALB) = FALBLY-NTRALB-FALBC-UALB+SIALB (7.163)

D(ISALB) = FALBC-FALBLY (7.164)

FALBC = ((ZPALB-ZISALB)*((PC)↑ 2)*(6.9204*1E-5.0)) (7.165)

FALBY = (ZISALB)*(LRR) (7.166)

NTRALB = ((ZPALB)*(LPDRALB)-0.01076) (7.167)

so that there is a controlling factor over plasma albumin concentration through the implicit inclusion of liver protein metabolism. Urea is a waste product of that metabolism and may be derived from the current content of albumin:

MPUR1 = (PALB/SSPALB) (7.168)

MPUR2 = (SSMPUR)*(MPUR1) (7.169)

COMPARISON WITH OTHER MATHEMATICAL MODELS:

Ikeda et al (1979) used three compartments to represent protein dynamics; interstitial, plasma and pulmonary. Albumin dynamics are integrated with those of other globulins, and an implicit representation of protein turnover in the liver is included. The model of Ikeda and co-workers was tried in earlier prototypes and found to 'blow up' on long simulations although no satisfactory reason was found which accounted for this.

A simpler representation is offered by Cameron (1977). A single extracellular compartment is used with an implicit liver representation creating/destroying protein around a set point. From the extracellular content, two equations are used to derive interstitial and plasma albumin concentrations. Despite this being generally consistent with Rossing (1978) in that a loss of plasma protein will lead to a redistribution of body protein, the Cameron model was discarded due to inconsistencies with the research objectives. The three special features that required inclusion are: ability to simulate diminished albumin synthesis, ability to increase capillary permeability (for instance due to gross inflammation) and the ability to simulate albumin loss to urine (for instance in disease of Bowmans capsule). These phenomena are explicitly available.

VALIDATION:

The protein equations are dependent on the microvascular and cardiovascular representations to such an extent that the protein dynamics cannot be simulated without them. This was one of the tasks undertaken during holistic validation and the reader is directed to that part of Chapter 8 for further details.

7.3.2.10 Glucose dynamics

The glucose dynamics are taken from Ikeda et al (1979) and have been integrated with the Deland principles (Deland, 1975). The reason for including glucose is to model the special biochemical feature of cellular uptake of potassium brought about by insulin promoted glucose metabolism:

D(EGL) = ((SIGL/180)-EGLKI1-UGL) (7.170)

D(GLA) = ((ZEGL-(GLA1/18.0))-GLA)/15.0 (7.171)

EGLKI1 = ((SINI)*(CGL2)+(CGL1)*(GLA)) (7.172)

EGLKI2 = (CGL3)*(EGLKI1) (7.173)

COMPARISON WITH OTHER MATHEMATICAL MODELS:

The objectives of Cramp and Carson (1981) were to study short term regulation of glucose and to enhance the understanding of glucose homeostasis. It is an important model as it continued the movement away from the earlier simplistic approaches of implicit representation of physiology, by arbitrary adaption of non-linear mathematical functions, to explicitly based representations using known physiology and biochemistry, especially at the enzyme level. This is particularly important for areas of controversy or weak knowledge.

Despite the advantages of such a model (including glucose promoted metabolism by insulin) the key factor of concern for MFAB (potassium uptake by cells as a consequence of glucose metabolism promoted by insulin) was not paralleled by Carson and Cramp's objectives. Thus, the simple representation of Ikeda and co-workers model was adapted with its more complex representation of insulin-glucose-potassium action.

VALIDATION:

As the objectives related to this representation require joint analysis of glucose and potassium dynamics, the important points arising from validating this aspect of the model have been more

appropriately documented in Chapter 8. The simulation responses of Ikeda and co-worker's representation in their fluid-electrolyte model (for a 50 g infusion of glucose) was consistent in a qualitative sense with expected responses, although quantitative features were not assessed.

7.4 ASSUMPTIONS OF THE MODEL

Consolidating the important assumptions made during the development of MFAB adds transparency to the model by explicitly identifying the simplifications made and the theory used in controversial areas, increasing the model's falsifiability and consequently increasing ongoing validity by enabling adaptions and corrections to be made as and when necessary.

The first assumptions listed below are general in nature and relate to ideas of simplification (including parsimony) for example homogeneity and lumping.

1. All compartments contain a single species which undergoes complete mixing after each simulation step. Homogeneity excludes the effects of distance. A point to note here is that Flood et al (1984a) in their pragmatic review of extant fluid-electrolyte models observed that compartmental representation was on the whole more successful, both in efficiency of representation and accuracy of output, than distributed models. This implies that the assumption of homogenous compartments has been relatively successful.
2. Systemic and pulmonary circulations are lumped.

3. Compliance and resistances of each cardiovascular compartment are lumped.
4. Gastrointestinal tract is lumped.
5. Lymphatic capillaries are lumped.
6. Systemic capillaries are lumped.
7. Capillaries do not have the properties of compliance and resistance.
8. Molecular radii of electrolytes are equal.
9. Body temperature is constant.

Some assumptions relate to normal values:

10. Intake quantities of electrolytes per day are those normally associated with a Western diet (see values in Appendix 6).
11. Concentrations of analytes are those normally found in clinics within the United Kingdom and United States of America.

The exclusion of phenomena is also an assumption relating to the ideas of simplification (including parsimony):

12. The hormone PTH is excluded.
13. Vitamin D is excluded.
14. Vascular growth and destruction are excluded.
15. The gastrointestinal chloride-bicarbonate exchange is excluded.
16. Digestion and excretion of food stuffs other than fluid and electrolytes are excluded.
17. Energy dynamics are excluded.
18. Behavioural aspects relating to hunger and thirst have been excluded (in the critically ill patient they are subject

usually to the overriding control of the physician through parenteral feeding).

19. The Gibbs-Donnan effect is excluded.
20. Oxygen dynamics are excluded.

The majority of the following assumptions relate to theoretically uncertain ideas and matters of controversy:

21. 'Third Factor' has been related to plasma colloid oncotic pressure.
22. Transmembrane dynamics are not affected by intracellular and extracellular H^+ ion concentration as the intracellular component and effect on the pumps were not satisfactorily achieved.
23. Proton excretion is represented by an additive sum of urine loss for bicarbonate, ammonium and titratable acid.
24. Proton secretion is matched for electrical charge solely by sodium, thus excluding potassium involvement.
25. Chloride excretion is passive against all other electrolyte excretion according to the net charges involved.
26. Vasodilatory properties of magnesium are not considered to be significant.
27. Gastrointestinal absorption is not affected by body requirements (hence the exclusion of PTH and Vitamin D).
28. Normal gastrointestinal absorption is complete.
29. Pressure and flow in the cardiovascular model are linearly related.
30. The heart is non-pulsatile.
31. Stimuli acting on hormonal secretion do so as an additive weighted sum.

32. Controllers act according to set point theory.
33. Protein (apart from albumin) are pnysically inert in the microvascular system.
34. Arterial pressure is represented as having significant effect on capillary pressure.
35. The close relationship between magnesium and calcium renal dynamics is not interactively represented (both have similar T_m dynamics).
36. A chloride pump in the loop of Henle is not represented and hence the renal relationships with magnesium and calcium (that may also exist) are not represented.
37. The movement of ions across membranes is simulated using a pump for each cation and diffusion for anions.
38. The renin and angiotensin aspects of the RAA system are not considered to be relevant over an eight hour period associated with clinical decisions.
39. The maculla densa theory is valid.
40. Amino acid concentration for protein metabolism is assumed to be constant.

7.5 CONCLUSION

MFAB has been presented as a complex non-linear, lumped parameter, control system model. It has been presented in such a way as to enhance its validity by comparing its representations with those of other workers; by making an initial attempt at validating segments (albeit theoretical validity in many cases); and by consolidating the model assumptions thus adding transparency (the effects of which are also considered further in Chapter 8).

ANALYTES	EXTRACELLULAR		INTRACELLULAR
	PLASMA	INTERSTITIAL	
SODIUM	———	———	———
POTASSIUM	———	———	———
CHLORIDE	———	———	———
BICARBONATE	———	———	———
MAGNESIUM	———	———	———
CALCIUM	———	———	———
PHOSPHATE	———	———	———
UREA	———	———	———
ALBUMIN	———	———	
CARBON DIOXIDE	———	———	———
PROTONS	———		
GLUCOSE	———	———	

Fgiure 7.1 Compartmental breakdown of the analytes of MFAB.

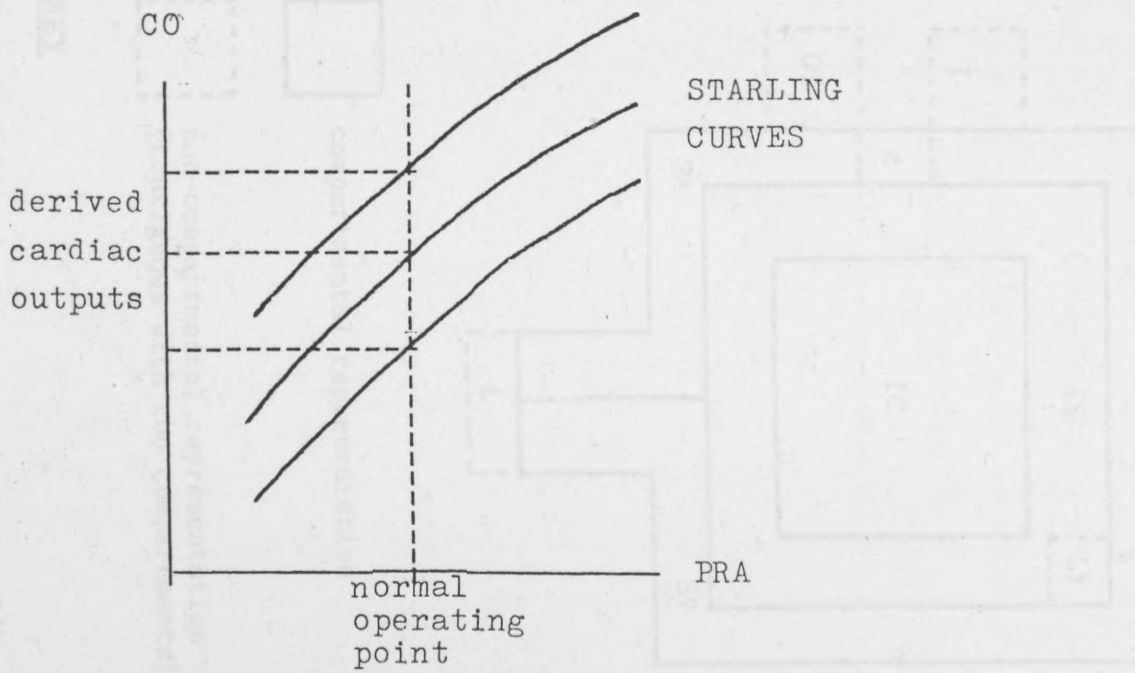

Figure 7.2 Starling curves for cardiac output in MFAB.

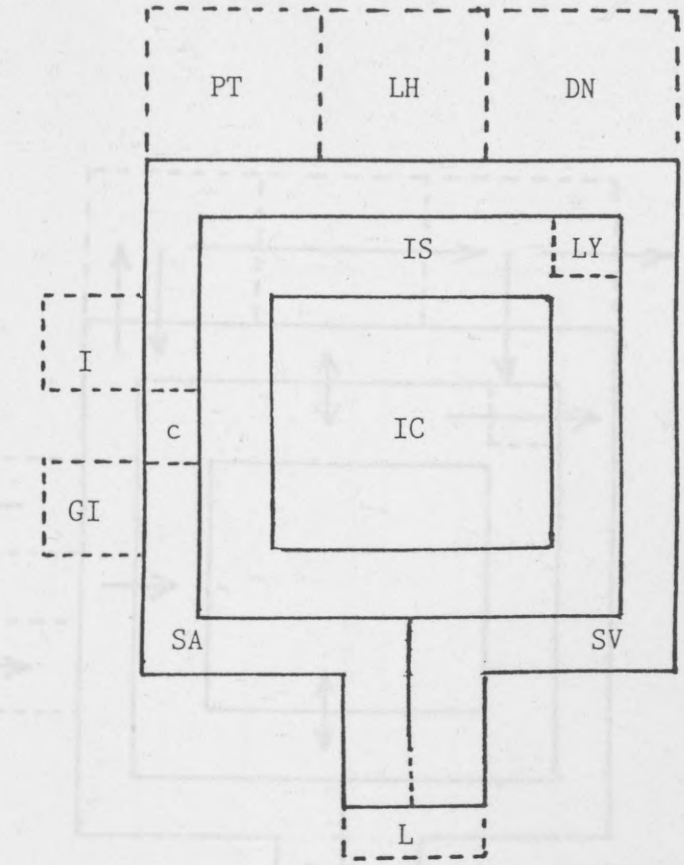

compartmental representation

non-compartmental representation
(contiguous with the compartments)

KEY

C	capillaries	LH	loops of Henle
DN	distal nephron	LY	lymphatics
GI	gastrointestial	PT	proximal tubule
I	insensible route	SA	systemic arteries
IC	intracellular	SV	systemic veins
L	lung		

Figure 7.3 General compartmental structure of MFAB.

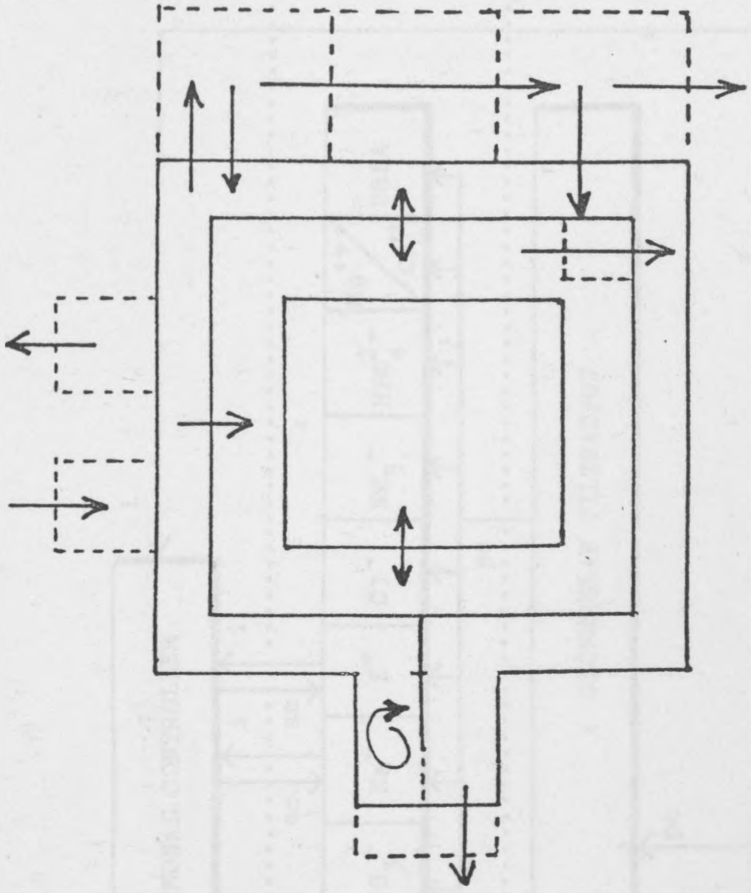

KEY

mass flow

metabolic production

Figure 7.4 Routes available within the compartmental structure of MFAB

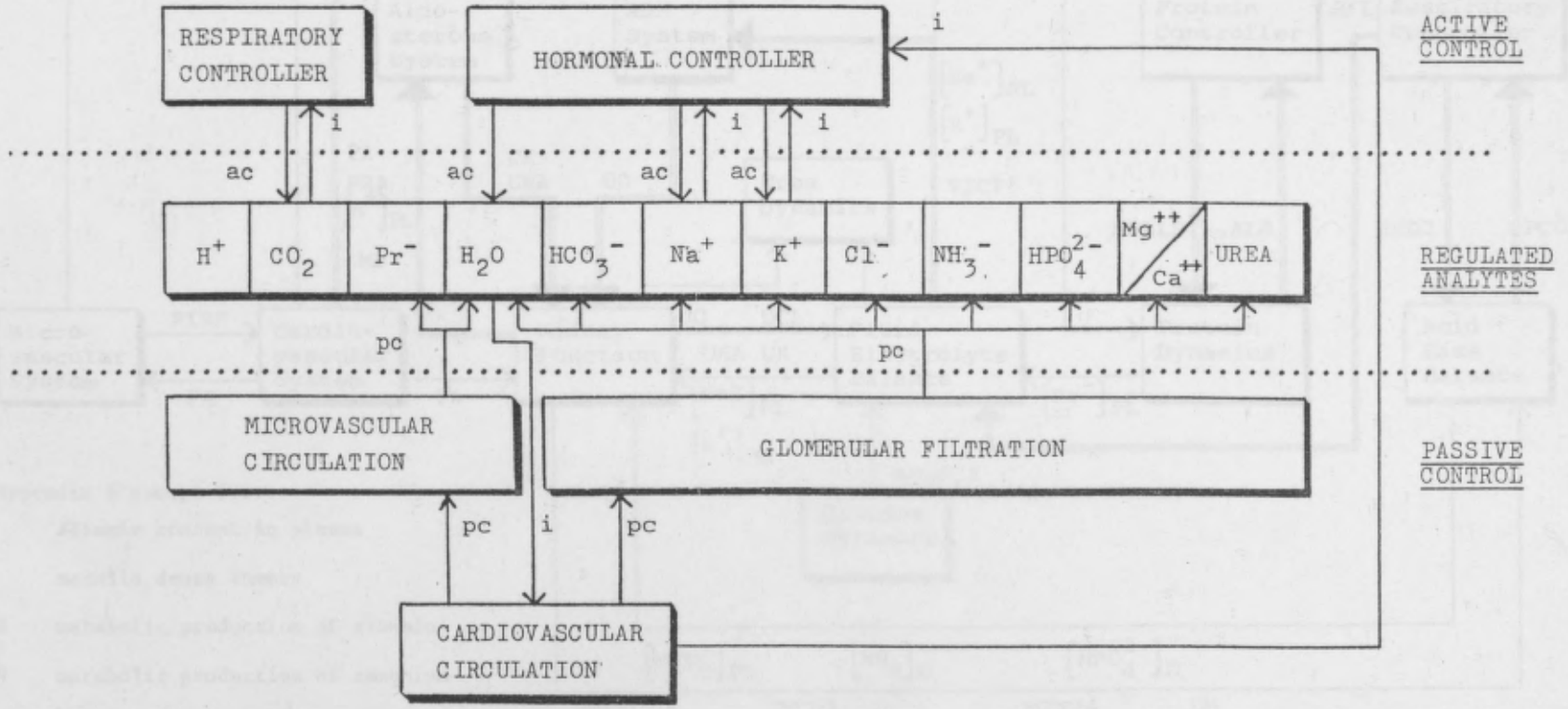

ac= active control
pc= passive control
i= information

Figure 7.5 The relationships between active control, passive regulation and the analytes of MFAB.

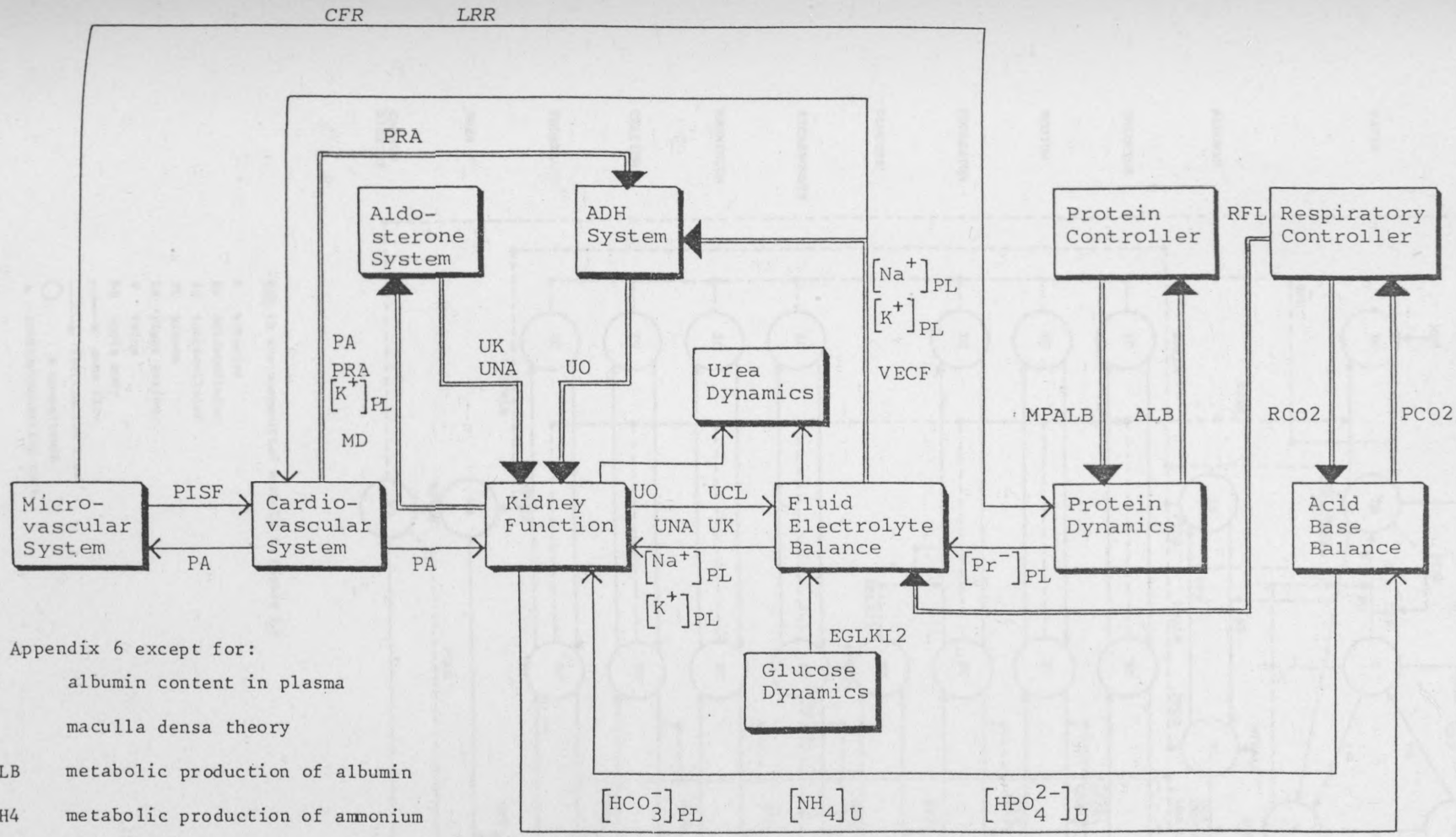

Key: see Appendix 6 except for:

ALB	albumin content in plasma
MD	maculla densa theory
MPALB	metabolic production of albumin
MPNH4	metabolic production of ammonium
RCO2	respiratory loss of carbon dioxide
UH	urine proton flow

Figure 7.6 Submodel structure and interconnections in MFAB, (single line represents, subsystem output flow, double line represents control flow).

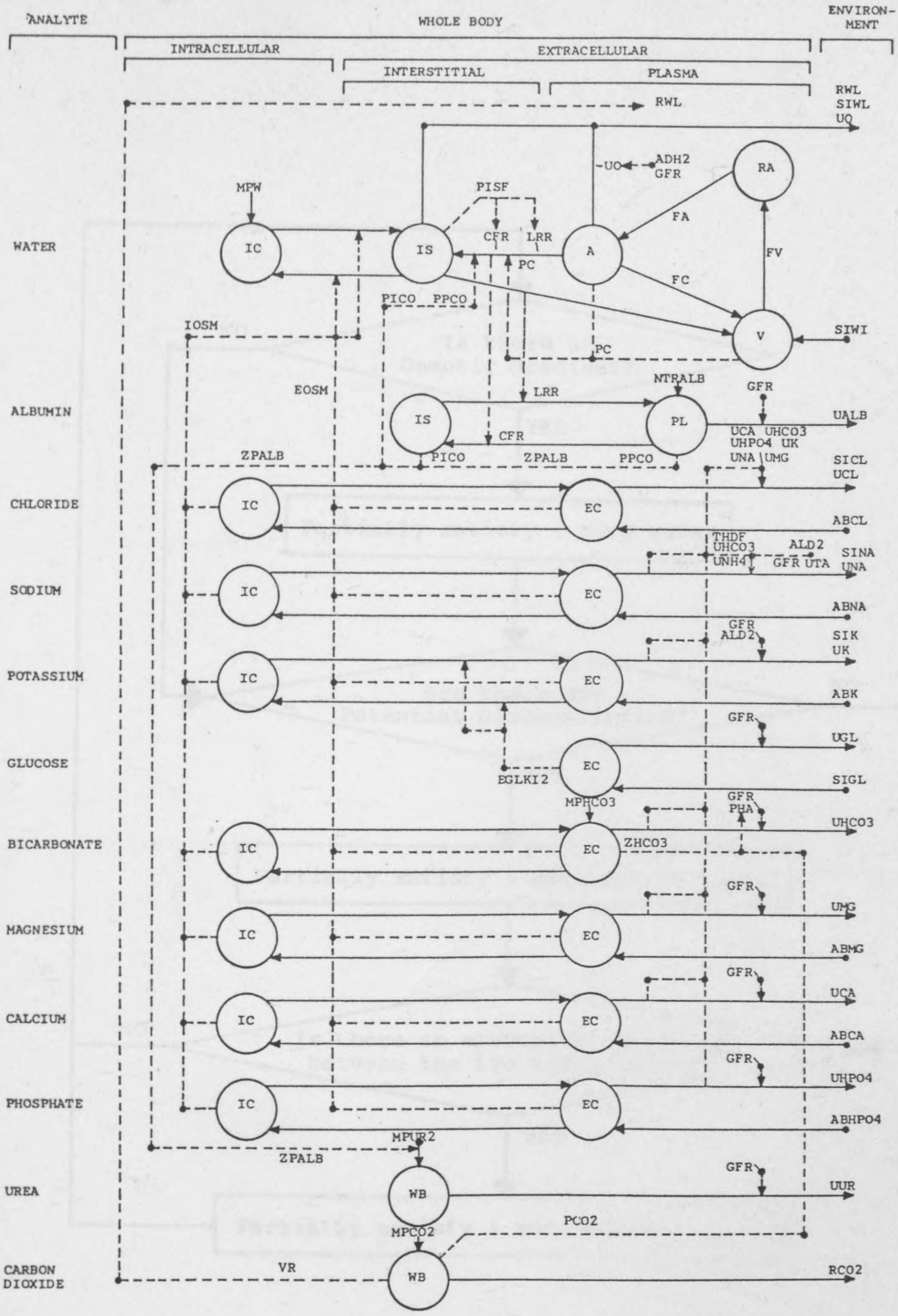

KEY to the unspecified symbols in Figure 7.7

A	arteries
EC	extracellular
IC	intracellular
PL	plasma
RA	right atrium
V	veins
WB	whole body
——→	mass flow
- - - - →	information flow
○	a compartment
•	source/connecting node

Figure 7.7 Compartmental fluxes and main information flows in MFAB.

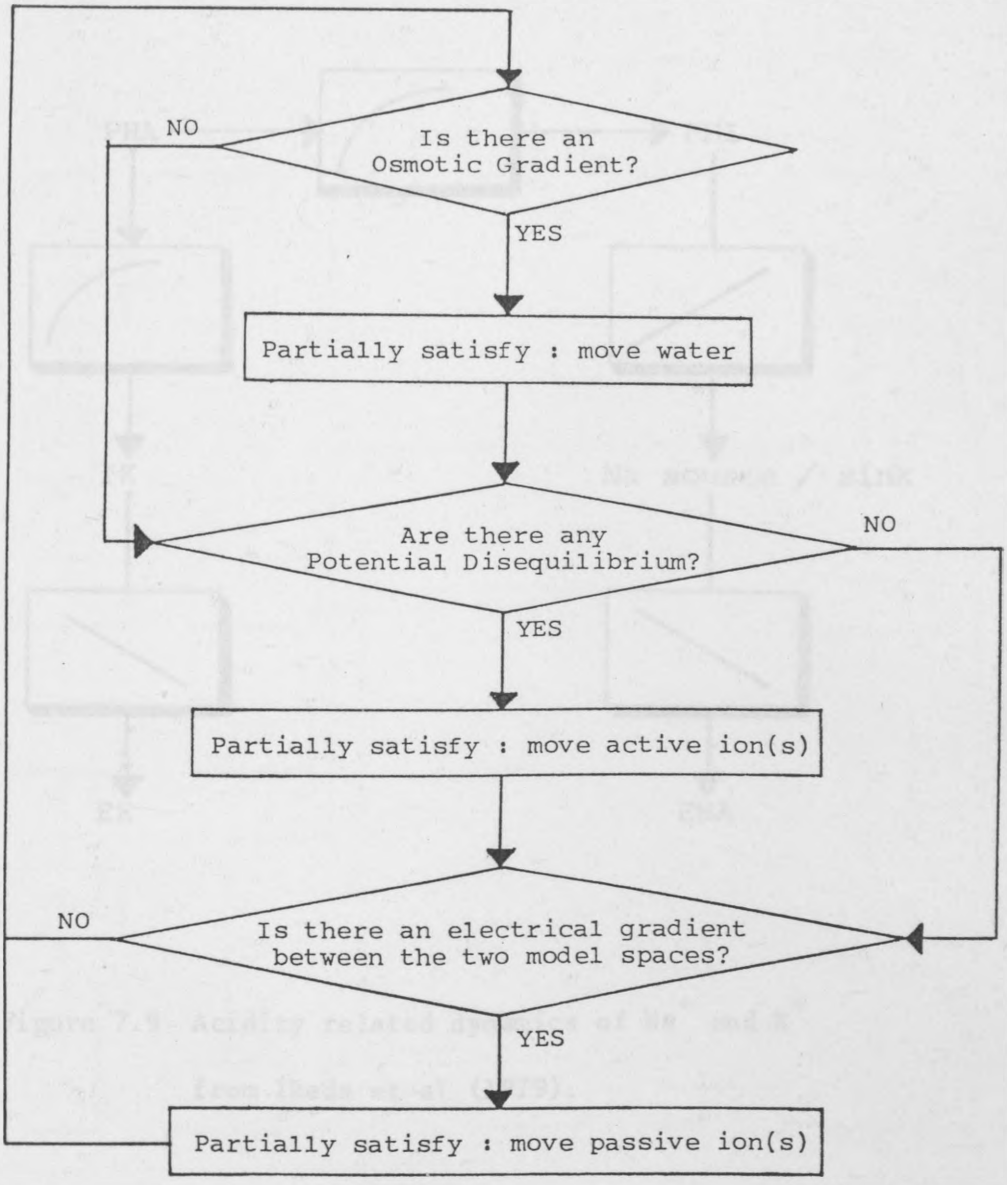

Figure 7.8 Solving the simple blood model of Deland (1975).

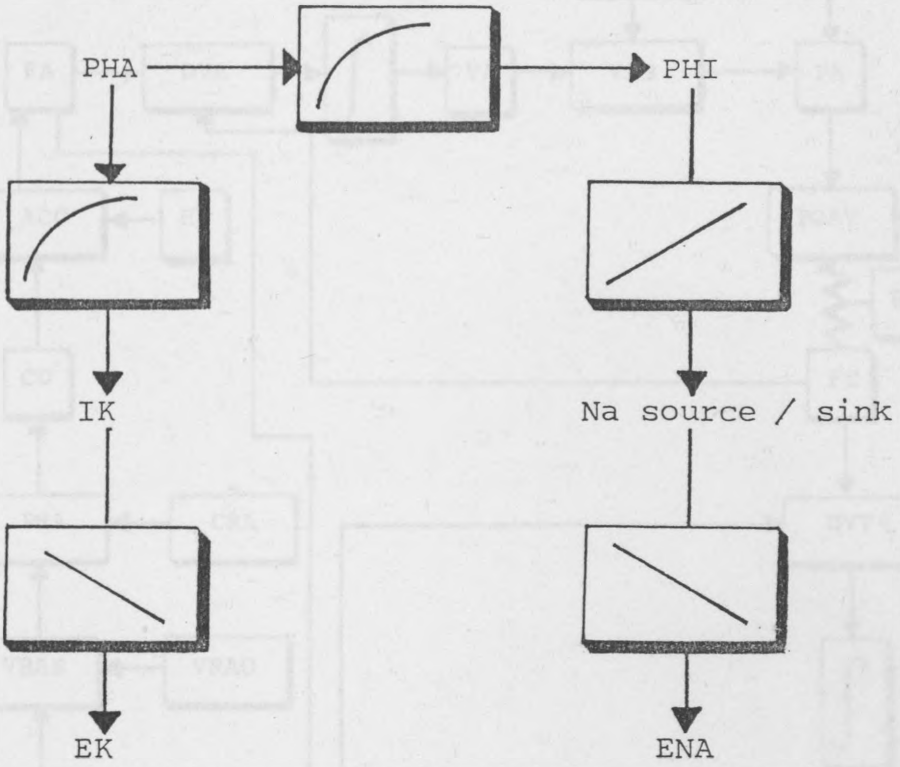

Figure 7.9 Acidity related dynamics of Na^+ and K^+ from Ikeda et al (1979).

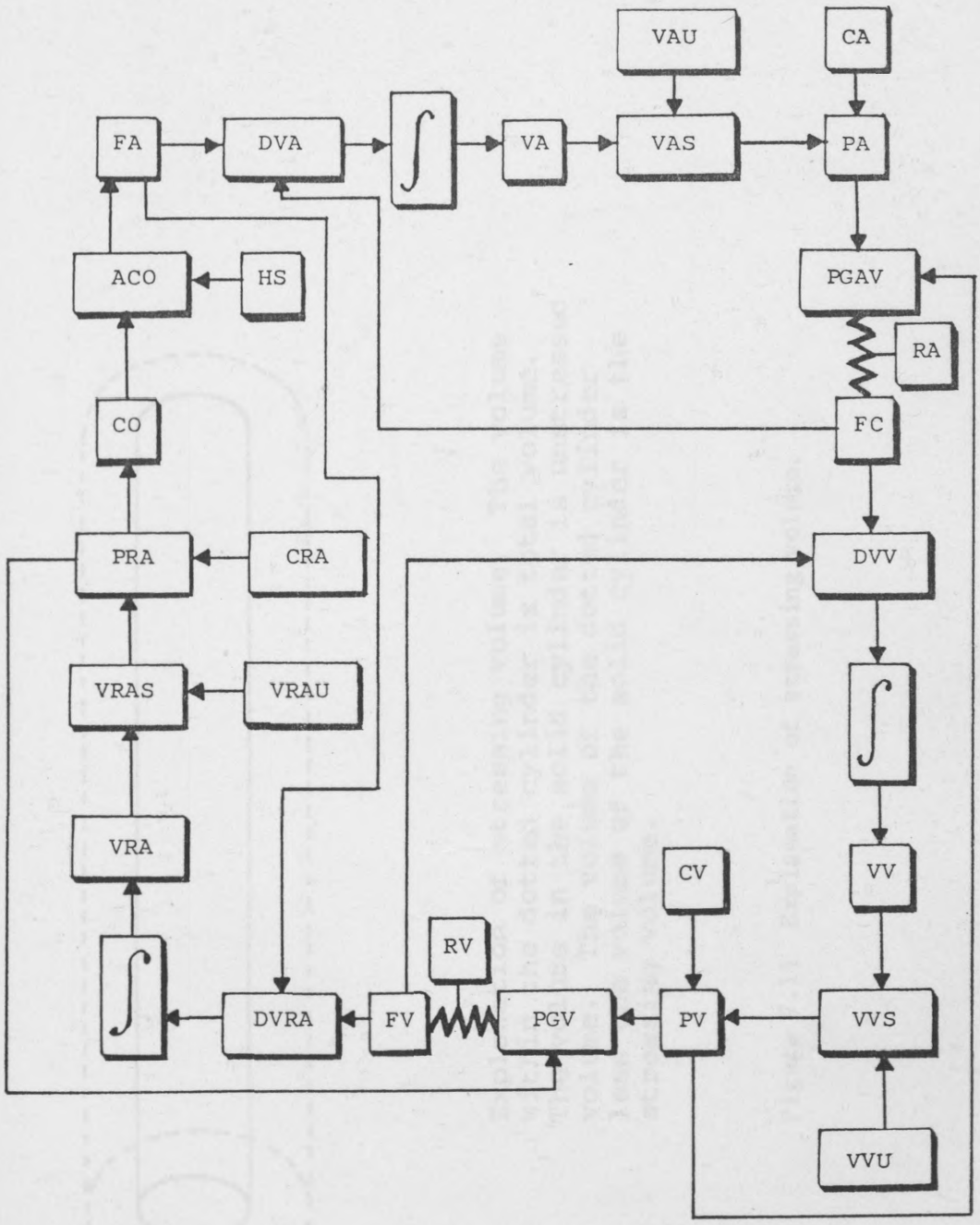

Figure 7.10 Original structure for the cardiovascular model of Parkin (1984).

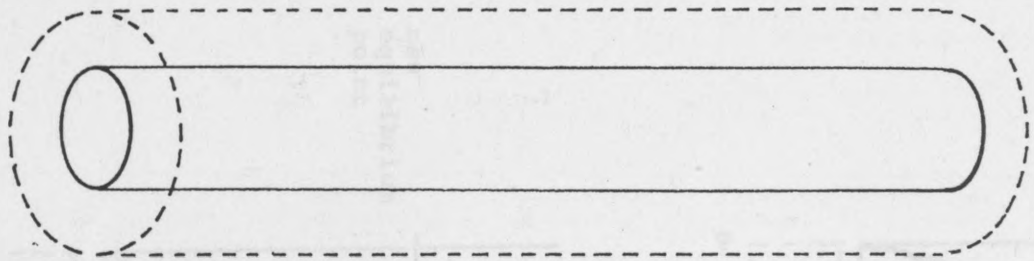

Explanation of stressing volume. The volume within the dotted cylinder is total volume. The volume in the solid cylinder is unstressed volume. The volume of the dotted cylinder less the volume of the solid cylinder is the stressing volume.

Figure 7.11 Explanation of stressing volume.

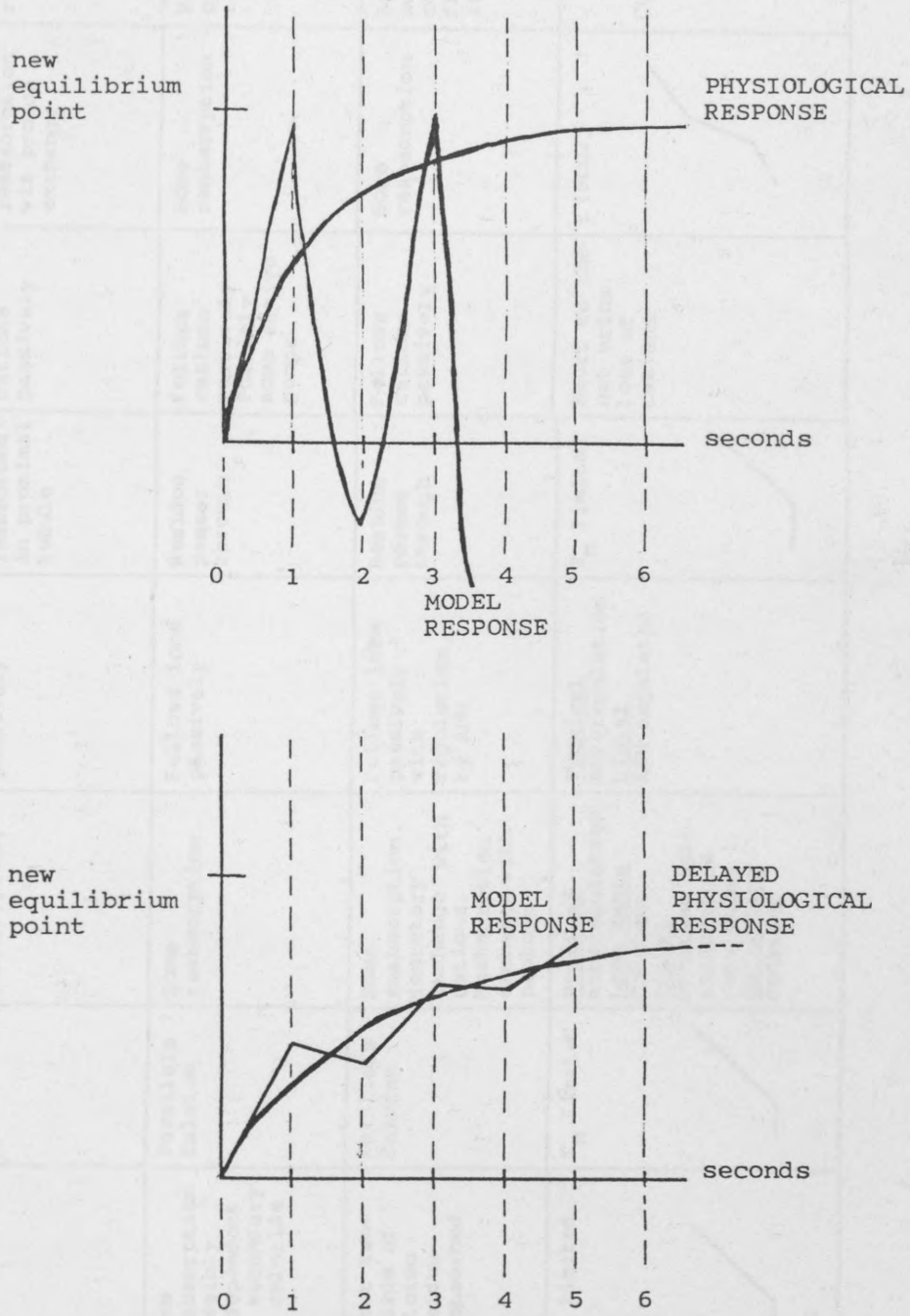

Fgiure 7.12 Effect on stability of changing the time constant of the cardiovascular model:

(a) 5 seconds;

(b) 15 seconds.

ISOTONIC ULTRA-FILTRATE	Na^+	Ca^{++}	Mg^{++}	K^+	H_2O	HPO_4^-	Cl^-	HCO_3^-	UREA	GLUCOSE
ISOTONIC PROXIMAL TUBULE	Active pumping out of filtrate	Parallels Sodium	Parallels Sodium	Isotonic reabsorption	Follows ions passively	Almost all reabsorbed in proximal tubule	Follows cations passively	High level of reabsorption via proton exchange	Isotonic reabsorption	Total reabsorption up to a known level - above that passes through
(on exit) HYPOTONIC LOOPS OF HENLE	Some reabsorption from ascending limb	Some reabsorption possibly independent or secondary to chloride	Parallels Calcium	Some reabsorption	Follows ions passively	Residue passes through	Follows cations passively. Possibly some active pumps	Some reabsorption	Residue passes through	Residue passes through
(on exit) HYPERTONIC DISTAL NEPHRON	Aldosterone regulated reabsorption with acid exchange	About two-thirds of Calcium residue reabsorbed	Parallels Calcium	Some reabsorption. Secretory exchange with cations. Reabsorption exchange with protons	Follows ions passively with regulation by ADH	Residue passes through	Follows cations passively	Some reabsorption	Some additional collection from the intestinum	Residue passes through
MODEL REALISATION	Proximal Autoregulation Loop Henle Constant Distal Constant Aldosterone controlled reabsorption Collecting Constant less proton exchange	T_m limited 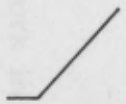	T_m limited 	Proximal Autoregulation Loop Henle Constant Distal Constant with Aldosterone regulation Collecting Constant	Proximal Autoregulation Distal ADH regulated	T_m limited 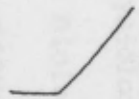	Equal to the net urine loss of cations	f (PCO2) 	Constant	T_m limited 

Figure 7.13 Comparison of MFAB renal analyte dynamics with currently accepted physiology.

CHAPTER 8

VALIDATION OF MFAB

8.1 INTRODUCTION

The description of MFAB in Chapter 7 includes some notes on theoretical validity (looking at the system of ideas which purport to explain things without necessarily dealing with the facts as presented by experience). These are given for each subsystem. The notes, with the listing of the main model assumptions, are appropriately placed in the thesis in that the model physiology and biochemistry can quickly be assessed by those with biological experience. Model validity is thus enhanced by providing transparency and increasing falsifiability (in a Popperian sense; Magee, 1979). As an initial step this is useful, although a model with the complexity of MFAB must undergo a variety of validatory tests to increase overall confidence. This may be of the form carried out by Pullen (1976) or Flood et al (1984b), where qualitative and quantitative feature analysis was carried out. However, more wide ranging validatory programmes are available, as developed and documented by Leaning (1980).

8.2 VALIDATION CRITERIA AND METHODOLOGIES OF LEANING (1980)

8.2.1 Introduction

The work of Leaning (1980) provides an excellent framework in which model validation may be carried out. Validation criteria are made explicit and standard methodologies have been developed. Furthermore, for special cases the development of methodologies from 'first principles' is discussed; and as an alternative, the

less time-consuming adaption of standard methodologies for less standard problems is covered. The work is enhanced by extensive case studies.

8.2.2 Concepts And Ideas

This subsection is designed only to draw out the main concepts and ideas which are pertinent to the validation of MFAB (this leaves untouched a wealth of intellect which is important reading for any dedicated modeller). For utilitarian modelling objectives (for example, where the purpose of developing the model is for clinical application and the improvement of health care) the pertinent standard Leaning methodology is the δ - methodology (described in the following subsection).

Also specified for models with utilitarian objectives are both an intended range of application R_I as well as the wider system of interest WSOI. This distinction is important as 'the representational criteria over R_I may be relaxed if the model obviously meets its utilitarian objectives over the WSOI'. Furthermore, as the model should be isomorphic with R_I it should also embody an explanation of R_I and may therefore satisfy general scientific objectives (for example, enchancing the understanding of hormone control). Setting and satisfying scientific objectives (generally speaking to improve the understanding in areas of weak knowledge and controversy) is therefore a useful way of testing model validity and, if successful, can only lead to the enhancement of pragmatic validity. For the purposes of assessing general scientific objectives, the later stages of the δ-methodology are not always appropriate (to be discussed later).

The criteria which are used in validation exercises have been made explicit by Leaning. These are described below.

Consistency validity criteria. The model should contain or entail no logical contradictions. In mathematical models this can be checked by examining algebraic loops. For computer programs with multi-conditional branching points it may be difficult to determine consistency completely.

Algorithmic validity criteria. These are a number of tests for checking that the algorithm for solution (analytical), or simulation of the model, are correct and lead to accurate solutions. Algorithms for numerical approximation may be checked for stability and asymptotic convergence (for example, Euler, Runge-Kutta or Gear's methods for integrating differential equations). Rounding off errors should also be tested.

Empirical validity criteria. This requires that the model should correspond to data available. This may be done at all levels (see Figure 8.1 for an example relating to MFAB) in strict validation, although a 'level of validation' may be chosen at an appropriate level of resolution. Validation may be carried out via qualitative and quantitative feature analysis and by sensitivity tests.

Theoretical validity criteria. This entails model comparison with currently accepted theories and models that apply to R_I. The model should cohere with the accepted models and theories. Theoretical validity criteria are important in examining assumptions, structure, elementary submodels and so on.

Pragmatic validity criteria. These are tests of the model in satisfying general and specific utilitarian objectives. This should involve a definition of the measure of effectiveness in the SOI and then determining whether the objective has been achieved. As some models will modify the WSOI once in use, a model may have to be assessed in terms of the potential benefit it offers or the understanding that it gives to people involved in the practical situation.

Heuristic validity criteria. These tests are concerned with the assessment of the potential of the model for scientific understanding and discovery, that is, its role as a heuristic device. They are mostly concerned with whether a model will be fruitful or promising for future developments. Specific criteria may include the resolution of an outstanding anomaly or giving better understanding.

8.2.3 The δ -Methodology

The four stages of the δ-methodology are shown in Figure 8.2 and are described below.

The symbols V_{ALG}, V_{CON}, V_{EMP}, V_{PRAG1} and V_{PRAG2} denote the types of validity criteria and refer to algorithmic, consistency, empirical, direct pragmatic and general pragmatic validity criteria respectively.

The standard δ-methodology is appropriate for when the model is to be used as a predictive device to improve the WSOI. The first

stage makes initial tests of consistency, algorithmic validity and stability.

The second stage consists of comparing model responses with data from R_I as a test of predictive validity. This essentially involves empirical validity criteria (based or acting on observation or experience, typically qualitative and quantitative feature analysis, and sensitivity analysis).

The third stage is concerned with the use of the model in the WSOI, that is, the direct pragmatic validity.

8.2.4 Validation Of A Renal Model (Uttamsingh, 1981) Using an Adapted δ-methodology: A Validation Programme For MFAB?

A validation programme may be developed from 'first principles', or may take the form of one of the standard validation methodologies, or the form of an adapted standard methodology.

Leaning (1980) developed a programme of validation for the renal model of Uttamsingh (1981), who had essentially utilitarian modelling objectives. Making developments from 'first principles' would have been excessively time consuming, however, the standard δ-methodology was not entirely appropriate (the second stage did not consider theoretical validity and the third and fourth stages were inappropriate for the general scientific objectives). Consequently the standard δ-methodology was adapted by brief consideration of model objectives, data and appropriate validity criteria.

As MFAB shares the utilitarian modelling objectives of the renal model, the suitability of the adapted δ-methodology as a validation programme for MFAB can be assessed by comparison of the three above considerations for MFAB. Thus, Leaning's text structure and content have been similarly replicated below for MFAB, allowing direct comparison with the study of the renal model.

The objectives of MFAB are utilitarian in nature. They have been declared as the improvement of the overall quality of patient health care and the optimisation of time and cost, by providing prediction of clinical states; improving diagnosis, prognosis and patient management. Optimal therapy may reduce patient stay-time and consequently reduce nursing hours in some instances, whilst possibly increasing those factors by maintaining life in other instances. R_I is therefore the clinical states of FAB during clinical decision making periods (assumed to be 8 hours). The WSOI is therefore the management of patients undergoing fluid therapy (in the ITU). These parts of the overall SOI of MFAB are consistent with the renal model, differing only in R_I by the clinical states of interest (although many subsystems are the same by label).

There are other similarities between the two modelling objectives. Patient representation (patient-related as some of the parameters are specific to the patient rather than patient-specific where all of the parameters would have to be specific to the patient) is achieved in both cases. To achieve this, individual patient subsystems are given initial conditions for state-variables and some parameters.

The observations on sources of data presented by Leaning on the renal model may equally have been written for MFAB (with minor adaptions). Three sources of data are required:

(i) data from the physiological-biochemical systems for representational validity;

(ii) data concerning the future clinical state for predictive validation;

(iii) data from WSOI on the effectiveness of the model used.

Data source (ii) is separated from the superset, data source (i), because predictive empirical validity of the model is directly related to pragmatic validity (for utilitarian objectives).

Other case study observations of Leaning hold for MFAB. The model has not been used in practice (that is, not for clinical application) therefore, no data are currently available for source (iii). (Currently is emphasised as it is the intention that a thorough clinical validation be undertaken by clinical experts; provisions for which have been made at The Royal Free Hospital and School of Medicine in London for a microcomputer implemented version of MFAB).

Data used to run a simulation of MFAB are obviously available and are documented in Appendix 6. Empirical validation can compare the major variables of the human which are easily measurable and routinely taken. As declared in Chapter 1 (the introduction to the thesis) there are large data banks on such variables. Other published sources exist. For non-measurable variables (such as

intracellular contents of analytes) assessment of qualitative behaviour by experts is of great value.

Comparison of the model with these sources must take account of uncertainty. Uncertainty may be in the form of important yet unrecorded events such as exceptional fluid loss through vomiting or diarrhoea. Uncertainty in clinical measurement is generally recognised and may come about due to human error such as insufficient cleansing of plain bottles for urine sampling. These errors are occasionally prominent (possibly accounting for the outliers in Figure 6.1) but may also be hidden from human observation.

By taking expert opinion, it was found that total intra-person variability for plasma sodium concentration is about 70 percent of total variability (the reference range of the population), that is about 1 mmol l^{-1}. Thus, if at least two values in succession differed by 3 mmol l^{-1} then it is likely that the steady-state has been disturbed. The intra-person variability for plasma potassium concentration is 0.2 mmol l^{-1}. Estimated percentage uncertainty on measurement (source, Leaning, 1980) of the major variables of interest is: arterial pressure $\pm$5 percent; plasma sodium $\pm$ 1 percent; plasma potassium $\pm$5 percent; and plasma urea $\pm$ 2 percent.

Uncertainty may also be related to model simplification where effects on the patient which change R_I are not modelled. Furthermore, clinical measurements of analyte concentrations and

other clinical variables are usually taken at particular times of day, every day, and thus may show seasonal (daily) bias.

It is evident that, although some of the data considerations vary in their precise nature, the overall nature of MFAB in comparison to the renal model is very similar. This is not surprising as the same utilitarian objectives are shared, whilst many of the subsystems of R_I are also shared (by label). For these reasons it was decided that the appropriate validity criteria and programme of validation used on Uttamsingh's renal model would hold for MFAB. The adapted δ-methodology is therefore described in the following subsection.

8.2.5 An Adapted δ-methodology: A Programme For Validiating MFAB

The stages of the adapted δ-methodology are shown in Figure 8.3. The symbol V_{HEUR} denotes heuristic validity criteria and V_{THEOR} denotes theoretical validity criteria.

The first stage is as described in the standard δ-methodology of subsection 8.2.3. The second stage is aimed at determining the representational validity of the model, both at an overall level and submodel level with tests of theoretical coherency and empirical correspondence. In this way, the validity of the model mechanisms that generate the predictions, as well as the predictions, can be determined. The importance of domain knowledge (current theory, understanding and new data) is obviously essential in the second stage. Multilevel validation of MFAB may be carried out in a similar way to Leaning's disassembly of the renal model, see Figure 8.1 for MFAB. In going from level 1 to

level 5 the validity of the overall model is built up deductively and areas of confidence or uncertainty can be identified. At the same time inferences may be made 'down' the tree about the validity of individual submodels.

After the second stage the methodology splits according to whether scientific or utilitarian validity is being examined. The third and fourth stage of the utilitarian branch are as those in the standard δ-methodology. The scientific branch is concerned with increasing understanding of the areas of weak or controversial knowledge in particular. Contradicting assessments of validity may occur between the two branches.

8.2.6 Summary

A well thought out programme of validation was perceived as being essential for a model with the complexity of MFAB. The work of Leaning (1980) was found to offer substantial insight into validity of models, whilst also offering an adapted standard methodology appropriate for a full validation programme on MFAB.

8.3 RESULTS OF VALIDATION

8.3.1 Initial Tests

8.3.1.1 V_{CON}

Despite the large number of equations involved with MFAB, assessment of consistency was found to be relatively easy. This is in part due to the ongoing nature of validation (see Figure 10.2) so that consistency is considered at the development stage of each submodel. At the whole model level, consistency can be assessed

via the simulation program. From this it can be seen that multi-conditional branching is not a common feature. Ensuring consistency at this level was therefore a relatively easy task.

8.3.1.2 V_{ALGO}

During steady-state simulation studies it was found that the model would remain in the steady-state indefinitely over time if not perturbed. This implies no numerical aberrations. It was found necessary, however, to take some parameters to five or six decimal places, and also to declare high solution accuracy from the minicomputer. These actions are common-place for a model with the complexity of MFAB.

Stability and asymptotic convergence of integration was considered specifically for the cardiovascular submodel (see 7.3.2.2). This highlighted the fact that MFAB has a wide range of time constants and therefore is comprised of a stiff set of equations. This type of problem can be tackled in several ways.

It is important that the integration time step is reduced to ensure asymptotic convergence for the smallest time constant. This was found to be an integration step of one second for the cardiovascular submodel. Thus the integration step of MFAB could have been set to one second, however, the remaining submodels were found to reach asymptotic convergence with an integration step of one minute. Substantial and unnecessary solution time on the computer would therefore be used.

Guyton et al (1972) also encountered this problem. Their set of equations are 'stiffer'than those of MFAB. They overcame this problem by solving initially with a short integration step for the rapid transients, and increased the integration step length during simulation.

There are obvious implications here for pragmatic validity. Ikeda et al (1979) shared the utilitarian objectives of the current research and recognised that the speed of solution of their model was too slow to meet those objectives. The respiratory system holds the majority of the rapid transients and was seen by Ikeda and co-workers as an essential subsystem for simplification. The lessons from their studies were carried forward into this thesis where a simple respiratory representation was developed.

A further alternative was to solve the cardiovascular system every second and the remainder of the model every minute (similar to Guyton and co-workers approach). This proved to be least time consuming whilst maintaining output of similar accuracy. Consequently this method was used. As simulation time is relatively quick the pragmatic valdidity for R_I with respect to MFAB's usefulness in the WSOI is satisfied.

A point of note here is that certain aspects of Leaning's adapted &-methodology are not as distinctly separated as Figure 8.3 implies.

8.3.2 Representational Validity

8.3.2.1 V_{THEOR}

This part of the validation process is extensively presented at a submodel level in Chapter 7. It was necessary to make comparisons between the generally accepted knowledge presented in Chapters 2 to 4 and the model representation of MFAB, and to make explicit the ways controversial areas highlighted in those earlier Chapters are represented in MFAB. This is most effectively carried out in the context of submodel development as presented in Chapter 7. Also presented in that Chapter was a comparison of submodel representations of MFAB against those of other models. This is also an important element of theoretical validation.

The conclusion that can be drawn is that MFAB is generally theoretically sound. Where it has been necessary to represent areas of controversy or weak knowledge, that representation has been made explicit, the assumptions noted and hence transparency attained. Transparency leads to increased falsifiability, and to increased adaptability of the model as new theories and evidence surface.

Chapter 7 did not consider theoretical validity at the overall model level. This is attainable by considering the structure and interactions displayed in Figure 7.6. This was accepted unanimously by medical experts.

8.3.2.2 V_{EMP}

Sensitivity testing is an extensively used scientific method of creating an experimental environment in which to test a hypothesis (MFAB for example). All bar one parameter are held constant and the one parameter is varied by set amounts (that is $\pm$5%, $\pm$10% and $\pm$ 15%). The relative response of model variables are documented and considered for realistic changes. In this way the hypothesis (MFAB for example) can be tested. (Note that, as stated by Leaning, 1980, these are precisely the tests required when scientific objectives have been set).

However, this method of hypothesis testing has been criticised, for example by Reynolds (1980) as '.... the systemic methods of thinking on the contrary would ideally require that all variables and their interactions are to be seen simultaneously and as a whole'. This quote serves the purpose of highlighting the comprehensive nature of Leaning's adapted δ-methodology in that, at this stage of representational validation, both scientific (via sensitivity tests) and systemic (via perturbation analysis) viewpoints are catered for.

Two types of parameter had to be assessed. These were the parameters associated with 'real' phenomena (such as the constant for molecular attraction) and other non-specified constants which appear as numerical prefixes in the model. The following equation for sensitivity testing was used:

$$r_{zx} = \frac{(z_{x+a}/z_o)}{((x_o+a)/x_o)} \qquad (8.1)$$

During sensitivity analysis all computed and state variables were found to be stable to parameter changes except for those detailed below. These showed an emerging pattern of sensitivity :

VARIABLE	RANGE FOR r
VAS	1.0—0.59
LRR	1.0—0.69
UO	1.0—0.33
UNA	1.0—0.82
UMG	1.0—0.51
UCA	1.0—0.76
UCL	1.0—0.83
UHCO3	1.0—0.58
NRAS	1.0—1.99
UCH	1.0—0.84
VA	1.0—0.85

Comments:

By tracing the logical connections in MFAB the following general hierarchical causal flows were identified:

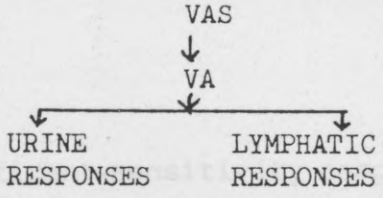

The implication is that the cardiovascular system, although apparently sound in isolation, does not integrate well into MFAB. The previous sound responses of the prototype FAB3 (reported by Flood et al, 1984b) and its integrated cardiovascular subsystem (from Ikeda et al, 1979) suggests that the use of the latter may be more appropriate.

Table 8.1 Details of sensitivity test on MFAB (with comments).

where; r_{zx} is the sensitivity coefficient relating z to changes in x, a is the designated change, x_o and z_o refer to the steady-state values of x and z at t=0 respectively, and z_{x+a} refers to the new steady-state value of z following the change a on x.

If x is a parameter which does not change model structure (for instance a constant input), then the criteria used to determine whether r_{zx} is significantly sensitive is whether it represents a physiologically realistic change. This can be determined by drawing on expert knowledge and empirical evidence (including medical textbooks and other physiological literature). However, if x is a parameter which alters model structure (for instance, filtration coefficients) which is often pathological in nature, then expert knowledge (practical experience) plays a dominant role in determining the significance of sensitivity measurements on the model.

The significant sensitivity responses are detailed in Table 8.1. It is clear that the model, on the whole, responds well to parameter changes of both a physiological and a pathological nature. This increases confidence in the model structure with respect to level 3 and level 4 of Figure 8.1. The results are not surprising as a number of important segments of the model, (which have been drawn from other research groups), have been well validated, either integrated in a wider system or in their own right.

Other tests of empirical validity involved both qualitative and quantitative feature analysis. Some observations can be made prior

to reporting the results of validation carried out during the current research programme.

At the submodel level the cardiovascular system has undergone extensive testing by its author Dr G Parkin, although this as yet has not been documented. Other submodels, previously incorporated in full FAB models, have been involved in validation tests by their original authors, for example, the hormone representations taken from Ikeda et al (1979) and the technique of intracellular fluid and electrolyte dynamics adapted from DeLand (1975). Furthermore, an earlier version of MFAB (which included all the submodels except the gastrointestinal system, glucose dynamics and intracellular dynamics of analytes) underwent an extensive qualitative and quantitative feature analysis at level 3 of Figure 8.1 (Flood et al, 1984b). The aim of the validation reported below was to assess model performance at levels 3, 4 and 5 of Figure 8.3.

Qualitative feature analysis involves perturbing the model physiologically or pathologically (level 3 and 4 respectively) and also by, at a later stage, applying fluid therapy to the model (level 5). The direction of the responses are noted and compared to known responses (clinical data) or expected responses (assessed by experts). Identifying a set of tests which are wide ranging and domain orientated was undertaken by a medical expert.

Quantitative feature analysis also involves perturbing the model both physiologically and pathologically (level 3 and 4 respectively), however, it is the measurable features of the

dynamic response of model variables which are investigated (for instance delay in response and peak value attained). The data for such tests was not freely available for the human. It was drawn from Journal publications, from as early as 1949. For both qualitative and quantitative features, relevant data became more difficult to acquire the higher the level considered (refer to Figure 8.1). Figure 8.4 provides the basis for interpretation of the Tables for quantitative feature analysis.

The results are documented in Tables 8.2 and 8.3 for a qualitative feature analysis at level 3, and Tables 8.4 and 8.5 for a quantitative feature analysis at level 3. Table 8.6 details a qualitative feature analysis and Table 8.7 a quantitative feature analysis, both at level 4. Table 8.8 shows the results of a qualitative feature analysis at level 5.

The Tables for qualitative feature analysis can be interpreted as follows. A test T may have an effect on one of the analytes A. The variable response may be to rise (+) to fall (-) or no response (0). The model response of an analyte in either the plasma (PL) or intracellular (IC) fluid is presented on the left hand side of the respective matrix block. There are two exceptions, the column for VICF relates only to the intracellular fluid, and the matrix block (Pr^{-}, IC) relates to interstitial protein concentration. On the right hand side of each block is the known or expected physiological/pathological response. There is occasionally no entry for the known or expected responses (which serves to highlight areas of controversy and weak knowledge). At the right hand side of each row and at the bottom of each column are the

A / T	ADH	ALD	Na^+	K^+	Cl^-	Mg^{++}	Ca^{++}	Urea	Pr^-	Gluc.	pH	PCO_2	HCO_3^-	H_2O	VICF	Σr
1) PL	0 0	0	0 0	0 0	0 0	0 0	0 0	0 0	0 0	- -	0 0	0 0	0 0	0 0	0 0	14/14
IC	·	·	0 0	+ +	0 0	0 0	0 0	·	0 0	·	·	·	0 0	0 0	·	8/8
2) PL	0	0	0	0	0	0	0	0	0	+ +	0	0	0	0	0	1/1
IC	·	·	0	+ +	0	0	0	·	0	·	·	·	0	0	·	1/1
3) PL	- -	0	- -	- -	- -	- -	- -	- -	- -	- -	0 0	0 0	- -	+ +	+ +	14/14
IC	·	·	- -	- -	- -	- -	- -	·	- -	·	·	·	- -	+ +	·	8/8
4) PL	+ +	0	+ +	- +	-	+	-	-	+ +	0 0	0 0	0 0	0 0	- -	— —	8/9
IC	·	·	+ +	+ +	+	+	+	·	+ +	·	·	·	+ 0	- -	·	4/5
5) PL	- -	0	+ +	- -	+ +	-	+	- 0	+ +	0 0	0 0	0 0	0 0	- -	— —	11/12
IC	·	·	- -	+ +	- -	+	—	·	+ +	·	·	·	- 0	- -	·	5/6
6) PL	+	-	0	-	0	-	0	0	+	0	0	0	-	—	-	0/0
IC	·	·	0	0	0	0	0	·	+	·	·	·	-	—	·	0/0
7) PL	+ +	-	+ +	0 -	0	-	0	- -	0	0	0	-	-	+ +	+ +	5/6
IC	·	·	- 0	- -	-	-	-	·	0	·	·	·	-	+ +	·	2/3
Σc	5/5	0/0	9/10	9/11	6/6	4/4	4/4	3/4	8/8	5/5	4/4	4/4	6/8	10/10	5/5	

Table 8.2 Qualitative feature analysis of MFAB at level 3 of Figure 8.1: Part I.

A / T	ADH	ALD	Na^+	K^+	Cl^-	Mg^{++}	Ca^{++}	Urea	Pr^-	Gluc.	pH	PCO_2	HCO_3^-	H_2O	VICF	Σ r	I-II %
1) PL	0 0	-	0 0	0 0	0 0	0 0	0 0	0 0	0 0	0 0	0 0	- -	- -	0 0	—	14/14	100
IC	*	*	- -	- -	- -	- -	- -	*	0 0	*	*	*	- 0	0 0	*	7/8	94
2) PL	+ +	-	+ +	- -	+ +	-	+	0	+	0	—	+ +	+ +	—	0	6/6	100
IC	*	*	0 0	+	-	+	-	*	+	*	*	*	-	—	*	1/1	100
3) PL	+ +	+	0 -	+ +	0	-	0	0 0	0	0	0	+	-	0 0	+ +	5/6	95
IC	*	*	- -	+ +	-	0	-	*	0	*	*	*	-	0 0	*	3/3	100
4) PL	+ +	-	0 0	- -	0 0	-	0	0 0	+	0	0	-	-	- -	- -	7/7	94
IC	*	*	0 0	- -	0 0	-	-	*	+	*	*	*	-	- -	*	4/4	89
5) PL	— —	-	0 -	- -	0 -	- -	0 -	-	+ +	0	0	—	-	+ +	+ +	6/9	81
IC	*	*	- -	- -	- -	- -	- -	*	0 0	*	*	*	-	+ +	*	7/7	92
6) PL	— —	-	0	-	0	-	0	+ +	0	0	0	+	-	+ +	+ +	4/4	100
IC	*	*	-	-	-	-	-	*	0	*	*	*	-	+ +	*	1/1	100
7) PL	0 0	-	0	0 +	0 0	-	0	-	+	0	0 0	+ +	- -	-	—	5/6	100
IC	*	*	-	- -	- -	-	-	*	0	*	*	*	- -	—	*	3/3	83
Σ c	7/7	0/0	8/10	10/11	8/9	4/4	3/4	4/4	4/4	1/1	2/2	3/3	4/5	10/10	5/5		
I-II %	100	.	85	86	93	100	88	100	100	100	100	100	77	100	100		

Table 8.3 Qualitative feature analysis of MFAB at level 3 of Figure 8.1: Part II.

RESPONSE \ FEATURE	DELAY		RISE/FALL TIME		PEAK TIME		PEAK VALUE		SETTLING TIME	
1) URINE OUTPUT	2 - 3 mins	2 mins	45 - 75 mins	39 mins	60± 15 mins	41 mins	10 - 12 ml min^{-1}	6 ml min^{-1}	60 - 105 mins	95 mins
2) GLUCOSE CONCENTRATION EXTRACELLULAR FLUID	0 mins	0 mins	55 - 60 mins	42 mins	57± 3 mins	42 mins	50 mg dl^{-1}	130 mg dl^{-1}	90 - 100 mins	didn't up to 480 mins
POTASSIUM CONCENTRATION EXTRACELLULAR FLUID	0 mins	0 mins	55 - 60 mins	240 mins	57± 3 mins	240 mins	-0.5 mEq l^{-1}	-0.54 mEq l^{-1}	didn't up to 480 mins	didn't up to 480 mins
3) ADH	0 - 10 mins	15 mins	55 - 65 mins	47 mins	60± 5 mins	62 mins	-1 AU	-0.83 AU	40 - 80 mins	150 mins
OSMOLALITY OF EXTRACELLULAR FLUID	2 - 5 mins	2 mins	85 - 95 mins	58 mins	90± 5 mins	60 mins	-7±3 mmol l^{-1}	-11.9 mmol l^{-1}	100 - 150 mins	160 mins
4) URINE OUTPUT	2 - 5 mins	3 mins	70 mins	59 mins	72± 3 mins	62 mins	13.5 ml min^{-1}	9 ml min^{-1}	160 - 240 mins	184 mins

Table 8.4 Quantitative feature analysis of MFAB at level 3 of Figure 8.1: Part I.

RESPONSE \ FEATURE	DELAY		RISE/FALL TIME		PEAK TIME		PEAK VALUE		SETTLING TIME	
1) URINE OUTPUT	2 - 5 mins	2 mins	150 - 210 mins	268 mins	180± 33 mins	270 mins	6 ml min^{-1}	5.3 ml min^{-1}	didn't up to 360 mins	didn't up to 360 mins
UREA CONCENTRATION PLASMA	2 - 5 mins	2 mins	170 - 190 mins	300 mins	180± 10 mins	300 mins	3.4 mmol l^{-1}	5.67 mmol l^{-1}	didn't up to 360 mins	didn't up to 360 mins
2) EXTRACELLULAR VOLUME	-	-	6.5 days	5.25 days	6.5 days	5.25 days	2 l	1.3 l	-	-
SODIUM CONCENTRATION PLASMA	-	-	2 days	1.5 days	2 days	1.5 days	9 mmol l^{-1}	6.3 mmol l^{-1}	-	-
3) PARTIAL PRESSURE CARBON DIOXIDE	-	-	-	-	-	-	15 mmHg	14 mmHg	-	-

Table 8.5 Quantitative feature analysis of MFAB at level 3 of Figure 8.1: Part II.

T \ A	ADH	ALD	Na^+	K^+	Cl^-	Mg^{++}	Ca^{++}	Urea	Pr^-	Gluc.	pH	PCO_2	HCO_3^-	H_2O	VICF	Σ_r
1) PL	0 0	0	0 0	0 0	0 0	- 0	0 0	0 0	0 0	0 0	0 0	0 0	0 0	0 0	0 0	13/14
IC	*	*	- 0	0 0	- 0	0 0	- 0	*	0 0	*	*	*	0 0	0 0	*	5/8
2) PL	- -	-	- -	- -	- -	- -	- -	- -	- -	0 -	0 0	0 0	0 -	+ +	+ +	12/14
IC	*	*	- -	- -	- -	- -	- -	*	0 -	*	*	*	0 -	+ +	*	6/8
3) PL	+ +	-	0 -	- -	0 -	- -	0 -	- -	0 -	0 0	0 0	- -	- -	- -	+ +	10/14
IC	*	*	0	0	0	0	0	*	+	*	*	*	-	+ +	*	1/1
4) PL	+ +	0	+ +	+ +	+ +	+ +	+ +	+ +	+ +	0 -	0 0	+ 0	+ 0	- -	- -	11/14
IC	*	*	+	0	0	0	0	*	+	*	*	*	0	- -	*	1/1
5) PL	+ +	-	+ +	+ +	+ +	+	0	+ +	+ +	+ +	- -	+ +	- -	- -	- -	12/12
IC	*	*	0	0	0	0	0	*	+	*	*	*	-	- -	*	1/1
6) PL	+ +	0	+ +	0 +	+ +	+	+	+ +	+ +	0	- -	+ +	- -	- -	- -	10/11
IC	*	*	0	0	0	0	0	*	+ +	*	*	*	-	- -	*	2/2
7) PL	+ +	0	+ +	0 +	0 +	-	0	0 0	+ +	0 +	0	+	-	- -	- -	6/9
IC	*	*	0	0	-	0	0	*	+ +	*	*	*	-	- -	*	2/2
Σ_c	7/7	0/0	7/9	7/9	6/9	5/6	4/6	7/7	9/11	3/6	6/6	5/6	5/8	14/14	7/7	

Table 8.6 Qualitative feature analysis of MFAB at level 4 of Figure 8.1

RESPONSE \ FEATURE	DELAY		RISE/FALL TIME		PEAK TIME		PEAK VALUE		SETTLING TIME	
1) ADH	-	-	60 - 70 mins	60 mins	65±5 mins	60 mins	-0.6 AU	-0.725 AU	remains at peak value	continues on very slow fall
PLASMA OSMOLALITY	-	-	65 - 75 mins	60 mins	70±5 mins	60 mins	-12±2 mmol l^{-1}	-20.2 mmol l^{-1}	remains at peak value	continues on very slow fall
2) PROTEIN CONCENTRATION INTERSTITIAL	-	-	-	-	-	-	5 - 6 g l^{-1}	1.2 g l^{-1}	-	-
LYMPHATIC FLOW RATE	-	-	-	-	-	-	55 - 65 mmol l^{-1}	77 mmol l^{-1}	-	-
3) BICARBONATE CONCENTRATION PLASMA	-	-	-	-	-	-	1.5± 0.3 mmol l^{-1}	5.9 mmol l^{-1}	-	-

Table 8.7 Quantitative feature analysis of MFAB at level 4 of Figure 8.1.

A / T	ADH	ALD	Na^+	K^+	Cl^-	Mg^{++}	Ca^{++}	Urea	Pr^-	Gluc.	pH	PCO_2	HCO_3^-	H_2O	VICF	Σr
1) PL	0 0	0	+ 0	0 0	+ 0	0 0	0 0	0 0	0 0	0 0	0 0	0 0	0 0	0 0	+ 0	11/14
IC	*	*	- 0	0 0	- 0	0 0	0 0	*	0 0	*	*	*	0 0	0 0	*	6/8
2) PL	0 0	0	0 0	- 0	+ 0	- 0	+ 0	- 0	0 0	0 0	0 0	0 0	- 0	0 0	+ 0	7/14
IC	*	*	- 0	0 0	0 0	- 0	0 0	*	0 0	*	*	*	0 0	0 0	*	6/8
3) PL	0 0	0	+ 0	+ 0	0 0	0 0	0 0	0 0	0 0	0 0	0 0	0 0	0 0	0 0	+ 0	11/14
IC	*	*	0 0	0 0	0 0	- 0	0 0	*	0 0	*	*	*	0 0	0 0	*	7/8
4) PL	0 0	0	0 0	+ 0	0 0	0 0	0 0	0 0	0 0	0 0	0 0	0 0	0 0	0 0	+ 0	12/14
IC	*	*	- 0	0 0	- 0	- 0	- 0	*	0 0	*	*	*	0 0	0 0	*	4/8
Σc	4/4	0/0	3/8	5/8	4/8	4/8	6/8	3/4	8/8	4/4	4/4	4/4	7/8	8/8	0/4	

Table 8.8 Qualitative feature analysis of MFAB at level 5 of Figure 8.1.

(Compared to normal 0 on right hand side of each block).

'success' summations Σr and Σc respectively. Where a feature analysis is presented in two parts (I and II) the summations from part I are carried forward onto part II and shown as an overall percentage of 'success'.

The tests of Figure 8.2 are as follows:

1. Insulin infusion.
2. Glucose loading.
3. Intravenous input of 5% dextrose.
4. Venous water loss.
5. Application of an ADH antagonist.
6. Application of an aldosterone antagonist.
7. Sodium loading.

For Figure 8.3:

1. Sodium depletion.
2. Rise in metabolic production of CO_2.
3. Potassium loading.
4. Potassium depletion.
5. Protein loading.
6. Urea loading.
7. Chloride depletion.

For Table 8.4:

1. 1000 ml H_2O infused into a dehydrated man (16 hrs) over 5 mins. Source, Ikeda et al (1979).
2. 50 g infusion of glucose over 50 mins. Source, Perez et al (1977).

3. 1000 ml H_2O infused into a normal man over 60 mins. Source Kuroda et al (1980).
4. 637 ml of 10% NaCl infused into a dehydrated man (16 hrs) over 65 mins. Source, Dean and McCance (1949).

For Table 8.5:

1. 200 ml of 50% urea infused into a normal man over 2 mins. Source, Dean and McCance (1949).
2. Aldosterone held at 4x normal level. Source, Marver and Kokko (1983).
3. Inhalation of 7% CO_2 (approximated in MFAB by holding metabolic production of CO_2 at 4x normal). Source, Brackett et al (1965).

For Table 8.6:

1. Hyperactive heart.
2. Hypoactive heart.
3. Increased capillary permeability as a result of endotoxic shock (shock syndrome).
4. Reduced metabolic production of protein as a result of liver disease.
5. Diabetes ketoacidosis, metabolic disorder of glucose.
6. Diarrhoea.
7. Vomiting.

For Table 8.7:

1. Patient with hypovasopresin, infused with 200 cc kg^{-1} of H_2O over 45 mins. Source, Robertson (1983).

2. Patient with acute hypercapnia, partial pressure of CO_2 at 54 mmHg. Source, Brackett et al (1965).
3. Model simulation of 2x permeability of capillaries. Source, Bert and Pinder (1982).

For Table 8.8 (comparison to normal patient):

1. Post operative fluid response, no fluid treatment, immediately post 3rd day diuresis.
2. Albumin boosting to patient with disorder in protein metabolism during liver disease.
3. Patient with diabetes ketoacidosis, metabolic disorder of glucose, 60 units of insulin and 20 mmol of potassium (slowly).
4. Patient with diarrhoea, 20 mmol of potassium (slowly).

It can be seen that in the qualitative feature analysis agreement is good, although the response of a normal person is better than a person in an abnormal condition. The abnormal patient response to fluid therapy proved to be very promising.

Quantitative feature analysis also proved to be promising. Occasional notable discrepancies appeared, however, these are discrepancies with limited sets of measurements. Acquisition of real clinical data is essential for further quantitative analysis, however, the data requirements are high (to achieve a representative picture) and are in direct conflict with the medical norms (and sensitivity to the Principles of the Data Protection Act, Chapter 35, pp 35).

Studies of the dynamic responses (samples are shown in Figures 8.5-9) are pleasing.

Overall, the representational validity of the model has shown that the essential structure and processes of the human FAB system are well represented in MFAB.

8.3.3 Heuristic Considerations, V_{HEUR}

The assessment of a model (such as MFAB) for potential scientific understanding and discovery was not explicitly declared in the research objectives. It is, however, an integral part of model development such as that undertaken in Chapter 7.

Potentially, MFAB offers the opportunity for researchers to investigate theories in weak and controversial areas. Interest has been shown in this area from The Westminster Hospital in London (for hormone response) and The Royal Alfred Hospital in Melbourne (for a new theory of cardiac output regulation).

Simple tests of model performance may be undertaken, for instance, the removal of the aldosterone control with sodium and potassium perturbations, thus assessing the role of controversial control systems. Alternatively, a whole FAB system response to closed-loop control of fluid infusion to changes in cardiac output, via a theoretical algorithm, can be monitored and the theory assessed.

As yet practical results of such activities have not been fully realised, however, the potential is clear.

8.3.4 Pragmatic Validation, V_{PRAG}

Making measurements on effectiveness of the model in the SOI are not yet appropriate as the actual implementation in the clinic is a goal which lies beyond the research programme (although Chapter 9 does consider some important pragmatic issues). Future assessment may not be an easy task as there is a high probability that the model's use in the WSOI will modify the WSOI itself.

Considering the potential held by MFAB within the SOI does approach the question of pragmatic validity. The potential of any mathematical model in the clinical environment (assuming good representational validity) lies in the mode of presentation to the clinical user.

It is necessary that the model itself produces the required output quickly and presents the output in an easily accessible form for the user. This is basically a methodological problem which spans the whole task of clinical modelling, from development to implementation (see Chapter 10 for an in depth analysis of modelling methodology). An appropriate methodology for the modelling process would ensure the model approaches optimum complexity (minimum) whilst ensuring that the model outputs are those of clinical importance. An appropriate methodology for (microcomputer) implementation would ensure that the package has a tailored logic to suit the user. The selection of the most suitable hardware is equally as important, as solving the technical problems of implementation may be time consuming and shifts the emphasis away from the important methodological issues.

The Apple II implementation of FAB3 (a prototype of MFAB, see Chapter 9) is typical of the traditional approach of simulation teams, where the basic model is presented with basic output. It does however prove the point that a complex model such as MFAB can be implemented on microcomputer with solutions available relatively quickly (as opposed to the traditional implementation of Ikeda et al, 1979, where model solution was far in excess of the acceptable user wait-time).

To achieve future pragmatic validity the necessary support will need to be provided as computer-software. Such a package must contain features relating to the user-machine interface; these should include menu entry, access to parameter change by key-stroking, screen representation of parameters in physiological terms and output in graphical format. In addition the mathematical model itself should be tailored to the user.

8.4 CONCLUSION

The validity of MFAB can be summarized as follows. It has good consistency and as an algorithm shows stability and asymptotic convergence with no numerical aberrations. From the theoretical viewpoint it is as sound as current knowledge permits. Representational validity is good. The latter two branches of the adapted δ-methodology, for heuristic and pragmatic validity, have (as suggested by Leaning) led to different conclusions. As a heuristic tool it does hold potential as it stands. However, with respect to pragmatic issues the mathematical model does not provide immediate potential. Alongside an appropriate methodology,

however, MFAB as a knowledge base could provide the dynamic quantitative information necessary to develop a model with immediate potential. Implementation of a complex model is presented in Chapter 9.

As a point of note, the clinical treatments discussed in this Chapter are paliative and do not consider the primary disease (as disease processes are not modelled in MFAB).

Chapters 7 and 8 have documented the development of one complex FAB model. Chapter 9 considers the role of complex FAB models in fluid therapy and consequently studies some of the pragmatic issues discussed above.

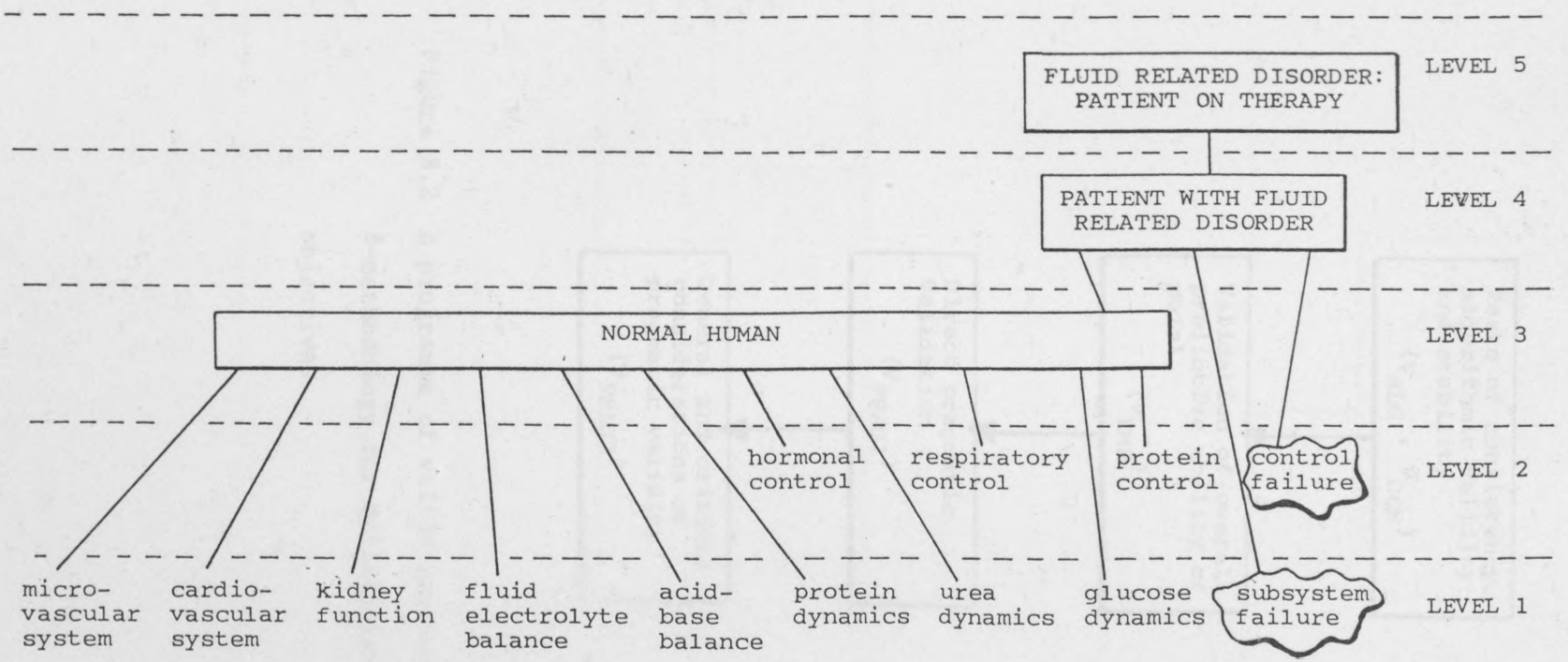

Figure 8.1 Hierarchy of validation at the representational stage for MFAB.

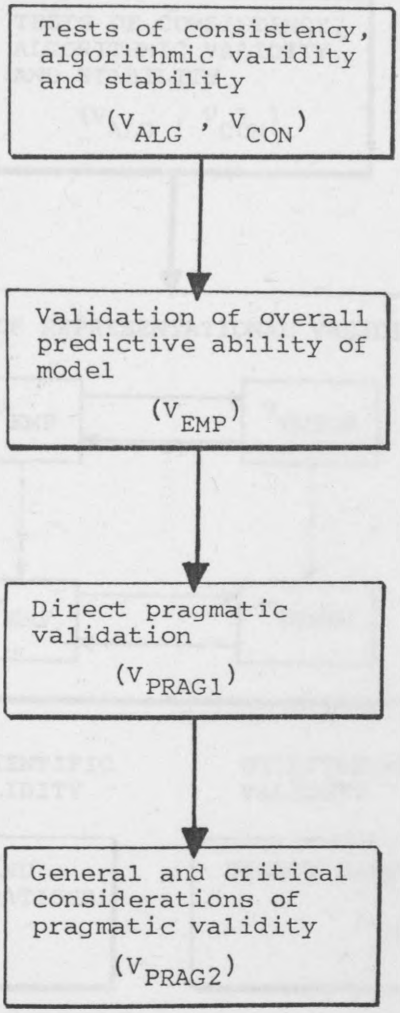

Figure 8.2 A programme of validation based on the δ-methodology for utilitarian modelling objectives

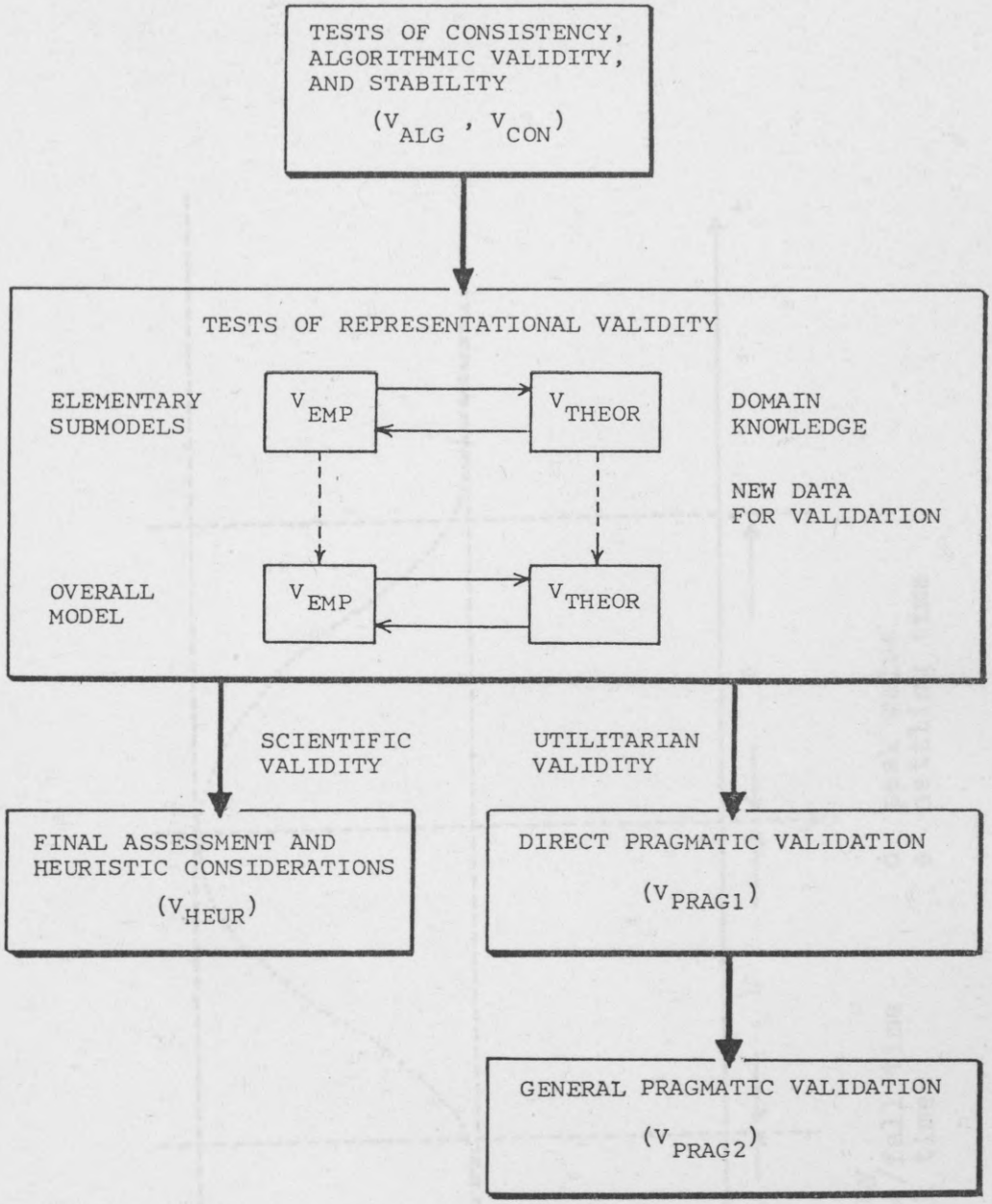

Figure 8.3 An adapted δ-methodology as a programme for validating MFAB.

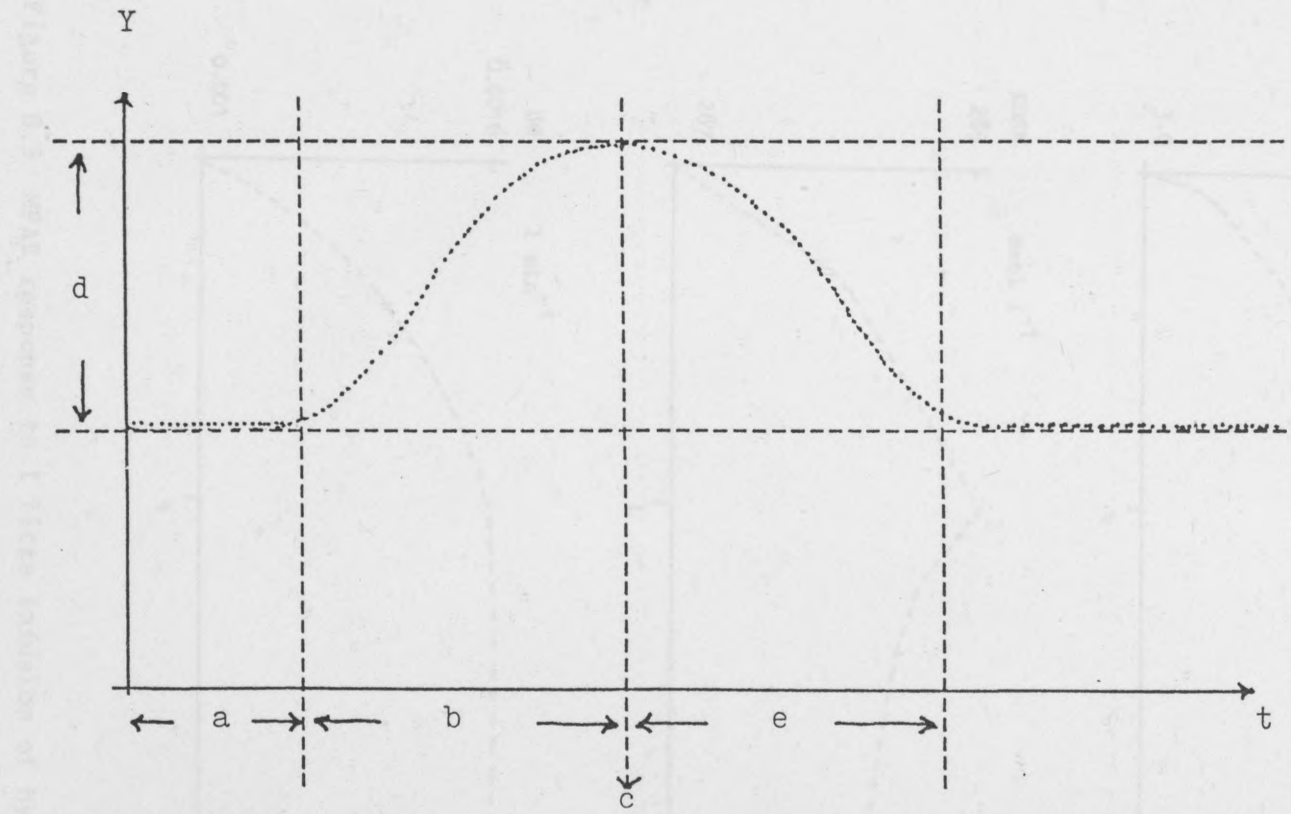

Figure 8.4 An explanation of the headings of Tables detailing quantitative feature analysis.

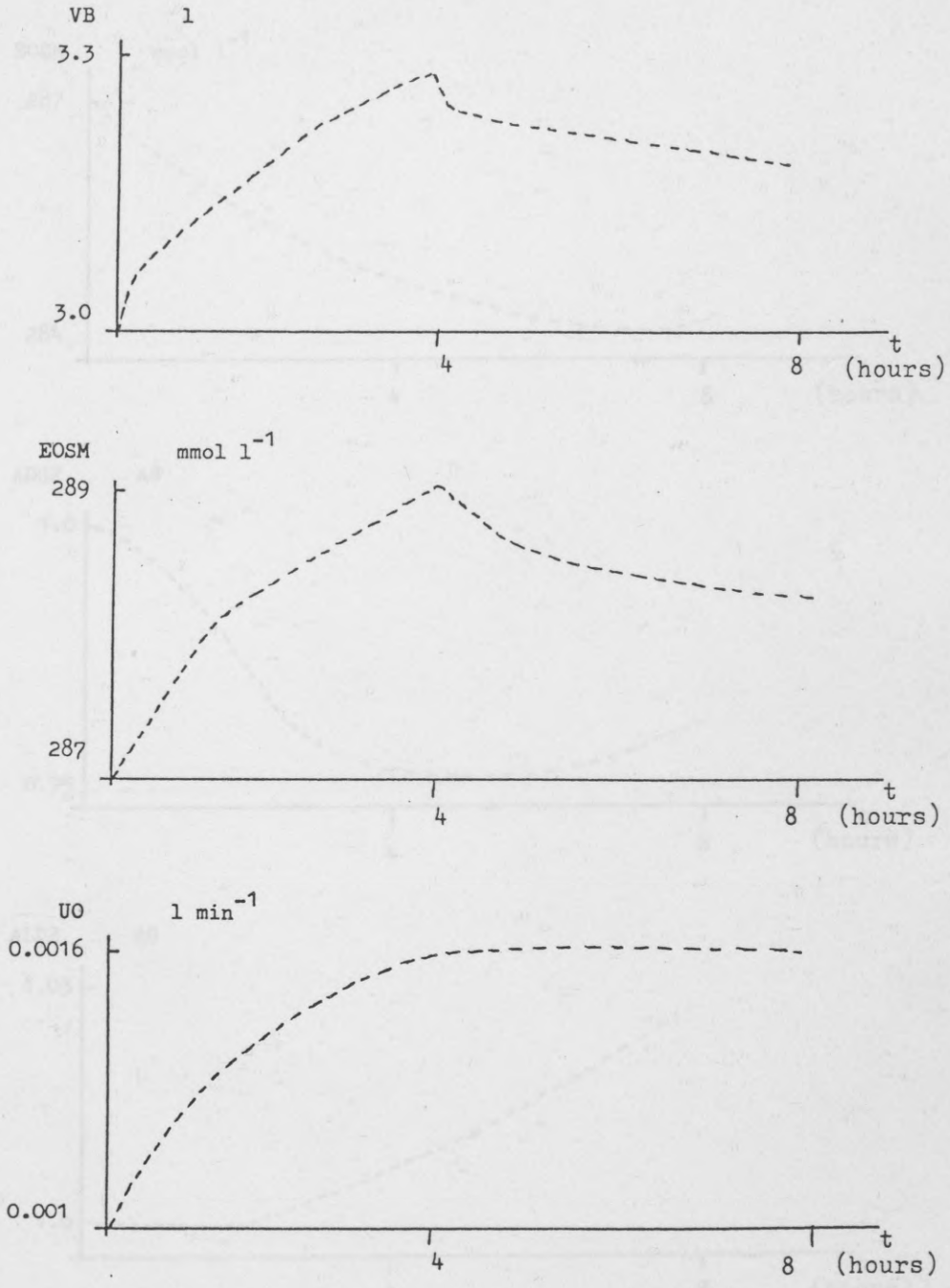

Figure 8.5 MFAB response to 1 litre infusion of hypertonic saline over 4 hrs; urine output, extracellular osmolality and blood volume.

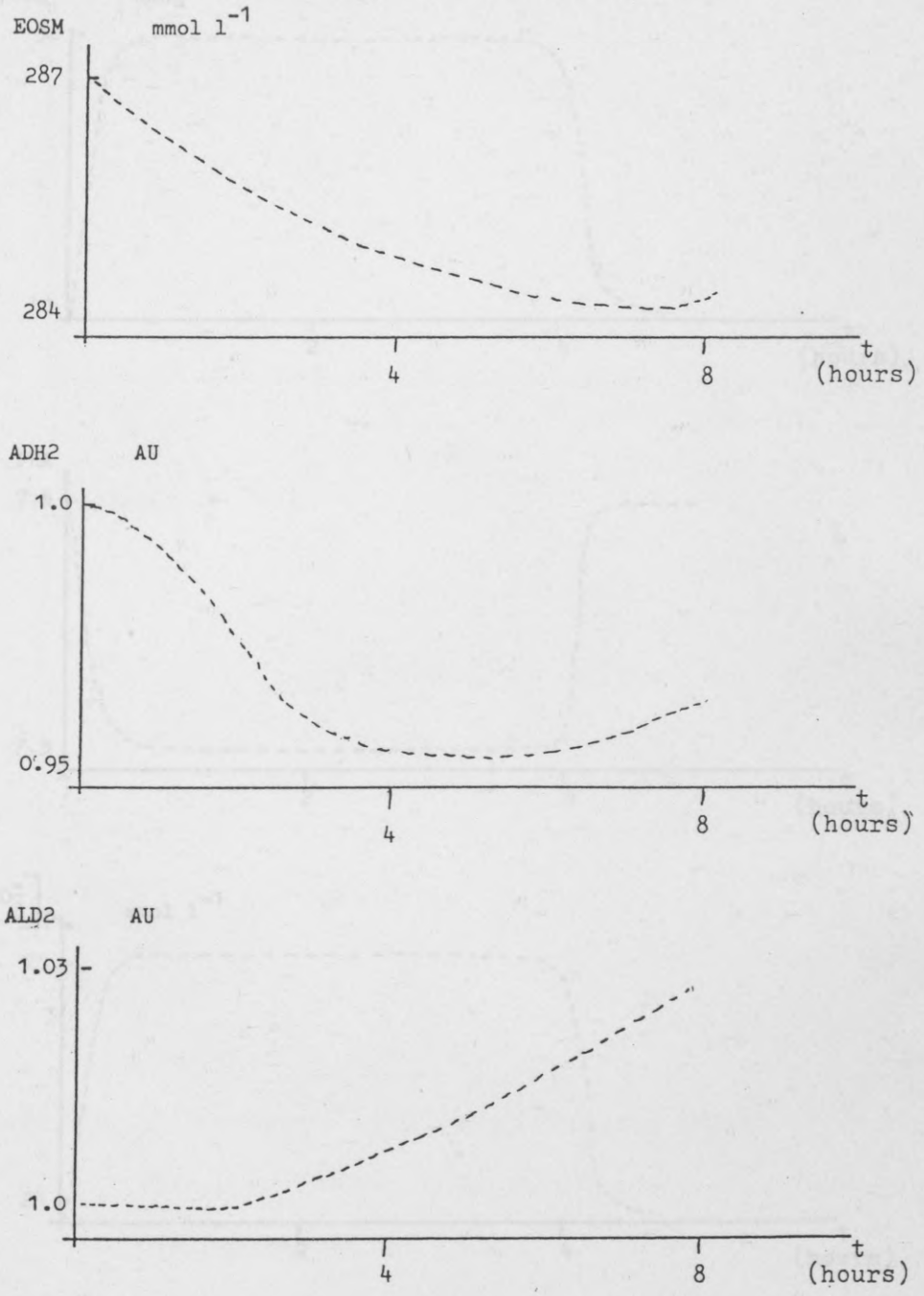

Figure 8.6 MFAB response to Na^+ depletion over 8 hrs; extracellular osmolality, antidiuretic hormone and aldosterone.

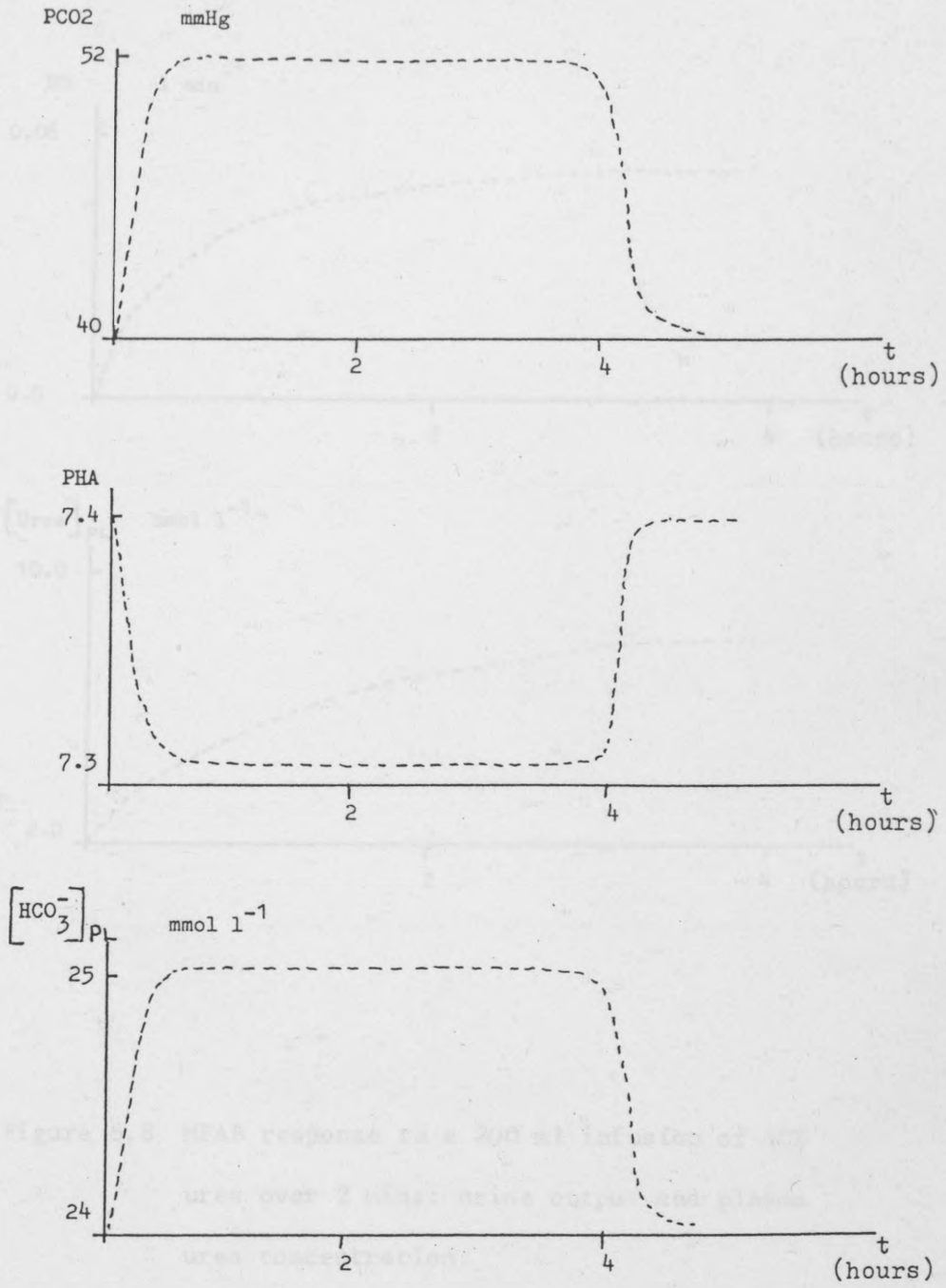

Figure 8.7 MFAB response to a 3x increase in carbon dioxide metabolic rate: partial pressure of carbon dioxide, blood acidity and plasma bicarbonate concentration.

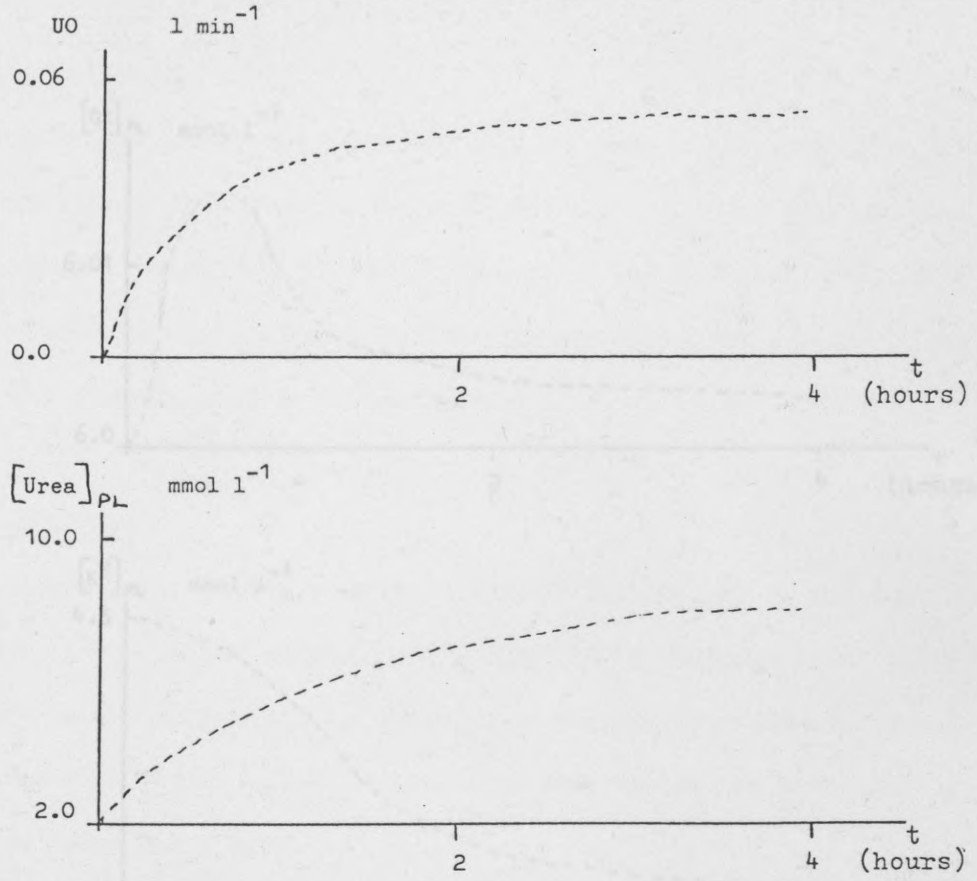

Figure 8.8 MFAB response to a 200 ml infusion of 50% urea over 2 mins: urine output and plasma urea concentration.

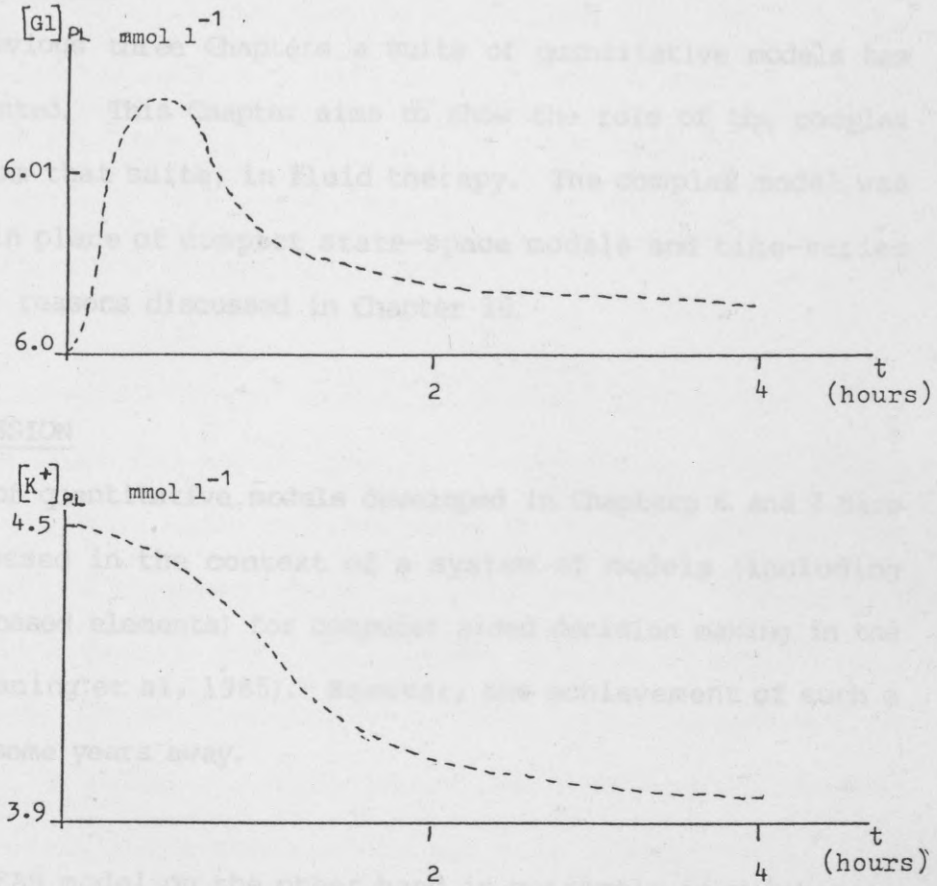

Figure 8.9 MFAB response to a 50 g infusion of glucose over 50 mins: plasma concentration and plasma potassium concentration.

CHAPTER 9

THE ROLE OF A COMPLEX FAB MODEL IN FLUID THERAPY

9.1 INTRODUCTION

In the previous three Chapters a suite of quantitative models has been presented. This Chapter aims to show the role of the complex model, from that suite, in fluid therapy. The complex model was favoured in place of compact state-space models and time-series models for reasons discussed in Chapter 10.

9.2 DISCUSSION

The suite of quantitative models developed in Chapters 6 and 7 have been discussed in the context of a system of models (including knowledge-based elements) for computer aided decision making in the clinic (Leaning et al, 1985). However, the achievement of such a system is some years away.

A complex FAB model on the other hand is currently in existence, has been properly validated (it is trustable because of its accurate performance) and may therefore be useful for the evaluation of diagnostic hypotheses and for prediction of the outcome of treatment alternatives. To achieve this effectively, the model should be able to simulate abnormalities of structure and process and assess typical fluid therapies for those abnormalities. Section 9.3 makes explicit these facilities for MFAB.

Groth (1985) stated that:

> "Models as pre-processors of clinical labaoratory data ... where complex conceptual models are required to capture the relationship between the primary pathological event and changes in blood and urine chemical variables ... can potentially be very useful. Raw laboratory data, for example concentration values, can be transformed into new quantities, more closely related to pathological process and therefore more discriminative than a single concentration. The predictive power of a valid biodynamical model may be used both for prognosis and to calculate non-measurable state-variables of the model, for instance cellular concentration, therefore producing potential test variables for diagnostic purpose".

Groth also noted, on the alignment of a model to a patient, that even in the least successful cases the understanding of the actual diagnostic and therapeutic problems would be sharpened and this may lead to rules of thumb which are clinically useful. However, as was shown in Chapter 7, individual patient data can be used to make the simulator patient-related (where some of the parameters are specific to the patient). Groth stated that such complex patient-related models, for example MFAB, can usually only be run in a forward mode to answer 'what if' questions. But this alone must be seen as a major step forward from static analysis. Section 9.4 presents one possible method of improving patient-relatedness by increasing the number of patient-specific parameters and hence improving patient prediction.

Alongside transparency and validity, technical realisation is one of the main criteria for clinical acceptance. Microcomputers have the advantage of being readily available when needed. As an example, section 9.5 details an implementation of FAB3 (a prototype of MFAB) on an Apple II microcomputer. A further and potentially

more acceptable method of implementation is in dedicated (special purpose) equipment. This may entail dissassembly of MFAB into a number of algorithms producing a library of:

> "certified diagnostic models which would then be helpful to the clinician for processing selected data from patient data-bases in search of diagnostic information", Groth (1985).

This may see MFAB being integrated in a system of models similar to that discussed in Chapter 10.

A promising way of gaining acceptability of models in a clinical environment is to expose medical staff to them at an early stage. This may be done by using models as teaching aids, and indeed the Apple II implementation of section 9.5 may well prove useful for this purpose. A more adventurous approach is to allow doctors and students (and any other relevant staff) to be able to develop their own versions of the model. This may be achieved by implementing the model using a simulation language such as MICRODYNAMO, with which alterations to the model can easily be made. The advantage of such a language is that only the relationships and structure of the model need be considered. The user is sheltered from such prohibitive aspects as the strict format of FORTRAN (a commonly used high level language) and concerns about integration (asymptotic convergence and stability).

The following three sections are supportive of the above discussion.

9.3 SIMULATING ABNORMALITIES AND FLUID THERAPY WITH MFAB

9.3.1 Introduction

The aim of this section is to identify some major and commonly found abnormalities in FAB (detailed in Chapter 3), and to show how these and their related fluid therapies may be simulated with MFAB by manual change of parameters. These changes are requested during simulation. It should be noted that section 9.4 describes conceptually a method which may be used to allow observations on the patient to determine the parameters automatically. The parameters discussed below relate to the A vector catalogued in Appendix 6 with their associated normal values.

9.3.2 Cardiovascular System

All heart related disorders cause a changed cardiac output because heart performance is altered. This may be enforced on the model by varying the value of A(4), the heart strength, from 1 (normal health) to 0 (cardiac arrest) or beyond 1 for hyperactivity.

Any clogging of arteries or veins by accumulation of substances on the walls causes a reduced diameter, consequently resistances rise and flow decreases. This can be effected by increasing the resistances related to the problem, that is, A(5) and A(6) for resistances of arteries and veins respectively.

Hardening of the arteries implies that arterial compliance has fallen, consequently A(1) should be reduced, and if suspected for the right atrium or the veins A(2) or A(3) should be decreased respectively.

To simulate fluid therapy parameters A(12) - A(18) may be adjusted to produce the desired concentration and constitutents for any water input that is made via A(23). (Note, parameters A(12) - A(18) may either be set at a steady-state input value which would require switching off the gastrointestinal system, or may be used to feed the model as described below and as required by the coded program in Appendix 7).

9.3.3 Gastrointestinal System

If the 'feeding' values are used for parameters A(12) - A(18) then the model should be fed every 8 hours, that is, three 'meals' a day. Each 'meal' is designed to provide enough water, sodium, potassium, chloride, magnesium, calcium and phosphate to maintain the model in dynamic equilibrium. By changing A(19) from 0 to 1 (false/true) a feed occurs. There is no obligation to feed the model in the case of a critically ill patient where intravenous methods are used, however, parameters A(12) - A(18) will need to be set to treatment values and the gastrointestinal system switched off.

Vomiting may be simulated by setting A(20) to 1 (true). Until A(20) is reset at 0 (false) the model will reject all feeding. Diarrhoea may be simulated by setting A(31) to a value between 0 and 0.9. The degree of severity of diarrhoea is described by the value of A(31), so that a value of 0 represents an acute case where the gastrointestinal system is not absorbing food.

9.3.4 Microvascular System

Lymphatic return can be restricted by varying the constant multiplication factor A(38) from 1 (no change) down to 0 (for total occlusion). This also has a relative effect on protein return. To increase permeability of capillaries, for example during inflammation, the capillary filtration coefficient A(27) can be increased.

9.3.5 Kidney System

Kidney disorders may be represented by varying the value of the steady-state GFR parameter A(50). Normally this is set at 0.1 l min^{-1}, however, if permeability at the glomerulus increases during a disease state then A(50) may be increased accordingly. If renal mass is reduced and plasma clearance rate falls then A(50) should be decreased. A reduction to 0 means total loss of renal function.

9.3.6 Hormones

Hormone secretion may be affected during certain abnormalities, for instance, in pituitary disease such as diabetes insipidus. To bring about reduced ADH or aldosterone response, the 'antagonist' parameters A(57) and A(62) may be reduced respectively. These may be set at a value between 0 and 0.9. The lower the value the less effective the endocrine metabolism, and at 0 there is no hormonal response.

9.3.7 Acid-Base Dynamics

The metabolic production rate of carbon dioxide can be varied according to the health of the patient by changing the parameter representation A(69) from its normal value.

9.3.8 Protein

The metabolic production and destruction rate of protein by the liver can be varied by changing the related constant A(73) from its normal value.

9.3.9 Glucose

The effects of an intravenous insulin input can be investigated by changing the normal input rate A(75) from 0 to a desired value. The behavioural characteristics of glucose metabolism are determined by the parameters A(76) - A(78). Metabolic disorders of glucose may be modelled by changing the value of these parameters appropriately. Glucose intake rate, which is normally set at 0, can be set at a desired rate using A(79).

9.3.10 Discussion

Therapeutic entry points and parameters relating to abnormal conditions in MFAB have been identified. These allow a wide range of input tests and model states to be investigated, although these are far from being exhaustive. It has not been possible to include a comprehensive set of facilities as there are so many possible areas of interest, however, small changes to the coding of MFAB could allow most types of abnormal condition to be simulated.

The results of making a number of these changes are investigated in the validation of MFAB as presented in Chapter 8.

9.4 ENHANCED DATA-PARAMETER MATCHING

When entering a simulation with MFAB, the user is asked a series of questions relating to easily attainable clinical data (that is, age, sex, height and weight). These data are translated into the state variables and some parameters of the patient (see subsection 7.2.3). Further adjustments to parameters can be made manually (as described in the previous subsection). To an extent, this latter activity proves difficult because of the complexity of the interactions within the model and the subjective nature of the parameter setting, and of course it may be time consuming (diminishing pragmatic validity). The idea of a second program to enable key model parameters to be adjusted automatically to match model prediction to clinical measurements thus has to be considered (Hinds et al, 1980).

The method which is most appropriate for a complex model such as MFAB is to select a set of parameters which may be varied simultaneously to optimise the model prediction. The set of parameters needs to include at least one of importance from each subsystem. This allows direct optimisation at the submodel level, whilst also considering the overall response. For example, Hinds et al (1980), in their data-parameter matching of a respiratory model described by Dickinson (1977), took arterial bicarbonate measurements and matched them by a calibration procedure involving the addition of a test load of 30 mmol of bicarbonate and (from the

subsequent steady-state level) calculation of the amount required to match the value measured in the patient. This was performed to a predetermined degree of accuracy for the submodel. The method is necessarily iterative and once completed other variables computed by the model can be compared with clinical measurements to assess overall accuracy and consistency. The development of such a program requires extensive studies, but the benefits are likely to be high.

Of more immediate consequence is the accessibility of MFAB to medical personnel in its current stage of development. This need has been tackled with the microcomputer implementation of FAB3 (a prototype of MFAB) which is presented in the following section.

9.5 MICROCOMPUTER IMPLEMENTATION OF FAB3 (A PROTOTYPE OF MFAB)

9.5.1 Introduction

FAB3 is a prototype of MFAB. It has been presented by Flood et al (1984b) including details of a promising qualitative and quantitative feature analysis. The essential differences between FAB3 and MFAB are in: the electrolyte representation where intracellular contents were not considered; the protein dynamics where a satisfactory representation had not at that stage been developed; the gastrointestinal system which had not been considered important at that stage; and the cardiovascular system where the representation of Ikeda et al (1979) was used before the model of Dr G Parkin had been considered.

9.5.2 The Program: Use And Details

In this subsection the reader is taken through a run of the package. Some program details are also given at appropriate points in the text. For details on: the program development from the FORTRAN coding; technical data; and the Apple II program coding and nomenclature of FAB3 refer to Appendix 8.

Initially the Apple II microcomputer and peripheral devices have to be turned on and the diskette loaded into the disk drive. The menu program is automatically loaded and run. The screen reads:

```
WELCOME TO THE
INTERACTIVE FAB
  SIMULATION

WHICH MODEL DO YOU REQUIRE?

1 - ACID/BASE SYSTEM
2 - FLUID/ELECTROLYTE & HORMONE SYSTEM
3 - GENERAL SYSTEM
4 - EXIT FROM PROGRAM
```

The user has to select one of the three models or exit the program. The GENERAL SYSTEM is in fact FAB3, however, two segmented versions of FAB3 are available. Both have the advantage of running at a faster real time speed than FAB3 and may be preferred by the user when the interest is more specific. The user must type in the number of his choice and press 'return'. The title of the model is initially displayed and the user is asked to press any key to proceed. For example, if the fluid-electrolyte and hormone system were selected the screen would read:

PRESS ANY KEY TO PROCEED

Once this has been carried out there is a short delay whilst the model is initialised. The user is then asked to select three variables for graphic output:

SPECIFY 3 VARIABLES FOR GRAPHIC OUTPUT

These must come from the list of dependent variables, must be specified by the appropriate number and must either be separated by commas or by pressing the 'return' key after each variable entry. The next question is asked:

TYPE MIN. & MAX. VALUES FOR
VARIABLE (a)

Variable a is the first of the three declared dependent variables. The user must use his expert knowledge to define the minimum and maximum values of the y axis of the graph for each variable in turn. The range is determined by the purpose of the simulation. The user who does not have expert knowledge will soon learn the expected ranges of variables to given perturbations. Appropriate range declaration is important as too large a range will confine the graph to a small strip of the screen, whereas, if the range is too small the graph may leave the screen thus stopping the program.

In the event of this happening the computer should be turned off and back on, where the menu will be re-run.

Having successfully declared the variables and their ranges, the system then asks if the user wishes to perturb the system:

DO YOU WISH TO PERTURB THE SYSTEM?

(ANSWER ONLY WHEN READY TO CONTINUE)

The response needs to be either Y for yes or N for no. If N is typed in then a steady-state simulation begins. If Y is typed then the vector number of the independent variable is requested:

WHICH VARIABLE DO YOU WISH TO ALTER?

The independent variable number must be entered and the 'return' key pressed. The system response is to give the current value and ask for a new value.

PRESENT VALUE (x)

NEW VALUE?

The new value should be entered and the 'return' key pressed. The opportunity to change further parameters is offered until an N is typed in response to the perturbation question.

The graph is then plotted. The y axis is given ten equally spaced dimension markers. Three different coloured markers of the dependent variables starting values are also drawn on the y axis

(on both the LHS and the RHS of the screen). Beneath the graph is the information required to explain the graphical display. For each of the three variables being displayed the number, range and colour is specified. Two numbers are displayed on the bottom right of the screen. The top 'clock' times the simulation in simulation-time, and the bottom 'clock' keeps a constant record of the last time the system was perturbed in simulation-time, see Figure 9.1 (although only shown in black and white).

The graph is plotted whilst the simulation is running and continues up to 4 hours 39 minutes. At this point the 279 available columns on the graphics are completely used. The screen then clears and initial dependent variable flags are again positioned on a blank graph, whence simulation continues. The user should note that Apple II graphics exhibits some idiosyncracies. The plotted points will either be the defined variable colour or some shade of it, depending on whether the point plotted is an odd or even numbered row (although it is easy to distinguish each variable).

A further user facility is the ability to leave the simulation or to make perturbations. By pressing any key during simulation the opportunity to abort is given. If simulation is to continue then the perturbation routine described above comes into use. This facility can be used to freeze the graph at desired times.

9.5.3 Comments

Substantial program documentation is given in Appendix 8. This gives general access to the prototype FAB model. Experience of this implementation makes quite clear the feasability and usefulness of such a system, consequently a further implementation using MFAB, or a future model developed using the proposed methodology of Chapter 10, is strongly recommended.

9.6 CONCLUSION

The role of a complex dynamic model of the FAB system in clinical medicine has been discussed in this Chapter and it has been shown that such a model offers substantial promise. Such a model, if properly treated, can be implemented on a microcomputer so that outputs are both easy to assess and quickly achievable. Graphical output with representation of parameters in physiological terms has obvious user-friendly qualities. Future development of multitasking systems will also be advantageous as speed of simulation and presentation of output may be improved. For example, a graphics window whilst other tasks are being dealt with from keyboard entry and VDU response. In addition, enhancing data-parameter matching will tune the model more closely to the patient, thus improving user acceptability. This will certainly be an improvement on the static use of clinical data, but does however require a substantial programme of development.

The work presented in this Chapter does not assume that the model MFAB is the ideal model for such an implementation. The following Chapter makes investigations into the methodology used to develop

MFAB and considers the possibility that a different methodology may produce a more appropriate model.

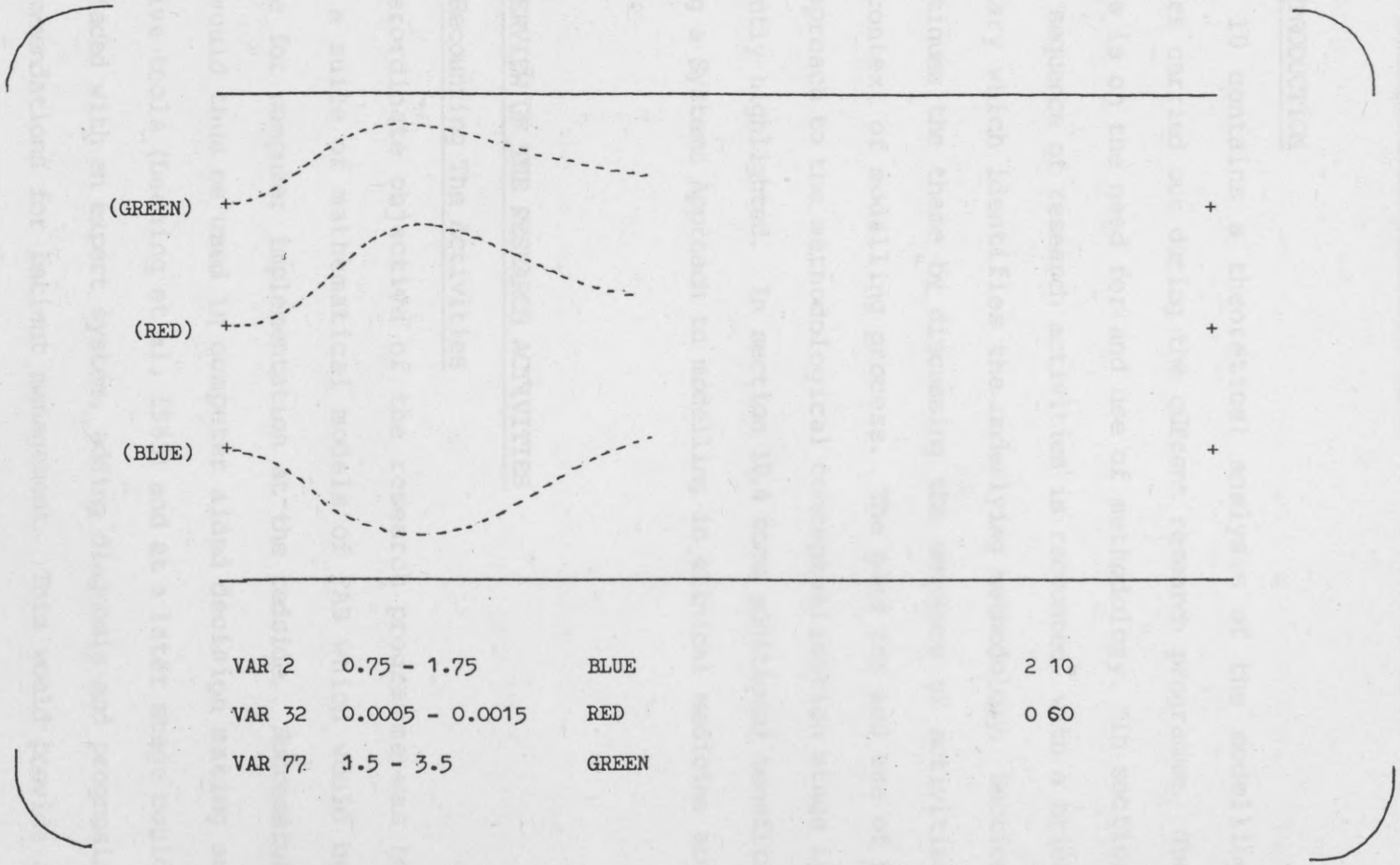

Figure 9.1 Screen output of FAB3 microcomputer implementation.

CHAPTER 10

THE ROLE OF SYSTEMS SCIENCE IN CLINICAL MEDICINE

10.1 INTRODUCTION

Chapter 10 contains a theoretical analysis of the modelling activities carried out during the current research programme. The emphasis is on the need for and use of methodology. In section 10.2 the sequence of research activities is recounted, with a brief commentary which identifies the underlying methodology. Section 10.3 continues the theme by discussing the sequence of activities in the context of modelling process. The need for and use of a novel approach to the methodological conceptualisation stage is consequently highlighted. In section 10.4 some additional benefits of taking a Systems Approach to modelling in clinical medicine are outlined.

10.2 OVERVIEW OF THE RESEARCH ACTIVITIES

10.2.1 Recounting The Activities

The superordinate objective of the research programme was to produce a suite of mathematical models of FAB which would be available for computer implementation at the bedside. Successful models would thus be used in computer aided decision making as predictive tools (Leaning et al, 1985) and at a later stage could be interfaced with an expert system, adding diagnosis and prognosis and recommendations for patient management. This would provide a system of models for computer aided decision making (Cramp et al, 1985; Cramp and Carson, 1985).

The research method was as follows:

(i) A sentential model of the structure and processes of FAB was constructed and then translated into a set of graph-theoretic models.

(ii) Extant FAB mathematical models were reviewed in detail (Flood et al, 1984a). This review identified techniques that have been used and other potential techniques which although not apparent in the extant models, displayed some possibilities for future use.

The conceptual models developed during the early parts of the research appeared to be compatible with the wealth of complex, non-linear, lumped-parameter, control system, extant models. Further consideration led to the following definition of the SOI:

$$A \underline{\cup} B \qquad (10.1)$$

where; A is the set relating to the patient FAB system, B is the set relating to clinical control over A. The research progressed from here:

(iii) As a consequence of (i) and (ii) and the definition of the SOI an isomorphic model representation was developed in the form of a complex, non-linear, lumped-parameter, control system model (Carson et al, 1985; Flood et al, 1984b, 1985b, 1985c).

(iv) Other experimental models were developed using techniques identified as potentially useful. These were ARIMA, TF and simple compartmental models, with recursive estimation of parameters on the latter two (Flood et al, 1985a).

(v) An appraisal of (i)-(iv) was undertaken and is detailed below.

10.2.2 Appraisal Of The Activities

It was found that the above definition of the SOI was not entirely appropriate and caused some setbacks in achieving the research objectives (to be discussed later). A modified definition of the SOI has therefore been formulated:

$$((A \underline{\cup} B) \underline{\cap} C \underline{\cup} D) \qquad (10.2)$$

where; C is the set of clinical observations regularly made on $A \underline{\cup} B$, D is a set of a minimal number of other variables (unknown) that explain the generative mechanisms behind C. This definition ensures that key observation variables are included, and not only satisfies clinician needs, but also includes parsimony as an explicit goal. An important implication of having a set of 'unknown' variables is that a fresh approach to the conceptualisation stage is required (to be discussed in detail in section 10.3).

One of the research objectives was to provide compatibility for a sister knowledge-based system. This would produce a system of models able to make current and future assessments in relation to current state and a series of alternative treatments. The structure of the system is perceived to be of the form shown in Figure 10.1.

It became apparent that this system could at best have a patient-related (some parameters specific to the patient) rather than a patient-specific (all parameters specific to the patient) dynamic model. This is explained below.

An expert system could be used to diagnose the patient for t=0 and then set the parameters of the patient model, thus transforming the data into information. However, inserting MFAB (the complex model presented in Chapter 7) in the patient-representational block of Figure 10.1 would impose insurmountable problems for the knowledge-based component. Handling the number of rules required by such a logic-based system is not conceivable by today's standards.

A less complex model was required. The compact compartmental model (presented in Chapter 6) provides a degree of patient-specificity. However, the simplicity required of the models for initial tests of the Extended Kalman Filter (for recursive estimation) proved to be non-compatible with their proposed use. The main reasons being a paucity in the observations available and a limited representation of the generative mechanisms.

ARIMA and TF models (presented in Chapter 6) were also developed. Aside from the problems of applying these techniques in a clinical environment (a new model is required for every set of data) and the a priori assumptions that are made (the system is linear and physically realisable) there appears to be another major drawback. They are black-box models of data that are not based on structural physiological hypotheses. However, if the dynamics are not well understood or if they are rapidly changing (as in disease situations) they may well be seen as advantageous in their representation.

After considering all these factors, it was concluded that neither black-box (input-output) nor white-box (isomorphic) models were appropriate for the continuation of the research programme. A grey-box (a mixture of implicitly and explicitly expressed representations) model, addressing the needs of the clinician was deemed appropriate. It was perceived that from a base of clinical observations and using an appropriate set of guidelines a minimal number of implicit and explicit functions could be developed, thus producing the required parsimonious grey-box model. This is of course a methodological problem.

Further analysis and development of existing methodologies was therefore necessary. This is the subject of the following section.

10.3 TOWARDS A NEW METHODOLOGY FOR MODELLING DYNAMIC PATIENT-CLINICIAN SYSTEMS

10.3.1 Introduction

The need for a new methodological approach has been identified. This section aims to build the foundations of such an approach. To achieve this, philosophical and methodological issues and the use of techniques will be discussed. Such words, however, are used in a variety of contexts and thus have rather loose interpretations. To add clarity to this discussion, the following operational definitions (based on Checkland, 1984) are offered:

(i) Philosophy: a broad non-specific guideline for action.

(ii) Technique: a precise specific programme of action which will produce a standard result.

(iii) Methodology: lacks the precision of a technique but will be a firmer guide to action than a philosophy.

A methodology thus follows the systematic and iterative guidelines of the related philosophy. However, a methodology has rules for 'things' that should be done and sets a constitution of things that could be done (Jenkins, 1983). This allows the modeller(s) to express a personality on the process by adopting the constitution according to current perceptions. A methodology without a constitution is, therefore, nothing more than a technique.

10.3.2 Modelling Philosophy

The modelling methodology of Carson et al (1983) (redefined as a philosophy according to the above presented operational definitions) is one view of the modelling process, see Figure 10.2. The modelling process passes through a phase of conceptualisation. The achievement of equations with estimated parameters depends on the nature of the system. Failure to attain full quantification is usually due to a paucity of laws, theory and/or data. A good example of the latter point is the model of Blaine et al (1972), which yields considerably more than a signed-digraph but less than would be provided by a fully quantitative simulation model (Flood et al, 1984a).

This modelling process was considered in the context of modelling purpose(s). Finkelstein and Carson (1985) discussed three types of purpose for mathematical modelling. These are; description, prediction and explanation. The essence of each type of purpose is presented below.

(i) Description: for the sake of conciseness and economy of description and the resultant ease of analysis and handling of data.

(ii) Prediction: to determine how a system would respond to a stimulus.

(iii) Explanation: explanatory power lies in the ways in which different features of system behaviour and structure are shown to depend upon each other.

Figure 10.3 highlights a variety of sequences that a modeller may follow and shows that the essence of the three types of use of models discussed by Finkelstein and Carson holds true for qualitative as well as quantitative models.

The following observations can be made by considering Figure 10.3 in the light of Figure 10.2:

(a) Block 1 and consequently Block 2 can be reached by using laws, theory and data.

(b) If Block 2 has been achieved to a reasonable degree of satisfaction, then it would be meaningful to progress from Block 3 and/or Block 4.

(c) For Block 3 and Block 4, validation will at best be qualitative in nature, for example, the tracing of an impulse input to a signed-digraph as discussed in Chapter 4.

(d) Block 5 may be achieved from Block 2, although it is not necessary that the parameters are estimated.

(e) Block 6 and Block 7 can be meaningfully achieved only after the parameters have been identified and the model validated. If this can not be achieved then observation (c) holds for Block 6 and Block 7.

Experience of following these sequences has shown that the transition from Block 1 to Block 2 is probably the single most important step in the modelling process. This is because at this conceptual stage the structure and complexity of the model are determined.

The modelling philosophy of Carson et al (1983) concentrates on realisation, identification and validation (although problem conceptualisation is not excluded). Appropriate techniques are also discussed. It was therefore perceived that concentrating on developing a conceptualisation stage would be a useful if not necessary contribution. Furthermore, the addition of rules to the philosophy (mostly via the conceptualisation stage) would add a necessary degree of context-specificity, thus producing a methodology for dynamic modelling in clinical medicine.

10.3.3 Approaches To Conceptualisation In Modelling Methodologies

A structure has been designed with which approaches to conceptualisation may be analysed, see Figure 10.4. Figure 10.4a is the simplified version, having only four possible matrix entries representing four extremes of approach. Figure 10.4b shows the set of possible matrix mixes which are more typical of real world methodologies

Expert consultation is where the modeller is the ultimate filter of all data available or gathered. The constitutents (which compose or make up the whole), the composition (the structuring of the constitutents in the whole) and the interactions (the process introducing the fourth dimension time) of the model are exclusively determined by the modeller, see Figure 10.5a.

In process consultation the modeller acts as a filter. Process consultation differs in that the constituents, composition and interactions of the developing model are determined (to varying degrees) by people involved with the SOI. These people may be internal to the SOI (for example, a clinician in a hospital) or they may be external to the SOI (for example, the Health Minister). The process consultants are usually key members of the SOI, see Figure 10.5b.

A modeller may also employ mathematical, computational and heuristic tools during the filtering process in further search for a parsimonious representation. These may be formally developed techniques such as pattern recognition (Attinger, 1985) or looser diagrammatic methods such as 'rich pictures' (Checkland, 1984). Some filtering is done intuitively (often due to a paucity of data) when the modeller is forced to make educated guesses about constitutents, composition and/or interactions. Two examples follow.

Checkland (1984) has developed a methodology for real world problem solving in human activity systems. Continual emphasis is put on

the inappropriateness of techniques and very little emphasis is placed on process consultation. Rich pictures (a first phase of conceptualisation), for example, are entirely the subjective interpretation of the expert consultants. In the matrix of 10.4a, this tends strongly towards conceptual approach 1.

Interpretive Structural Modelling (ISM) has been developed for hierarchical structuring of objectives and other intents. This approach emphasises process consultation (although expert consultation is not totally excluded) and a mixture of human and technique interpretation. In the 'matrix' of Figure 10.4b this tends towards conceptual approach 2∩4.

As the objectives of the current research programme are aimed ultimately at producing user friendly packages, it seems appropriate that process consultation is used. Furthermore, technique interpretation could, if properly constructed, be usefully employed in selecting the model variables. The following subsection presents some guidelines for selecting model variables.

10.3.4 Selection Of Variables

The task of selecting the variables for inclusion in a model can be considered in the light of Figure 10.6. This is an adapted version of a diagram first conceived by Onno Raddemaker. It can be seen that as the number of variables included rises, the predictive ability rises to a peak value beyond which the continuing decrease in manipulability and increase in numerical errors (especially during computer simulation) tends to force the predictive ability downwards. Furthermore, by increasing model complexity it is easy

to fit short term model output to empirical data, however, this is at the expense of medium to long term accuracy brought about by increased model uncertainty.

An optimality curve can be drawn by lumping these concepts together. This relates the model to the modelling objectives. The optimal number of variables may be at the point X on the abscissa axis. This axis should be thought of as an ordinal scale where variables are included from left to right in order of importance.

The modelling activities of top-down (starting with a number of variables $> X$, then simplifying the model towards X), and bottom-up (starting from a base of variables $< X$, then moving towards X) are conceptually accessible from Figure 10.6. However, necessary in any bottom-up approach is an initial top-down exercise to achieve a base of variables.

In graphical terms, neither top-down nor bottom-up are seen as smooth functions. Rather they are negative exponential oscillatory functions, see Figure 10.7.

Whether a top-down or a bottom-up approach is taken, and whether expert or process consultaton is adopted, and whether human or technique interpretation is used, depends on the modelling situation, that is; the nature of the system, resources, objectives and the modellers viewpoint. The author's viewpoint in relation to these factors is detailed below.

10.3.5 Foundations Of A Novel Conceptual Approach

The preceeding subsections suggest that expert consultation with human interpretation was used during the research programme. As a consequence of this consultation and the original definition of the SOI, a complex model (MFAB) was developed. The point Y in Figure 10.6 represents MFAB's theoretical position in relation to the research objectives. A substantial amount of unnecessary detail was included, however, a top-down of the complex model is not seen as the most suitable way of achieving the optimum detail.

The implications of Figure 10.6 with respect to the objectives of the current research (and indeed the author's viewpoint), suggest that bottom-up is appropriate. This would ensure that variables are included in order of importance, that only the necessary variables are represented (adding parsimony), and that with an appropriate base of variables (important clinical observations) the model is tailored to the user.

Furthermore, consideration of findings in this Chapter has led to the conclusion that conceptual approach 4, the process consultation with technique interpretation, is appropriate in the development of decision making aids for the clinic. Process consultation would further ensure that clinicians needs are satisfied, user friendliness being of prime importance, whilst technique interpretation would help ensure that parsimony is attained, minimum complexity being essential for maximum versatility of the model.

If a conceptualisation stage were developed along these lines and integrated with the philosophy of Carson et al (1983), then the result would be a novel and surely essential methodology for the development of dynamic models as clinical decision making tools.

The future development of a domain-specific methodology would provide a systematic approach to modelling activities, but at each systematic step it would be the systemic thinking that enables the whole system to be represented effectively. To achieve this the Systems Scientist will need to be both a reductionist and a holistic thinker in the course of his activities.

Furthermore, it has been curious to note that implementation of models designed for clinical use is the exception rather than the rule. The development of a domain-specific methodology may go some way to solving the user acceptability component of that problem by tailoring the model specification to the demands of the clinical user.

A theme of section 10.3 has been the interaction required between the Systems Scientist and the medical profession. The following section discusses the benefits that accrue for both parties by adopting a Systems Approach.

10.4 SYSTEMS SCIENCE IN CLINICAL MEDICINE

The foregoing sections in this Chapter have detailed a variety of methodological issues. Other aspects of Systems Science can play an important role in clinical medicine. These are discussed below.

It was shown in Chapter 2 that Systems Science can contribute substantially to the understanding of physiological functions and pathological conditions (and consequently health care by increasing awareness). This is often achieved by using models to test controversial and new theories of physiological function. The complex model (MFAB) is currently being used for these purposes at The Westminster Hospital in London and The Royal Alfred Hospital in Melbourne, respectively.

The concept of control has helped to explain physiological and biochemical homeostasis, and has also increased understanding of the external control loop (clinician control) when pathological and other disorders occur. Unlike feedback control found within a patient's body (although not exclusively found, for instance sensitivity to rates of change could be considered as feedforward) this research has identified clinician control as (if not exclusively at least substantially) feedforward. It is the clinician's persistent consideration of future patient state that initiated the current modelling activities, with the aim to constructing tools with which future patient states can be investigated. Furthermore, the current state can be explicated and classified through model simulation.

Medical application of dynamic models has however, continued to pose a number of special problems. Although biochemical and physiological subsystems are relatively hard, so that quantification can readily be applied, acceptance of models in the clinic can not automatically be assumed. Problems of

implementation and acceptance occur due to the contrasting soft nature of the target human activity system labelled the clinic. Pope et al (1983) showed how effective a soft Systems Analysis of the role of the clinical laboratory could be in improving diagnosis and management of liver disease. This study is suggestive in the ways that we modellers may best direct our activities to ensure the earliest possible acceptance and implementation of model-based computer-aided decision-making tools.

Systems Science provides a framework for thought. This framework is transferable from situation to situation and develops with each new venture. It is for this reason that the study of physiology and (in particular) medicine has contributed substantially to Systems Science.

This symbiotic (association to the mutual advantage of) and synergistic (success arising directly and exclusively from the joint relationship of) relationship occurred within the bounds of an Action Research (as defined by Checkland, 1984). A programme of action has been undertaken within the problem situation, whilst in parallel, research into Systems Science has continued. Consequently, implementation in the clinic has become a realistic target, whilst ideas about methodologies have also developed and methodological approaches have been refined.

These observations relate closely to the writings of M'Pherson (1974), where he commented that Systems Science is not distinctly a Science. Rather, it moves between Science and Philosophy, at times

dealing with the application of a scientific approach, whilst at other times looking critically at the approach itself.

10.5 CONCLUSION

In this penultimate Chapter, an account of the activities of the research allowed the modelling approach to be critically analysed. The analysis showed severe limitations in existing modelling methodologies, particularly in relation to modelling for clinical application. A new context-sensitive methodological approach was discussed. This provides an important and yet fundamental step, necessary if clinical application is to be effectively realised.

At a more general level, it has also been noted that Systems Science provides an excellent framework within which this type of research programme may be carried out.

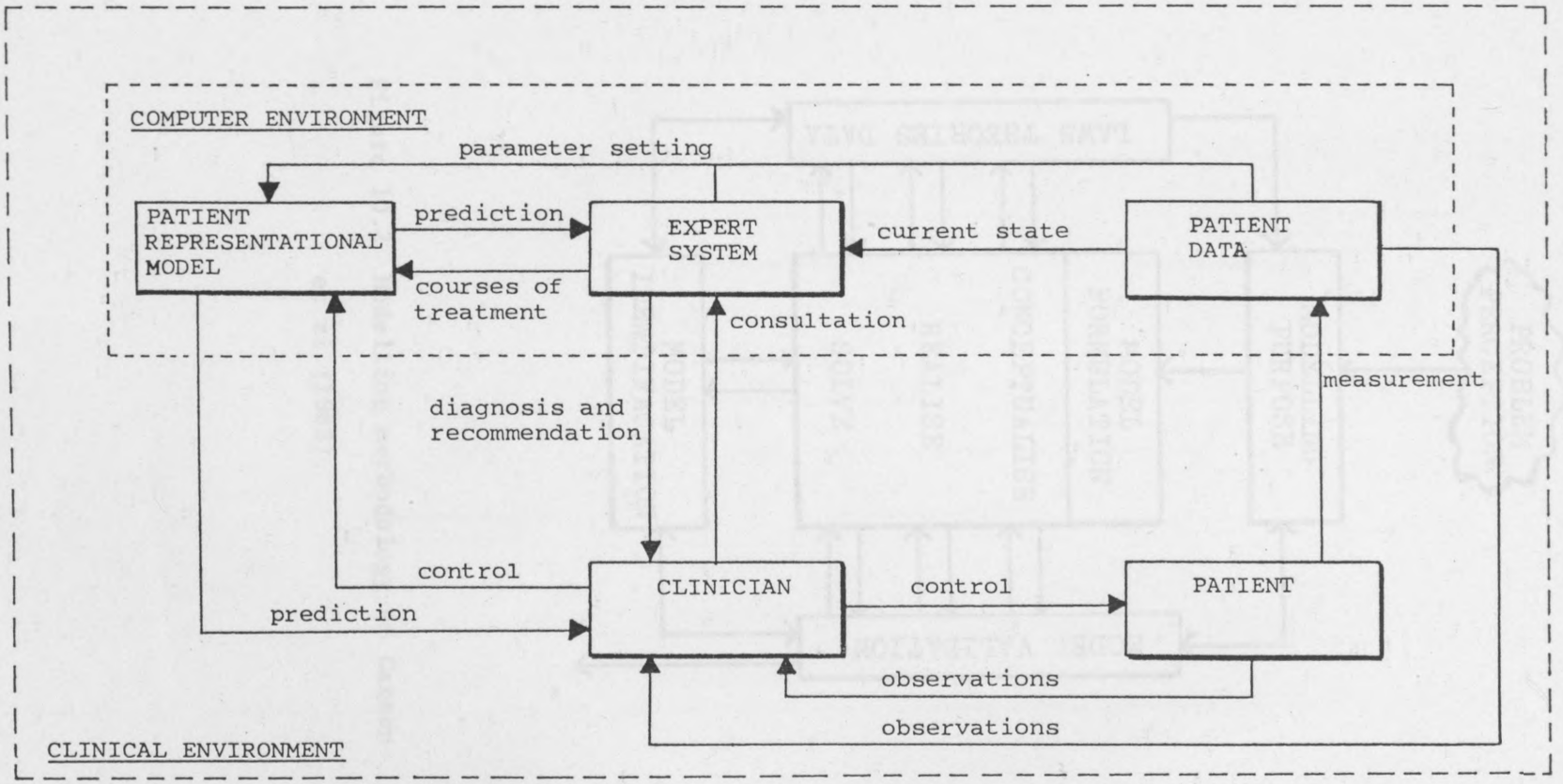

Figure 10.1 A structure for a system of systems, designed to produce a tool for clinical decision making.

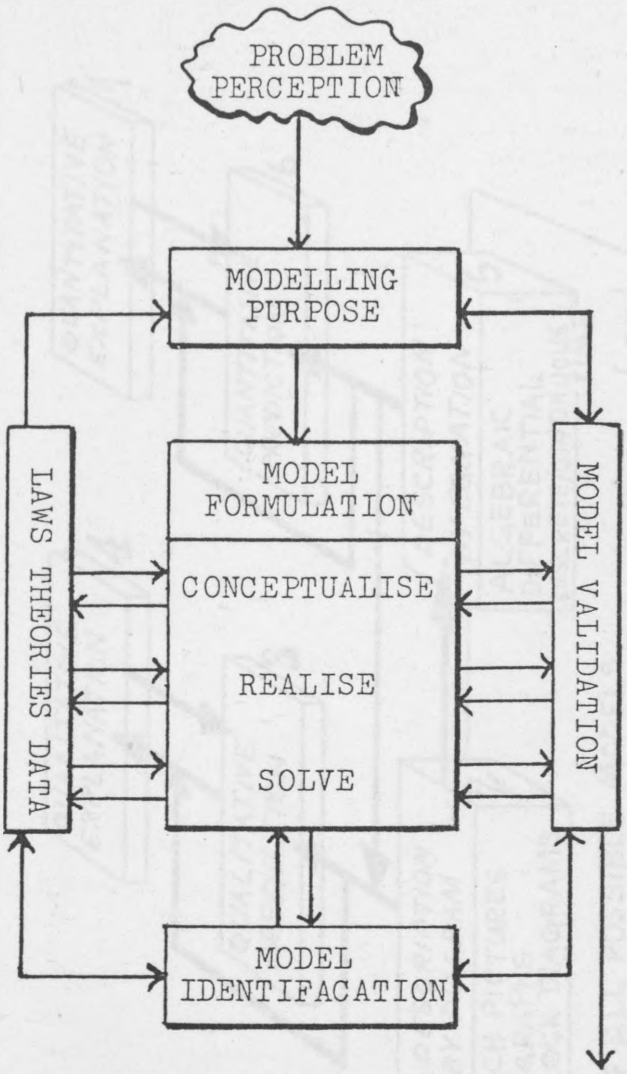

Figure 10.2 Modelling methodology of Carson et al (1983).

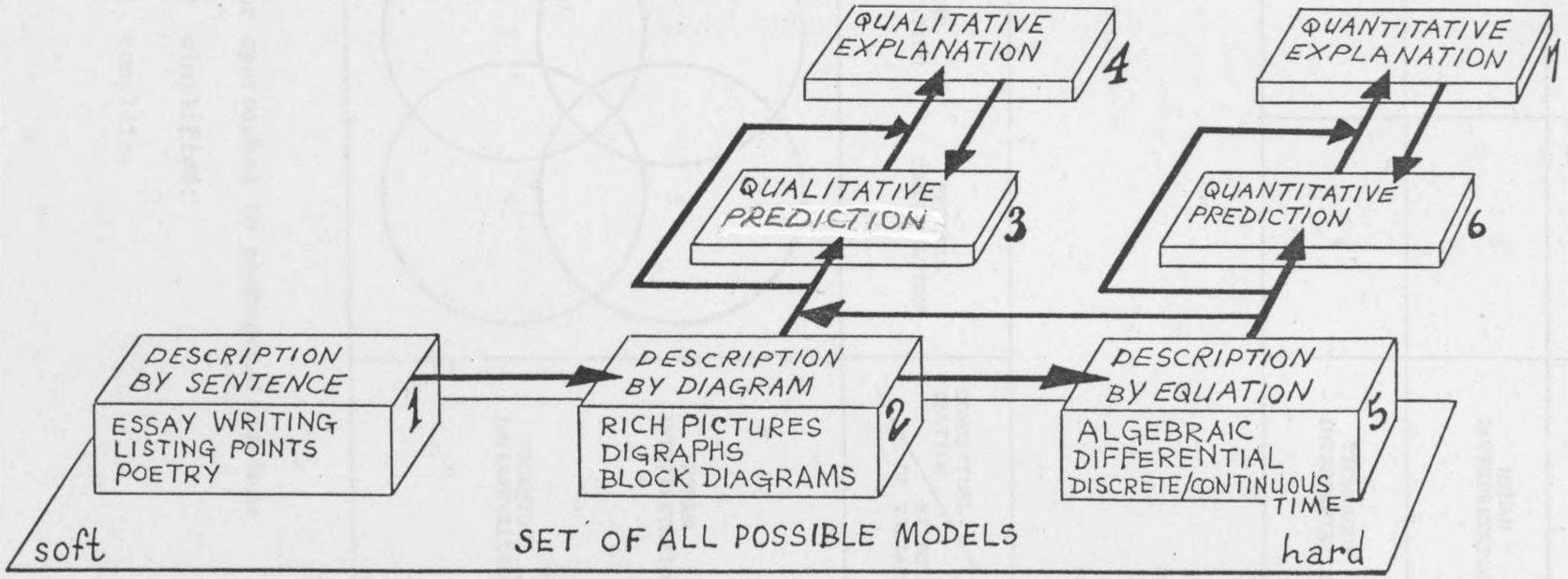

Figure 10.3 Modelling process.

(a)

EXPERT CONSULTATION	PROCESS CONSULTATION	CONCEPTUAL-ISATION / SELECTION OF VARIABLES
1	3	HUMAN INTERPRETATION
2	4	TECHNIQUE INTERPRETATION

(b)

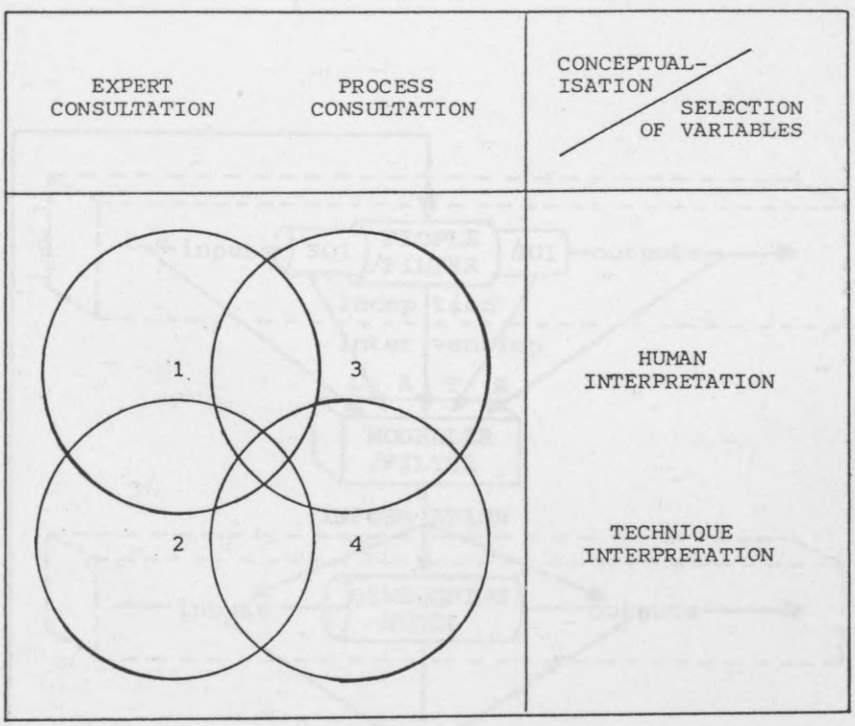

Figure 10.4 Four approaches to conceptualisation:

(a) simplified;

(b) complete.

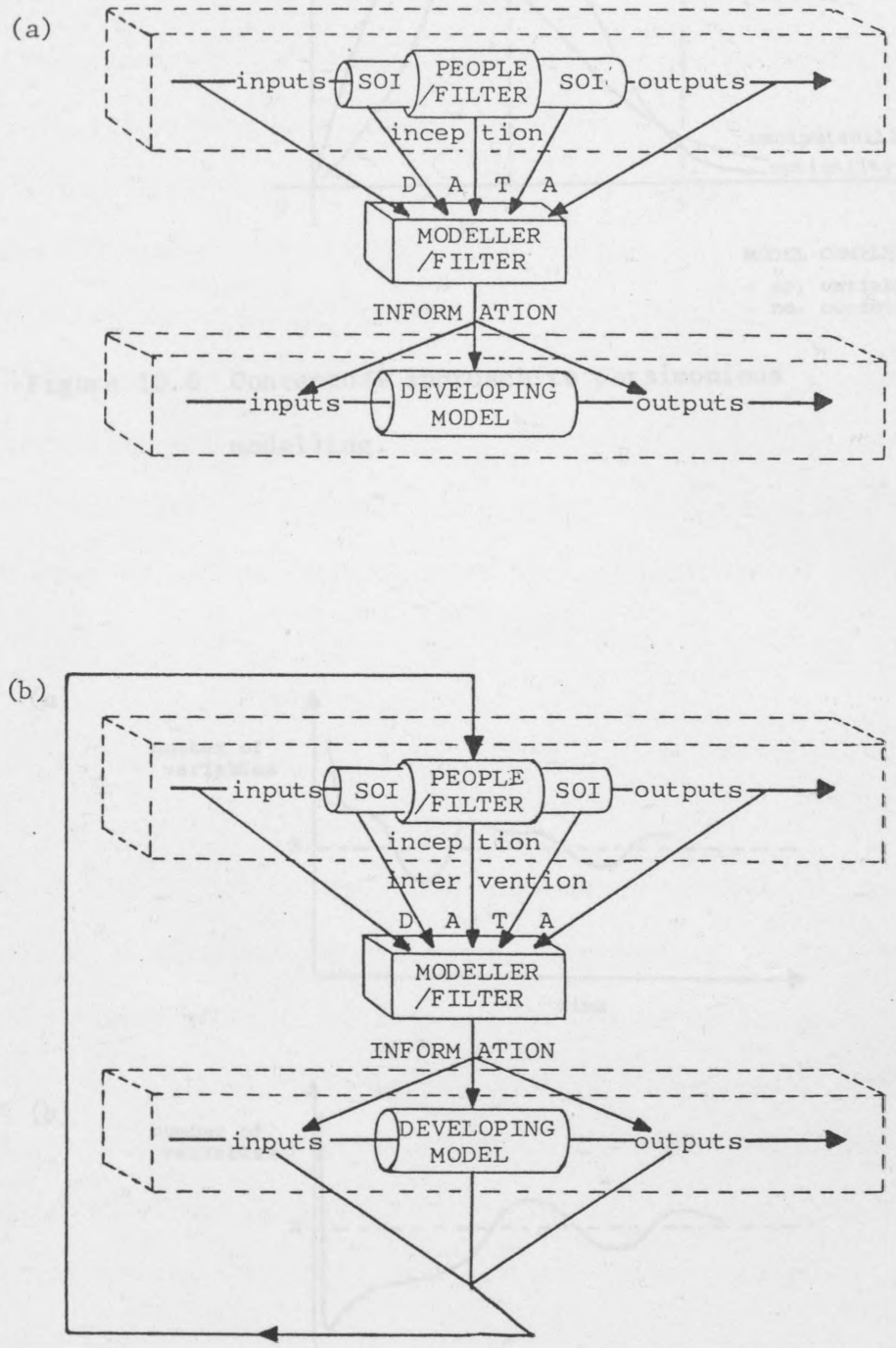

Figure 10.5 Representations of:

(a) expert consultation;

(b) process consultation.

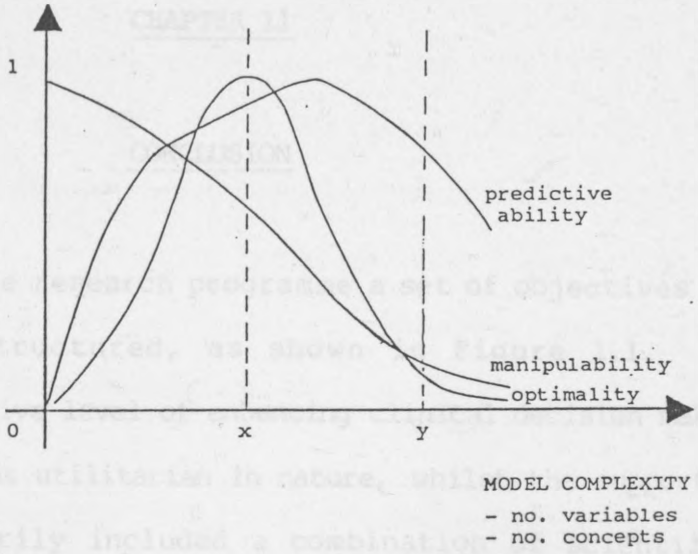

Figure 10.6 Conceptual approach to parsimonious modelling.

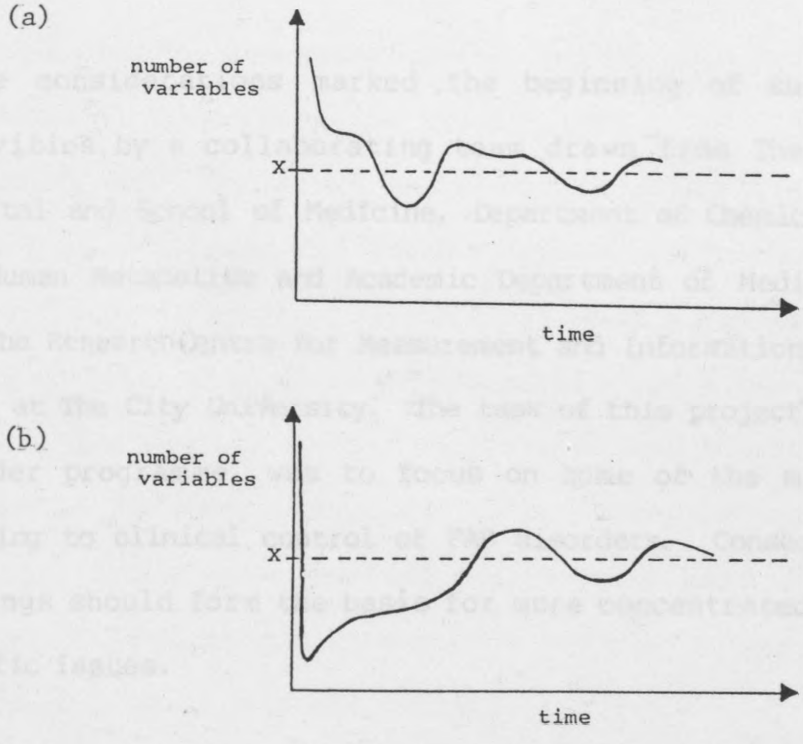

Figure 10.7 Graphical representation of:

(a) top down modelling;

(b) bottom up modelling.

CHAPTER 11

CONCLUSION

At the outset of the research programme a set of objectives was formulated and structured, as shown in Figure 1.1. The superordinate objective level of enhancing clinical decision making in the FAB domain was utilitarian in nature, whilst the supporting objectives necessarily included a combination of scientific, technical and practical features; tackling model development, construction and implementation. The raw material available for these activities was the ever growing laboratory-produced data bank on plasma and urine samples, with the computer being the obvious processor.

These considerations marked the beginning of such research activities by a collaborating team drawn from The Royal Free Hospital and School of Medicine, Department of Chemical Pathology and Human Metabolism and Academic Department of Medical Physics, and The ResearchCentre for Measurement and Information in Medicine based at The City University. The task of this project, set within a wider programme, was to focus on some of the major issues relating to clinical control of FAB disorders. Consequently, the findings should form the basis for more concentrated efforts on specific issues.

Significant contributions have been made to Systems Science, Physiology and Medicine. Systems Science has benefited through the identification of weaknesses in methodological approaches.

Contributions to physiology have arisen via clarification of controlling systems of FAB and via increased insight of intra-extracellular ion dynamics. Advantages to medicine are apparent with the development of computer based decision support aids for clinical decision making on critically ill patients. The following discussion supports these statements.

An approach to mathematical modelling documented by Carson et al (1983) provided the basis for model development. The research programme consisted of three distinct but highly inter-connected stages; those of conceptualisation, mathematical analysis, and practical and theoretical issues relating to model development and implementation. A systemic approach was adopted throughout.

In developing the conceptual model, the FAB system needed to be specified at two cybernetic levels; that of physiological and biochemical self-regulation, and that consisting of the exterior control loop between clinician, patient and a computer-based decision support system. At the first level a number of areas of weak knowledge and points of controversy were identified, for example, the precise mechanisms of hormonal control. Further analysis of the control structure using graph-theory confirmed the essential features of control which have been proposed in biochemical publications, however, the precise mix and contribution of stimuli is still somewhat unclear.

The next phase involved identifying the essential structure and processes of FAB which were to be represented mathematically. The

review confirmed the appropriateness of the general modelling approach being adopted, and also highlighted those areas of the FAB system where agreement has yet to be reached as to the appropriate mathematical realisation to be adopted. In addition, the review highlighted the relevance of alternative mathematical and statistical techniques in relation to differing modelling purposes.

The first quantitative approach investigated was clinical time-series which drew heavily on data supplied from clinical tests. Three specific techniques were considered under this heading; univariate ARIMA modelling, bivariate TF modelling and compact state-space modelling. They differed in the data sample size required and the need for knowledge of the underlying physiological system's dynamics.

The univariate and bivariate approaches would require data sets with $N > 50$ which realistically requires on-line monitoring (especially for patients whose stay is relatively short). This may be practicable in the future given the development of specially designed bedside equipment. The recursive implementation of discrete TF models, updating estimates of patient parameters, was found to be promising and ideally suited to situations where new data will continually be supplied.

Compact state-space models were found to have the advantage of codifying pathophysiological processes, therefore, the initial requirement of the statistical approaches on data set size could be relaxed.

The second quantitative approach considered was the frequently used complex compartmental approach. A model of that nature was developed alongside an algorithm to tune the model parameters to patient data. Unlike the statistical approaches which inherently contain measures of validity, the complex model required an explicit well thought out validation programme. That developed by Leaning (1980) was adopted and against this the model performed well.

The question of pragmatic validity, however, required that the use of such a model in clinical medicine be considered and consequently gave rise to the third distinct section of the research.

This was investigated by highlighting the features of a microcomputer implementation that was developed; especially in relation to user interface, available ways of simulating abnormalities, and by showing that tuning of the model parameters to those of the patient could be done effectively.

Another aspect of pragamatic validity questions the appropriateness of a model selected for implementation in a decision support structure. The complex model was perceived as being the appropriate type of model (at least currently, whilst on-line monitoring is developed), however, the question of whether the model could be improved in structure, process and complexity was considered. An analysis of methodology highlighted substantial weaknesses, especially relating to conceptualisation. A series of novel ideas were consequently put forward.

One of the major achievements of the research has been the documentation of a wide range of important matters relating to the provision of a computer-based decision support for clinical application in the domain of FAB. This has drawn together information which previously had been documented separately in the respective literatures of Systems Science, Physiology and Medicine. The piecing together of other research efforts alongside developments carried out during for example the current programme, has thrown new light on the problem of clinical application, in particular the importance of developing the modelling methodology and tailoring the software itself for the intended range of application.

Since the work described in this thesis represents a portion of a major ongoing research programme, it is inevitable that as well as making significant contributions to knowledge in its own right it should also have highlighted areas where future work is required. A set of recommendations is therefore listed below:

1. Investigations of a scientific nature into areas of controversy and weak knowledge relating to FAB, possibly with compartmental models.
2. Development of efficient bias-free recursive estimators.
3. Interfacing on-line monitoring with time-series and compact state-space models, including a recursive estimator on the parameters.
4. Development of an appropriate methodology for clinical modelling with utilitarian objectives.

5. (Subsequent to 4.), the development of a tailored mathematical model and microcomputer implementation for FAB.
6. Development of a sophisticated parameter setting algorithm for clinical compartmental models.

The work described in this thesis should thus act as a stimulus for further developments in this important and challenging area of medicine.

REFERENCES

Allen, T.H., Peng, M.T., Chen, K.P., Huang, T.F., Chang, C., and Fang, H.S. (1956). Prediction of blood volume in man from body weight and cube of height. Metabolism, 5, 328.

Attinger, E.O. (1985). Parsimonious systems description: A necessary first step in the development of predictive indicators, in: Carson, E.R., and Cramp, D.G. (eds), Computers and Control in Clinical Medicine. New York: Plenum.

Badke, F. (1972). A model of body water and salt regulation. Biomed. Sci. Instrum., 9, 103-107.

Beketov, A.I., and Korneliuk, I.K. (1981). [Effect of noradrenaline and agiotensin II on the brain and kidney blood supply with changes in systemic arterial pressure]. Farmakol Toksikol, 44(4), 414-7 (English abstract).

Beneken, J.E.W. (1965). A mathematical approach to cardiovasular function. The uncontrolled human system. Institute of Medical Physics TNO, Report no. 21415/6, Utrecht, The Netherlands.

Bert, J.L., and Pinder, K.L. (1982). Analog simulation of the human microvascular exchange system. Simulation, 39(3), 89-95.

Bigelow, J.H., DeHaven, J.C., and Shapley, M.L. (1973). Systems analysis of the renal function. J. Theoret. Biol., 41,287-322.

Blaine, E.H., Davis, J.O., and Harris, P.D. (1972). A steady-state control analysis of the Renin-Angiotensin-Aldosterone system. Circ. Res., 30, 713-30.

Box, G.E.P., and Jenkins, G.M. (1976). Time Series Analysis. Forecasting and Control. San Francisco. Holden-Day 2nd edn.

Boyers, D.G., Cuthbertson, J.G., and Luetscher, J.A. (1972). Simulation of the human cardiovascular system: A model with normal response to posture, blood loss, transfusion and autonomic blockade. Simulation, 18, 197-206.

Brackett, N.C., Cohen, J.J., and Schwartz, W.B. (1965). Effect of increasing degrees of acute hypercapnia on acid-base equilibrium. New Eng. J. Med., 272(1), 6-12.

Brown, T.A., Roberts, F.S., and Spencer, J. (1972). Pulse Processes on Signed Digraphs: A Tool for Analyzing Energy Demand. R-926-NSF, The Rand Corporation, Santa Monica, California.

Cage, P.E., Carson, E.R., and Britton, K.E. (1977). A model of the human renal medulla. Comput. Biomed. Res., 10, 561-84.

Cameron, W.H. (1977). A model framework for computer simulation of overall renal function. J. Theoret. Biol., 66, 551-72.

Carson, E.R., Cobelli, C., and Finkelstein, L. (1983). Mathematical Modelling of Metabolic and Endocrine Systems: Model Formulation, Identification and Validation. New York: Wiley.

Carson, E.R., Cramp, D.G., Flood, R.L., and Leaning, M.S. (1985). A mathematical model of fluid-electrolyte dynamics for clinical application. IEEE 7th Annual Conference on Frontiers of Engineering and Health Care. New York: IEEE.

Chatfield, C. (1980). The Analysis of Time Series. London. Chapman and Hall, 2nd edn.

Checkland, P. (1984). Systems Thinking, Systems Practice. Chichester: Wiley.

Coleman, T.G., Bower, J.D., and Guyton, A.C. (1970). Chronic hemodialysis and circulatory function. Simulation, 15, 222-228.

Cramp, D.G., and Carson, E.R. (1981). The dynamics of short-term blood glucose regulation, in: Cobelli, C., and Bergman, R.N. (eds), Carbohydrate Metabolism. Chichester: Wiley, pp349-68.

Cramp, D.G., and Carson, E.R. (1985). Design requirements for a user-friendly computer aided decision support system in laboratory medicine. Proc. 2nd IFAC Conference on Analysis, Design and Evaluation of Man-Machine Systems, Oxford: Pergamon.

Cramp, D.G. Carson, E.R., and Leaning, M.S. (1985). Some design features for a user-friendly computer-aided decision support system incorporating mathematical models, in : Artificial Intelligence in Medicine, Amsterdam: North Holland.

Cunningham, D.J., Hey En., Patrick, J.M., and Lloyd, B.B. (1963). The effect of noradrenaline infusion on the relation between pulmonary ventilation and the alveolar PO2 and PCO2 in man. Ann. N.Y. Acad. Sci. 109: 756-71.

Curthoys, N.P., and Lowry, O.H. (1973). Glutamate and glutamine distribution in the rat nephron in Acidosis and Alkalosis. Am. J. Physiol. 224, 884-9.

de la Salle, S., Leaning, M.S., Carson, E.R., Edwards, P.R., and Finkelstein, L. (1985). Control system modelling of hormonal dynamics in the management of thyroid disease. Proc. 9th IFAC Congress, Oxford: Pergamon.

du Bois, D., and du Bois, E.F. (1916). A formula to estimate the approximate surface area if height and weight be known. Arch. Intern. Med., 17, 863-71.

Dean, R.F.A., and McCance, R.A. (1949). J. Physiol. Lond., 109, 25.

Defares, J.G., Derksen, H.E., and Duyff, J.W. (1960). Acta. Pysiol. Pharmacol. Neerlandica, 9, 327.

DeHaven, J.C., and Shapiro, N.Z. (1967). On the control of urine formation. Supplementum ad Nephron, 4, 1-63.

DeHaven, J.C., and Shapiro, N.Z. (1970). Simulation of renal effects of antidiuretic hormone (ADH) in man. J. Theoret. Biol., 28, 261-286.

Deland, E.C. (1971). The classical structure of blood chemistry, in: Alfred Benzon Foundation Symposium IV. Oxygen Affinity of Hemoglobin and the Red Cell Acid-Base Status, Munksgaard, Copenhagen.

Deland, E.C. (1975). Classic electrolyte distribution and tranposrt-mathematical principles. Adv. Pathology, 1, 21-28.

Deland, E.C., and Bradham, G.B. (1966). Fluid balance and electrolyte distribution in the human body. Ann. N.Y. Acad. Sci., 128, 795-809.

Deland, E.C., Dell, R.B., and Ramakrishnan, R. (1978). Simulation and research models as teaching tools, in: Deland, E.C. (ed), Information Technology in Health Science Education. New York: Plenum.

Deland, E.C., Wintress, R.W., Dell, R.B., and Zuckerman, A. (1972). Fluidmod: A versatile CAI system for medical students, in: 1st USA-Japan Computer Conference, Tokyo. American Federation of Information Processors Society.

Dick, D.E. (1968). A Hybrid Computer Study of Major Transients in the Canine Cardiovascular System. PhD dissertation. Madison: University of Wisconsin.

Dickinson, C.J. (1977). A Computer Model of Human Respiration. Lancaster: MTP Press Limited.

Dickinson, C.J., and Shephard, P. (1971). A digital computer model of the systemic circulation and kidney, for studying renal and circulatory interactions involving electrolytes and body fluid compartments ('Macpee'). J. Physiol., 216, 11-12.

Diem, K., and Lenter, C. (1970). Documenta Geigy, 7th edn. Basle: J.R. Geigy S.A., pp 255.

Dunn, M.J. (1973).Ouablin-uninhibited sodium transport in human erythrocytes. Evidence against a second pump. J. Clin. Invert 52, 658-70.

Regulation of Water and Electrolytes

Elkington, J.R. (1960). Circulation, 21, 1184-92.

Emery, B., Moran, F., and Pack, A. (1971). A ventilation drive simulation of pulmonary gas exchange in man. Proc. Physiol. Soc., 222, 38P-39P.

Eykhoff, P. (1974). Systems Identification and State Estimation. Chichester: Wiley.

Fadali, M.S., Steadman, J.W., and Jacqust, R.G. (1979). Control of blood volume and extracellular fluid osmolality in humans. Biomed. Sci. Instrum., 15, 67-71.

Fincham, W.F. (1963). A Study of the Mechanicms Regulating the Composition of the Human Blood by means of an Electrical Analogue Computer. PhD thesis, London: University of London.

Finkelstein, L., and Carson, E.R. (1985). Mathematical Modelling of Dynamic Biological Systems. 2nd ed. Letchworth: Research Studies Press.

Flood, R.L., Carson, E.R., Leaning, M.S., and Cramp, D.G. (1984a). Fluid-electrolyte and acid-base balance: A pragmatic review of extant mathematical models. MIM/RLF-ERC-MSL-DGC/1. London. The City University.

Flood, R.L., Carson, E.R., Leaning, M.S., and Cramp, D.G. (1984b). The control of body fluid volume in man: a mathematical modelling approach. 2nd Colloquium on Theoretical Biology and Medicine, Angers, France, September.

Flood, R.L., Carson, E.R., Leaning, M.S., and Cramp, D.G. (1985a). Clinical time-series analysis, modelling and recursive estimation, in: Billing, S.A., and Young, P. (eds), Proc. 7th IFAC Symposium on Identification and System Parameter Estimation. Oxford: Pergamon.

Flood, R.L., Cramp, D.G., Leaning, M.S., and Carson, E.R. (1985b). MFAB: A complex mathematical model of the fluid-electrolyte, acid-base dynamics. (To be published).

Flood, R.L., Leaning, M.S., Cramp, D.G., and Carson, E.R. (1985c). A complex model of the fluid-electrolyte acid-base (FAB) system: Mathematical realisation. MIM/RLF-MSL-DGC-ERC/2. London: The City University.

Gardner, M.L.G. (1978). Medical Acid-Base Balance The Basic Principles. London: Cassell Ltd.

Gray, J.S. (1945). The multiple factor theory of respiratory regulaiton. AAF School of Aviation Medicine, report no. 386(1).

Grodins, F.S., and James, G. (1963). Mathematical models of respiratory regulation. Ann. N.Y. Acad. Sci., 109, 852-868.

Grodins, F.S., Buell, J., and Bart, A.J. (1967). Mathematical analysis and digital simulation of the respiratory control system. J. Appl. Physiol., 22, 260-276.

Groth, T.L. (1985). The role of biodynamic models in computer-aided diagnosis, in: Carson, E.R., and Cramp, D.G. (eds), Computers and Control in Clinical Medicine. New York: Plenum.

Guyton, A.C. (1976). Textbook of Medical Physiology. New York: W.B. Saunders and Co.

Guyton, A.C., and Coleman, T.G. (1967). Long term regulation of the circulation: interrelationships with body fluid volume, in: Reeve, E.B., and Guyton, A.C. (eds), Physical Bases of Circulatory Transport: Regulation and Exchange. Philadelphia: W.B. Saunders and Co.

Guyton, A.C., Coleman, T.G., and Granger, H.J. (1972). Circulation: Overall regulation. Annu. Rev. Physiol., 34, 13-46.

Hinds, C.J., Ingram, D., Adams, L., Cole, P.V., Dickinson, C.J., Kay, J., Krapez, J.R., and Williams, J. (1980). An evaluation of the clinical potential of a comprehensive model of human respiration in artificially ventillated patients. Clin. Sci., 58, 83-91.

Horgan, J.D., and Lange, R.L. (1963). IEEE Intl. Conv. Rec., pp 149-157.

Hume, R. (1966). Prediction of lean body mass from height and weight. J. Clin. Path., 19, 389-91.

Hume, R., and Weyers, E. (1971). Relationship between total body water and surface area in normal and obese subjects. J. Clin. Path., 24, 234-38.

Ikeda, N., Marumo, F., Shirtataka, M., and Sato, T. (1979). A model of overall regulation of body fluids. Ann. Biomed. Eng., 7, 135-66.

Jenkins, G. (1983). Reflections on Management Science. J. Appl. Syst. Anal., 10, 15-39.

Kohn, M.C., and Chiang, E. (1982). Metabolic network sensitivity analysis. J. Theoret. Biol., 98, 109-26.

Kohn, M.C., and Garfinkel, D. (1978). Computer simulation of entry into glycolysis and lactate output in the ischemic rat heart. J. Mol. Cell. Cardio., 10(9), 79-96.

Kohn, M.C., and Letzkus, W. (1983). A graph-theoretical analysis of metabolic regulation. J. Theoret. Biol., 100, 293-304.

Kohn, M.C., Achs, M.J., and Garfinkel, D. (1979). Computer simulation of metabolism in pyruvate-perfused rate heart. II. Krebs cycle. Am. J. Physiol., 237 (3), R159-66.

Koshikawa, S., Yoshitoshi, Y., Maeda, T., and Schimizu, K. (1964). Shindan to Chiryo, 39, 1691.

Koushanpour, E., and Stipp, G.K. (1982). Mathematical simulation of the body fluid regulating system in dog. J. Theoret. Biol., 99, 203-235.

Koushanpour, E., Tarcia, R.R., and Stevens, W.F. (1971). Mathematical simulation of normal nephron function in rat and man. J. Theoret. Biol., 31, 177-214.

Kuroda, E., Fujii, K., Higuchi, M., Sato, T., Imamura, M., and Kajiya, F. (1980). [A mathematical model of the body fluid control system]. Iyodenshi to Seitai Kagoku, 18, 194-200. (In Japanese).

Landis, E.M., and Pappenheimer, J.R. (1963). Exchange of substances through the capillary walls, in: Hamilton, W.F., and Dow, P. (eds), Handbook of Physiology, Section II: Circulation. Washington D.C.: American Physiological Society.

Leaning, M.S. (1980). The Validity and Validation of Mathematical Models. PhD thesis, London: City University.

Leaning, M.S. (1984). Unpublished notes.

Leaning, M.S., Flood, R.L., Cramp, D.G., and Carson, E.R. (1985). A system of models for fluid-electrolyte dynamics. Trans. Biomed. Eng. (In press).

Ljung, L. (1979). Asymptomatic behaviour of the Extended Kalman Filter as parameter estimator for linear systems. IEEE Trans. Automat. Contr., AC-24, 36-50.

Lote, C.J. (1982). Principles of Renal Physiology. London: Croom Helm Ltd.

Magee, B. (1979). Popper. Glasgow: Fontana.

Marver, D., and Kokko, J.P. (1983). Renal target sites and the mechanism of action of Aldosterone. Min. Elect. Metab., 9, 1-18.

Mcleod, J. (1965). PHYSBE-A physiological simulation benchmark experiment. Simulation, 7, 324-29.

Meredith, J.F. (1957). An Investigation of the Mechanisms Maintaining Sodium and Water Balance in Animals. PhD thesis, Durham: University of Durham.

Merletti, R., and Weed, H.R. (1972). Mathematical description of the body fluid control system. Proc. 5th IFAC Conf. Paris, 25.1, 1-19.

Milhorn, H.T., Benton, R., Ross, R., and Guyton, A.C. (1965). A mathematical model of the human respiratory control system. Biophys. J., 5, 27-46.

Millerschoen, N.R., and Riggs, D.S. (1969). Homeostatic control of plasma osmolality in dog and the effect of ethanol. Am. J. Physiol., 217, 431-37.

M'Pherson, P.K. (1974). A perspective on Systems Science and Systems Philosophy. Futures, June, 219-239.

Murray-Smith, D.J., and Pack, A.I. (1974). Dynamic modelling of respiratory gas exchange for clinical applications. Clin. Sci. Mod. Med., 46, 26P-27P.

Nadler, S.B. Hidalgo, J.U., and Block, T. (1962). Prediction of blood volume in normal human adults. Surgery, 51, 224-232.

Nagasaka, M., Schimizu, K., Maeda, T., Yoshitoshi, Y., Koshikawa, S., and Suzuki, K. (1969). Control of body fluid volume regarded as a feedback system. Med. Biol. Eng., 4, 567-574.

Nelson, C.R. (1973). Applied Time-Series Analysis for Managerial Forecasting. San Francisco: Holden-Day.

Noordergraaf, A., Jager, G.N., and Westerhof, N. (eds). (1963). Circulatory Analog Computers. North Holland: Amsterdam.

Pace, W.H. (1961). An Analogue computer model for the study of water and electrolyte flows in the extracellular and intracellular fluids. I.R.E. Trans Biomed. Elect., 8, 29-33.

Pace, N., and Rathbun, E.H. (1945). Studies on body composition; body water and chemically combined nitrogen content in relation to fat content. J. Biol. Chem., 158, 685-91.

Perez, G.O., Lespier, L., Knowles, R., Oster, J.R., and Vaamonde, C.A. (1977). Potassium homeostasis in chronic diabetes mellitus. Arch. Internal Med., 137, 1018-1022.

Peterson, J.L. (1977) ACM Com. Surveys, 9, 223.

Pope, C.M., Carson, E.R., and Cramp, D.G. (1983). A systems analysis of the laboratory in the diagnosis and management of liver disease. DSS/CMP-ERC-DGC/233. London: The City University.

Price, W.L. (1971). Graphs and Networks - An Introduction. London: Butterworth.

Pullen, H.E. (1976). Studies in the Modelling and Simulation of the Human Cardiovascular System with application to the Effects of Drugs. PhD thesis, London: The City University.

Reeve, E.B., and Chen, Y. (1973). Studies with a mass balance method of measuring fibrinogen synthesis, in: Protein Turnover, Cuba Foundation Symposium. North Holland: Amsterdam.

Reeve, E.B., and Kulhanek, L. (1967). Regulation of body water content: a preliminary analysis, in: Reeve, E.B., and Guyton, A.C. (eds), Physical Bases of Circulatory Transport: Regulation and Exchange. Philadelphia: Saunders W.B.

Retzlaff, J.A., Tauxe, W.N., Kiely, J.M., and Stroebel, C.F. (1969). Erythrocyte volume, plasma volume and lean body mass in adult men and women., Blood, 33, 649-61.

Reynolds, P.A. (1980). An Introduction to International Relations, 2nd ed. New York: Longman Inc.

Robertson, G.L. (1983). Thirst and vasopressin in normal and disordered states of water balance. J. Lab. Clin. Med., 101(3), 351-371.

Rossing, N. (1978). Intra- and extravascular distribution of albumin and immunoglobulin in man. Lymphology, 11, 138-42.

Sato, T., Yamashiro, S.M., Vega, D., and Grodins, F.S. (1974). Parameter sensitivity analysis of a network of systematic circulatory mechanics. Ann. Biomed. Eng., 2, 289-306.

Smith, K. (1980). Fluid and Electrolytes: A Conceptual Approach. Edinburgh: Churchill Livingstone.

Staff of the Division of Pathology. (1979). Practical Notes on Hospital Pathology. London: Royal Free Hospital Group.

Steinkamp, R.C., Cohen, N.L., Gaffey, W.R., McKey, T., Bron, G., Siri, W.E., Sargent, T.W., and Isaacs, E. (1965). Measures of body fat and related factors in normal adults. II. A simple clinical method to estimate body fat and lean body mass. J. Chron. Dis., 18, 1291-307.

Talbot, N.B., Richie, R.H., and Crawford, J.D. (1959). Metabolic Homeostasis. A Syllabus for those Concerned with the Care of Patients. Cambridge, Massachusetts: Harvard University Press.

Thoma, J.U. (1975). Introduction to Bond Graphs and their Applications. New York: Pergamon.

Toates, F.M., and Oatley, K. (1970). Computer simulation of thirst and water balance. Med. Biol. Eng., 8, 71-87.

Toates, F.M., and Oatley, K. (1977). Control of water excretion by antidiuretic hormone: some aspects of modelling the system. Med. Biol. Eng. Comput., 15, 579-88.

Uttamsingh, R.J. (1981). A Systems Approach to Renal Dialysis. PhD thesis, London: The City University.

Verney, E.G. (1948). The antidiuretic hormone and the factors which determine its release. Proc. Roy. Soc., Series B, 25-106.

Yates, F.E. (1978). Complexity and the limits to knowledge. Am. J. Physiol., 4, R201-R204.

Yoshitoshi, Y., and Nagasaka, M. (1962). Mod. Med. Osaka, 17, 1575.

Yoshitoshi, Y., Maeda, T., Nagasaka, M., and Koshikawa, S. (1955). Jap. Circul. J., 19, 206.

Young, P. (1974). Recursive approaches to time series analysis. Bulletin Institute of Mathematics and its Applications, 10, 209-224.

APPENDIX 1

THEORY RELATED TO ACID-BASE DYNAMICS

A comprehensive reading on this topic is available from Gardner (1978).

A buffer solution is one which will restrict a change in pH when an acid or a base is added. An acid is a proton donor, that is, anything which dissociates into one or more protons plus a conjugate base:

$$\text{acid} \rightleftharpoons \text{proton} + \text{conjugate base.}$$

A base is a proton acceptor, that is, anything which can combine with a proton to form a conjugate acid:

$$\text{base} + \text{proton} \rightleftharpoons \text{conjugate acid.}$$

The equilibrium position of any reaction can be described quantitatively by an equilibrium constant K.

If in equilibrium:

$$A + B \rightleftharpoons C + D$$

then:

$$K = \frac{[C].[D]}{[A].[B]}$$

so that:

$$pK = \frac{1}{\log K} = -\log K$$

which is a convenient way of representing K, as typical K values are very small. Similarly,

$$pH = \frac{1}{\log [H^+]} = -\log [H^+].$$

The lower the pK the stronger the acid. A useful combination of these equations has been derived and is known as the Henderson-Hasselbalch equation:

$$pH = pK + \log \frac{[base^-]}{[acid]}$$

A buffer functions best when $\frac{[base^-]}{[acid]} = 1$, that is, when the pH is close to the buffer's pK value.

APPENDIX 2

THEORY RELATED TO SIGNED-DIGRAPHS

A comprehensive account of graph-theory is available in Price (1971).

NOTATION

A digraph D has a set of V vertices and a binary relation E on V called the relation of adjacency. If xEy then there is a directed edge from x to y. A signed-digraph consists of a digraph together with an assignment of a sign, + or -, to each directed edge.

Consider a sequence of vertices x_1, x_2, x_3, ..., x_n and $\forall_i$, $x_i E x_{i+1}$, then the sequence is a path if the vertices are distinct, and a cycle if in addition $x_n E x_i$. The sign of a sequence is the product of the sign of its edges and the length of a sequence is n-1.

STRUCTURING CAPACITY

A signed-digraph is a compact structured representation of a less structured conceptual model which may be either sentential or merely a set of thoughts or ideas. The structuring capacity of the method is apparent when converting the information contained within the signed-digraph back to spoken/written language, where a strict grammatical format is attained. For instance, 'a rise/fall in plasma volume will cause a rise/fall in arterial pressure'.

PARTS OF A GRAPH

If a graph is G:

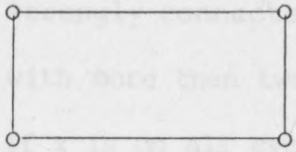

then a subgraph of G is:

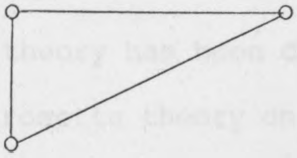

and a partial graph of G is:

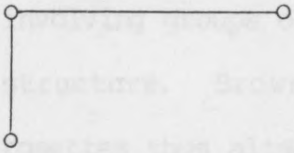

CONNECTIVITY

A digraph is strongly connected if for every pair of vertices v and t, v is reachable from t and t is reachable from v. It is unilateral if 'and' from above is replaced by 'or.' It is weakly connected if every pair of vertices is merely joined (without consideration of directedness). An ordinal scale representation of this is:

connected of degree 0 if disconnected

conencted of degree 1 if weak

connected of degree 2 if unilateral

connected of degree 3 if strong

ROSETTES

A digraph D(V,E) is a rosette if V > 1 and D is a single cycle or is strongly connected and has exactly one node x, the central node with more than two edges incident to it. D is an advanced rosette if x is on all cycles.

Rosettes have been introduced because a substantial amount of theory has been developed for these special cases. The use of rosette theory on complex systems has generally been contrived. For example, Brown et al (1972) analysed signed-digraphs of energy demand all of which were developed through a lengthy process involving groups of experts and none of which were of the rosette structure. Brown converted many of these signed-digraphs to rosettes thus altering the structure and inherent control features and hence the analysis lost relevance to the experts efforts.

The need for a signed-digraph analysis has already been stated but in short relates to complexity. As one of the main phenomena leading to complexity is asymmetry (Yates, 1978) it seems highly unlikely that rosette theory will have any relevance to physiological-biochemical systems.

PULSE PROCESSES

The emphasis of this theory is on stability, structure and control. The theory relating to pulse processes is drawn from Brown et al (1972) with some development added for the sake of clarity.

Suppose each vertex attains a value $V_i(t)$ at times t=0,1,2,.... The value $V_i(t+1)$ is determined from $V_i(t)$, from the pulse $P_i^o(t+1)$ introduced at vertex x_i at time t+1, and from the information about whether other vertices x_j adjacent to x_i went 'up or down' at the last time period, that is,

$$V_i(t+1) = V_i(t)+P_i^o(t+1)+ \Sigma_j \text{sgn}(x_j,x_i)P_j(t) \tag{A2.1}$$

where;

$$\text{sgn}(x_j,x_i) = \left.\begin{array}{l} +1 \text{ if } x_j,x_i \text{ is +ve} \\ -1 \text{ if } x_j,x_i \text{ is -ve} \\ 0 \text{ if there is no edge } x_j,x_i \end{array}\right\} \tag{A2.2}$$

and;

$$P_j(t) = \left.\begin{array}{ll} V_j(t)-V_j(t-1) & \text{if } t > 0 \\ P_j^o(0) & \text{if } t = 0 \end{array}\right\} \tag{A2.3}$$

so that $P_j(t)$ is the pulse at vertex x_j at time t. A pulse process is defined by an initial vector of values

$$V(0) = (V_1(0), V_2(0),...., V_n(0)) \tag{A2.4}$$

and by the vectors giving the outside pulse introduced at each node at each time period;

$$\underline{P}^o(t) = (P_1^o(t),P_2^o(t),....,P_n^o(t)) \tag{A2.5}$$

with the pulse vector;

$$\underline{P}(t) = (P_1(t),P_2(t),...,P_n(t)) \tag{A2.6}$$

The pulse at vertex x_j at time t is given by the ij entry of A^t, while the value at node xj at time t is given by the ij entry of $A+A^2+....+A^t$, where A is the signed adjacency matrix;

$$A = (a_{ij}), \qquad a_{ij} = \text{sgn}(x_i,x_j) \tag{A2.7}$$

If;

$$S = A^T \tag{A2.8}$$

then

$$\underline{P}(t) = S^{t-T}\underline{P}(T) \quad t > T \geq 0 \tag{A2.9}$$

$$\underline{V}(t)=\underline{P}(t-1)+P(t-1+1)+....+P(t) \tag{A2.10}$$

Stability in a system is assessed by:

(a) pulse stability if x_j under $P_j(t)$ is bounded in absolute value and;

(b) value stability if $V_j(t)$ is bounded in absolute value.

The theory described by Brown and coworkers can be described more clearly and efficiently by writing a set of coupled ordinary first order linear differential equations;

$$\left.\begin{aligned} \dot{x}_1 &= k_1x_1 + k_2x_2 + ... + k_nx_n \\ \dot{x}_2 &= l_1x_1 + l_2x_2 + ... + l_nx_n \\ \dot{x}_3 &= m_1x_1 + m_2x_2 + ... + m_nx_n \end{aligned}\right\} \tag{A2.11}$$

so that pulse stability relates to the vector $\dot{\underline{X}}$ and value stability to the vector $\underline{X}$ and the constants k_i, l_i and m_i are the values associated with the signed adjacency matrix. This set of equations can be simulated on a computer using a first order Euler integration routine.

APPENDIX 3

EQUATION REPRESENTATION OF THE SIGNED-DIGRAPHS OF FIGURES 4.1-4.

The set of differential equations representing the signed-digraph of Figure 4.1 is:

$$\dot{x}_1 = -x_2+x_9+x_{20}+x_{24}$$

$$\dot{x}_2 = x_4-x_5-x_6+x_7$$

$$\dot{x}_3 = x_2-x_9-x_{11}+x_{12}-x_{15}+x_{16}$$

$$\dot{x}_4 = x_1$$

$$\dot{x}_5 = x_3$$

$$\dot{x}_6 = -x_1$$

$$\dot{x}_7 = -x_3$$

$$\dot{x}_8 = x_5$$

$$\dot{x}_9 = x_8$$

$$\dot{x}_{10} = x_{11}+x_{15}$$

$$\dot{x}_{11} = -x_{10}-x_{13}+x_{14}$$

$$\dot{x}_{12} = -x_3+x_{13}-x_{14}+x_{21}-x_{22}$$

$$\dot{x}_{13} = x_{11}-x_{12}$$

$$\dot{x}_{14} = x_{13}$$

$$\dot{x}_{15} = -x_{10}+x_{17}-x_{18}$$

$$\dot{x}_{16} = -x_3-x_{17}+x_{18}+x_{25}-x_{26}$$

$$\dot{x}_{17} = -x_{15}+x_{16}$$

$$\dot{x}_{18} = x_{17}$$

$$\dot{x}_{19} = x_{12} - x_{20}$$

$$\dot{x}_{20} = -x_1 - x_{21} + x_{22}$$

$$\dot{x}_{21} = -x_{19}$$

$$\dot{x}_{22} = x_{19}$$

$$\dot{x}_{23} = x_{16} - x_{24}$$

$$\dot{x}_{24} = -x_1 - x_{25} + x_{26}$$

$$\dot{x}_{25} = -x_{23}$$

$$\dot{x}_{26} = x_{23}$$

The set of differential equations representing the signed-digraph of Figure 4.2 is:

$$\dot{x}_1 = x_{11}$$

$$\dot{x}_2 = x_{11}$$

$$\dot{x}_3 = x_2$$

$$\dot{x}_4 = x_3$$

$$\dot{x}_5 = x_4$$

$$\dot{x}_6 = x_5$$

$$\dot{x}_7 = x_2 + x_6$$

$$\dot{x}_8 = x_7$$

$$\dot{x}_9 = x_{10} - x_{14}$$

$$\dot{x}_{10} = x_1$$

$$\dot{x}_{11} = -x_9 + x_{12}$$

$$\dot{x}_{12} = x_{13}$$

$$\dot{x}_{13} = -x_{11}+x_{15}$$

$$\dot{x}_{14} = x_{13}$$

$$\dot{x}_{15} = -x_{8}-x_{16}+x_{18}$$

$$\dot{x}_{16} = x_{17}$$

$$\dot{x}_{17} = x_{2}+x_{6}$$

$$\dot{x}_{18} = x_{19}$$

$$\dot{x}_{19} = -x_{11}$$

The set of differential equations representing the signed-digraphs of Figure 4.3 is:

$$\dot{x}_{1} = x_{15}$$

$$\dot{x}_{2} = x_{10}$$

$$\dot{x}_{3} = x_{2}+x_{4}-x_{10}$$

$$\dot{x}_{4} = x_{5}$$

$$\dot{x}_{5} = x_{6}$$

$$\dot{x}_{6} = x_{7}$$

$$\dot{x}_{7} = x_{11}$$

$$\dot{x}_{8} = x_{4}+x_{10}$$

$$\dot{x}_{9} = -x_{8}$$

$$\dot{x}_{10} = x_{1}-x_{14}$$

$$\dot{x}_{11} = x_{9}+x_{12}$$

$$\dot{x}_{12} = -x_3$$

$$\dot{x}_{13} = x_{12}$$

$$\dot{x}_{14} = -x_9+x_{12}$$

$$\dot{x}_{15} = -x_{13}$$

The set of differential equations representing the signed-digraphs of Figure 4.4 is:

$$\dot{x}_1 = x_2$$

$$\dot{x}_2 = -x_1$$

$$\dot{x}_3 = x_2-x_4-x_6-x_7$$

$$\dot{x}_4 = x_5$$

$$\dot{x}_5 = -x_4$$

$$\dot{x}_6 = 0$$

$$\dot{x}_7 = x_3+x_{12}$$

$$\dot{x}_8 = x_3-x_9+x_{11}$$

$$\dot{x}_9 = x_8+x_{10}$$

$$\dot{x}_{10} = -x_9$$

$$\dot{x}_{11} = x_6$$

$$\dot{x}_{12} = -x_7$$

APPENDIX 4

THEORY RELATED TO ARIMA MODELLING AND TRANSFER FUNCTION MODELLING

Introductory texts on ARIMA and Transfer Function modelling include Chatfield (1980), Nelson (1973), however the comprehensive book of Box and Jenkins (1976) is very accessible.

VARIANCE AND COVARIANCE

Take n samples of x_i and y_i, i=1 to n, the mean values are:

$$\bar{x} = \sum_i^n x_i/n; \quad \bar{y} = \sum_i^n y_i/n \qquad \text{(A4.1;A4.2)}$$

the variances are:

$$\sigma_x^2 = \sum_i^n (x_i - \bar{x})^2/n; \quad \sigma_y^2 = \sum_i^n (y_i - \bar{y})^2/n \qquad \text{(A4.3;A4.4)}$$

and the covariances are:

$$\sigma_{xy}^2 = \sum_i^n (x_i - \bar{x})(y_i - \bar{y})/n \qquad \text{(A4.5)}$$

STATIONARITY

Strict stationarity is defined by the following equation:

$$p(x_t,\ldots,x_{t+k}) = p(x_{t+m},\ldots,x_{t+k+m}) \qquad \text{(A4.6)}$$

where p( ) is a probability density function. If a time-series is stationary then it is not dependent on t and it will remain in the space in the neighbourhood of the mean value.

AUTCORRELATION

Autocovariance (the prefix auto is used because it is the covariance between different observations in the same series) is defined by:

$$\gamma_j = C(x_t, x_{t+j}) \qquad \text{(A4.7)}$$

where C relates to covariance. This is equivalent to:

$$\gamma_j = E[(x_t - Ex_t)(x_{t+j} - Ex_{t+j})] \qquad \text{(A4.8)}$$

where E relates to the expected value. These will be positive if a higher/lower than average observation is followed by a higher/lower than average observation j periods later. Alternatively they will be negative if a higher/lower than average observation is followed by a lower/higher than average observation. Therefore a series of negative values implies a regular passage over the mean, whereas a series of positive values implies lengthy excursions away from the mean.

The autocorrelation function is:

$$\left.\begin{aligned} \rho_o &= \frac{\gamma_o}{\gamma_o} = 1 \\ \rho_1 &= \frac{\gamma_1}{\gamma_o} \\ \rho_2 &= \frac{\gamma_2}{\gamma_o} \\ &\text{etc.....} \end{aligned}\right\} \qquad \text{(A4.9)}$$

CORRELOGRAM

Is a graph of the autocorrelation function. If C_j is the estimate of γ_j, that is:

$$C_j = \frac{1}{n} \sum_{t=1}^{T} \left[(x_t - \bar{x})(x_{t+j} - \bar{x})\right] \quad j < 1,2,3 \ldots. \qquad \text{(A4.10)}$$

then r_j is the sample correlogram:

$$r_j = \frac{C_j}{C_o} \qquad j = 1,2,3... \qquad \text{(A4.11)}$$

which provides the basis for choice of an appropriate moving average model.

Distinguishing what is important from what is not in a sample correlogram can be done by a test of statistical significance of the sample autocorrelation. This is done by using Bartlett's formula so that a standard error for r_j is given by:

$$SE(r_j) = \frac{1}{\sqrt{n}}\left(1+2\sum_{n=1}^{q} r_i^2\right)^{\frac{1}{2}} \qquad j > q \qquad \text{(A4.12)}$$

Note, about 5% of autocorrelation coefficients will show spurious significance.

PARTIAL AUTOCORRELATION

With the estimates of r_j, the Yule-Walker equations can be written:

$$\left.\begin{aligned} r_1 &= \phi_1 + \phi_2 r_1 + \ldots + \phi_p r_{p-1} \\ &\vdots \qquad\qquad \vdots \\ r_p &= \phi_1 r_{p-1} + \phi_2 r_{p-2} + \ldots + \phi_p \end{aligned}\right\} \qquad \text{(A4.13)}$$

so that estimates of the ϕ_j can be made resulting in the set of $\hat{\phi}_j . \hat{\phi}_{jj}$ denotes the value of $\hat{\phi}_j$ implied for the solution of the system for p=j and $\hat{\phi}_{jj}$ are referred to as the estimated partial autocorrelations. If the time order of the autoregression is p^* then:

$$\hat{\phi}_{jj} \simeq 0 \qquad j > p \qquad \text{(A4.14)}$$

ANALYSIS OF NON-STATIONARY TIME SERIES

Differencing is an important filter in that the differences of many non-stationary series are stationary.

MOVING AVERAGE PROCESS

A moving average process occurs when $\Theta_i=0$ for $i>q$ in the following equation:

$$x_t = \mu+U_t-\theta U_{t-1}- \ldots . -\theta_q U_{t-q} \qquad \text{(A4.15)}$$

where μ and Θ are fixed parameters and the time series $(\ldots,U_{t-1},U_t,\ldots)$ is a sequence of identically and independently distributed random disturbances with mean zero and variance σ_u^2, often referred to as white noise because the observations are a moving average in the disturbances reaching back q periods. This is therefore in terms of the current disturbance and all past disturbances.

AUTOREGRESSIVE PROCESS

An autoregressive process is in terms of the current disturbance and all past observations:

$$x_t = \emptyset_1 x_{t-1}+\emptyset_2 x_{t-2}+\ldots+\emptyset_p x_{t-p}+ \delta + U_t \qquad \text{(A4.16)}$$

The term autoregressive comes from the fact that (A4.16) is essentially a regression equation in which x_t is related to its own past values instead of to a set of independent variables.

ARIMA PROCESS

An autoregressive integrated moving average process is a natural extension to the above processes. A given observation in a time-series generated by an ARIMA(p,d,q) process may be expressed in terms of past observation of order p, and current and past disturbances of order q, where the series has been filtered by differencing d times to give stationarity:

$$x_t = (1+\phi_1)x_{t-1}+(\phi_2-\phi_1)x_{t-2}+ \ldots . +(\phi_p-\phi_{p-1})-$$

$$\phi_p x_{t-p-1}+\mu+U_t-\theta_1 U_{t-1}- \ldots . - \theta_q U_{t-q} \qquad \text{(A4.17)}$$

INVERTIBILITY

Invertibility requires that the coefficients on past disturbances become small as i gets large and do so rapidly enough so that $\sum_{i=1}^{\infty} \pi_i$ converges (π is for coefficients in general), that is, the coefficients sum to less than unity.

T-RATIO

The t-ratio is the null hypothesis that

$\beta_i^* = 0$, that is:

$$\text{Prob}\left(-1.96 < \frac{\hat{\beta}_i-\beta_i}{SD(\beta_i)} < 1.96\right) \qquad \text{(A4.18)}$$

for a 95 percent confidence, where SD is standard deviation and $\hat{\beta}_i$ is the parameter estimate. If the t-ratio $\geq |1|$, β_i is said to be significantly different from zero.

CONFIDENCE INTERVAL

The 95 percent confidence interval is defined by:

$$\hat{\beta}_i-1.96SD(\hat{\beta}_i)<\beta_i<\hat{\beta}_i+1.96SD(\hat{\beta}_i) \qquad \text{(A4.19)}$$

METHODOLOGY FOR ARIMA MODELLING AND THE IDENTIFICATION OF THE APPROPRIATE MINITAB FACILITIES

MINITAB is a statistical software package developed at Pond Laboratory, University Park, PA16802, USA. The methodology for ARIMA modelling was developed by Box and Jenkins (1976) and has three stages: identification; estimation; diagnostic checking.

Identification consists of selecting tentative classes of (p,d,q) model and making preliminary estimates of the ϕ_j and θ_j parameters (refer to Table A4.1). Identification, which is largely subjective, relies on the estimated autocorrelation function, r_j, and the estimated partial autocorrelation function $\hat{\phi}_{jj}$. The MINITAB facilities useful for identification are:

DESCribe - simple descriptive statistics.

LAG - sets one time-series, the same values, n lags behind the donor statistics: especially for seasonal models.

ACF - helps identify stationarity/non-stationarity; degree of differencing required; identification of the order of the moving average process.

PACF - identification of the autoregressive process.

DIFF - finds difference of time-series.

In estimation, the model parameters for a given (p,d,q) model are estimated, the maximum likelihood estimation is often used. The MINITAB facilities for estimation are:

ARIMA - using the information from the identification stage, this estimates the parameters of the model.

STORAGE - stores information about ARIMA.

CONSTANT - places a constant on ARIMA.

STARTING - allows initial parameter estimates to be entered by user.

Class of processes	*Autocorrelations*	*Partial autocorrelations*
Moving average	Spikes at lags 1 through q, then cut off	Tail off
Autogressive	Tail off according to $\rho_j = \phi_1\rho_{j-1} + \ldots + \phi_p\rho_{j-p}$	Spikes at lags 1 through ρ, then cut off
Mixed autoregressive-moving average	Irregular pattern at lags 1 through q, then tail off according to $\rho_j = \phi_1\rho_{j-1} + \ldots + \phi_p\rho_{j-p}$	Tail off

Table A 4.1 Characetristic behaviour of autocorrelations and partial autocorrelations for three classes of processes (Source: Nelson, 1973)

The validity of the final model is assessed in diagnostic checking, where the whiteness of the residuals and the significance of adding AR or MA terms are considered. The MINITAB facility is:

ARIMA - (see above)

In addition to this, MINITAB has the facility to forecast an ARIMA model and gives confidence limits using FORECAST.

CROSS-CORRELATION

Cross-correlation is achieved in a similar way to equation (A4.5) for the covariance and (A4.9) for the autocorrelation function. The cross-correlation function for a bivariate process is defined by:

$$\gamma_{xy}(j) = E\left[(x_t-\mu_x)(x_{t+j}-\mu_x)\right] \qquad \text{(A4.20)}$$

and hence the cross correlation coefficient at lag j is:

$$\rho_{xy}(j) = \frac{\gamma_{xy}(j)}{\sigma_x \sigma_y} \qquad \text{(A4.21)}$$

TRANSFER FUNCTION MODELLING

The idea of Transfer Function (TF) modelling is to produce a combined transfer function-noise model of the form:

$$y_t = \delta^{-1}(B)\ \omega(B) x_{t-b} + N_t \qquad \text{(A4.22)}$$

where; x_t and y_t are the input and output series respectively, $\delta(B) = 1-\delta_1 B-\delta_2 B^2-\ldots-\delta_r B^r$ and $\omega(B) = \omega_0-\omega_1 B-\ldots-\omega_s B^s$ are polynomials of orders r and s, r is the left hand operator, s is the right hand operator, b is the delay parameter (or "dead time"), N_t is the noise component, B is the backward shift operator. This

is based on the linear general model for representing continuous dynamic systems:

$$(1+\Xi_1 D+ \ldots +\Xi_R D^R)Y(t) = g(1+H_1 D+ \ldots +H_s D^s)X(t-\Gamma) \qquad \text{(A4.23)}$$

which in the case of discrete dynamic systems has the general linear difference equation:

$$(1+\zeta_1 \nabla+ \ldots +\zeta_r \nabla^r)y_t = g(1+\eta_1 \nabla+ \ldots +\eta_s \nabla^s)x_{t-b} \qquad \text{(A4.24)}$$

a transfer function of order r,s. This can be written as:

$$\delta(B)y_t = \omega(B)x_{t-b} \qquad \text{(A4.25)}$$

If it is known that the input is variable then x_t and y_t are deviations at t from equilibrium, thus the inertia of the system can be represented by the general linear filter:

$$\left.\begin{aligned} y_t &= \nu_o x_t + \nu_1 x_{t-1} + \nu_2 x_{t-2} + \ldots \\ &= (\nu_o + \nu_1 B + \nu_2 B + \ldots)x_t \\ &= \nu(B)x_t \end{aligned}\right\} \qquad \text{(A4.26)}$$

so that the transfer function of the model may be written as:

$$\nu(B) = \delta^{-1}(B)\,\omega(B) \qquad \text{(A4.27)}$$

which is the ratio of two polynomials.

(A4.28)

As in ARIMA stochastic models, stability has to be considered, thus the roots of $\delta(B) = 0$ must lie outside of the unit circle.

APPENDIX 5

RECURSIVE ESTIMATION OF TRANSFER FUNCTION AND PHYSIOLOGICALLY-BASED MODELS

The following theory is based on Young (1974).

TRANSFER FUNCTION MODELS

The aim is to set a cost function J and minimise the loss with respect to $\underline{a}$ the vector of model parameters. Figure A5.1 shows the cost function as an assumed parabola such that if the gradient is positive a value to correct the parameters must be deducted, and if the gradient is negative a value to correct the parameters must be added.

The cost function is:

$$J \triangleq \sum_{i=1}^{k} \left[\underline{X}_i^T \hat{\underline{a}} - y_i \right]^2 \qquad \text{(A5.1)}$$

where: $\underline{X}_i$ is a vector of past observations and past inputs, and $y_i = \underline{X}_i^T \underline{a} + \varepsilon_{yi}$ with ε_{yi} as an error term. Minimising (A5.1) with respect to $\underline{a}$ gives:

$$\nabla_{\hat{a}} (J_1) = \left[\sum_{i=1}^{k} \underline{X}_i \underline{X}_i^T \right] \hat{\underline{a}} - \sum_{i=1}^{k} \underline{X}_i y_i = 0 \qquad \text{(A5.2)}$$

which is better shown as:

$$\begin{bmatrix} \Sigma x_1 x_1 & \Sigma x_1 x_2 \cdots & \Sigma x_1 x_n \\ \vdots & \Sigma x_2 x_2 \cdots & \Sigma x_2 x_n \\ \Sigma x_n x_1 & \Sigma x_n x_2 \cdots & \Sigma x_n x_n \end{bmatrix} \begin{bmatrix} a_1 \\ \vdots \\ a_n \end{bmatrix} - \begin{bmatrix} \Sigma x_1 y \\ \vdots \\ \Sigma x_n y \end{bmatrix} = 0 \qquad \text{(A5.3)}$$

where y is a scalar. This can be represented by:

$$M.\hat{\underline{a}} = b \qquad \text{(A5.4)}$$

so that:

$$\hat{\underline{a}} = M^{-1}.b \qquad \text{(A5.5)}$$

To achieve $\hat{\underline{a}}$, a matrix inversion at every k is necessary. To find a recursive form without inversion it can be noted that:

$$M_k = \sum_{i=1}^{k-1} \underline{X}(i)\underline{X}(i)^T + \underline{X}(k)\underline{X}(k)^T \qquad \text{(A5.6)}$$

which can be rewritten as:

$$M_k = M_{k-1} + \underline{X}(k)\underline{X}(k)^T \qquad \text{(A5.7)}$$

and similarly:

$$b_k = b_{k-1} + \underline{X}_k y_k \qquad \text{(A5.8)}$$

Details of matrix manipulation in Eykhoff (1974) lead to the following expression:

$$M = M^{-1} - M^{-1}\underline{X}[I+\underline{X}^T M^{-1}\underline{X}]^{-1}\underline{X}^T M^{-1} \qquad \text{(A5.9)}$$

which can be rewritten as:

$$M = M^{-1} - M^{-1}\underline{X}[1+\underline{X}^T M^{-1}\underline{X}]^{-1}\underline{X}^T M^{-1} \qquad \text{(A5.10)}$$

that is:

$$M_k = M_{k-1} - M_{k-1}\underline{X}_k[1+\underline{X}_k^T M_{k-1}\underline{X}_k]^{-1}\underline{X}_k^T M_{k-1} \qquad \text{(A5.11)}$$

Therefore, using the error covariance matrix defined by:

$$M_k^* = \sigma^2 M_k \qquad \text{(A5.12)}$$

where; σ^2 is the variance of the sequence of errors; the following two equations can be drawn up for the recursive estimation:

$$\hat{\underline{a}}_k = \hat{\underline{a}}_{k-1} - \frac{M_k^*}{\sigma^2}[\underline{X}_k\underline{X}_k^T\hat{\underline{a}}_{k-1} - \underline{X}_k y_k] \qquad \text{(A5.13)}$$

and:

$$M_k^* = M^*_{k-1} - M^*_{k-1}\underline{X}_k[\sigma^2+\underline{X}_k^T M_{k-1}\underline{X}_k]^{-1}\underline{X}_k^T M^*_{k-1} \qquad \text{(A5.14)}$$

where; $[\sigma^2+\underline{X}_k^T M_{k-1}\underline{X}_k]$ is simply a scalar quantity so that there is no need for direct matrix inversion.

STATE-SPACE MODELS

Considering a continuous-time stochastic system described by the following state-space differential equation:

$$\dot{\underline{X}} = A\underline{X}+B\underline{U}+D\underline{\zeta} \qquad \text{(A5.15)}$$

where; dot notation represents differentiation with respect to time, $\underline{X}$ is an n dimensional state vector, U is a l dimensional vector of inputs, $\underline{\zeta}$ is an m dimensional vector of zero mean white noise disturbances representing model uncertainty and system (patient) variability. A, B and D are nxn, nxq and nxm matrices respectively. The model (clinical) outputs may be represented by:

$$\underline{Y}_k = C\underline{X}_k+\underline{\eta}_k \qquad \text{(A5.16)}$$

where; $\underline{Y}$ is an n dimensional observation vector, $\underline{n}$ is an n dimensional vector of white measurement noises, and C is a pxn observation matrix.

A situation may arise where some of the parameters of A and/or B are unknown, but where both the system states and the unknown parameters require estimation. The solution to the problem lies in the knowledge of the input vector $\underline{U}$ and discrete observations of the system behaviour taken from (A5.16).

One approach is the Extended Kalman Filter (EKF), where the state vector is augmented with the unknown parameters $\underline{a}$. The augmented state vector thus becomes:

$$\underline{X} = \begin{bmatrix} \underline{X} \\ \hline \underline{a} \end{bmatrix} \qquad \text{(A5.17)}$$

If the parameters are all assumed to be time invariant then $\dot{\underline{a}} = [0]$.

The initial prediction is of the form:

$$\hat{\underline{X}}_{k|k-1} = \hat{\underline{X}}_{k-1} + \int_{t_{k-1}}^{t_k} \underline{f}(\hat{\underline{X}}_{k-1}, U)\,dt \qquad \text{(A5.18)}$$

with the covariance P:

$$P_{k|k-1} = \underline{\Phi}_k P_{k-1} \underline{\Phi}_k^T + Q \qquad \text{(A5.19)}$$

where; $\underline{\Phi}_k$ is the linear state transition matrix from t_{k-1} to t_k :

$$\underline{\Phi}_k \triangleq e^{F\Delta t} = I + F_k \Delta t + F_k^2 \frac{\Delta t^2}{2} + \ldots + F_k^n \frac{\Delta t^n}{n!} \qquad \text{(A5.20)}$$

where Δt is the sampling interval and F_k is the Jacobian matrix with elements $\frac{\partial f_i}{\partial x_j}$ (evaluated at $\hat{\underline{X}}_{k-1}$) and n is chosen to assure satisfactory convergenece. Q is the discrete time covariance matrix of $\underline{\zeta}$.

The second stage of correction is of the form:

$$\hat{\underline{X}}_k = \hat{\underline{X}}_{k\ k-1} + K_k (\underline{Y}_k - \underline{g}(\hat{\underline{X}}_{k|k-1})) \qquad \text{(A5.21)}$$

where; K_k is the Kalman gain matrix:

$$K_k = P_{k|k-1} C_k^T (C_k P_{k|k-1} C_k^T + R)^{-1} \qquad \text{(A5.22)}$$

with R being the covariance matrix of the output noise $\underline{n}_k$. The linearised output matrix C_k has elements $\frac{\partial y_i}{\partial x_j}$ (evaluated at $\hat{\underline{x}}_{k-1}$).

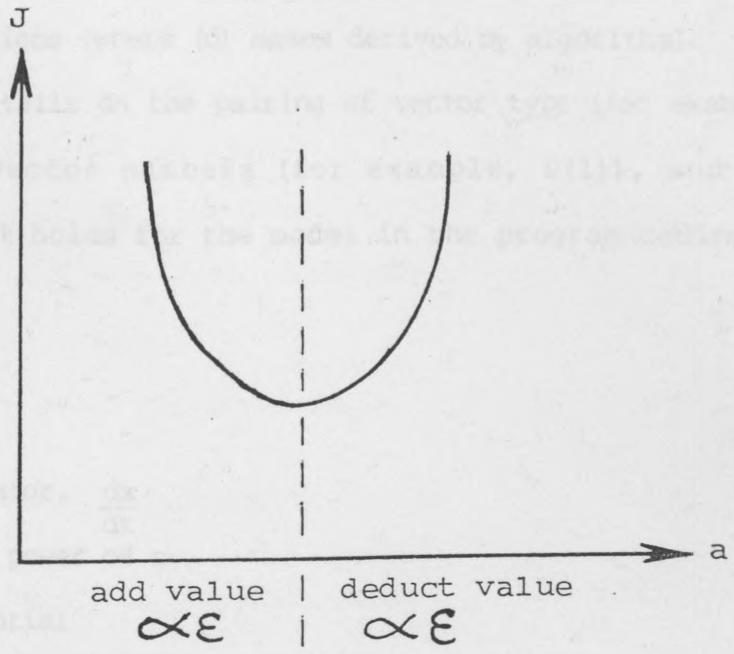

Figure A5.1 Assumed parabular shape of a cost function J.

APPENDIX 6

NOMENCLATURE OF MFAB

The functions and nomenclature of MFAB (presented in Chapter 7) are detailed below in alphabetical order, including normal steady-state value, and dimensions (where (d) means derived by algorithm). This is followed by details on the pairing of vector type (for example, P, X, A) with vector numbers (for example, P(1)), and the representation it holds for the model in the program coding of Appendix 7.

FUNCTIONS

D(x)	D operator, $\frac{dx}{dt}$
↑n	to the power of n
DEXP	exponential
LOG10	log to the base of 10
SQRT	square root
1EN	times ten to the power of N

NOMENCLATURE *

Symbolic represen-	description	steady-state value	dimensions
AADH	ADH antagonist	1	AU
AALD	Aldosterone antagonist	1	AU
ABCA	Calcium absorbed by GI system	0.007	mM min^{-1}
		or 3.36	mM $8hr^{-1}$
ABCL	Chloride absorbed by GI system	0.1328	mM min^{-1}
		or 57.744	mm $8hr^{-1}$
ABHPO4	Phosphate absorbed by GI system	0.025	mM min^{-1}
		or 12.0	mM $8hr^{-1}$

* Note: insensible loss rate of analytes should be added to the respective intake rates.

ABK	Potassium absorbed by GI system		0.047	mM min^{-1}
		or	22.56	mM $8hr^{-1}$
ABMG	Magnesium absorbed by GI system		0.008	mM min^{-1}
		or	3.84	mM $8hr^{-1}$
ABNA	Sodium absorbed by GI system		0.12	mM min^{-1}
		or	57.6	mM $8hr^{-}$
ABW	Water absorbed by GI system		0.001	l min^{-1}
		or	0.48	l $8hr^{-1}$
ADH1	State of ADH metabolism		0	AU
ADH2	Normalised ADH effector		1	AU
ALD1	State of aldosterone metabolism		0	AU
ALD2	Normalised aldosterone effector		1	AU
ANCO	Starling curve shifter		(d)	AU
APCA	Calcium actual potential across membrane		(d)	AU
APK	Potassium actual potential across membrane		(d)	mv
APMG	Magnesium actual potential across membrane		(d)	mv
APNA	Sodium actual potential across membrane		(d)	mv
CA	Compliance in arteries		(d)	mmHg
CAEC	Extracellular 'charge'		0	mEq
CAIC	Intracellular 'charge'		0	mEq
CAM	Cation flow across membrane		0	mEq min^{-1}
CAME	Combined factors for deriving extracellular anion flux		0	AU
CAMI	Combined factors for deriving intracellular anion flux		0	AU
CFC	Capillary filtration coefficient		0.0066	AU
CFR	Capillary filtration rate		0.002	l min^{-1}
CGL1	First constant of glucose metabolism		1	AU

CGL2	Second constant of glucose metabolism	1	AU
CGL3	Third constant of glucose metabolism	0.03	AU
CH	Intra-extracellular 'charge' imbalance	0	mEq
CI	Cardiac index	(d)	$l\ min^{-1}\ m^{-2}$
CLANE	Chloride fraction of extracellular anions	0.8	AU
CLANI	Chloride fraction of intracellular anions	0.18	AU
CO	Cardiac output	(d)	$l\ s^{-1}$
CPISF	Ratio of VISF by it's steady-state	1	AU
CRA	Compliance in right atrium	0.005	l mmHg
CV	Compliance in veins	(d)	l mmHg
DNK	Potassium excreted from distal nephron	0.121	$mM\ min^{-1}$
DNNA	Sodium excreted from distal nephron	1.17	$mM\ min^{-1}$
DTU	Water load passing to distal nephron	0.01	$l\ min^{-1}$
ECA	Extracellular calcium content	(d)	mM
ECL	Extracellular chloride content	(d)	mM
EGL	Extracellular glucose content	(d)	g
EGLKI1	First glucose metabolic effector on D(IK)	0	AU
EGLKI2	Second glucose metabolic effector on D(IK)	0	AU
EHCO3	Extracellular bicarbonate content	(d)	mM
EHPO4	Extracellular phosphate content	(d)	mM
EK	Extracellular potassium content	(d)	mM
EMG	Extracellular magnesium content	(d)	mM
ENA	Extracellular sodium content	(d)	mM
EOSM	Extracellular osmolality	287	$mM\ l^{-1}$

EPAVR	PHA effector on VR	1	AU
EPCO2VR	PCO2 effector on VR	1	AU
FA	Flow in arteries	(d)	$l\ s^{-1}$
FALBC	Albumin flow from capillaries	0.04	$g\ min^{-1}$
FALBLY	Albumin flow from lymphatic system	0.04	$g\ min^{-1}$
FC	Flow in capillaries	(d)	$l\ s^{-1}$
FV	Flow in veins	(d)	$l\ s^{-1}$
GFR1	VEC effect on GFR	0.1	$l\ min^{-1}$
GFR2	PA effect on GFR	1	AU
GFR3	Actual GFR	0.1	$l\ min^{-1}$
GFR4	GFR including THDF	0.02	$l\ min^{-1}$
GLA	Glucose effector on D(IK)	0	AU
GLA1	Constant associated with glucose metabolism	108	AU
GLW	Gastrointestinal water loss	0	$l\ min^{-1}$
HCO3ANE	Bicarbonate fraction of extracellular anions	0.19	AU
HCO3ANI	Bicarbonate fraction of intracellular anions	0.39	AU
HPO4ANE	Phosphate fraction of extracellular anions	0.01	AU
HPO4ANI	Phosphate fraction of intracellular anions	0.43	AU
HS	Heart strength	1	AU
HT	Height	Variable	cm
ICA	Intracellular calcium content	(d)	mM
ICL	Intracellular chloride content	(d)	mM
IHCO3	Intracellular bicarbonate content	(d)	mM
IHPO4	Intracellular phosphate content	(d)	mM
IK	Intracellular potassium content	(d)	mM
IMG	Intracellular magnesium content	(d)	mM

INA	Intracellular sodium content	(d)	mM
IOSM	Intracellular osmolality	287	mM l^{-1}
ISALB	Interstitial albumin content	(d)	g
KCH	Constant related to CH	0.01	AU
KCP	Constant related to Pc	5.9286	AU
LHK	Potassium excreted from loop of Henle	0.045	mM min^{-1}
LHNA	Sodium excreted from loop of Henle	1.4	mM min^{-1}
LPDRALB	Liver production/destruction rate of albumin	0.00027	AU min^{-1}
LRR	Lymphatic return rate	0.002	l min^{-1}
MAC	Molecular attraction coefficient	0.9288	AU
MDUHCO3	Modified bicarbonate excretion rate	2.4	mM min^{-1}
MPCO2	Metabolic production rate of CO_2	10.42	mM min^{-1}
MPHCO3	Metabolic production rate of HCO_3^-	0.015	mM min^{-1}
MPUR1	Protein effector for urea production rate	1	AU
MPUR2	Metabolic production rate of urea	0.15	mM min^{-1}
MPW	Metabolic production rate of water	0.0005	l min^{-1}
MUHCO3	Modifier to bicarbonate excretion	1	AU
NCRCLIO	Normalised conc. ratio chloride I/O	1	AU
NCRCLOI	Normalised conc. ratio chloride O/I	1	AU
NCRHCO3IO	Normalised conc. ratio bicarbonate I/O	1	AU
NCRHCO3OI	Normalised conc. ratio bicarbonate O/I	1	AU
NCRHPO4IO	Normalised conc. ratio phosphate I/O	1	AU
NCRHPO4OI	Normalised conc. ratio phosphate O/I	1	AU
NCSF	Net capillary Starling force	0.3	mmHg
NTRALB	Net turnover rate albumin in liver	0	g min^{-1}

OLRR	Occlusion to lymphatic return rate	1	AU
PA	Arterial pressure	100	mmHg
PALB	Plasma albumin content	(d)	g
PC	Capillary pressure	17	mmHg
PCO2	Partial pressure of CO_2	40	mmHg
PDCA	Potential disequilibirum for calcium	1	AU
PDK	Potential disequilibrium for potassium	1	AU
PDMG	Potential disequilibrium for magnesium	1	AU
PDNA	Potential disequilibrium for sodium	1	AU
PGAV	Pressure gradient arteries-veins	97	mmHg
PGVRA	Pressure gradient veins-right atrium	3	mmHg
PHA	pH of blood	7.4	AU
PHAA	State of pH effector on UTA	7.4	AU
PHU	pH of urine	6	AU
PHUA	State of PHU effector on UNH4	6	AU
PIC	Intracellular protein 'charge'	(d)	mv
PICO	Interstitial colloid osmotic pressure	5	mmHg
PISF	Interstitial fluid pressure	-6.3	mmHg
PPCA	Pump potential for calcium	(d)	mv
PPCO	Plasma colloid osmotic pressure	28	mmHg
PPK	Pump potential for potassium	(d)	mv
PPMG	Pump potential magnesium	(d)	mv
PPNA	Pump potential sodium	(d)	mv
PRA	Right arterial pressure	0	mmHg
PTK	Potassium excreted from proximal tubule	0.09	mM min^{-1}

PTNA	Sodium excreted from proximal tubule	2.8	mM min^{-1}
PV	Venous pressure	3	mmHg
RA	Resistance in arteries	(d)	mmHg l^{-1}min
RV	Resistance in veins	(d)	mmHg l^{-1}min
RWL	Respiratory water loss	0.0005	l min^{-1}
SA	Surface area	variable	m^2
SICL	Insensible chloride loss	0.0072	mM min^{-1}
SIGL	Rate of glucose intake	0	g min^{-1}
SIK	Insensible potassium loss	0.006	mM min^{-1}
SINA	Insensible sodium loss	0.0072	mM min^{-1}
SINI	Intravenous insulin input	0	mM min^{-1}
SIWI	Intravenous water input	0	l min^{-1}
SIWL	Insensible water loss	0.0003	l min^{-1}
SSAPCA	Steady-state APCA	(d)	mv
SSAPK	Steady-state APK	(d)	mv
SSAPMG	Steady-state APMG	(d)	mv
SSAPNA	Steady-state APNA	(d)	mv
SSCRIOCL	Steady-state conc. ratio chloride I/O	(d)	AU
SSCRIOHCO3	Steady-state conc. ratio bicarbonate I/O	(d)	AU
SSCRIOHPO4	Steady-state conc. ratio phosphate I/O	(d)	AU
SSCROICL	Steady-state conc. ratio chloride O/I	(d)	AU
SSCROIHCO3	Steady-state conc. ratio bicarbonate O/I	(d)	AU
SSCROIHPO4	Steady-state conc. ratio phosphate O/I	(d)	AU
SSECO2	Steady-state excretion rate CO_2	10.42	mM min^{-1}
SSGFR	Steady-state GFR	0.1	l min^{-1}

SSICA	Steady-state calcium intracellular content	(d)	mM
SSIK	Steady-state potassium intracellular content	(d)	mM
SSIMG	Steady-state magnesium intracellular content	(d)	mM
SSINA	Steady-state sodium intracellular content	(d)	mM
SSLRR	Steady-state lymphatic return rate	0.002	1 min^{-1}
SSMPHCO3	Steady-state metabolic production bicarbonate	0.015	mM min^{-1}
SSMPUR	Steady-state metabolic production urea	0.15	mM min^{-1}
SSPALB	Steady-state plasma albumin content	(d)	g
SSPCO2	Steady-state partial pressure of carbon dioxide	40	mmHg
SSPHA	Steady-state pH blood	7.4	AU
SSPGLOB	Steady-state plasma globulin content	(d)	g
SSRWL	Steady-state respiratory water loss	0.0005	1 min^{-1}
SSUNH4	Steady-state ammonium excretion	0.024	mM min^{-1}
SSUTA	Steady-state titratable acid excretion	0.0068	mM min^{-1}
SSVECF	Steady-state volume extracellular fluid	(d)	l
SSVISF	Steady-state volume interstitial fluid	(d)	l
TBW	Total body water	(d)	l
TCADH	Time constant ADH targetting	15	min
TCALD	Time constant aldosterone targetting	30	min
TCCA	Transfer coefficient EC $\leftrightarrow$ IC ions	0.004	AU
TCEI	Transfer coefficient EC $\leftrightarrow$ H_2O	0.0003	AU
THDF	Third Factor	1	AU
TOTANE	Total anion extracellular content	(d)	mEq

TOTANI	Total anion intracellular content	(d)	mEq
UALB	Urine loss albumin	0	g min^{-1}
UCA	Urine loss calcium	0.007	mM min^{-1}
UCH	Net cations in urine output	0.1328	mM min^{-1}
UCL	Urine loss of chloride	0.1328	mM min^{-1}
UFCA	Calcium content in ultrafiltrate	0.5	mM min^{-1}
UFCL	Chloride content in ultrafiltrate	10.4	mM min^{-1}
UFGL	Glucose content in ultrafiltrate	0.6	g min^{-1}
UFHCO3	Bicarbonate content in ultrafiltrate	2.4	mM min^{-1}
UFHPO4	Phosphate content in ultrafiltrate	0.11	mM min^{-1}
UFMG	Magensium content in ultrafiltrate	0.3	mM min^{-1}
UGL	Urine loss glucose	0	mM min^{-1}
UHCO3	Urine loss bicarbonate	0.015	mM min^{-1}
UHPO4	Urine loss phosphate	0.025	mM min^{-1}
UK	Urine loss potassium	0.047	mM min^{-1}
UMG	Urine loss magnesium	0.008	mM min^{-1}
UNA	Urine loss sodium	0.12	mM min^{-1}
UNH4	Urine loss ammonium	0.024	mM min^{-1}
UO	Urine output	0.001	l min^{-1}
UTA	Urine loss titratable acid	0.017	mM min^{-1}
UTA1	First stage for titratable acid 'excretion'	0.007	mM min^{-1}
UUR	Urine loss urea	0.15	mM min^{-1}
VA	Arterial volume of blood	(d)	l
VAS	Arterial stressing volume	(d)	l
VAU	Unstressed arterial volume	(d)	l
VEC	Extracellular fluid volume	(d)	l
VICF	Intracellular fluid volume	(d)	l
VISF	Interstitial fluid volume	(d)	l

VPL	Plasma volume	(d)	l
VR	Ventilation rate to unity	1	AU
VRA	Right atrial volume	(d)	l
VRAS	Right atrial stressing volume	(d)	l
VRAU	Unstressed right atrial volume	(d)	l
VV	Venous volume	(d)	l
VVS	Venous stressing volume	(d)	l
VVU	Unstressed venous volume	(d)	l
WCO2	Whole body CO_2 content	(d)	l
WT	Weight	variable	kg
WTKALD	Weight of ZEK on aldosterone release	0.5	AU
WTNALD	Weight of LHNA on aldosterone release	0.1	AU
WTOSADH	Weight of EOSM on aldosterone release	0.5	AU
WTPAADH	Weight of PA on ADH release	1	AU
WTPAALD	Weight of PA on aldosterone release	0.001	AU
WUR	Whole body urea content	(d)	mM
ZECA	Extracellular calcium conc.	5	mM l^{-1}
ZECL	Extracellular chloride conc.	104	mM l^{-1}
ZEGL	Extracellular glucose conc.	6	mM l^{-1}
ZEHCO3	Extracellular bicarbonate conc.	24	mM l^{-1}
ZEHPO4	Extracellular phosphate conc.	1.1	mM l^{-1}
ZEK	Extracellular potassium conc.	4.5	mM l^{-1}
ZEMG	Extracellular magnesium conc.	3	mM l^{-1}
ZENA	Extracellular sodium conc.	140	mM l^{-1}
ZICA	Intracellular calcium conc.	0.45	mM l^{-1}
ZICL	Intracellular chloride conc.	4	mM l^{-1}

ZIHCO3	Intracellular bicarbonate conc.	9	mM l^{-1}
ZIHPO4	Intracellular phosphate conc.	10	mM l^{-1}
ZIK	Intracellular potassium conc.	140	mM l^{-1}
ZIMG	Intracellular magnesium conc.	30	mM l^{-1}
ZINA	Intracellular sodium conc.	9	mM l^{-1}
ZPLPR	Plamsa protein conc.	70	g l^{-1}
ZISALB	Interstitial albumin conc.	20	g l^{-1}
ZPALB	Plasma albumin conc.	40	g l^{-1}
ZWCO2	Whole body carbon dioxide conc.	25	mM l^{-1}
ZWUR	Whole body urea conc.	25	mM l^{-1}

EXPLANATION OF VECTORS FROM MFAB CODING (IN APPENDIX 7)

State variables: X( )

1. VICF	2. VISF	3. VA
4. VV	5. VRA	6. ENA
7. EK	8. ECL	9. EHCO3
10. EMG	11. ECA	12. EHPO4
13. INA	14. IK	15. ICL
16. IHCO3	17. IMG	18. ICA
19. IHPO4	20. WUR	21. PALB
22. ISALB	23. WCO2	24. PHAA
25. PHUA	26. ADH1	27. ALD1
28. EGL	29. GLA	

Computed variables: P( )

1. VB	2. FA	3. FC
4. FV	5. CO	6. PA
7. PGAV	8. PGVRA	9. PRA
10. PV	11. VAS	12. VRAS

13. VVS	14. VPL	15. ZENA
16. ZEK	17. ZECL	18. ZEHCO3
19. ZEMG	20. ZECA	21. ZEHPO4
22. ZINA	23. ZIK	24. ZICL
25. ZIHCO3	26. ZIMG	27. ZIHPO4
28. ZWUR	29. ZPALB	30. ZISALB
31. ZPLPR	32. EOSM	33. IOSM
34. CFR	35. LRR	36. UO
37. RWL	38. NCSF	39. PISF
40. PC	41. PICO	42. PPCO
43. CPISF	44. VR	45. UNA
46. UK	47. UCL	48. UHCO3
49. UMG	50. UCA	51. UHPO4
52. UUR	53. ZICA	54. PDNA
55. APNA	56. PPNA	57. CAIC
58. CAEC	59. CH	60. PDK
61. APK	62. PPK	63. PDMG
64. APMG	65. PPMG	66. PDCA
67. APCA	68. PPCA	69. ZWCO2
70. EPAVR	71. EPCO2VR	72. MPUR1
73. MPUR2	74. ZEGL	75. CAM
76. NCRCLOI	77. NCRCLIO	78. NCRHCO3OI
79. NCRHCO3IO	80. NCRHPO4OI	81. NCRHPO4IO
82. TOTANI	83. TOTANE	84. CLANI
85. CLANE	86. HCO3ANI	87. HCO3ANE
88. HPO4ANI	89. HPO4ANE	90. GFR1
91. GFR2	92. GFR3	93. GFR4
94. THDF	95. DTU	96. ALD2

97. UFHPO4	98. UFCA	99. UFMG
100. UFHCO3	101. MUHCO3	102. MDUHCO3
103. PTK	104. LHK	105. DNK
106. PTNA	107. LHNA	108. DNNA
109. NRAS	110. UFCL	111. UCH
112. UTA1	113. UTA	114. UNH4
115. ADH2	116. ALD2	117. PCO2
118. PHA	119. PHU	120. FALBLY
121. NTRALB	122. FALBC	123. UALB
124. EGLKI1	125. EGLKI2	126. UGL

Parameters: A( )

1. CA	2. CRA	3. CV
4. HS	5. RA	6. RV
7. VAU	8. VRAU	9. VVU
10. ANCO	11. VRBC	12. ABW
13. ABNA	14. ABK	15. ABCL
16. ABMG	17. ABCA	18. ABHPO4
19. IFEED	20. IVOM	21. SIWL
22. MPW	23. SIWI	24. SSRWL
25. SSVISF	26. KCP	27. CFC
28. SSLRR	29. SSMPHCO3	30. SSMPUR
31. IDIAR	32. SSPGLOB	33. SINA
34. SIK	35. SICL	36. TCEI
37. MAC	38. OLRR	39. SSINA
40. TCCA	41. SSAPNA	42. KCH
43. PIC	44. SSIK	45. SSAPK
46. SSIMG	47. SSAPMG	48. SSICA
49. SSAPCA	50. SSGFR	51. SSVECF

52. SSUTA	53. SSUNH4	54. WTOSADH
55. WTPAADH	56. TCADH	57. AADH
58. WTKALD	59. WTPAALD	60. WTNALD
61. TCALD	62. AALD	63. SSCRIOCL
64. SSCRIOHCO3	65. SSCRIOHPO4	66. SSCROICL
67. SSCROIHCO3	68. SSCROIHPO4	69. MPCO2
70. SSECO2	71. SSPHA	72. SSPCO2
73. LPDRALB	74. GLA1	75. SINI
76. CGL1	77. CGL2	78. CGL3
79. SIGL	80. TPRINT	

Note. The following two computed variables are used in the coding of MFAB but are not shown in the description of MFAB in Chapter 7.

NRAS Net rate of acid secretion

VB Blood volume (including VRBC; volume of the red blood cells).

In addition, the following parameters are used during simulation of MFAB as coded in Appendix 7.

IDIAR Logic switch to impose diarrohea

IFEED Logic switch to impose feed

IVOM Logic switch to impose vomitting

TPRINT Frequencey of results in form of tables (mins)

Other important symbolic codings are:

ITH Hour counter

ITM Minute counter

ITS Second counter

IPOKE Next entry to POKER subroutine counter.

The following print out gives: the patient-related algorithm output for state variables X(I), computed variables, P(I), and parameters, A(I), of a 70 Kg, 30 year old, 170 cm man (see overleaf).

INITIAL CONDITIONS INITIAL CONDITIONS INITIAL CONDITIONS INITIAL CONDITIONS INITIAL CONDITIONS INITIAL CONDITIONS

AGE 29 YRS HEIGHT 170 CMS WEIGHT 70 KGS

COMPUTED VARIABLES

5.20080	P 1	0.09221	P 2	0.09221	P 3	0.09221	P 4	0.09221	P 5	100.00000	P 6
97.00000	P 7	3.00000	P 8	0.00000	P 9	3.00000	P 10	0.43442	P 11	0.00000	P 12
0.37206	P 13	3.20080	P 14	140.00000	P 15	4.50000	P 16	104.00000	P 17	24.00000	P 18
3.00000	P 19	5.00000	P 20	1.10000	P 21	9.00000	P 22	140.00000	P 23	4.00000	P 24
9.00000	P 25	30.00000	P 26	10.00000	P 27	2.50000	P 28	40.00000	P 29	20.00000	P 30
70.00000	P 31	287.00000	P 32	287.00000	P 33	0.00200	P 34	0.00200	P 35	0.00100	P 36
0.00050	P 37	0.30000	P 38	-6.30000	P 39	17.00000	P 40	5.00000	P 41	28.00000	P 42
1.00000	P 43	1.00000	P 44	0.12000	P 45	0.04700	P 46	0.13280	P 47	0.01500	P 48
0.00800	P 49	0.00700	P 50	0.02500	P 51	0.15000	P 52	0.45000	P 53	1.00000	P 54
72.70502	P 55	72.70502	P 56	0.00000	P 57	0.00000	P 58	0.00000	P 59	1.00000	P 60
-91.06786	P 61	-91.06786	P 62	1.00000	P 63	-30.50000	P 64	-30.50000	P 65	1.00000	P 66
31.89560	P 67	31.89560	P 68	25.00000	P 69	1.00000	P 70	1.00000	P 71	1.00000	P 72
0.15000	P 73	6.00000	P 74	0.00000	P 75	1.00000	P 76	1.00000	P 77	1.00000	P 78
1.00000	P 79	1.00000	P 80	1.00000	P 81	570.54236	P 82	1962.81006	P 83	0.17391	P 84
0.80558	P 85	0.39130	P 86	0.18590	P 87	0.43478	P 88	0.00832	P 89	0.10000	P 90
1.00000	P 91	0.10000	P 92	0.02000	P 93	1.00000	P 94	0.01000	P 95	0.00000	P 96
0.11000	P 97	0.50000	P 98	0.30000	P 99	2.40000	P100	1.00000	P101	2.40000	P102
0.09000	P103	0.04500	P104	0.12100	P105	2.80000	P106	1.40000	P107	1.17000	P108
0.01600	P109	10.40000	P110	0.13300	P111	0.00700	P112	0.01700	P113	0.02400	P114
1.00000	P115	1.00000	P116	40.00000	P117	7.40000	P118	6.00000	P119	0.04000	P120
0.00000	P121	0.04000	P122	0.00000	P123	0.00000	P124	0.00000	P125	0.00000	P126

STATE VARIABLES

24.80619	X 1	12.00300	X 2	1.04016	X 3	0.13002	X 4	4.03062	X 5	2128.53125	X 6
68.41708	X 7	1581.19482	X 8	364.89111	X 9	45.61139	X10	76.01898	X11	16.72417	X12
223.25574	X13	3472.86719	X14	99.22478	X15	223.25574	X16	744.18579	X17	11.16279	X18
248.06192	X19	100.02498	X20	128.03195	X21	240.05997	X22	1000.24976	X23	7.40000	X24
6.00000	X25	0.00000	X26	0.00000	X27	91.22278	X28	0.00000	X29		

PARAMETERS

0.00434	A 1	0.00500	A 2	0.12402	A 3	1.00000	A 4	1051.90771	A 5	32.53323	A 6
0.60574	A 7	0.13002	A 8	3.65856	A 9	1.10656	A10	2.00000	A11	0.00100	A12
0.12000	A13	0.04700	A14	0.13280	A15	0.00800	A16	0.00700	A17	0.02500	A18
0.00000	A19	0.00000	A20	0.00030	A21	0.0050	A22	0.00000	A23	0.00050	A24
12.00300	A25	5.92860	A26	0.00667	A27	0.00200	A28	0.01500	A29	0.15000	A30
1.00000	A31	96.02397	A32	0.00720	A33	0.00600	A34	0.00720	A35	0.00030	A36
0.92880	A37	1.00000	A38	223.25574	A39	0.00400	A40	72.70502	A41	0.01000	A42
4388.21484	A43	3472.86719	A44	-91.06786	A45	744.18579	A46	-30.50000	A47	11.16279	A48
31.89560	A49	0.10000	A50	15.20380	A51	0.00680	A52	0.02400	A53	0.50000	A54
1.00000	A55	15.00000	A56	1.00000	A57	0.50000	A58	0.00100	A59	0.10000	A60
30.00000	A61	1.00000	A62	0.03846	A63	0.37500	A64	9.09091	A65	26.00000	A66
2.66667	A67	0.11000	A68	10.42000	A69	10.42000	A70	7.40000	A71	40.00000	A72
0.00027	A73	108.00000	A74	0.00000	A75	1.00000	A76	1.00000	A77	0.03000	A78
0.00000	A79	10.00000	A80								

APPENDIX 7

CODING OF MFAB

See over page:

```
C*************************************************************************

(        1) C*************************************************************************
(        2) C
(        3) C       NFAB1F.FTN : A PATIENT-RELATED SIMULATION MODEL OF THE
(        4) C                    FLUID-ELECTROLYTE, ACID-BASE SYSTEM FOR
(        5) C                    NON-PAEDIATRIC PATIENTS. THIS VERSION DESIGNED
(        6) C                    TO RUN SENSITIVITY ANALYSIS.
(        7) C
(        8) C       AUTHOR     : ROBERT LOUIS FLOOD
(        9) C
(       10) C       RESEARCH   : TOWARDS THE DEGREE OF DOCTOR OF PHILOSOPHY.
(       11) C                    RESEARCHED JOINTLY AT THE CITY UNIVERSITY
(       12) C                    LONDON AND THE ROYAL FREE HOSPITAL ALSO
(       13) C                    LONDON. FUNDED BY THE SERC.
(       14) C
(       15) C       HARDWARE   : PRIME 550
(       16) C
(       17) C       LANGUAGE   : FORTRAN 4
(       18) C
(       19) C*************************************************************************
(       20) C
(       21)         REAL*4 HT,WT,TBW,AVA,AVV,SA,CI,SC
(       22)         INTEGER*2 J,K,JAGE,ISEX,ITH,ITM,ITS,IPOKE,ITT
(       23)         DIMENSION DX(29),X(29),P(126),A(80),AC(80),Z(3)
(       24)         DIMENSION XC(29),XS(29),PC(126),PS(126)
(       25)         DIMENSION POOL(7,3),PABS(7,3),PTC(7,3),PABZ(7)
(       26) C
(       27) C       READ IN DATA
(       28) C       ************
(       29) C
(       30) C       PARAMETERS
(       31) C
(       32)         DO 1000 I=1,126
(       33)         READ (6,*) P(I)
(       34) 1000    CONTINUE
(       35) C
(       36) C       CONSTANTS
(       37) C
(       38)         DO 1010 I=1,80
(       39)         READ(6,*) A(I)
(       40) 1010    CONTINUE
(       41) C
(       42) C       STATE VARIABLES (MAINLY COMPARTMENTAL VALUES)
(       43) C
(       44)         DO 1020 I=1,29
(       45)         READ(6,*)X(I)
(       46)         DX(I)=0
(       47) 1020    CONTINUE
(       48) C
(       49) C       100 MIN ALDLAY INITIAL CONDITIONS.
(       50) C
(       51)         Z(1)=100
(       52)         Z(2)=4.5
(       53)         Z(3)=1.4
(       54) C
(       55) C       PATIENT-RELATED ALGORITHM
(       56) C       *************************
(       57) C       (SEE NOTES ON P-RELATED CF P-SPECIFIC : M.S.LEANING)
(       58) C
(       59)         WRITE(1,50)
(       60)         WRITE(1,10)
```

```
C*************************************************************************
(        61)          WRITE(1,50)
(        62)          WRITE(1,20)
(        63)          WRITE(1,30)
(        64)          WRITE(1,40)
(        65)          WRITE(1,50)
(        66)  5       WRITE(1,60)
(        67)          WRITE(1,50)
(        68)  10      FORMAT('WELCOME TO THE FAR SIMULATION. ')
(        69)  20      FORMAT('THERE ARE A NUMBER OF QUESTIONS YOU WILL BE REQUIRED TO')
(        70)  30      FORMAT('ANSWER IN ORDER THAT THE COMPARTMETENTS AND THE PARAME-')
(        71)  40      FORMAT('RS OF THE MODEL MAY BE INITIALISED')
(        72)  50      FORMAT('*')
(        73)  60      FORMAT('KEY IN 1 WHEN READY TO PROCEED')
(        74)  C
(        75)          READ(1,*)J
(        76)          IF(J.NE.1)GOTO 5
(        77)  C
(        78)  C       DETERMINE PATIENTS SEX
(        79)  C
(        80)  61      WRITE(1,62)
(        81)  62      FORMAT('STATE PATIENTS SEX, M=1, F=0')
(        82)          READ(1,*)ISEX
(        83)          IF(ISEX.NE.1.AND.ISEX.NE.0)GOTO 61
(        84)  C
(        85)  C       DETERMINE PATIENTS AGE
(        86)  C
(        87)  65      WRITE(1,70)
(        88)          WRITE(1,50)
(        89)  70      FORMAT('STATE PATIENTS AGE IN WHOLE YRS.[15 YRS & OVER]')
(        90)          READ(1,*)JAGE
(        91)          IF(JAGE.GT.14)GOTO 100
(        92)          WRITE(1,80)JAGE
(        93)  80      FORMAT('PATIENT AGE =',I3,'YRS OLD.  UNDER 15 NOT ACCEPTED. ')
(        94)  85      WRITE(1,90)
(        95)          WRITE(1,50)
(        96)  90      FORMAT('KEY IN 1 TO RESTATE AGE, 0 TO LEAVE PROGRAM. ')
(        97)          READ(1,*)J
(        98)          IF(J.NE.1.AND.J.NE.0)GOTO 85
(        99)          IF(J.EQ.1)GOTO 65
(       100)          STOP
(       101)  100     CONTINUE
(       102)  C
(       103)  C       DETERMINE PATIENTS WEIGHT
(       104)  C
(       105)          WRITE(1,110)
(       106)          WRITE(1,50)
(       107)  110     FORMAT('STATE PATIENTS WEIGHT IN KGS')
(       108)          READ(1,*)WT
(       109)  C
(       110)  C       DETERMINE PATIENTS HEIGHT
(       111)  C
(       112)          WRITE(1,120)
(       113)          WRITE(1,50)
(       114)  120     FORMAT('STATE PATIENTS HEIGHT IN CMS')
(       115)          READ(1,*)HT
(       116)          WRITE(1,50)
(       117)  C
(       118)  C       PRINT PATIENT DETAILS ON VDU SO THAT USER MAY IDENTIFY ERRORS
(       119)  C
(       120)  121     IF(ISEX.EQ.1)GOTO 123
```

```
C*************************************************************************
(       121)          WRITE(1,122)
(       122) 122      FORMAT('THE FEMALE PATIENT HAS THE FOLLOWING DETAILS')
(       123)          GOTO 125
(       124) 123      WRITE(1,124)
(       125) 124      FORMAT('THE MALE PATIENT HAS THE FOLLOWING DETAILS')
(       126) 125      WRITE(1,130)JAGE,WT,HT
(       127)          WRITE(1,50)
(       128) 130      FORMAT(' AGE ',I3,' WEIGHT ',I3,' HEIGHT ',I3)
(       129)          WRITE(1,140)
(       130) 140      FORMAT('KEY IN 1 TO CORRECT DETAILS, 0 TO CONTINUE')
(       131)          READ(1,*)J
(       132)          IF(J.EQ.0)GOTO 210
(       133)          WRITE(1,150)
(       134) 150      FORMAT('IS AGE CORRECT, 1=YES, 0=NO')
(       135)          READ(1,*)J
(       136)          IF(J.EQ.1)GOTO 170
(       137)          WRITE(1,160)
(       138) 160      FORMAT('KEY IN CORRECT VALUE')
(       139) 161      READ(1,*)JAGE
(       140)          IF(JAGE.GT.14)GOTO 170
(       141)          WRITE(1,162)JAGE
(       142) 162      FORMAT('PATIENT AGE ',I3,' .UNDER 15 NOT ACCEPTED.')
(       143)          WRITE(1,163)
(       144) 163      FORMAT('RESTATE AGE')
(       145)          GOTO 161
(       146) 170      WRITE(1,180)
(       147) 180      FORMAT('IS WEIGHT CORRECT, 1=YES, 0=NO')
(       148)          READ(1,*)J
(       149)          IF(J.NE.0.AND.J.NE.1)GOTO 170
(       150)          IF(J.EQ.1)GOTO 190
(       151)          WRITE(1,160)
(       152)          READ(1,*)WT
(       153) 190      WRITE(1,200)
(       154) 200      FORMAT('IS HEIGHT CORRECT, 1=YES, 0=NO')
(       155)          READ(1,*)J
(       156)          IF(J.NE.0.AND.J.NE.1)GOTO 190
(       157)          IF(J.EQ.1)GOTO 205
(       158)          WRITE(1,160)
(       159)          READ(1,*)HT
(       160) 205      WRITE(1,202)
(       161) 202      FORMAT('IS SEX CORRECT, 1=YES, 0=NO')
(       162)          READ(1,*)J
(       163)          IF(J.NE.0.AND.J.NE.1)GOTO 205
(       164)          IF(J.EQ.1)GOTO 208
(       165)          WRITE(1,62)
(       166)          READ(1,*)ISEX
(       167)          WRITE(1,50)
(       168) 208      GOTO 121
(       169) 210      CONTINUE
(       170)          WRITE(1,50)
(       171) C
(       172) C        FORMULA TO CALCULATE TOTAL BODY FLUID FROM INFORMATION
(       173) C        PREVIOUSLY ATTAINED IN THE PROGRAM AND TO CALCULATE
(       174) C         THE INITIAL COMPARTMENTAL FLUID VOLUMES.
(       175) C
(       176)          IF(ISEX.EQ.0)TBW=-42.8+0.379*HT+0.227*WT
(       177)          IF(ISEX.EQ.1)TBW=-14.2+0.197*HT+0.296*WT
(       178)          X(1)=0.62*TBW
(       179)          X(2)=0.3*TBW
(       180)          A(25)=X(2)
```

```
C*************************************************************************
(       181)          P(14)=0.08*TBW
(       182)          P(1)=P(14)+A(11)
(       183)          A(51)=P(14)+X(2)
(       184)          X(3)=0.2*P(1)
(       185)          X(5)=0.775*P(1)
(       186)          X(4)=0.025*P(1)
(       187)          WRITE(1,220)TBW
(       188)  220     FORMAT('TOTAL BODY WATER IS ',F6.2,' LITRES DIVIDED INTO')
(       189)          WRITE(1,230)X(1)
(       190)  230     FORMAT('           ',F6.2,' LITRES INTRACELLULAR')
(       191)          WRITE(1,240)X(2)
(       192)  240     FORMAT('           ',F6.2,' LITRES INTERSTITIAL')
(       193)          WRITE(1,250)P(14)
(       194)  250     FORMAT('AND        ',F6.2,' LITRES PLASMA')
(       195)          WRITE(1,50)
(       196)  C
(       197)  C       PARAMETER VALUE SETTING IN ACCORDANCE WITH VOLUME
(       198)  C       DERIVATIONS CARRIED OUT ABOVE
(       199)  C
(       200)  C       CHANGES IN THE ARTERIAL SECTION
(       201)  C
(       202)          AVA=X(3)/0.85
(       203)          A(7)=AVA*0.495
(       204)          P(11)=X(3)-A(7)
(       205)          A(1)=P(11)/P(6)
(       206)  C
(       207)  C       CHANGES IN THE VENOUS SECTION
(       208)  C
(       209)          AVV=X(5)/3.25
(       210)          A(9)=AVV*2.95
(       211)          P(13)=X(5)-A(9)
(       212)          A(3)=P(13)/P(10)
(       213)  C
(       214)  C       CHANGES IN THE RIGHT ATRIAL SECTION
(       215)  C
(       216)          A(8)=X(4)
(       217)  C
(       218)  C       DERIVING THE APPROPRIATE CARDIAC OUTPUT AND FLOWS ACCORDING TO
(       219)  C       SEX, AGE AND SIZE.  NOTE THAT FLOWS RELATED TO THE
(       220)  C       CARDIOVASCULAR SYSTEM ARE CONVERTED TO FLOWS PER SECOND.
(       221)  C       AS RESISTANCES ARE ALSO DIMENSIONED IN UNITS PER TIME,
(       222)  C       THEY ADDITIONALLY ARE CONVERTED INTO UNITS PER SECOND.
(       223)  C
(       224)          SA=0.00718*((HT)**0.725)*((WT)**0.425)
(       225)          CI=-0.029*JAGE+3.9
(       226)          P(5)=CI*SA/60
(       227)          IF(ISEX.EQ.0)P(5)=P(5)*0.9
(       228)          A(10)=P(5)/(5.0/60.0)
(       229)          A(6)=P(8)/P(5)
(       230)          A(5)=P(7)/P(5)
(       231)          P(2)=P(5)*A(4)
(       232)          P(3)=P(7)/A(5)
(       233)          P(4)=P(8)/A(6)
(       234)  C
(       235)  C       CALCULATING COMPARTMENTAL ANALYTE CONTENTS.
(       236)  C       THE LEFT HAND VALUE IS THE STEADY STATE CONCENTRATION IN MEQ.L
(       237)  C       FOR 6-20 AND G.L FOR 21-22.
(       238)  C
(       239)          X(6)=P(15)*(X(2)+P(14))
(       240)          X(7)=P(16)*(X(2)+P(14))
```

```
C*****************************************************************
(       241)          X(8)=P(17)*(X(2)+P(14))
(       242)          X(9)=P(18)*(X(2)+P(14))
(       243)          X(10)=P(19)*(X(2)+P(14))
(       244)          X(11)=P(20)*(X(2)+P(14))
(       245)          X(12)=P(21)*(X(2)+P(14))
(       246)          X(13)=P(22)*X(1)
(       247)          X(14)=P(23)*X(1)
(       248)          X(15)=P(24)*X(1)
(       249)          X(16)=P(25)*X(1)
(       250)          X(17)=P(26)*X(1)
(       251)          X(18)=P(53)*X(1)
(       252)          X(19)=P(27)*X(1)
(       253)          X(20)=P(28)*TBW
(       254)          X(21)=P(29)*P(14)
(       255)          X(22)=P(30)*X(2)
(       256)          X(23)=P(69)*(P(14)+X(1)+X(2))
(       257)          X(28)=P(74)*(X(2)+P(14))
(       258)          A(32)=30.0*P(14)
(       259)  C
(       260)  C       SETTING VALUES INVOLVED IN TRANSMEMBRANE ION DISTRIBUTION
(       261)  C
(       262)          A(39)=X(13)
(       263)          A(44)=X(14)
(       264)          A(46)=X(17)
(       265)          A(48)=X(18)
(       266)          A(41)=-61*(DLOG10(P(22)/P(15)))
(       267)          P(55)=A(41)
(       268)          P(56)=A(41)
(       269)          A(45)=-61*(DLOG10(P(23)/P(16)))
(       270)          P(61)=A(45)
(       271)          P(62)=A(45)
(       272)          A(47)=-61*(DLOG10((SQRT(P(26)))/(SQRT(P(19)))))
(       273)          P(64)=A(47)
(       274)          P(65)=A(47)
(       275)          A(49)=-61*(DLOG10((SQRT(P(53)))/(SQRT(P(20)))))
(       276)          P(67)=A(49)
(       277)          P(68)=A(49)
(       278)          A(43)=X(13)+X(14)-X(15)-X(16)+(2*X(17))+(2*X(18))-(2*X(19))
(       279)          P(82)=X(15)+X(16)+X(19)
(       280)          P(83)=X(8)+X(9)+X(12)
(       281)          A(63)=P(24)/P(17)
(       282)          A(64)=P(25)/P(18)
(       283)          A(65)=P(27)/P(21)
(       284)          A(66)=P(17)/P(24)
(       285)          A(67)=P(18)/P(25)
(       286)          A(68)=P(21)/P(27)
(       287)  C
(       288)  C       WRITE THE INITIAL CONDITIONS
(       289)  C
(       290)          WRITE(5,1022)
(       291)  1022    FORMAT(4('*************************'))
(       292)          WRITE(5,1024)
(       293)  1024    FORMAT(6('INITIAL CONDITIONS    '))
(       294)          WRITE(5,1022)
(       295)          WRITE(5,1031)
(       296)          WRITE(5,1021)JAGE,HT,WT
(       297)          WRITE(5,1031)
(       298)  1021    FORMAT('AGE ',I2,' YRS  HEIGHT ',I3,' CMS  WEIGHT ',I3,' KGS')
(       299)          WRITE(5,1026)
(       300)  1026    FORMAT('COMPUTED VARIABLES')
```

```
C**********************************************************************
(      301)          WRITE(5,1028)
(      302)  1028    FORMAT('******************')
(      303)          WRITE(5,1030)(P(I),I,I=1,126)
(      304)  1030    FORMAT(6(F12.5,2X,'P',I3,4X))
(      305)          WRITE(5,1031)
(      306)          WRITE(5,1031)
(      307)  1031    FORMAT(' ')
(      308)          WRITE(5,1032)
(      309)  1032    FORMAT('STATE VARIABLES')
(      310)          WRITE(5,1028)
(      311)          WRITE(5,1034)(X(I),I,I=1,29)
(      312)  1034    FORMAT(6(F12.5,2X,'X',I2,5X))
(      313)          WRITE(5,1031)
(      314)          WRITE(5,1036)
(      315)  1036    FORMAT('PARAMETERS')
(      316)          WRITE(5,1028)
(      317)          WRITE(5,1038)(A(I),I,I=1,80)
(      318)  1038    FORMAT(6(F12.5,2X,'A',I2,5X))
(      319)          WRITE(5,1031)
(      320)          WRITE(5,1031)
(      321)          WRITE(5,1031)
(      322)          WRITE(5,1031)
(      323)          WRITE(5,1022)
(      324)  C
(      325)  C       SETTING AC(I), A FIXED VECTOR HOLDING THE INITIAL
(      326)  C       VALUES OF THE CONSTANT PARAMETERS, FOR THE CURRENT PATIENT.
(      327)  C       SIMILARLY XC(I) AND PC(I) ARE SET.
(      328)  C
(      329)          DO 1050 I=1,80
(      330)          AC(I)=A(I)
(      331)  1050    CONTINUE
(      332)          DO 1055 I=1,126
(      333)          PC(I)=P(I)
(      334)  1055    CONTINUE
(      335)          DO 1060 I=1,29
(      336)          XC(I)=X(I)
(      337)  1060    CONTINUE
(      338)  C       **********************************************
(      339)  C       FROM HERE ON THE PROGRAM GOES INTO SIMULATION PHASE
(      340)  C       WHERE THE DERIVED INITIAL VALUES FROM THE PATIENT
(      341)  C       RELATED ALGORITHM ARE ENTERED INTO THE DYNAMIC
(      342)  C       MODEL.
(      343)  C       **********************************************
(      344)  C
(      345)  C       INITIALISE THE TIME COUNTERS
(      346)  C
(      347)          DO 251 I=1,4
(      348)          DO 251 J=1,3
(      349)          PTC(I,J)=0
(      350)  251     CONTINUE
(      351)          IPOKE=99999
(      352)          ITH=0.0
(      353)          ITM=0.0
(      354)          ITS=0.0
(      355)          SC=1.0
(      356)  252     CONTINUE
(      357)  C
(      358)  C       SUBROUTINE WHICH MAY BE CALLED TO MAKE CHANGES TO ANY OF
(      359)  C       THE CONSTANT, A(I), PARAMETERS. THIS ALLOWS PHYSIOLOGICAL
(      360)  C       INPUTS AND DISTURBANCES, ASWEL AS PATHOLOGICAL
```

```
C*************************************************************************
(      361) C       DISTURBANCES TO BE EFFECTED ON THE SIMULATION.
(      362) C          NOTE THAT THIS SUBROUTINE HOLDS THE ENTRY TO
(      363) C       SUBROUTINE INFO, WHICH PROVIDES INFORMATION ON THE
(      364) C       TYPES OF CHANGES AND DISORDERS WHICH MAY BE EFFECTED
(      365) C       ON THIS FAB MODEL.
(      366) C
(      367)         CALL POKER(A,AC,IPOKE,ITM,SC)
(      368) C
(      369) C       ASCERTAIN WHETHER THE POKER SUBROUTINE IS REQUIRED
(      370) C
(      371) 255     IF(IPOKE.EQ.ITM)GOTO 252
(      372) C
(      373) C       CALL SIMULATION SUBROUTINES
(      374) C       ***************************
(      375) C
(      376) C
(      377) C       SUBROUTINE TO IMPOSE 100 MIN DELAY ON ALDOSTERONE
(      378) C       SECRETION.
(      379) C
(      380)         CALL ALDLAY(P,Z,ITM)
(      381) C
(      382) C       SUBROUTINE TO SOLVE THE ALGEBRAIC EQUATIONS AT INTERVALS
(      383) C       OF ONE SECOND
(      384) C
(      385) 256     CALL ALGEBS(DX,X,P,A)
(      386) C
(      387) C       SUBROUTINE TO SOLVE THE DIFFFERENTIAL EQUATIONS AT INTERVALS
(      388) C       OF ONE SECOND.
(      389) C
(      390)         CALL INTEGS(DX,X,P,A,PABZ)
(      391) C
(      392) C       UPDATING SECOND COUNTERS
(      393) C
(      394)         ITS=ITS+1
(      395)         IF(ITS.NE.60) GOTO 256
(      396)         ITS=0.0
(      397) C
(      398) C       SUBROUTINE TO SOLVE ALGEBRAIC EQUATIONS AT INTERVALS
(      399) C       OF ONE MINUTE
(      400) C
(      401)         CALL ALGEBM(DX,X,P,A,POOL,PARS,PTC,PABZ,Z)
(      402) C
(      403) C       SUBROUTINE TO SOLVE THE DIFFERENTIAL EQUATIONS AT INTERVALS
(      404) C       OF ONE MINUTE
(      405) C
(      406)         CALL INTEGM(DX,X,P,A,PABZ)
(      407) C
(      408) C       UPDATING MINUTE TIME COUNTER
(      409) C
(      410)         ITM=ITM+1
(      411) C
(      412) C       PRINT OUT THE CURRENT PATIENT STATE.
(      413) C
(      414)         ITT=ITT+1
(      415)         IF(ITT.NE.A(80))GOTO 9135
(      416)         WRITE(5,9000)
(      417) 9000    FORMAT(6('**********'))
(      418)         WRITE(5,9010)ITM
(      419) 9010    FORMAT('RESULTS AT TIME PERIOD',2X,I3,7X)
(      420)         WRITE(5,9000)
```

```
C**********************************************************************
(      421)          WRITE(5,9045)
(      422)          WRITE(5,9045)
(      423)          WRITE(5,9045)
(      424)          WRITE(5,9045)
(      425)          WRITE(5,9045)
(      426)          WRITE(5,9020)
(      427) 9020     FORMAT('COMPUTED VARIABLES')
(      428)          WRITE(5,9030)
(      429) 9030     FORMAT('********************')
(      430)          WRITE(5,9040)(P(I),I,I=1,126)
(      431) 9040     FORMAT(6(F12.5,2X,'P',I3,4X))
(      432)          WRITE(5,9045)
(      433)          WRITE(5,9045)
(      434)          WRITE(5,9045)
(      435)          WRITE(5,9045)
(      436)          WRITE(5,9045)
(      437) 9045     FORMAT(1X)
(      438)          WRITE(5,9050)
(      439) 9050     FORMAT('STATE VARIABLES')
(      440)          WRITE(5,9030)
(      441)          WRITE(5,9060)(X(I),I,I=1,29)
(      442) 9060     FORMAT(6(F12.5,X,'X',I2,5X))
(      443)          WRITE(5,9045)
(      444)          WRITE(5,9070)
(      445) 9070     FORMAT('RATE OF CHANGE SV')
(      446)          WRITE(5,9030)
(      447)          WRITE(5,9080)(DX(I),I,I=1,29)
(      448) 9080     FORMAT(6(F12.5,X,'DX',I2,4X))
(      449)          WRITE(5,9045)
(      450)          WRITE(5,9045)
(      451)          WRITE(5,9045)
(      452)          WRITE(5,9045)
(      453)          WRITE(5,9000)
(      454) 9090     CONTINUE
(      455)          DO 9095 I=1,126
(      456)          PS(I)=(P(I)/PC(I))/SC
(      457) 9095     CONTINUE
(      458)          DO 9100 I=1,29
(      459)          XS(I)=(X(I)-XC(I))/SC
(      460) 9100     CONTINUE
(      461)          WRITE(5,9000)
(      462)          WRITE(5,9110)ITM
(      463) 9110     FORMAT('SENSITIVITY TEST AT TIME PERIOD',2X,I3,7X)
(      464)          WRITE(5,9000)
(      465)          WRITE(5,9045)
(      466)          WRITE(5,9115)
(      467) 9115     FORMAT('SENSITIVITY OF COMPUTED VARIABLES')
(      468)          WRITE(5,9120)
(      469) 9120     FORMAT(3('**********'))
(      470)          WRITE(5,9125)(PS(I),I,I=1,126)
(      471) 9125     FORMAT(6(F12.5,2X,'PS',I3.3X))
(      472)          WRITE(5,9048)
(      473) 9048     FORMAT('SENSITIVITY OF STATE VARIABLES')
(      474)          WRITE(5,9120)
(      475)          WRITE(5,9130)(XS(I),I,I=1,29)
(      476) 9130     FORMAT(6(F12.5,2X,'XS',I2,4X))
(      477)          WRITE(5,9045)
(      478)          WRITE(5,9000)
(      479)          ITT=0
(      480) 9135     CONTINUE
```

```
C**********************************************************************
(      481) C
(      482) C       STOP COMMAND. EIGHT HOUR CLINICIAN DECISION PERIOD ASSUMED.
(      483) C
(      484)        IF(ITM.NE.480.0)GOTO 255
(      485)        STOP
(      486)        END
(      487)
(      488)
(      489)
(      490)
(      491)
(      492)
(      493)
(      494)
(      495)
(      496)
(      497) C
(      498) C      ALDLAY : SUBROUTINE TO IMPOSE 100 MIN DELAY ON
(      499) C      ************************************************
(      500) C                ALDOSTERONE SECRETION.
(      501) C                ********************
(      502) C
(      503)        SUBROUTINE ALDLAY(P,Z,ITM)
(      504)        DIMENSION P(126),Z(3),Q(100),R(100),S(100)
(      505)        DIMENSION QA(100),RA(100),SA(100)
(      506)        INTEGER*2 ITM
(      507) C
(      508) C      SET UP INITIAL DELAY VECTORS.
(      509) C
(      510)        IF(ITM.GT.0)GOTO 5010
(      511)        DO 5000 I=1,100
(      512)        Q(I)=P(6)
(      513)        R(I)=P(16)
(      514)        S(I)=P(107)
(      515) 5000   CONTINUE
(      516)        GOTO 5030
(      517) C
(      518) C      UPDATE DELAY VECTORS.
(      519) C
(      520) 5010   DO 5020 I=2,100
(      521)        QA(I)=Q(I-1)
(      522)        RA(I)=R(I-1)
(      523)        SA(I)=S(I-1)
(      524) 5020   CONTINUE
(      525)        DO 5025 I=2,100
(      526)        Q(I)=QA(I)
(      527)        R(I)=RA(I)
(      528)        S(I)=SA(I)
(      529) 5025   CONTINUE
(      530)        Q(1)=P(6)
(      531)        R(1)=P(16)
(      532)        S(1)=P(107)
(      533) C
(      534) C      BRINGING FORWARD THE RELEVANT PARAMETER STATES FROM
(      535) C      100 MINS EARLIER IN THE SIMULATION.
(      536) C
(      537)        Z(1)=Q(100)
(      538)        Z(2)=R(100)
(      539)        Z(3)=S(100)
(      540) 5030   CONTINUE
```

```
C*************************************************************************

(      541) C
(      542) C       SENDING SUBROUTINE BACK TO MAIN PROGRAMME.
(      543) C
(      544)         RETURN
(      545)         END
(      546)
(      547)
(      548)
(      549)
(      550)
(      551)
(      552)
(      553)
(      554)
(      555) C
(      556) C       ALGEBS : SUBROUTINE TO SOLVE THE ALGEBRAIC EQUATIONS
(      557) C       ***************************************************
(      558) C             AT ONE SECOND INTERVALS.
(      559) C             ************************
(      560) C
(      561)         SUBROUTINE ALGEBS(DX,X,P,A)
(      562)         DIMENSION DX(29),X(29),P(126),A(80)
(      563)         REAL*4 NCOA,NCOB
(      564) C
(      565) C       CARDIOVASCULAR SYSTEM
(      566) C
(      567)         P(12)=X(4)-A(8)
(      568)         P(9)=P(12)/A(2)
(      569)         NCOA=(((P(9)+4)*6)**2.6)
(      570)         NCOB=(5000+(((P(9)+4)*6)**2.6))
(      571)         P(5)=(NCOA/NCOB)*11.447515*A(10)/60
(      572)         P(2)=P(5)*A(4)
(      573)         P(11)=X(3)-A(7)
(      574)         P(6)=(P(11)/A(1)-100)*.05+100
(      575)         P(7)=P(6)-P(10)
(      576)         P(3)=P(7)/A(5)
(      577)         P(13)=X(5)-A(9)
(      578)         P(10)=P(13)/A(3)
(      579)         P(8)=P(10)-P(9)
(      580)         P(4)=P(8)/A(6)
(      581)         P(1)=X(3)+X(4)+X(5)
(      582)         P(14)=P(1)-A(11)
(      583) C
(      584) C       SEND SUBROUTINE BACK TO MAIN PROGRAM
(      585) C
(      586)         RETURN
(      587)         END
(      588)
(      589)
(      590)
(      591)
(      592)
(      593)
(      594)
(      595)
(      596)
(      597)
(      598) C
(      599) C       INTEGS : SUBROUTINE TO SOLVE DIFFERENTIAL EQUATIONS
(      600) C       ***************************************************
```

```
C*****************************************************************
(      601) C                AT ONE SECOND INTERVALS.
(      602) C                ************************
(      603) C
(      604)          SUBROUTINE INTEGS(DX,X,P,A,PABZ)
(      605)          DIMENSION DX(29),X(29),P(126),A(80)
(      606)          DIMENSION PABZ(7)
(      607)          INTEGER*2 I,J
(      608) C
(      609) C        THE DIFFERENTIAL EQUATIONS
(      610) C
(      611)          DX(3)=(P(2)-P(3))/15
(      612)          DX(4)=(P(4)-P(2))/15
(      613)          DX(5)=(P(3)-P(4))/15+((PABZ(1)+A(23)+P(35)-P(36)-P(34))/60)
(      614) C
(      615) C        SOLVING THE FIRST ORDER LINEAR DIFFERENTIAL
(      616) C        WITH ONE INTEGRATION STEP.
(      617) C
(      618)          DO 9000 I=3,5
(      619)          X(I)=X(I)+DX(I)
(      620) 9000     CONTINUE
(      621) C
(      622) C        SENDING SUBROUTINE BACK TO MAIN PROGRAMME
(      623) C
(      624)          RETURN
(      625)          END
(      626)
(      627)
(      628)
(      629)
(      630)
(      631)
(      632)
(      633)
(      634)
(      635)
(      636) C
(      637) C        POKER : SUBROUTINE TO SIMULATE PHYSIOLOGICAL AND
(      638) C        ***********************************************
(      639) C                PATHOLOGICAL DISTURBACES.
(      640) C                *************************
(      641) C
(      642)          SUBROUTINE POKER(A,AC,IPOKE,ITM,SC)
(      643)          DIMENSION A(80),AC(80)
(      644)          INTEGER*2 I,J,IPOKE,ITM
(      645)          REAL*4 SC
(      646) 8000 WRITE(1,8010)
(      647) 8010     FORMAT('DO YOU WISH TO DISTURB THE SYSTEM 1=Y 0=N')
(      648)          READ(1,*)I
(      649)          IF(I.NE.0.AND.I.NE.1)GOTO 8000
(      650)          IF(I.EQ.0)IPOKE=99999
(      651)          IF(I.EQ.0) GOTO 8990
(      652) 8040     WRITE(1,8050)
(      653) 8050     FORMAT('TYPE WHICH I OF A(I) PARAMETERS REQUIRED FOR CHANGE')
(      654)          READ(1,*)I
(      655)          WRITE(1,8055)I, AC(I)
(      656) 8055     FORMAT('NORMAL VALUE OF A(',I3,')=',F10.4)
(      657)          WRITE(1,8060)I,A(I)
(      658) 8060     FORMAT('CURRENT VALUE OF A(',I3,')=',F10.4)
(      659) 8065     WRITE(1,8070)
(      660) 8070     FORMAT('NOW TYPE IN THE NEW VALUE')
```

```
C**********************************************************************
(      661)          READ(1,*)A(I)
(      662)          IF(AC(I).EQ.0)GOTO 8079
(      663)          SC=(A(I)/AC(I))
(      664) 8079     SC=1.0
(      665)          WRITE(1,8080)I,A(I)
(      666) 8080     FORMAT('NEW VALUE OF A(',I3,') =',F10.4)
(      667) 8090     WRITE(1,8100)
(      668) 8100     FORMAT('IS THAT THE CORRECT VALUE 1=Y 0=N')
(      669)          READ(1,*)J
(      670)          IF(J.NE.0.AND.J.NE.1) GOTO 8090
(      671)          IF(J.EQ.0) GOTO 8065
(      672) 8105     WRITE(1,8110)
(      673) 8110     FORMAT('DO YOU WISH TO CHANGE ANOTHER A(I) VALUE 1=Y 0=N')
(      674)          READ(1,*)J
(      675)          IF(J.NE.0.AND.J.NE.1) GOTO 8105
(      676)          IF(J.EQ.1) GOTO 8040
(      677) 8115     WRITE(1,8120)
(      678) 8120     FORMAT('TYPE IN HOW MANY MINUTES UNTIL NEXT CHANGES')
(      679)          READ(1,*)J
(      680) 8125     WRITE(1,8130)J
(      681) 8130     FORMAT('CONFIRM THAT YOU MEAN ',I3,' MINUTES 1=Y 0=N')
(      682)          READ(1,*)K
(      683)          IF(K.NE.0.AND.K.NE.1) GOTO 8125
(      684)          IF(K.EQ.0) GOTO 8115
(      685)          IPOKE=ITM+J
(      686) C
(      687) C        SEND SUBROUTINE BACK TO MAIN PROGRAM
(      688) C
(      689) 8990     RETURN
(      690)          END
(      691)
(      692)
(      693)
(      694)
(      695)
(      696)
(      697)
(      698)
(      699)
(      700)
(      701) C
(      702) C        ALGEBM : SUBROUTINE TO SOLVE ALGEBRAIC EQUATIONS
(      703) C        ***********************************************
(      704) C                 AT ONE MINUTE INTERVALS.
(      705) C                 ************************
(      706)          SUBROUTINE ALGEBM(DX,X,P,A,POOL,PABS,PTC,PABZ,Z)
(      707)          DIMENSION DX(29),X(29),P(126),A(80),Z(3)
(      708)          DIMENSION POOL(7,3),PABS(7,3),PTC(7,3),PABZ(7)
(      709)          INTEGER*2 I,J
(      710)          REAL*4 PABA,PABB
(      711) C
(      712) C        GASTRO INTESTINAL SYSTEM
(      713) C
(      714)          GOTO 7015
(      715) C
(      716) C        SECTION TO CANCEL FEED IF GI COMPARTMENTS NOT AVAILABLE.
(      717) C
(      718) 7000     I=I+17
(      719)          WRITE(1,7010)I
(      720) 7010     FORMAT('NO COMPARTMENTS FOR A(',I3,') CURRENT FEED CANCELLED')
```

```
C**********************************************************************
(      721)          A(12)=0
(      722)          A(13)=0
(      723)          A(14)=0
(      724)          A(15)=0
(      725)          A(16)=0
(      726)          A(17)=0
(      727)          A(18)=0
(      728)          GOTO 7150
(      729)  C
(      730)  C       ASCERTAIN WHETHER FEEDING REQUIRED.  IF YES THEN CHECK
(      731)  C       WHETHER ANY FEEDING COMPARTMENTS AVAILABLE.  IF ALSO YES
(      732)  C       THEN FEED.  COMPARTMET SELECTED AUTOMATICALLY,
(      733)  C       TIME COUNTER IS THEN TRIGGERED OFF.
(      734)  C
(      735)  7015    IF(A(19).EQ.0)GOTO 7150
(      736)          A(19)=0
(      737)  C
(      738)  C       SUBSTANCE A(12)
(      739)  C
(      740)          IF(A(12).EQ.0)GOTO 7022
(      741)          I=1
(      742)          IF(POOL(I,1).EQ.0.OR.POOL(I,2).EQ.0.OR.POOL(I,3).EQ.0)GOTO 7018
(      743)          GOTO 7000
(      744)  7018    DO 7020 J=1,3
(      745)          IF(POOL(I,J).NE.0)GOTO 7020
(      746)          PTC(I,J)=0
(      747)          POOL(I,J)=A(12)
(      748)          J=3
(      749)  7020    CONTINUE
(      750)  C
(      751)  C       SUBSTANCE A(13)
(      752)  C
(      753)  7022    IF(A(13).EQ.0)GOTO 7030
(      754)          I=2
(      755)          IF(POOL(I,1).EQ.0.OR.POOL(I,2).EQ.0.OR.POOL(I,3).EQ.0)GOTO 7025
(      756)          GOTO 7000
(      757)  7025    DO 7027 J=1,3
(      758)          IF(POOL(I,J).NE.0)GOTO 7027
(      759)          PTC(I,J)=0
(      760)          POOL(I,J)=A(13)
(      761)          J=3
(      762)  7027    CONTINUE
(      763)  C
(      764)  C       SUBSTANCE A(14)
(      765)  C
(      766)  7030    IF(A(14).EQ.0)GOTO 7042
(      767)          I=3
(      768)          IF(POOL(I,1).EQ.0.OR.POOL(I,2).EQ.0.OR.POOL(I,3).EQ.0)GOTO 7033
(      769)          GOTO 7000
(      770)  7033    DO 7035 J=1,3
(      771)          IF(POOL(I,J).NE.0)GOTO 7035
(      772)          PTC(I,J)=0
(      773)          POOL(I,J)=A(14)
(      774)          J=3
(      775)  7035    CONTINUE
(      776)  C
(      777)  C       SUBSTANCE A(15)
(      778)  C
(      779)  7042    IF(A(15).EQ.0)GOTO 7060
(      780)          I=4
```

```
C*********************************************************************
(      781)          IF(POOL(I,1).EQ.0.OR.POOL(I,2).EQ.0.OR.POOL(I,3).EQ.0)GOTO 7045
(      782)          GOTO 7000
(      783) 7045     DO 7050 J=1,3
(      784)          IF(POOL(I,J).NE.0)GOTO 7050
(      785)          PTC(I,J)=0
(      786)          POOL(I,J)=A(15)
(      787)          J=3
(      788) 7050     CONTINUE
(      789) C
(      790) C        SUBSTANCE A(16)
(      791) C
(      792) 7060     IF(A(16).EQ.0)GOTO 7090
(      793)          I=5
(      794)          IF(POOL(I,1).EQ.0.OR.POOL(I,2).EQ.0.OR.POOL(I,3).EQ.0)GOTO 7070
(      795)          GOTO 7000
(      796) 7070     DO 7080 J=1,3
(      797)          IF(POOL(I,J).NE.0)GOTO 7080
(      798)          PTC(I,J)=0
(      799)          POOL(I,J)=A(16)
(      800)          J=3
(      801) 7080     CONTINUE
(      802) C
(      803) C        SUBSTANCE A(17)
(      804) C
(      805) 7090     IF(A(17).EQ.0)GOTO 7120
(      806)          I=6
(      807)          IF(POOL(I,1).EQ.0.OR.POOL(I,2).EQ.0.OR.POOL(I,3).EQ.0)GOTO 7100
(      808)          GOTO 7000
(      809) 7100     DO 7110 J=1,3
(      810)          IF(POOL(I,J).NE.0)GOTO 7110
(      811)          PTC(I,J)=0
(      812)          POOL(I,J)=A(17)
(      813)          J=3
(      814) 7110     CONTINUE
(      815) C
(      816) C        SUBSTANCE A(18)
(      817) C
(      818) 7120     IF(A(18).EQ.0)GOTO 7150
(      819)          I=7
(      820)          IF(POOL(I,1).EQ.0.OR.POOL(I,2).EQ.0.OR.POOL(I,3).EQ.0)GOTO 7130
(      821)          GOTO 7000
(      822) 7130     DO 7140 J=1,3
(      823)          IF(POOL(I,J).NE.0)GOTO 7140
(      824)          PTC(I,J)=0
(      825)          POOL(I,J)=A(18)
(      826)          J=3
(      827) 7140     CONTINUE
(      828) 7150     CONTINUE
(      829) C
(      830) C        CALCULATE THE AMOUNTS TO BE ABSORBED FROM THE GI SYSTEM.
(      831) C        AND CLEAR THE PREVIOUS AMOUNTS ABSORBED.
(      832) C
(      833)          DO 7155 I=1,7
(      834)          PABZ(I)=0.0
(      835) 7155     CONTINUE
(      836)          DO 7160 I=1,7
(      837)          DO 7160 J=1,3
(      838)          PABA=.125*(DEXP(.04*PTC(I,J)))
(      839)          PABB=.125*(DEXP(.059*PTC(I,J)))
(      840)          PABS(I,J)=-POOL(I,J)*(PABA-PABB)
```

```
C**********************************************************************
(       841) C
(       842) C       IF AMOUNT TO ABSORB IS > THAN THAT AVAILABLE THEN REDUCE IT TO
(       843) C       THE AMOUNT WHICH IS AVAILABLE.  THIS PREVENTS -VE ABSORPTION
(       844) C       WHICH MAY NOT OCCUR IN COMPARTMENTAL ANALYSIS.
(       845) C
(       846)         IF(PABS(I,J).GT.POOL(I,J))PABS(I,J)=POOL(I,J)
(       847) C
(       848) C       WHEN THE GI COMPARTMENT BECOMES SMALL IT IS EMPTIED INTO
(       849) C       THE PLASMA COMPARTMENT.
(       850) C
(       851)         IF(POOL(I,J).LE.0.0013)PABS(I,J)=POOL(I,J)
(       852) C
(       853) C       COMPUTE THE ACCUMULATING AMOUNTS TO BE ABSORBED.
(       854) C
(       855)         PABZ(I)=PABZ(I)+PABS(I,J)*A(31)
(       856) 7160    CONTINUE
(       857) C
(       858) C       VOMIT
(       859) C
(       860) 7300    IF(A(20).NE.1)GOTO 7320
(       861)         DO 7310 I=1,7
(       862)         DO 7310 J=1,3
(       863)         POOL(I,J)=0
(       864)         PABS(I,J)=0
(       865)         PABZ(I)=0
(       866) 7310    CONTINUE
(       867) 7320    CONTINUE
(       868) C
(       869) C       UPDATE POOL VOLUME.
(       870) C
(       871)         DO 7325 I=1,7
(       872)         DO 7325 J=1,3
(       873)         POOL(I,J)=POOL(I,J)-PABS(I,J)
(       874) C
(       875) C       UPDATE EXPONENTIAL COUNTERS.
(       876) C
(       877)         PTC(I,J)=PTC(I,J)+1
(       878) 7325    CONTINUE
(       879) C
(       880) C       RESPIRATORY WATER LOSS
(       881) C
(       882)         P(37)=A(24)*P(44)
(       883) C
(       884) C       MICROVASCULAR DYNAMICS.
(       885) C
(       886)         P(43)=X(2)/A(25)
(       887)         IF(P(43).LE.0.9)P(39)=-15.0
(       888)         IF(P(43).GT.0.9.AND.P(43).LE.1.0)P(39)=87.0*P(43)-93.3
(       889)         IF(P(43).GT.1.0.AND.P(43).LE.2.0)P(39)=-6.3*((2.0-P(43))**10)
(       890)         IF(P(43).GT.2.0)P(39)=P(43)-2.0
(       891)         P(40)=((P(10)*A(26))+P(6))/(A(26)+1.0)
(       892)         P(41)=P(30)*0.25
(       893)         P(42)=P(31)*0.4
(       894)         P(38)=P(40)+P(41)-P(39)-P(42)
(       895)         P(34)=A(27)*P(38)
(       896)         P(35)=A(28)*(24.0/(1.0+(DEXP(-.4977*P(39)))))*A(38)
(       897) C
(       898) C       CALCULATION OF CONCENTRATION OF ANALYTES.
(       899) C
(       900)         P(15)=X(6)/(X(2)+P(14))
```

```
C*****************************************************************
(       901)          P(16)=X(7)/(X(2)+P(14))
(       902)          P(17)=X(8)/(X(2)+P(14))
(       903)          P(18)=X(9)/(X(2)+P(14))
(       904)          P(19)=X(10)/(X(2)+P(14))
(       905)          P(20)=X(11)/(X(2)+P(14))
(       906)          P(21)=X(12)/(X(2)+P(14))
(       907)          P(22)=X(13)/X(1)
(       908)          P(23)=X(14)/X(1)
(       909)          P(24)=X(15)/X(1)
(       910)          P(25)=X(16)/X(1)
(       911)          P(26)=X(17)/X(1)
(       912)          P(53)=X(18)/X(1)
(       913)          P(27)=X(19)/X(1)
(       914)          P(28)=X(20)/(P(14)+X(1)+X(2))
(       915)          P(29)=X(21)/P(14)
(       916)          P(30)=X(22)/X(2)
(       917)          P(31)=(X(21)+A(32))/P(14)
(       918)          P(74)=X(28)/(P(14)+X(2))
(       919) C
(       920) C        CALCULATING THE INTRA- AND EXTRACELLULAR OSMOLALITIES
(       921) C
(       922)          P(33)=(P(22)+P(23)+P(24)+P(25)+P(26)+P(27)+P(28)+104.05)*A(37)
(       923)          P(32)=(P(15)+P(16)+P(17)+P(18)+P(19)+P(20)+P(21)+P(28))
(       924)          P(32)=(P(32)+P(74)+18.9)*A(37)
(       925) C
(       926) C        TRANSMEMBRANE ION DYNAMICS
(       927) C
(       928) C        CALCULATING INTRA- AND EXTRACELLULAR CHARGES.
(       929) C
(       930)          P(57)=X(13)+X(14)-X(15)-X(16)+2*X(17)+2*X(18)-2*X(19)-A(43)
(       931)          P(58)=X(6)+X(7)-X(8)-X(9)+2*X(10)+2*X(11)-2*X(12)
(       932)          P(58)=P(58)-(.9925856*(X(21)+X(22)+A(32)))
(       933)          P(59)=P(57)-P(58)
(       934) C
(       935) C        ACTIVELY PUMPED IONS.
(       936) C
(       937)          P(55)=-61*(DLOG10(P(22)/P(15)))
(       938)          P(61)=-61*(DLOG10(P(23)/P(16)))
(       939)          P(64)=-61*(DLOG10(SQRT(P(26))/SQRT(P(19))))
(       940)          P(67)=-61*(DLOG10(SQRT(P(53))/SQRT(P(20))))
(       941)          P(56)=A(41)+P(59)*A(42)
(       942)          P(62)=A(45)-P(59)*A(42)
(       943)          P(65)=A(47)-P(59)*A(42)
(       944)          P(68)=A(49)+P(59)*A(42)
(       945)          P(54)=P(55)/P(56)
(       946)          P(60)=P(61)/P(62)
(       947)          P(63)=P(64)/P(65)
(       948)          P(66)=P(67)/P(68)
(       949) C
(       950) C        PASSIVE MOVING IONS.
(       951) C
(       952)          P(75)=DX(13)+DX(14)+2*DX(17)+2*DX(18)
(       953)          IF(P(75).GE.0)GOTO 7330
(       954)          P(77)=(P(24)/P(17))/A(63)
(       955)          P(79)=(P(25)/P(18))/A(64)
(       956)          P(81)=(P(27)/P(21))/A(65)
(       957)          P(82)=X(15)+X(16)+X(19)
(       958)          P(84)=X(15)/P(82)
(       959)          P(86)=X(16)/P(82)
(       960)          P(88)=X(19)/P(82)
```

```
C*************************************************************************
(      961)          GOTO 7340
(      962) 7330     P(76)=(P(17)/P(24))/A(66)
(      963)          P(78)=(P(18)/P(25))/A(67)
(      964)          P(80)=(P(21)/P(27))/A(68)
(      965)          P(83)=X(8)+X(9)+X(12)
(      966)          P(85)=X(8)/P(83)
(      967)          P(87)=X(9)/P(83)
(      968)          P(89)=X(12)/P(83)
(      969) 7340     CONTINUE
(      970) C
(      971) C        GLUCOSE/INSULIN EFFECTS ON POTASSIUM TRANSMEMBRANE ACTIVITY
(      972) C
(      973)          P(124)=((A(75)*A(77))+(A(76)*X(29)))
(      974)          P(125)=P(124)*A(78)
(      975) C
(      976) C        KIDNEY DYNAMICS.
(      977) C
(      978) C
(      979) C        GFR.
(      980) C
(      981)          P(90)=A(50)*(X(2)+P(14))/A(51)
(      982)          IF(P(6).LT.40)P(91)=0
(      983)          IF(P(6).GE.40.AND.P(6).LT.80)P(91)=.02*P(6)-0.8
(      984)          IF(P(6).GE.80.AND.P(6).LT.100)P(91)=-0.005*((P(6)-100)**2)+1
(      985)          IF(P(6).GE.100)P(91)=1
(      986)          P(92)=P(91)*P(90)
(      987)          IF(P(42).LE.28)P(94)=-5.0*((P(42)/28)-1)+1
(      988)          IF(P(42).GT.28)P(94)=1
(      989)          P(93)=P(94)*0.2*P(92)
(      990) C
(      991) C        RENAL UREA DYNAMICS.
(      992) C
(      993)          P(52)=0.6*P(92)*P(28)
(      994) C
(      995) C        RENAL PHOSPHATE DYNAMICS.
(      996) C
(      997)          P(97)=P(21)*P(92)
(      998)          IF(P(97).LE.0.11)P(51)=5.0*P(97)/22.0
(      999)          IF(P(97).GT.0.11)P(51)=P(97)-0.085
(     1000) C
(     1001) C        RENAL CALCIUM DYNAMICS.
(     1002) C
(     1003)          P(98)=P(20)*P(92)
(     1004)          IF(P(98).LT.0.493)P(50)=0
(     1005)          IF(P(98).GE.0.493)P(50)=P(98)-0.493
(     1006) C
(     1007) C        RENAL MAGNESIUM DYNAMICS.
(     1008) C
(     1009)          P(99)=P(19)*P(92)
(     1010)          IF(P(99).LT.0.292)P(49)=0
(     1011)          IF(P(99).GE.0.292)P(49)=P(99)-0.292
(     1012) C
(     1013) C        RENAL BICARBOATE DYAMICS.
(     1014) C
(     1015)          P(100)=P(18)*P(92)
(     1016)          P(101)=(1.333333)-(P(117)/120.0)
(     1017)          P(102)=P(101)*P(100)
(     1018)          IF(P(102).LE.2)P(48)=0
(     1019)          IF(P(102).GT.2.AND.P(102).LE.4)P(48)=0.16395*((P(102)-2)**2.61)
(     1020)          IF(P(102).GT.4)P(48)=P(102)-3
```

```
C*************************************************************************
(      1021) C
(      1022) C       RENAL POTASSIUM DYNAMICS.
(      1023) C
(      1024)         P(103)=P(93)*P(16)
(      1025)         P(104)=P(103)*0.5
(      1026)         P(105)=(0.9*P(104))+(0.01778*P(16)*P(116))
(      1027)         P(46)=P(105)*0.39004
(      1028) C
(      1029) C       RENAL SODIUM DYNAMICS.
(      1030) C
(      1031)         P(109)=(-P(48)+P(114)+P(113))
(      1032)         IF(P(109).LT.0)P(109)=0
(      1033)         P(106)=P(93)*P(15)
(      1034)         P(107)=P(106)*0.5
(      1035)         P(108)=(0.9*P(107))-(P(116)*0.09)
(      1036)         P(45)=(P(108)*0.11624)-P(109)
(      1037)         IF(P(45).LT.0)P(45)=0
(      1038) C
(      1039) C       RENAL CHLORIDE DYNAMICS.
(      1040) C
(      1041)         P(110)=P(92)*P(17)
(      1042)         P(111)=P(45)+P(46)+P(114)+2*P(50)+2*P(49)-P(48)-0.073
(      1043)         IF(P(111).GT.P(110))P(47)=P(110)
(      1044)         IF(P(111).LE.P(110))P(47)=P(111)
(      1045)         IF(P(111).LT.0)P(47)=0
(      1046) C
(      1047) C      RENAL GLUCOSE DYNAMICS.
(      1048) C
(      1049)         IF((P(74)*P(92)).LT.0.65)P(126)=0.0
(      1050)         IF((P(74)*P(92)).GE.0.65)P(126)=P(74)*P(92)-0.65
(      1051) C
(      1052) C       RENAL EXCRETION OF TITRATABLE ACID.
(      1053) C
(      1054)         IF(X(25).LE.4)P(112)=0
(      1055)         IF(X(25).GT.4.AND.X(25).LE.5)P(112)=(A(52)*(-2.5*X(24)+19.5))
(      1056)         IF(X(25).GT.4.AND.X(25).LE.5)P(112)=P(112)*(X(25)-4)
(      1057)         IF(X(25).GT.5)P(112)=A(52)*(-2.5*X(24)+19.5)
(      1058)         P(113)=P(112)+((0.001*P(116))+0.009)
(      1059) C
(      1060) C       RENAL AMMONIUM EXCRETION.
(      1061) C
(      1062)         P(114)=A(53)*(-0.5*X(25)+4)
(      1063) C
(      1064) C       URINE FORMATION.
(      1065) C
(      1066)         P(95)=(P(52)+0.312+(1.86*(P(103)+P(103))))/P(32)
(      1067)         P(36)=P(95)-(P(115)*0.9*P(95))
(      1068)         IF(P(36).LT.0.0003472)P(36)=0.0003472
(      1069) C
(      1070) C       HORMONAL CONTROL.
(      1071) C
(      1072) C       ADH.
(      1073) C
(      1074)         P(115)=1.1/(1+DEXP(-0.5*(X(26)+4.605)))*A(57)
(      1075) C
(      1076) C       ALDOSTERONE.
(      1077) C
(      1078)         P(96)=(Z(2)-4.5)*A(58)-(Z(1)-100)*A(59)-(Z(3)-1.4)*A(60)
(      1079)         P(116)=10/(1.0+DEXP(-0.439445*(X(27)-5.0)))*A(62)
(      1080) C
```

```
C
C       ACID-BASE DYNAMICS.
C
        P(69)=X(23)/(X(1)+X(2)+P(14))
        P(117)=2.5*(P(69)-23)+35
        P(118)=6.099+(DLOG10(P(18)/(0.03*P(117))))
C
C       RESPIRATORY UNIT.
C
        P(70)=DEXP(7.0*(A(71)-P(118)))
        P(71)=DEXP(0.138*(P(117)-A(72)))
        P(44)=(P(70)+P(71))/2
C
C       PROTEIN DYNAMICS.
C
        P(72)=40/P(29)
        P(73)=P(72)*A(30)
        P(122)=(P(29)-P(30))*((P(40)**2)*(6.9204*(1E-6)))
        P(120)=P(30)*P(35)
        P(121)=P(29)*A(73)-.01076
        IF(P(92).GE.0.1)P(123)=(P(129)*(A(50)-.1)/10)
        IF(A(50).LT.0.1)P(123)=0
C
C       SEND SUBROUTINE BACK TO MAIN PROGRAM
C
        RETURN
        END
C
C
C
C
C
C
C
C
C
C       INTEGM : SUBROUTINE TO SOLVE DIFFERENTIAL EQUATIONS
C       ***************************************************
C                AT ONE MINUTE INTERVALS.
C                ************************
        SUBROUTINE INTEGM(DX,X,P,A,PABZ)
        DIMENSION DX(29),X(29),P(126),A(80)
        DIMENSION PABZ(7)
        REAL*4 DIFF
C
C       THE DIFFERENTIAL EQUATIONS.
C
        DX(1)=(P(33)-P(32))*A(36)+A(22)
        DX(2)=P(34)-P(35)-A(21)-P(37)
        DX(6)=PABZ(2)-P(45)-A(33)-DX(13)
        DX(7)=PABZ(3)-P(46)-A(34)-DX(14)
        DX(8)=PABZ(4)-P(47)-A(35)-DX(15)
        DX(9)=A(29)-P(48)-DX(16)+((P(14)+X(2))*11.605*(7.4-P(118)))
        DX(10)=PABZ(5)-P(49)-DX(17)
        DX(11)=PABZ(6)-P(50)
        DX(12)=PABZ(7)-P(51)-DX(13)
        DX(13)=(A(39)*P(54)-X(13))*A(40)
        DX(14)=(X(14)-A(44)*P(60))*A(40)+P(125)
        DX(17)=(X(17)-A(46)*P(63))*A(40)
```

```
C*************************************************************************
(      1141)          DX(18)=(A(48)*P(66)-X(18))*A(40)
(      1142)          IF(P(75).GE.0)GOTO 6005
(      1143)          DIFF=(P(77)*P(84)/A(63))+(P(79)*P(86)/A(64))+(P(81)*P(88)/A(65))
(      1144)          DX(15)=P(75)*((P(77)*P(84)/A(63))/DIFF)
(      1145)          DX(16)=P(75)*((P(79)*P(86)/A(64))/DIFF)
(      1146)          DX(19)=P(75)*((P(81)*P(08)/A(65))/2*DIFF)
(      1147)          GOTO 6007
(      1148)  6005    DIFF=(P(76)*P(85)/A(66))+(P(78)*P(87)/A(67))+(P(80)*P(89)/A(68))
(      1149)          DX(15)=P(75)*((P(76)*P(85)/A(66))/DIFF)
(      1150)          DX(16)=P(75)*((P(78)*P(87)/A(67))/DIFF)
(      1151)          DX(19)=P(75)*((P(80)*P(89)/A(68))/2*DIFF)
(      1152)  6007    CONTINUE
(      1153)          DX(20)=P(73)-P(52)
(      1154)          DX(21)=P(120)-P(121)-P(122)-P(123)
(      1155)          DX(22)=P(122)-P(120)
(      1156)          DX(23)=A(69)-(P(44)*A(70))
(      1157)          DX(24)=(P(118)-X(24))/200
(      1158)          DX(25)=(P(119)-X(25))/300
(      1159)          DX(26)=((A(54)*(P(32)-287))-(A(55)*(P(6)-100))-X(26))/A(56)
(      1160)          DX(27)=(P(96)-X(27))/A(61)
(      1161)          DX(28)=(A(79)/180.0)-P(124)-P(126)
(      1162)          DX(29)=((P(74)-(A(74)/18.0))-X(29))/15.0
(      1163)  C
(      1164)  C       SOLVING THE FIRST ORDER LINEAR DIFFERENTIAL
(      1165)  C       EQUATIONS WITH ONE INTEGRATION STEP.
(      1166)  C
(      1167)          DO 6010 I=1,23
(      1168)          IF(I.EQ.3)I=6
(      1169)          IF(I.EQ.13)I=15
(      1170)          IF(I.EQ.17)I=19
(      1171)          X(I)=X(I)+DX(I)
(      1172)  6010    CONTINUE
(      1173)  C
(      1174)  C       SOLVING THE FIRST ORDER NON-LINEAR DIFFERENTIAL
(      1175)  C       EQUATIONS WITH TEN INTEGRATION STEPS.
(      1176)  C
(      1177)          DO 6020 I=13,29
(      1178)          DO 6020 J=1,10
(      1179)          IF(I.EQ.15)I=17
(      1180)          IF(I.EQ.19)I=24
(      1181)          X(I)=X(I)+0.1*DX(I)
(      1182)  6020    CONTINUE
(      1183)  C
(      1184)  C       SEND SUBROUTINE BACK TO MAIN PROGRAM
(      1185)  C
(      1186)          RETURN
(      1187)          END
```

APPENDIX 8

DOCUMENTATION FOR APPLE II IMPLEMENTATION OF FAB3

(A PROTOTYPE OF MFAB)

PROGRAM DEVELOPMENT

FAB3 was initially developed as a mathematical model using FORTRAN IV on a PRIME 550 minicomputer. This was translated to APPLESOFT for the Apple II microcomputer. The program size was 17K (excluding variable storage space required during simulation), run time was slow and model output restricted to listings of forecasted values. A number of changes were therefore necessary to improve the run time efficiency and output representation.

In an attempt to increase runtime efficiency the 100 minute aldosterone delay was changed. The values of the variables which are used to stimulate aldosterone release were kept in arrays of dimension 100 and in the FORTRAN representation updating was achieved by shifting each value up one place in the array and inserting a new value for the first element. This involved 100 operations per array. The Apple II version was altered so that a pointer is used to move down each array (rather than all elements moved up each array) and a new value is inserted into the element specified by the pointer once that element has been read, before the pointer is incremented by 1. This therefore involves only 1 operation per array.

Graphics were also introduced as an attempt to improve output representation. In early attempts one variable was selected for

graphic output, its value at each minute was stored during simulation and the forecast array plotted at the end of the simulation.

Further problems were encountered. The section of memory on the Apple II which handles graphics is situated in the middle of the available memory. This reduced the room available for the original program and made future development difficult unless memory space used by the program was reduced. The initial FORTRAN coding was laid out for ease of understanding and contained a large number of comment statements. These were all removed from the APPLESOFT version and furthermore, statements were combined into multiple lines. This successfully reduced the program requirements to 11K of memory.

The two main concerns of run time and interactive facilities dominated the remainder of the development exercise. Improving both of these was seen to be essential for the eventual aim of producing a user friendly package.

The large mathematical model (FAB3) was segmented to produce two smaller models (models emphasising hormones and acid-base dynamics). It would be an easy task to include other submodels in the package. A shell program was written for these models (containing lines and routines common to the different models) which allows real time interaction. This involves the selection of three dependent variables for graphic output. In addition independent variables can be changed by breaking the simulation.

Breaking was achieved by checking the contents of memory location - 16384 (if this is greater than 127 then a key has been pressed) so that simulation may be broken simply by pressing any key. If this action is carried out then the user is asked a number of questions relating to the continuation of the simulation (see subsection 9.5.2 for an example run of the package).

A menu program was then developed which allows the user to select a version, which is then loaded from disc and run. Using this method, memory space requirements were reduced and user-friendliness increased, however, the run time of the model remained unacceptibly slow. It was therefore necessary to gain access to a program compiler.

The BASIC language is an interpreter so that during simulation each statement is translated into machine code each time it is encountered and before it can be executed. A compiler translates the BASIC program into machine code in advance of a simulation (which can be stored for future use) and thus removes the need for translation during simulation. This reduced run time to approximately a third of the non-compiled version, although disc space requirement increased. The latter problem did not cause problems during simulation as compiled versions may be directed to store areas (thus over-writing graphic memory space can be prevented).

A number of other improvements were made including:

- FAB3 as a menu option;
- a menu option to exit the package;

- automatic loading and running of menu (effected by changing the initialisation of the floppy disc);
- mobility between the menu options.

TECHNICAL DATA

Memory requirements:

General model	12.5k
Acid-base model	11.2k
Hormone model	10.7k
Available memory	21.0k

DISC SPACE REQUIREMENTS (1/2K units):

	Basic version	Compiled version	Total
General model	25	41	66
Acid-base model	23	35	58
Hormone model	22	34	56
Menu	4	-	4
Initialisation	2	-	2
Computer (optional)	-	-	170
Available disc space			496
Remaining disc space			140

PROGRAM SPEED: time to simulate 1h simulation time

General model: 57 second real time

Acid-base model: 41 seconds real time

Hormone model: 37 seconds real time

P( ) Vector Number	Description	Initial Value
1.	Factor determining HCO_3^- excretion rate	2.4 AU
2.	Effect of ADH (ratio to normal)	1.0 AU
3.	Effect of aldosterone (ratio to normal)	1.0 AU
4.		
5.	Effect of HCO_3^- excretion (ratio to normal)	1.0 AU
6.	Glomerular Filtration Rate (GFR)	0.1 $l min^{-1}$
7.	Factor of GFR	1.0 AU
8.	Factor of Na^+ and K^+ renal excretion	0.0
9.	Plasma osmolality	287.0 $mOsm\ l^{-1}$
10.		
11.		
12.	Systemic arterial pressure	100 mm Hg
13.	Capillary pressure	17 mm Hg
14.	$P\ CO_2$	40 mm Hg
15.	Net capillary Starling forces	0.3 mm Hg
16.	pH of arterial blood	7.4
17.		
18.		
19.	Interstitial colloid osmotic pressure	5.0 mm Hg
20.	Interstitial fluid pressure	-6.3 mm Hg
21.	Plasma colloid osmotic pressure	28 mm Hg
22.	Pulmonary venous pressure	4.0 mm Hg
23.	Systemic venous pressure	3.0 mm Hg
24.	Capillary filtration rate	0.002 $l min^{-1}$
25.	Cardiac output	5.0 $l min^{-1}$
26.	Fraction of cardiac output	4.0 $l min^{-1}$
27.	Net H_2O flux ICF $\longleftrightarrow$ ECF	0.0 $l min^{-1}$
28.	Lymphatic return rate	0.002 $l min^{-1}$
29.		
30.		
31.	Rate of urinary excretion distal tubule	0.01 $l min^{-1}$
32.	Urine output	0.001 $l min^{-1}$
33.	Standard bicarbonate at pH = 7.4	24.0 $mEq\ l^{-1}$

34.	Effect of TA, OA, phosphate on Cl^- renal excretion	0.038 AU
35.		
36.	Effect of volume expansion (pressure diuresis)	1.0 AU
37.	Blood volume	5.0 l
38.	Extracellular fluid volume	15.0 l
39.	Extracellular fluid Cl^- concentration	104.0 $mEql^{-1}$
40.	Extracellular fluid HCO_3^- concentration	4.5 $mEql^{-1}$
41.	Extracellular fluid K^+ concentration	4.5 $mEql^{-1}$
42.	Intracellular fluid K^+ concentration	140.0 $mEql^{-1}$
43.	Extracellular fluid Na^+ concentration	140.0 $mEql^{-1}$
44.	Extracellular fluid OA concentration	6.0 mMl^{-1}
45.	Plasma protein effect on STBC	15.5 $mEql^{-1}$
46.	Interstitial protein concentration	20.0 gl^{-1}
47.	Extracellular fluid phosphate concentration	1.1 $mEql^{-1}$
48.	Plasma protein concentration	70.0 hl^{-1}
49.	Extracellular fluid urea concentration	2.5 $mEql^{-1}$
50.	Renal excretion rate of HCO_3^-	0.015 $mEqmin^{-1}$
51.	Renal excretion rate of Cl^-	0.1328 $mEqmin^{-1}$
52.	Albumin concentration in plasma	40.0 gl^{-1}
53.	Rate of K^+ excretion in distal tubule	0.1205 $mEqmin^{-1}$
54.	Net flux K^+ ECF $\longleftrightarrow$ ICF	0.0 $mEqmin^{-1}$
55.	Net flux K^+ ECF $\longleftrightarrow$ ICF(normalised)	1.0 AU
56.	Renal excretion rate K^+	0.047 $mEqmin^{-1}$
57.	Rate of Na^+ excretion in distal tubule	1.17 $mEqmin^{-1}$
58.	Effect of Na^+ lost in Urine	0.016 $mEqmin^{-1}$
59.	Rate of Na^+ excretion in loop of Henle	1.4 $mEqmin^{-1}$
60.		
61.	Renal excretion rate of Na^+	0.12 $mEqmin^{-1}$
62.	Renal excretion rate of OA	0.01 $mMmin^{-1}$
63.	Whole body CO_2 concentration	25.0 $mEql^{-1}$
64.	Arterial pH effect on CO_2 excretion via lung	1.0 AU
65.	PCO_2 effect on CO_2 excretion via lung	1.0 AU 1 min^{-1}
66.	Respiratory water loss	0.0005 1 min^{-1}
67.	Ventilation rate (ratio to normal)	1.0 AU

68.	Renal excretion rate phosphate	0.025 $mMmin^{-1}$
69.		
70.		
71.		
72.	Renal excretion rate of urea	0.15 $mEq\,min^{-1}$
73.	Effects of various phenomena on ALD release	0.0 AU
74.		
75.	Intracellular fluid volume	25.0 l
76.	Interstitial fluid volume	12.0 l
77.	Plasma volume	3.0 l
78.	Extracellular chloride content	1560.0 mEq
79.		
80.	Extracellular potassium content	67.5 mEq
81	Intracellular potassium content	3500.0 mEq
82.	Extracellular sodium content	2100.0 mEq
83.	Extracellular organic acid content	90.0 mEq
84.	Whole body CO_2 content	1000.0 mEq
85.	Interstitial protein content	240.0 g
86.	Albumin synthesis rate	0.0 $gmin^{-1}$
87.	Plasma albumin content	120.0 g
88.	Extracellular phosphate content	16.5 mEq
89.	Extracellular urea content	100.0 mEq
90.	Factor determining ADH release rate	0.0 AU
91.	Factor determining aldosterone release rate	0.0 AU

A( ) Vector Number	Description	Initial Value
1.	ACTH	1.0 AU
2.	Parameter of left heart performance	0.2 AU
3.	Parameter of right heart performance	0.3 AU
4.	Parameter for capillary pressure	5.9286 AU
5.	ADH antagonist	1.0 AU
6.	Capillary filtration coefficient	0.0067 AU
7.	Transfer coefficient H^+ ECF $\longleftrightarrow$ ICF	5.0 AU

8.	Weight of ECF Na^+ concentration on ALD secretion	0.5 AU
9.	Transfer coefficient K^+ ECF $\longleftrightarrow$ ICF	0.0008 AU
10.	Maculladensa weighting on ALD secretion	0.1 AU
11.	Systemic arterial pressure weighting on ALD secretion	0.001 AU
12.	Na^+, K^+, ECF concentration effect on GFR	0.2 AU
13.	Pulmonary venous pressure weighting on ALD secretion	0.1 AU
14.	Transfer coefficient H_2O ECF $\longleftrightarrow$ ICF	0.0003 mEq min^{-1}
15.	Proportional constant between CO and blood volume	1.0 AU
16.	Drinking rate	0.00013 l min^{-1}
17.	Rate of insensible H_2O loss	0.0003 l min^{-1}
18.	Steady-state lymphatic return rate	0.002 l min^{-1}
19.	Rate of metabolic water production	0.0005 l min^{-1}
20.	Total resistance in pulmonary circulation	3.0 mm Hg min^{-1}
21.	Total resistance in systemic circulation	20.0 mm Hg min^{-1}
22.	Steady-State CO_2 excretion rate via lung	10.42 mEq min^{-1}
23.	Steady-State CO_2 metabolic production	10.42 mEq min^{-1}
24.	Steady-state interstitial fluid volume	12.0 l
25.	Volume red blood cells	2.0 l
26.	Intake rate K^+	0.047 mEq min^{-1}
27.	Steady-state excretion rate NH_4	0.024 mEq min^{-1}
28.	Intake rate Na^+	0.12 mEq min^{-1}
29.	Aldosterone antagonist reduces effectiveness (< 1.0)	1.0 AU
30.	Intake rate of urea	0.15 mEq
31.	Steady-state GFR	0.1 l min^{-1}
32.	Steady-state ECF volume	15.0 l
33.	Time constant for ADH secretion	15.0 min
34.	Time constant for aldosterone secretion	30.0 min
35.	Plasma osmolality weighting on ADH secretion	0.5 AU
36.	Pulmonary venous pressure weighting on ADH secretion	1.0 AU
37.	Intravenous H_2O input	0.0 AU
38.	Intake rate of phosphate	0.025 mM min^{-1}
39.	Intake rate of OA	0.01 mM min^{-1}

40.	Intake rate of Cl^-	0.1328 mEq min^{-1}
41.	Steady-state PCO_2	40.0 mm Hg
42.	Steady-state pH of arterial blood	7.4
43.	Albumin loss rate from plasma	0.0 g min^{-1}
44.	Decrease albumin synthesis (due to loss in	0.0 g l^{-1}
45.	Protein substitute infusion	0.0 g min^{-1}
46.	Respiratory H_2O loss in steady-state	0.0005 l min^{-1}
47.	Plasma albumin conc.	40 g l^{-1}
48.	Interstitial albumin conc.	20 g l^{-1}

Note: There are some blank entries which occured during model development.

PROGRAM CODING

```
]LIST

100  TEXT : HOME : VTAB 6
110  PRINT "           WELCOME TO THE"
120  PRINT : PRINT "          INTERACTIVE  FAB"
130  PRINT : PRINT "             SIMULATION": PRINT : PRINT
140  PRINT "     WHICH MODEL DO YOU REQUIRE ?": PRINT : PRINT
150  PRINT " 1 - ACID / BASE SYSTEM": PRINT
160  PRINT " 2 - FLUID/ELECTROLYTE & HORMONE SYSTEM": PRINT

180  PRINT " 3 - GENERAL SYSTEM": PRINT
190  PRINT " 4 - EXIT FROM PROGRAM": PRINT
290  INPUT I: ON I GOTO 310,320,340,400
310  PRINT  CHR$ (4) + "BLOAD RUNTIME" +  CHR$ (13) +  CHR$ (4) + "BRUN PH"
320  PRINT  CHR$ (4) + "BLOAD RUNTIME" +  CHR$ (13) +  CHR$ (4) + "BRUN HORM1"

340  PRINT  CHR$ (4) + "BLOAD RUNTIME" +  CHR$ (13) +  CHR$ (4) + "BRUN FAB1"
400  END
```

```
]PR#0
]LIST PH

100  HOME : VTAB 8: PRINT  TAB( 11);"ACID / BASE AND": PRINT
105  PRINT  TAB( 12);"HORMONE MODEL"
110  VTAB 21: PRINT  TAB( 7);"PRESS ANY KEY TO PROCEED": GET A$
120  DIM A(48),P(91),Q(100),R(100),S(100),T(100)
420  FOR I = 1 TO 91: READ P(I): NEXT
510  FOR I = 1 TO 48: READ A(I): NEXT
550  FOR I = 1 TO 100:Q(I) = P(12):R(I) = P(22):S(I) = P(41):T(I) = P(59): NEXT
:O = 1
610 X =  - 1:Y = 159:Z = 279:W = 127:V = 0:U = 60:S = 1:J = V: HGR : VTAB 21
620  PRINT "SPECIFY 3 VARIABLES FOR GRAPHIC OUTPUT": INPUT A,B,C
625 A1 = P(A):B1 = P(B):C1 = P(C)
630  PRINT : PRINT : PRINT : PRINT "TYPE MIN. & MAX. VALUES FOR"
640  PRINT "VARIABLE ";A;" ";: INPUT K,L
650  PRINT "VARIABLE ";B;" ";: INPUT N,P
660  PRINT "VARIABLE ";C;" ";: INPUT Q,R: GOTO 700
670  PRINT : PRINT : PRINT
680  PRINT "DO YOU WISH TO ABORT THE SIMULATION ?": PRINT "( Y OR N ) ?": PRINT
: INPUT A$: IF A$ = "Y" THEN 9000
700  PRINT "DO YOU WISH TO PERTURB THE SYSTEM ?": PRINT "( Y OR N ) ?"
710  PRINT "(ANSWER ONLY WHEN READY TO CONTINUE)": INPUT A$
740  IF A$ <  > "Y" THEN 790
750  PRINT "WHICH VARIABLE DO YOU WISH TO ALTER ?": PRINT : PRINT.: INPUT D
760  PRINT "PRESENT VALUE ";A(D);"  NEW VALUE ?": PRINT : PRINT : INPUT E
770 A(D) = E:F = H:G = M
780  PRINT "ANY OTHER PERTURBATIONS ?": PRINT "( Y OR N ) ?": PRINT : INPUT A$:
GOTO 740
790  POKE  - 16368,0: IF J > V THEN 810
800  HGR : HCOLOR= 3: HPLOT V,Y TO Z,Y: HPLOT V,Y TO V,V: HPLOT Z,Y TO Z,V
801  FOR I = 0 TO 144 STEP 16: HPLOT V,I TO 2,I: HPLOT 277,I TO Z,I: NEXT
802 YA = Y - Y * (A1 - K) / (L - K): HCOLOR= 6: HPLOT V,YA TO 6,YA: HPLOT 273,YA
 TO Z,YA
804 YB = Y - Y * (B1 - N) / (P - N): HCOLOR= 5: HPLOT V,YB TO 6,YB: HPLOT 273,YB
 TO Z,YB
806 YC = Y - Y * (C1 - Q) / (R - Q): HCOLOR= 1: HPLOT V,YC TO 6,YC: HPLOT 273,YC
 TO Z,YC
810  VTAB 21: PRINT "VAR.";A; TAB( 8);K; TAB( 13);"- ";L; TAB( 21);"BLUE": IF G
> 9 THEN 820
815  PRINT "VAR.";B; TAB( 8);N; TAB( 13);"- ";P; TAB( 21);"RED"; TAB( 33);F;": "
;G: GOTO 830
820  PRINT "VAR.";B; TAB( 8);N; TAB( 13);"- ";P; TAB( 21);"RED"; TAB( 33);F;":";
G
830  PRINT "VAR.";C; TAB( 8);Q; TAB( 13);"- ";R; TAB( 21);"GREEN": IF J > V THEN
 850
840 J = J + S: IF  PEEK ( - 16384) > W THEN 670
850 X = X + S: IF X > Z THEN X = V: IF X = V THEN 800
860  HCOLOR= 6: HPLOT X,Y - Y * (P(A) - K) / (L - K)
870  HCOLOR= 5: HPLOT X,Y - Y * (P(B) - N) / (P - N)
880  HCOLOR= 1: HPLOT X,Y - Y * (P(C) - Q) / (R - Q)
890 H =  INT (J / U):M = J - H * U: IF M > 9 THEN 900
895  VTAB 21: PRINT "VAR.";A; TAB( 8);K; TAB( 13);"- ";L; TAB( 21);"BLUE"; TAB(
33);H;": ";M: GOTO 7030
900  VTAB 21: PRINT "VAR.";A; TAB( 8);K; TAB( 13);"- ";L; TAB( 21);"BLUE"; TAB(
33);H;":";M
7030 P(26) = P(37) * A(15) - 1:P(12) = P(26) * A(21) + 20
7060 P(23) = P(26) / A(3) - 10.3333: IF P(23) < 0 THEN P(23) = 0
7080 P(22) = P(26) / A(2) - 16: IF P(22) < 0 THEN P(22) = 0
7110 P(24) = A(6) * P(15):P(15) = P(13) - P(21) - P(20) + P(19):P(21) = .4 * P(4
8)
7140 P(19) = .25 * P(46):I = P(76) / A(24): IF I <  = .9 THEN P(20) =  - 15
7170  IF I > .9 AND I <  = 1 THEN P(20) = 87 * I - 93.3
7180  IF I > 1 AND I <  = 2 THEN P(20) =  - 6.3 * ((2 - I) ^ 10)
7190  IF I > 2 THEN P(20) = I - 2:P(13) = ((P(23) * A(4)) + P(12)) / (A(4) + 1)
7220 P(38) = P(77) + P(76):P(37) = P(77) + A(25)
7250 P(63) = P(84) / (P(75) + P(76) + P(77)):P(14) = 2.5 * (P(63) - 23) + 35
7270 P(40) = P(33) - 11.605 * (P(16) - 7.4)
7280 P(16) = 6.099 + ( LOG (P(40) / (.03 * P(14))) /  LOG (10))
7290 P(64) =  EXP (7 * (A(42) - P(16))):P(65) =  EXP (.133 * (P(14) - A(41)))
7310 P(67) = (P(64) + P(65)) / 2:P(66) = A(46) * P(67)
```

```
7380 P(28) = A(18) * (24 / (1 + ( EXP ( - .4977 * P(20)))))
7390 P(55) = 1 + .5 *  LOG (P(41) / 4.5):P(54) = A(9) * (3500 * P(55) - P(81))
7400 P(27) = (A(14) * ((P(42) + 10.5) - 6 - P(41) - P(43)))
7430 P(43) = P(82) / P(38):P(41) = P(80) / P(38):P(42) = P(81) / P(75)
7510 P(9) = (((P(41) + P(43)) * 1.86) + P(49) + 15.73)
7540 P(2) = 1.1 / (1 +  EXP ( - .5 * (P(90) + 4.605))) * A(5)
7550 P(3) = 10 / (1 +  EXP ( - .4394 * (P(91) - 5))) * A(29)
7570 BA = A(1) - 1:BB = (S(0) - 4.5) * A(8):BC = (R(0) - 4) * A(13)
7600 BD = (T(0) - 1.4) * A(10):BE = (Q(0) - 100) * A(11):P(73) = BA + BB - BC -
BD - BE
7640 P(6) = P(7) * (A(31) * (P(39) / A(32))):P(8) = P(36) * P(6) * A(12)
7660  IF P(12) < 40 THEN P(7) = 0: IF P(12) >  = 100 THEN P(7) = 1
7670  IF P(12) >  = 40 AND P(12) < 80 THEN P(7) = .02 * P(12) - .8
7680  IF P(12) >  = 80 AND P(12) < 100 THEN P(7) = .01 * P(12)
7700  IF P(21) <  = 28 THEN P(36) =  - 5 * (P(21) / 28 - 1) + 1: IF P(21) > 28 T
HEN P(36) = 1
7740 P(72) = P(6) * P(49) * .6:P(31) = (P(72) + .312 + 1.86 * (P(57) + P(53))) /
 P(9)
7770 P(32) = P(31) - (P(2) * .9 * P(31)): IF P(32) < .5 / 1440 THEN P(32) = .5 /
 1440
7790 P(53) = (P(3) * P(41) * .01778) + (.45 * P(8) * P(41)):P(56) = P(53) * .390
04
7810 P(59) = (.5 * P(43) * P(8)):P(61) = P(57) * .11624 - P(58): IF P(61) < 0 TH
EN P(61) = 0
7840 P(58) = .007 + A(27) - P(50): IF P(58) < 0 THEN P(58) = 0:P(57) = .9 * P(59
) - .09 * P(3)
8220 P(75) = P(75) + P(27):P(76) = P(76) + (P(24) - P(28) - P(27))
8240 P(77) = P(77) + (A(16) + A(37) + A(19) + P(28)) - (A(17) + P(32) + P(24) +
P(66))
8300 P(80) = P(80) + (A(26) - P(56) - P(54))
8330 P(82) = P(82) + (A(28) - P(61))
8370 P(84) = P(84) + A(23) - A(22) * P(67)
8475  FOR I = 1 TO 10
8490 P(90) = P(90) + ((A(35) * (P(9) - 287)) - (A(36) * (P(22) - 4)) - P(90)) /
(A(33) * 10)
8510 P(91) = P(91) + (P(73) - P(91)) / (A(34) * 10): NEXT
8710 Q(0) = P(12):R(0) = P(22):S(0) = P(41):T(0) = P(59)
8750 O = O + 1: IF O > 100 THEN O = 1
8900  GOTO 840
9000  PRINT  CHR$ (4);"RUN MENU"
9100  DATA  2.4,1,1,0,1,.1,1,.02,287,461,0,100,17,40,.3,7.4,0,0,5,-6.3,28,4,3,.0
02,5,4,0,.002,0,0
9200  DATA  .01,.001,24,.038,0,1,5,15,104,24,4.5,140,140,6,15.5,20,1.1,70,2.5,.0
15,.1328,40
9300  DATA  .1205,0,1,.047,1.17,.016,1.4,0,.12,.01,25,1,1,.0005,1,.025,0,0,0,.15
,0,0
9350  DATA  25,12,3,1560,0,67.5,3500,2100,90,1000,240,0,120,16.5,100,0,0
9400  DATA  1,.2,.3,5.9286,1,.0067,5,.5,.0008,.1,.001,.2,.1,.0003,1,.0013,.0003,
.002,.0005,3,20
9500  DATA  10.42,10.42,12,2,.047,.024,.12,1,.15,.1,15,15,30,.5,1,0,.025,.01,.13
28,40,7.4
9600  DATA  0,0,0,.0005,40,20
```

```
]LOAD HORMONE
]LIST HORM1.

100  HOME : VTAB 8: PRINT  TAB( 8);"FLUID/ELECTROLYTE AND": PRINT
105  PRINT  TAB( 12);"HORMONE MODEL"
110  VTAB 21: PRINT  TAB( 7);"PRESS ANY KEY TO PROCEED": GET A$
120  DIM A(48),P(91),Q(100),R(100),S(100),T(100)
420  FOR I = 1 TO 91: READ P(I): NEXT
510  FOR I = 1 TO 48: READ A(I): NEXT
550  FOR I = 1 TO 100:Q(I) = P(12):R(I) = P(22):S(I) = P(41):T(I) = P(59): NEXT
:O = 1
610 X =  - 1:Y = 159:Z = 279:W = 127:V = 0:U = 60:S = 1:J = V: HGR : VTAB 21
620  PRINT "SPECIFY 3 VARIABLES FOR GRAPHIC OUTPUT": INPUT A,B,C
625 A1 = P(A):B1 = P(B):C1 = P(C)
630  PRINT : PRINT : PRINT : PRINT "TYPE MIN. & MAX. VALUES FOR"
640  PRINT "VARIABLE ";A;" ";: INPUT K,L
650  PRINT "VARIABLE ";B;" ";: INPUT N,P
660  PRINT "VARIABLE ";C;" ";: INPUT Q,R: GOTO 700
670  PRINT : PRINT : PRINT
680  PRINT "DO YOU WISH TO ABORT THE SIMULATION ?": PRINT "( Y OR N ) ?": PRINT
: INPUT A$: IF A$ = "Y" THEN 9000
700  PRINT "DO YOU WISH TO PERTURB THE SYSTEM ?": PRINT "( Y OR N ) ?"
710  PRINT "(ANSWER ONLY WHEN READY TO CONTINUE)": INPUT A$
740  IF A$ <  > "Y" THEN 790
750  PRINT "WHICH VARIABLE DO YOU WISH TO ALTER ?": PRINT : PRINT : INPUT D
760  PRINT "PRESENT VALUE ";A(D);"  NEW VALUE ?": PRINT : PRINT : INPUT E
770 A(D) = E:F = H:G = M
780  PRINT "ANY OTHER PERTURBATIONS ?": PRINT "( Y OR N ) ?": PRINT : INPUT A$:
GOTO 740
790  POKE  - 16368,0: IF J > V THEN 810
800  HGR : HCOLOR= 3: HPLOT V,Y TO Z,Y: HPLOT V,Y TO V,V: HPLOT Z,Y TO Z,V
801  FOR I = 0 TO 144 STEP 16: HPLOT V,I TO 2,I: HPLOT 277,I TO Z,I: NEXT
802 YA = Y - Y * (A1 - K) / (L - K): HCOLOR= 6: HPLOT V,YA TO 6,YA: HPLOT 273,YA
 TO Z,YA
804 YB = Y - Y * (B1 - N) / (P - N): HCOLOR= 5: HPLOT V,YB TO 6,YB: HPLOT 273,YB
 TO Z,YB
806 YC = Y - Y * (C1 - Q) / (R - Q): HCOLOR= 1: HPLOT V,YC TO 6,YC: HPLOT 273,YC
 TO Z,YC
810  VTAB 21: PRINT "VAR.";A; TAB( 8);K; TAB( 13);"- ";L; TAB( 21);"BLUE": IF G
> 9 THEN 820
815  PRINT "VAR.";B; TAB( 8);N; TAB( 13);"- ";P; TAB( 21);"RED"; TAB( 33);F;": "
;G: GOTO 830
820  PRINT "VAR.";B; TAB( 8);N; TAB( 13);"- ";P; TAB( 21);"RED"; TAB( 33);F;":";
G
830  PRINT "VAR.";C; TAB( 8);Q; TAB( 13);"- ";R; TAB( 21);"GREEN": IF J > V THEN
 850
840 J = J + S: IF  PEEK ( - 16384) > W THEN 670
850 X = X + S: IF X > Z THEN X = V: IF X = V THEN 800
860  HCOLOR= 6: HPLOT X,Y - Y * (P(A) - K) / (L - K)
870  HCOLOR= 5: HPLOT X,Y - Y * (P(B) - N) / (P - N)
880  HCOLOR= 1: HPLOT X,Y - Y * (P(C) - Q) / (R - Q)
890 H =  INT (J / U):M = J - H * U: IF M > 9 THEN 900
895  VTAB 21: PRINT "VAR.";A; TAB( 8);K; TAB( 13);"- ";L; TAB( 21);"BLUE"; TAB(
33);H;": ";M: GOTO 7030
900  VTAB 21: PRINT "VAR.";A; TAB( 8);K; TAB( 13);"- ";L; TAB( 21);"BLUE"; TAB(
33);H;":";M
7030 P(26) = P(37) * A(15) - 1:P(12) = P(26) * A(21) + 20
7060 P(23) = P(26) / A(3) - 10.3333: IF P(23) < 0 THEN P(23) = 0
7080 P(22) = P(26) / A(2) - 16: IF P(22) < 0 THEN P(22) = 0
7110 P(24) = A(6) * P(15):P(15) = P(13) - P(21) - P(20) + P(19):P(21) = .4 * P(4
8)
7140 P(19) = .25 * P(46):I = P(76) / A(24): IF I <  = .9 THEN P(20) =  - 15
7170  IF I > .9 AND I <  = 1 THEN P(20) = 87 * I - 93.3
7180  IF I > 1 AND I <  = 2 THEN P(20) =  - 6.3 * ((2 - I) ^ 10)
7190  IF I > 2 THEN P(20) = I - 2:P(13) = ((P(23) * A(4)) + P(12)) / (A(4) + 1)
7220 P(38) = P(77) + P(76):P(37) = P(77) + A(25)
7310 P(66) = A(46) * P(67)
7380 P(28) = A(18) * (24 / (1 + ( EXP ( - .4977 * P(20)))))
7390 P(55) = 1 + .5 *  LOG (P(41) / 4.5):P(54) = A(9) * (3500 * P(55) - P(81))
7400 P(27) = (A(14) * ((P(42) + 10.5) - 6 - P(41) - P(43)))
7430 P(43) = P(82) / P(38):P(41) = P(80) / P(38):P(42) = P(81) / P(75)
```

```
7510 P(9) = (((P(41) + P(43)) * 1.86) + P(49) + 15.73)
7540 P(2) = 1.1 / (1 +  EXP ( - .5 * (P(90) + 4.605))) * A(5)
7550 P(3) = 10 / (1 +  EXP ( - .4394 * (P(91) - 5))) * A(29)
7570 BA = A(1) - 1:BB = (S(0) - 4.5) * A(8):BC = (R(0) - 4) * A(13)
7600 BD = (T(0) - 1.4) * A(10):BE = (Q(0) - 100) * A(11):P(73) = BA + BB - BC -
BD - BE
7640 P(6) = P(7) * (A(31) * (P(38) / A(32))):P(8) = P(36) * P(6) * A(12)
7660  IF P(12) < 40 THEN P(7) = 0: IF P(12) >  = 100 THEN P(7) = 1
7670  IF P(12) >  = 40 AND P(12) < 80 THEN P(7) = .02 * P(12) - .8
7680  IF P(12) >  = 80 AND P(12) < 100 THEN P(7) = .01 * P(12)
7700  IF P(21) <  = 28 THEN P(36) =  - 5 * (P(21) / 28 - 1) + 1: IF P(21) > 28 T
HEN P(36) = 1
7740 P(72) = P(6) * P(49) * .6:P(31) = (P(72) + .312 + 1.86 * (P(57) + P(53))) /
 P(9)
7770 P(32) = P(31) - (P(2) * .9 * P(31)): IF P(32) < .5 / 1440 THEN P(32) = .5 /
 1440
7790 P(53) = (P(3) * P(41) * .01778) + (.45 * P(8) * P(41)):P(56) = P(53) * .390
04
7810 P(59) = (.5 * P(43) * P(8)):P(61) = P(57) * .11624 - P(58): IF P(61) < 0 TH
EN P(61) = 0
7840 P(58) = .007 + A(27) - P(50): IF P(58) < 0 THEN P(58) = 0:P(57) = .9 * P(59
) - .09 * P(3)
8220 P(75) = P(75) + P(27):P(76) = P(76) + (P(24) - P(28) - P(27))
8240 P(77) = P(77) + (A(16) + A(37) + A(19) + P(28)) - (A(17) + P(32) + P(24) +
P(66))
8300 P(80) = P(80) + (A(26) - P(56) - P(54))
8330 P(82) = P(82) + (A(28) - P(61))
8475  FOR I = 1 TO 10
8490 P(90) = P(90) + ((A(35) * (P(9) - 287)) - (A(36) * (P(22) - 4)) - P(90)) /
(A(33) * 10)
8510 P(91) = P(91) + (P(73) - P(91)) / (A(34) * 10): NEXT
8710 Q(0) = P(12):R(0) = P(22):S(0) = P(41):T(0) = P(59)
8750 O = O + 1: IF O > 100 THEN O = 1
8900  GOTO 840
9000  PRINT  CHR$ (4);"RUN MENU"
9100  DATA  2.4,1,1,0,1,.1,1,.02,287,461,0,100,17,40,.3,7.4,0,0,5,-6.3,28,4,3,.0
02,5,4,0,.002,0,0
9200  DATA  .01,.001,24,.038,0,1.5,15,104,24,4.5,140,140,6,15.5,20,1.1,70,2.5,.0
15,.1328,40
9300  DATA  .1205,0,1,.047,1.17,.016,1.4,0,.12,.01,25,1,1..0005,1,.025,0,0,0,.15
,0,0
9350  DATA  25,12,3,1560,0,67.5,3500,2100,90,1000,240,0,120,16.5,100,0,0
9400  DATA  1,.2,.3,5.9286,1,.0067,5,.5,.0008,.1,.001,.2,.1,.0003,1,.0013,.0003,
.002,.0005,3,20
9500  DATA  10.42,10.42,12,2,.047,.024,.12,1,.15,.1,15,15,30,.5,1,0,.025,.01,.13
28,40,7.4
9600  DATA  0,0,0,.0005,40,20
```

```
]LIST FAB1

100  HOME : VTAB 8: PRINT  TAB( 12);"GENERAL MODEL"
110  VTAB 21: PRINT  TAB( 7);"PRESS ANY KEY TO PROCEED": GET A$
120  DIM A(48),P(91),Q(100),R(100),S(100),T(100)
420  FOR I = 1 TO 91: READ P(I): NEXT
510  FOR I = 1 TO 48: READ A(I): NEXT
550  FOR I = 1 TO 100:Q(I) = P(12):R(I) = P(22):S(I) = P(41):T(I) = P(59): NEXT
:O = 1
610 X =  - 1:Y = 159:Z = 279:W = 127:V = 0:U = 60:S = 1:J = V: HGR : VTAB 21
620  PRINT "SPECIFY 3 VARIABLES FOR GRAPHIC OUTPUT": INPUT A,B,C
625 A1 = P(A):B1 = P(B):C1 = P(C)
630  PRINT : PRINT : PRINT : PRINT "TYPE MIN. & MAX. VALUES FOR"
640  PRINT "VARIABLE ";A;" ";: INPUT K,L
650  PRINT "VARIABLE ";B;" ";: INPUT N,P
660  PRINT "VARIABLE ";C;" ";: INPUT Q,R: GOTO 700
670  PRINT : PRINT : PRINT
680  PRINT "DO YOU WISH TO ABORT THE SIMULATION ?": PRINT "( Y OR N ) ?": PRINT
: INPUT A$: IF A$ = "Y" THEN 9000
700  PRINT "DO YOU WISH TO PERTURB THE SYSTEM ?": PRINT "( Y OR N ) ?"
710  PRINT "(ANSWER ONLY WHEN READY TO CONTINUE)": INPUT A$
740  IF A$ <  > "Y" THEN 790
750  PRINT "WHICH VARIABLE DO YOU WISH TO ALTER ?": PRINT : PRINT : INPUT D
760  PRINT "PRESENT VALUE ";A(D);"  NEW VALUE ?": PRINT : PRINT : INPUT E
770 A(D) = E:F = H:G = M
780  PRINT "ANY OTHER PERTURBATIONS ?": PRINT "( Y OR N ) ?": PRINT : INPUT A$:
GOTO 740
790  POKE  - 16368,0: IF J > V THEN 810
800  HGR : HCOLOR= 3: HPLOT V,Y TO Z,Y: HPLOT V,Y TO V,V: HPLOT Z,Y TO Z,V
801  FOR I = 0 TO 144 STEP 16: HPLOT V,I TO 2,I: HPLOT 277,I TO Z,I: NEXT I
802 YA = Y - Y * (A1 - K) / (L - K): HCOLOR= 6: HPLOT V,YA TO 6,YA: HPLOT 273,YA
 TO Z,YA
804 YB = Y - Y * (B1 - N) / (P - N): HCOLOR= 5: HPLOT V,YB TO 6,YB: HPLOT 273,YB
 TO Z,YB
806 YC = Y - Y * (C1 - Q) / (R - Q): HCOLOR= 1: HPLOT V,YC TO 6,YC: HPLOT 273,YC
 TO Z,YC
810  VTAB 21: PRINT "VAR.";A; TAB( 8);K; TAB( 13);"- ";L; TAB( 21);"BLUE": IF G
> 9 THEN 820
815  PRINT "VAR.";B; TAB( 8);N; TAB( 13);"- ";P; TAB( 21);"RED"; TAB( 33);F;": "
;G: GOTO 830
820  PRINT "VAR.";B; TAB( 8);N; TAB( 13);"- ";P; TAB( 21);"RED"; TAB( 33);F;":";
G
830  PRINT "VAR.";C; TAB( 8);Q; TAB( 13);"- ";R; TAB( 21);"GREEN": IF J > V THEN
 850
840 J = J + S: IF  PEEK ( - 16384) > W THEN 670
850 X = X + S: IF X > Z THEN X = V: IF X = V THEN 800
860  HCOLOR= 6: HPLOT X,Y - Y * (P(A) - K) / (L - K)
870  HCOLOR= 5: HPLOT X,Y - Y * (P(B) - N) / (P - N)
880  HCOLOR= 1: HPLOT X,Y - Y * (P(C) - Q) / (R - Q)
890 H =  INT (J / U):M = J - H * U: IF M > 9 THEN 900
895  VTAB 21: PRINT "VAR.";A; TAB( 8);K; TAB( 13);"- ";L; TAB( 21);"BLUE"; TAB(
33);H;": ";M: GOTO 7030
900  VTAB 21: PRINT "VAR.";A; TAB( 8);K; TAB( 13);"- ";L; TAB( 21);"BLUE"; TAB(
33);H;":";M
7030 P(25) = P(37) * A(15):P(26) = P(25) - 1:P(12) = P(26) * A(21) + 20
7060 P(23) = P(26) / A(3) - 10.3333: IF P(23) < 0 THEN P(23) = 0
7080 P(22) = P(26) / A(2) - 16: IF P(22) < 0 THEN P(22) = 0
7110 P(24) = A(6) * P(15):P(15) = P(13) - P(21) - P(20) + P(19):P(21) = .4 * P(4
8)
7140 P(19) = .25 * P(46):I = P(76) / A(24): IF I <  = .9 THEN P(20) =  - 15
7170  IF I > .9 AND I <  = 1 THEN P(20) = 87 * I - 93.3
7180  IF I > 1 AND I <  = 2 THEN P(20) =  - 6.3 * ((2 - I) ^ 10)
7190  IF I > 2 THEN P(20) = I - 2:P(13) = ((P(23) * A(4)) + P(12)) / (A(4) + 1)
7220 P(38) = P(77) + P(76):P(37) = P(77) + A(25)
7250 P(63) = P(84) / (P(75) + P(76) + P(77)):P(14) = 2.5 * (P(63) - 23) + 35
7270 P(40) = P(33) - 11.605 * (P(16) - 7.4)
```

```
7280 P(16) = 6.099 + ( LOG (P(40) / (.03 * P(14))) /  LOG (10))
7290 P(64) =  EXP (7 * (A(42) - P(16))):P(65) =  EXP (.133 * (P(14) - A(41)))
7310 P(67) = (P(64) + P(65)) / 2:P(66) = A(46) * P(67)
7340 P(46) = P(85) / P(76):P(48) = (P(87) + 90) / P(77):P(52) = P(87) / P(77)
7380 P(28) = A(18) * (24 / (1 + ( EXP ( - .4977 * P(20)))))
7390 P(55) = 1 + .5 *  LOG (P(41) / 4.5):P(54) = A(9) * (3500 * P(55) - P(91))
7400 P(27) = (A(14) * ((P(42) + 10.5) - 6 - P(41) - P(43)))
7430 P(43) = P(82) / P(38):P(41) = P(80) / P(38):P(42) = P(81) / P(75)
7460 P(49) = P(89) / (P(38) + P(75))
7470 P(39) = P(78) / P(38):P(47) = P(88) / P(38):P(44) = P(83) / P(38)
7510 P(9) = (((P(41) + P(43)) * 1.86) + P(49) + 15.73)
7520 P(10) = (P(72) + 1.8623 * (P(56) + P(61))) / P(32)
7540 P(2) = 1.1 / (1 +  EXP ( - .5 * (P(90) + 4.605))) * A(5)
7550 P(3) = 10 / (1 +  EXP ( - .4394 * (P(91) - 5))) * A(29)
7570 BA = A(1) - 1:BB = (S(0) - 4.5) * A(8):BC = (R(0) - 4) * A(13)
7600 BD = (T(0) - 1.4) * A(10):BE = (Q(0) - 100) * A(11):P(73) = BA + BB - BC -
BD - BE
7640 P(6) = P(7) * (A(31) * (P(38) / A(32))):P(8) = P(36) * P(6) * A(12)
7660  IF P(12) < 40 THEN P(7) = 0: IF P(12) >  = 100 THEN P(7) = 1
7670  IF P(12) >  = 40 AND P(12) < 80 THEN P(7) = .02 * P(12) - .8
7680  IF P(12) >  = 80 AND P(12) < 100 THEN P(7) = .01 * P(12)
7700  IF P(21) <  = 28 THEN P(36) =  - 5 * (P(21) / 28 - 1) + 1: IF P(21) > 28 T
HEN P(36) = 1
7740 P(72) = P(6) * P(49) * .6:P(31) = (P(72) + .312 * 1.86 * (P(57) + P(53))) /
 P(9)
7770 P(32) = P(31) - (P(2) * .9 * P(31)): IF P(32) < .5 / 1440 THEN P(32) = .5 /
 1440
7790 P(53) = (P(3) * P(41) * .01778) + (.45 * P(8) * P(41)):P(56) = P(53) * .390
04
7810 P(59) = (.5 * P(43) * P(8)):P(61) = P(57) * .11624 - P(58): IF P(61) < 0 TH
EN P(61) = 0
7840 P(58) = .007 + A(27) - P(50): IF P(58) < 0 THEN P(58) = 0:P(57) = .9 * P(59
) - .09 * P(3)
7880 P(34) = P(62) + (P(68) * 1.8) - .0168: IF P(34) < 0 THEN P(34) = 0
7900 P(51) = P(61) - P(34) + P(56) + A(27) - P(50) - .0052: IF P(51) < 0 THEN P(
51) = 0
7930 XO = P(44) * P(6): IF XO <  = .6 THEN P(62) = XO / 60
7950  IF XO > .6 THEN P(62) = XO / 3 - .19:XP = P(47) * P(6)
7980  IF XP <  = .11 THEN P(68) = 5 * XP / 22: IF XP > .11 THEN P(68) = XP - .02
5
8010 P(5) =  - P(14) / 120 + 4 / 3:P(1) = P(40) * P(6) * P(5)
8030  IF P(1) > 2 AND P(1) <  = 4 THEN P(50) = .1638 * ((P(1) - 2) ^ 2.61)
8040  IF P(1) > 4 THEN P(50) = P(1) - 3
8060 P(33) = P(41) + P(43) - P(45) - P(39) - 1:P(45) = P(48) * .22143
8220 P(75) = P(75) + P(27):P(76) = P(76) + (P(24) - P(28) - P(27))
8240 P(77) = P(77) + (A(16) + A(37) + A(19) + P(28)) - (A(17) + P(32) + P(24) +
P(66))
8300 P(80) = P(80) + (A(26) - P(56) - P(54)):P(81) = P(81) + P(54)
8330 P(82) = P(82) + (A(28) - P(61)):P(83) = P(83) + (A(39) - P(62))
8370 P(84) = P(84) + (A(23) - (A(22) * P(67)))
8450 P(88) = P(88) + (A(38) - P(68)):P(89) = P(89) + (A(30) - P(72))
8475  FOR I = 1 TO 10
8490 P(90) = P(90) + ((A(35) * (P(9) - 287)) - (A(36) * (P(22) - 4)) - P(90)) /
(A(33) * 10)
8510 P(91) = P(91) + (P(73) - P(91)) / (A(34) * 10): NEXT
8710 Q(0) = P(12):R(0) = P(22):S(0) = P(41):T(0) = P(59)
8750 O = O + 1: IF O > 100 THEN O = 1
8800  GOTO 840
9000  PRINT  CHR$ (4);"RUN MENU"
9100  DATA  2.4,1,1,0,1,.1,1,.02,287,461,0,100,17,40,.3,7.4,0,0,5,-6.3,28,4,3,.0
02,5,4,0,.002,0,0
9200  DATA  .01,.001,24,.038,0,1,5,15,104,24,4.5,140,140,6,15.5,20,1.1,70,2.5,.0
15,.1328,40
9300  DATA  .1205,0,1,.047,1.17,.016,1.4,0,.12,.01,25,1,1,.0005,1,.025,0,0,0,.15
,0,0
9350  DATA  25,12,3,1560,0,67.5,3500,2100,90,1000,240,0,120,16.5,100,0,0
9400  DATA  1,.2,.3,5.9286,1,.0067,5,.5,.0008,.1,.001,.2,.1,.0003,1,.0013,.0003,
.002,.0005,3,20
9500  DATA  10.42,10.42,12,2,.047,.024,.12,1,.15,.1,15,15,30,.5,1,0,.025,.01,.13
28,40,7.4
9600  DATA  0,0,0,.0005,40,20
```

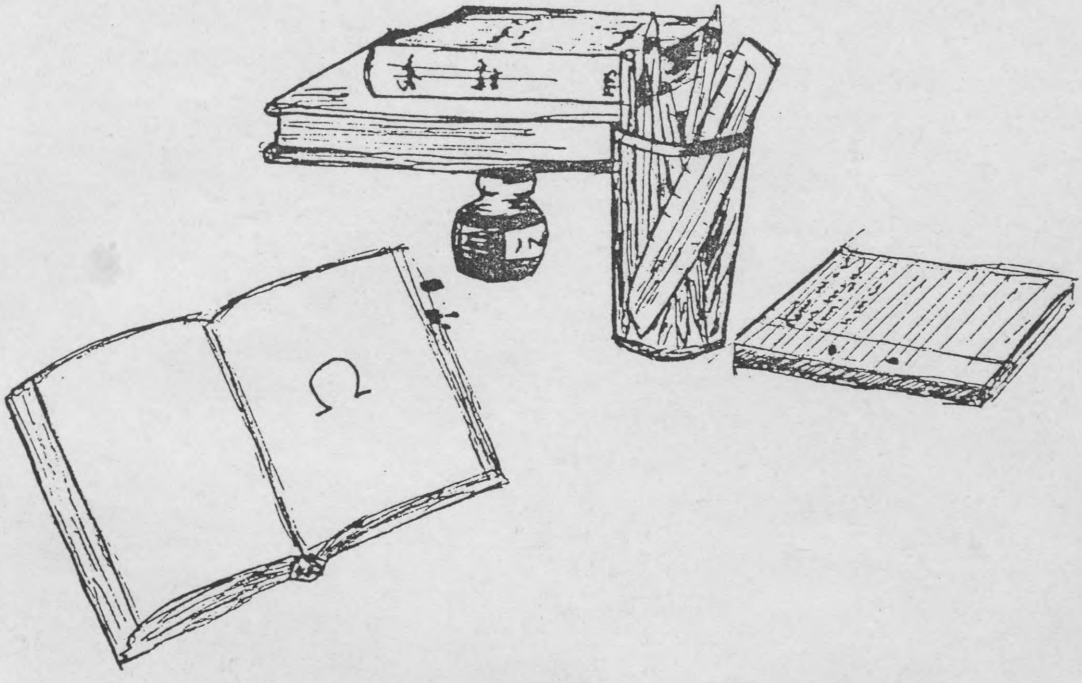

Figure A8.1 Ω